TESI DOCTORAL

MODELITZACIÓ DE RECEPTORS ACOBLATS A PROTEÏNA G:

disseny d'agonistes i antagonistes

MIREIA OLIVELLA I GARCIA

Gener 2004

Memòria presentada per Mireia Olivella i Garcia per optar al grau de Doctora en Bioquímica i Biologia Molecular.

Tesi Doctoral realitzada al Laboratori de Medicina Computacional, Institut de Neurociències, sota la direcció del Dr. Leonardo Pardo i Carrasco i la Dra. Mercedes Campillo i Grau.

Tesi adscrita al Departament de Bioquímica i Biologia Molecular, Universitat Autònoma de Barcelona.

AGRAÏMENTS

Durant aquests quatre anys hi ha hagut moments bons i dolents, d'encantament i desencantament, de motivació i de decepció, però finalment ha estat possible l'elaboració d'aquesta tesi gràcies a tots aquells que m'han acompanyat tant en l'espai professional com en el personal, espais que sovint es confonen.

Al meu director de tesi, al Leo, per encomanar-me la passió per la biologia, per la llibertat que m'ha donat, per la seva qualitat científica, per haver superat aquesta gran creu que suposa una doctoranda polititzada i tossuda, de qui encara m'agradaria aprendre'n moltes coses, per la immersió lingüística superada amb bona nota.

A la meva directora de tesi, la Merche, per estar sempre disposadíssima a ajudar-me, per la seva valuosa aportació en aquesta última etapa, de qui en valoro molt les seves ganes de fer les coses justes i ben fetes, per saber escoltar, per la seva comprensió, per l'esperit de superació.

Al David, a qui encara no perdono de veure't tant poc. M'has ajudat tant! Gràcies per la teva gran qualitat com a persona, pel teu gran compromís i coherència en les coses més quotidianes, que en el fons són les més importants.

Al Xavi, quatre anys dia a dia, ens hem fet un tip de riure, i també un tip de treballar, ets el company de feina perfecte. El despatx encara em sembla buit.

Al Joffre, perquè ens ho hem passat molt bé treballant, per les teves històries, pels batuts, per les platges de gossos i les bicicletes motoritzades.

Al Jesús, per les nostre xerrades, per l'interès, pel suport.

A la Gema per haver-me fet riure quan més em calia.

Al Joan, per ser al meu davant cada dia quan alço el cap, tant per parlar com per ajudar, poc temps i ja tenim un munt d'històries.

A la Teresa i la Ceci per ser l'alegria d'aquest departament, per fer que la feina sigui més que treballar.

A l'Arantxa i el Marc que m'han acompanyat aquests últims mesos, amb qui segur que treballarem a gust.

Als meus amics de l'ànima, què faria sense vosaltres! Pel vostre suport incondicional, pels vespres a les places, els múltiples sopars i les inoblidables rialles.

Al Menda, a la Putxi i al Guimi, gràcies per tornar a formar part del dia a dia.

Agraeixo molt especialment a l'Oriol que segueixi acompanyant-me quatre anys més com a parella, com a company d'un projecte de vida dur i idealista però increïblement fantàstic, que dóna sentit a la nostra vida.

I per últim als meus pares, que per bé o per mal, són els principals responsables que avui acabi aquesta tesi. Per haver dipositat incondicionalment tota la vostra confiança en mi, per animar-me a seguir endavant quan semblava que tot s'esfondrava.

Als meus pares

Qui sinó tots -i cadascú per torna-
podem crear des d'aquests límits d'ara
l'àmbit de llum on tots els vents s'exaltin,
l'espai de vent on tota veu ressoni?
Públicament ens compromet la vida,
públicament i amb tota llei d'indicis.
Serem allò que vulguem ser. Debades
fugim del foc si el foc ens justifica.

MIQUEL MARTÍ I POL

ÍNDEX

1. INTRODUCCIÓ 8

1.1. ELS RECEPTORS ACOBLATS A PROTEÏNA G 9
1.1.1. La importància dels GPCRS 9
1.1.2. Classificació dels GPCRS 10
1.1.3. Estructura general dels GPCRS 10
1.1.4. Informació estructural a través de l'anàlisis de seqüència dels gpcrs 11
1.1.5. Numeració dels GPCRS 12
1.1.6. Unió de lligands als GPCRs 12
1.1.7. Activació dels GPCRs 15
1.1.8. Divergències estructurals específiques dels GPCRS 19

1.2 . ELS RECEPTORS DE SEROTONINA 21
1.2.1. La serotonina 21
1.2.2. El receptor 5-HT_{1A} 21
1.2.3. El receptor 5-HT_4 22
1.2.4. El receptor 5-HT_7 22

1.3. ESTRUCTURA SECUNDÀRIA DELS RECEPTORS ACOBLATS A PROTEÏNA G 24
1.3.1. Les hèlix α 24
1.3.2. Efecte de l'entorn en la conformació de les hèlixs α 24
1.3.3. Residus que influeixen en l'estructura de les hèlixs α 25

2. RESUM GLOBAL DELS RESULTATS 27

2.1. INTRODUCCIÓ 27

2.2. L'EFECTE DE L'ENTORN EN LA CONFORMACIÓ DE LES HÈLIXS α 28

2.3. DESENVOLUPAMENT DE LA CAIXA DE METANS COM A MODEL DEL COR HIDROFÒBIC DE LES MEMBRANES LIPÍDIQUES 29

2.4. L'EFECTE DE LA PROLINA EN LA CONFORMACIÓ DE LES HÈLIXS α 31

2.5. MODES D'UNIÓ DELS RECEPTORS DE SEROTONINA AMB ELS SEUS LLIGANDS 32

2.6. CONSTRUCCIÓ D'UN MODEL TRIDIMENSIONAL PEL RECEPTOR 5-HT_{1A} A PARTIR DELS SEUS LLIGANDS 35

2.7. DISSENY DE LLIGANDS AGONISTES SELECTIUS AL RECEPTOR 5-HT_{1A} SENSE AFINITAT PEL RECEPTOR ADRENÈRGIC 36

2.8. ESTUDI DE LA UNIÓ ENTRE EL RECEPTOR 5-HT_4 I EL LLIGAND GR113808 36

2.9. MODEL D'INTERACCIÓ DELS ANTAGONISTES DEL RECEPTOR 5-HT_7 38

3. CONCLUSIONS 40

4. BIBLIOGRAFIA 43

5. COMPENDI DE PUBLICACIONS 52

5.1. INFLUENCE OF THE ENVIRONMENT IN THE CONFORMATION OF ALPHA-HELICES STUDIED BY PROTEIN DATABASE SEARCH AND MOLECULAR DYNAMICS SIMULATIONS 53

5.2.DESIGN, SYNTHESIS AND PHARMACOLOGICAL EVALUATION OF 5-HYDROXYTRYPTAMINE(1A) RECEPTOR LIGANDS TO EXPLORE THE THREE-DIMENSIONAL STRUCTURE OF THE RECEPTOR. 60

5.3 DESIGN AND SYNTHESIS OF S-(-)-2-[[4-(NAPHT-1-YL)PIPERAZIN-1-YL]METHYL]-1,4-DIOXOPERHYDROPYRROLO[1,2-A]PYRAZINE (CSP-2503) USING COMPUTATIONAL SIMULATION. A 5-HT_{1A} RECEPTOR AGONIST. 67

5.4. COMPUTATIONAL MODEL OF THE COMPLEX BETWEEN GR113808 AND THE 5-HT4 RECEPTOR GUIDED BY SITE-DIRECTED MUTAGENESIS AND THE CRYSTAL STRUCTURE OF RHODOPSIN 71

5.5. OPTIMIZATION OF THE PHARMACOPHORE MODEL FOR 5-HT7R ANTAGONISM. DESIGN AND SYNTHESIS OF NEW NAPHTHOLACTAM AND NAPHTHOSULTAM DERIVATIVES. 80

1. INTRODUCCIÓ

1.1. ELS RECEPTORS ACOBLATS A PROTEÏNA G

1.1.1. LA IMPORTÀNCIA DELS GPCRS

Els receptors acoblats a proteïna G (GPCRs) són una família de proteïnes integrals de membrana que responen a senyals extracel·lulars com amines biogèniques, pèptids, glicoproteïnes, lípids, ions, nucleòtids o proteases (Ji *et al.*, 1998). Aquests receptors s'encarreguen de transmetre el senyal extracel·lular cap a l'interior de la cèl·lula a través de la proteïna G. A grans trets podríem dir que la seva funció és amplificar la petita senyal extracel·lular rebuda fins a una resposta cel·lular.

S'ha pogut identificar més de 800 GPCRs en el genoma humà (veure FIGURA 1), alguns dels quals encara estan classificats com a "orphan receptors" (Shacham *et al.*, 2001), tot constituint una de les més grans famílies de proteïnes del genoma humà (Lander *et al.*, 2001; Venter *et al.*, 2001). S'ha estimat que més de la meitat de tots els fàrmacs actuals estan destinats a interaccionar amb aquest tipus de receptor (Flower, 1999) ja que moltes patologies es troben associades al funcionament anòmal dels GPCRs (Marinissen and Gutkind, 2001; Whitehead *et al.*, 2001). És així que cada vegada més els GPCRs estan esdevenint el focus on es centren els programes de genòmica funcional i la recerca en desenvolupament de fàrmacs (Howard *et al.*, 2001).

Malgrat la seva evident importància, una de les moltes claus que encara resten per resoldre és com aquests receptors transmeten els senyals extracel·lulars als sistemes efectors intracel·lulars i a través de quin mecanisme aquestes proteïnes passen d'un estat inactiu a un estat actiu.

1.1.2. CLASSIFICACIÓ DELS GPCRS

1.1.2.1. Classificació tradicional dels GPCRs

Tradicionalment, els GPCRs es divideixen en cinc famílies: la família dels receptors relacionats amb la rodopsina i el receptor β_2-adrenèrgic (família A), la família relacionada amb el receptor de glucagon (família B), la família relacionada amb el receptor metabotròpic (família C) i els receptors de les feromones del llevat (famílies D i E). Dins de la família dels receptors de la rodopsina/β_2 adrenèrgic, que és la família més estudiada, es classifiquen en receptors d'amines biogèniques, receptors de pèptids, receptors d'hormones i receptors de neurotransmissors, en funció del lligand endogen que s'hi uneix (Attwood and Findlay, 1994; Kolakowski, 1994).

1.1.2.2. Classificació filogenètica dels GPCRs del genoma dels mamífers

Molt recentment, a través d'anàlisis filogenètiques s'ha pogut classificar els GPCRs del genoma humà en cinc famílies principals: glutamat, rodopsina, adhesió, frizzled/tas2 i secretina (Fredriksson *et al.*, 2003) (veure FIGURA 2). La família de la rodopsina és la més gran i es classifica en 4 grups i un total de 13 subgrups. D'aquesta manera s'obté una classificació més refinada que l'antiga classificació global. Els membres dins de cada família comparteixen un origen evolutiu comú.

1.1.3. ESTRUCTURA GENERAL DELS GPCRS

La rodopsina bovina és l'únic GPCR que s'ha pogut cristal·litzar fins el moment (Palczewski *et al.*, 2000) a partir de cristal·lografia de raigs X. La rodopsina és única entre els GPCRS ja que el seu lligand, el retinal, es troba covalentment unit a la proteïna. Quan s'absorveix un fotó, a través de l'11-cis–retinal, es produeix la isomerització cap a all-trans-retinal, tot conduint a un canvi conformacional en el receptor que dóna lloc a la seva activació. Fins el moment s'han depositat tres estructures d'alta resolució en el Protein Data Bank a partir dels cristalls de rodopsina basats en mapes de densitat electrònica. La primera estructura (codi d'accés 1F88) es va

poder detallar a 2.8 Å de resolució. Posteriorment es va depositar una estructura més refinada (codi d'accés 1HZX) que incluia residus d'aminoàcids adicionals i cadenes de palmitoil (Teller *et al.*, 2001). L'estructura més recent depositada s'ha pogut detallar a 2.6 Å de resolució (codi d'accés 1L9H) i s'hi corretgeixen les posiscions de les molècules d'aigua (Okada *et al.*, 2002).

Tot i així prèviament a l'obtenció de l'estructura cristal·logràfica de la rodopsina, durant anys s'havien dut a terme diferents aproximacions per tal de proposar models tridimensionals de GPCRs. A través d'estudis de mutagènesi dirigida i d'estructures de baixa resolució obtingudes mitjançant difracció d'electrons s'havia proposat un model que ja preveia les característiques principals de la rodopsina (Baldwin *et al.*, 1997; Unger *et al.*, 1997) (veure FIGURA 3).

L'estructura cristal·logràfica de la rodopsina bovina confirma com l'estructura de la rodopsina i probablement de tots els GPCRs consisteix en un domini N terminal extracel·lular, un domini C terminal citoplasmàtic que conté una hèlix α paral·lela a la membrana cel·lular i set hèlixs α. Aquestes hèlixs transmembràniques (HTMs), aproximadament perpendiculars a la membrana cel·lular, estan connectades per llaços hidrofílics exposats de manera alterna a la part intracel·lular (LIC1, LIC2 i LIC3) i a la part extracel·lular (LEC1, LEC2 i LEC3). A més a més, existeix un pont disulfur entre la HTM3 i LEC2 (Palczewski *et al*., 2000; Teller *et al*., 2001) (veure FIGURA 4).

1.1.4. INFORMACIÓ ESTRUCTURAL A TRAVÉS DE L'ANÀLISIS DE SEQÜÈNCIA DELS GPCRS

La seqüència dels GPCRs revela una diversitat significativa entre els diferents membres de la família. La mida total dels GPCRs varia des de 300 aminoàcids en el cas del receptor de la hormona adrenocorticotrofina fins a 1100 aminoàcids pel receptor de glutamat. La majoria dels llaços extracel·lulars i intracel·lulars són d'entre 10 i 40 aminoàcids de llargada, però el tercer llaç i la regió C terminal intracel·lular pot arrivar a tenir fins a 150 aminoàcids. El domini N terminal extracel·lular pot contenir des de quatre fins a 50 aminoàcids (Mirzadegan *et al.*, 2003; Baldwin *et al*., 1997).

L'anàlisis de seqüència mostra com els receptors de la família de la rodopsina es caracteritzen per una sèrie de residus que es conserven i que es troben distribuits en les set hèlixs transmembràniques (Mirzadegan *et al*., 2003). A la HTM1 hi trobem un residu d'asparagina que es troba conservat en el 100% dels membres de la família de la rodopsina. A la HTM2 hi trobem un residu d'aspàrtic que es troba conservat en un 94%. A la HTM3 hi trobem el motiu conservat Asp-Arg-Tyr, a la HTM5 hi trobem el motiu conservat Phe-XX-Pro-(Ile/Met)-XXX-Tyr-(Ile/Val) i a la HTM 7 hi trobem el motiu molt conservat (Asn/Asp)-Pro-XX-Tyr. També s'han identificat patrons de conservació en els receptors de la família de la secretina però difereixen dels anteriors patrons de conservació (Harmar, 2001). En els receptors de la família de la rodopsina, el domini extracel·lular és el menys conservat, mentre que la zona citoplasmàtica es troba força conservada. La llargada dels llaços també suggereix la importància d'aquests elements en retenir una estructura similar entre els receptors (veure FIGURA 5). Quan s'alineen els patrons de conservació, es mostra una conservació més gran en la part transmembrànica més intracel·lular dels GPCRs, cosa que ens apunta a un mecanisme comú d'activació i de transducció del senyal en els receptors de la família de la rodopsina (Mirzadegan *et al*., 2003) (veure FIGURA 5).

1.1.5. NUMERACIÓ DELS GPCRS

Cada residu es numera amb el número de l'hèlix (de la 1 a la 7) i la seva posició respecte al residu més conservat de l'hèlix en la família dels GPCRs, al qual se li assigna arbitràriament la posició 50 (Ballesteros and Weinstein, 1995). Per exemple, segons aquest esquema el residu més conservat de la HTM 3 (l'Arg en el motiu (D/E)RY) se li assigna el número 3.50 ($Arg^{3.50}$), a l'Asp anterior el 3.49 ($Asp^{3.49}$) i a la Tyr posterior el 3.51 ($Tyr^{3.51}$) (veure FIGURA 6).

1.1.6. UNIÓ DE LLIGANDS ALS GPCRs

S'han dut a terme nombrosos estudis per a identificar els dominis implicats en la unió dels lligands en les diferents subclasses de GPCRs. Els llocs d'unió pels lligands endògens dels receptors de la família de la rodopsina són els més ben caracteritzats

(Kobilka, 1992; Savarese and Fraser, 1992; Strader *et al.*, 1995; Ji *et al*., 1998). No ha estat fins molt recentment que s'ha pogut identificar els llocs d'unió d'altres classes de lligands. Mentre que sembla que els pèptids i les hormones interaccionen amb els dominis extracel·lulars dels seus receptors, les amines biogèniques interaccionen amb el domini transmembrànic dels seus receptors. En aquest treball ens centrarem en l'estudi dels llocs d'unió de les amines biogèniques (veure FIGURA 7) als seus receptors, en particular la serotonina.

1.1.6.1. Amines biogèniques

Els llocs d'unió de les amines biogèniques (dopamina, epinefrina, norepinefrina, serotonina, histamina i acetilcolina) es troben en el domini transmembrànic del receptor. En el receptors de les amines biogèniques, els agonistes i antagonistes s'uneixen a les HTM 3, 5, 6 i 7 en el domini transmembrànic.

L'anàlisis de les seqüències alineades dels GPCRs ha portat a la identificació d'un nombre de residus que es troben altament conservats en les subfamílies de receptors. Utilitzant diferents tècniques com la mutagènesi dirigida, *affinity labeling*, *second site revertant mutations* i el mètode d'accessibilitat de cisteïnes substituïdes s'han anat identificant els llocs d'unió dels lligands.

La interacció més important és un pont salí entre el grup amino carregat dels lligands de les amines biogèniques i la cadena lateral carboxílica de l'$Asp^{3.32}$ (HTM3) (Strader *et al.*, 1991). Concretament, el residu $Asp^{3.32}$, que es troba conservat entre els receptors de les amines biogèniques s'ha trobat que estava implicat en la unió del grup positivament carregat de la dopamina (Mansour *et al.*, 1992), la serotonina (Wang *et al.*, 1993;Ho *et al.*, 1992), la histamina (Gantz *et al.*, 1992) i l'acetilcolina (Spalding *et al.*, 1994) amb els seus respectius receptors (veure FIGURA 7, 8 i 10). En alguns receptors i en alguns tipus de lligands, aquesta interacció amb l'amina protonada es comparteix amb el residu $Ser^{3.36}$ (Almaula *et al.*, 1996). En els receptors colinèrgic i histaminèrgics, la posició 3.40 sembla ser que també està implicat en la unió de lligands i en l'especificitat (Lu and Hulme, 1999; Ligneau *et al.*, 2000).

Molts lligands aminèrgics també formen una interacció important amb residus de la HTM5. Aquests residus de la HTM5 implicats en la unió dels lligands no es troben tant

conservats com l'Asp$^{3.32}$, però les posicions i les interaccions d'aquests residus sembla ser que sí que estan conservats (veure FIGURA 8 i 10). En els receptors de catecolamines la interacció existeix entre els residus Ser$^{5.42}$ i Ser$^{5.46}$ i els grups OH en meta i para dels agonistes de catecolamines, en concret en el rececptor β_2-adrenèrgic (Strader *et al.*, 1989), dopaminèrgic D_1 (Pollock *et al.*, 1992; Cox *et al.*, 1992), α_1-adrenèrgic (Cavalli *et al.*, 1996; Perez *et al.*, 1998) i dopaminèrgic D_2 (Mansour *et al.*, 1992). Utilitzant el mètode d'accessibilitat de cisteïnes substituïdes en el receptor β_2-adrenèrgic i per mutagènesi dirigida, es va trobar que la Ser$^{5.42}$ també estava implicada participava en la unió al grup meta-hidroxil de les catecolamines. A més a més sembla que aquesta Ser$^{5.42}$ juga un paper important en l'agonisme parcial del pindolol. En canvi els antagonistes que no presenten capacitat de formació de ponts d'hidrogen com el propanolol o alprenolol no s'uneixen a la Ser$^{5.42}$(Liapakis *et al.*, 2000). En diversos receptors serotoninèrgics, la Ser$^{5.42}$ i la Thr$^{5.43}$ sembla ser que interaccionen amb els lligands (Roth and Shapiro, 2001; Ho *et al.*, 1992; Johnson *et al.*, 1997). La histamina, a través dels nitrogens de l'imidazol també forma enllaços d'hidrogen i/o interaccions iòniques amb els receptors de la histamina H_1 i H_2: en el rececptor H_2, l'Asp$^{5.42}$ interacciona amb el N^{τ} de la histamina (Gantz *et al.*, 1992), mentre que en el receptor H_1 l'Asn$^{5.46}$ interacciona amb el N^{τ} (Ohta *et al.*, 1994; Moguilevsky *et al.*, 1995; Leurs *et al.*, 1994). En el receptor H_2, la Thr $^{5.46}$ interacciona amb el N^{π} de la histamina a través d'un enllaç d'hidrogen (Gantz *et al.*, 1992). La diferent afinitat per la mesulergina entre el receptor $5HT_{2A}$ humà i de rata és a causa de la Ser$^{5.46}$ que es troba substituïda per una Ala (Kao *et al.*, 1992), i la diferència d'afinitats entre els receptors $5HT_{2A}$ i $5HT_{2C}$ per a aquest fàrmac prové de la substitució de la posició 5.46 (Almaula *et al.*, 1996). Es pensa que aquesta Ser forma un enllaç per pont d'hidrogen amb el nitrogen N-1 de les triptamines i ergolines no substituïdes (Roth and Shapiro, 2001). En el receptor muscarínic M_1, l'Ala$^{5.46}$ també està implicada en la unió d'agonistes (Allman *et al.*, 2000).

El clúster de residus aromàtics a la HTM6 es troba molt conservat entre els receptors de les amines biogèniques i inclou els residus: Trp$^{6.48}$, Phe/Tyr$^{6.51}$ i Phe$^{6.52}$. S'ha trobat que aquests residus estan implicats en la unió de lligands i/o amb l'activació en molts receptors de les amines biogèniques (Choudhary *et al.*, 1993; Heitz *et al.*, 1999; Wess *et al.*, 1991; Javitch *et al.*, 1998; Roth *et al.*, 1997; Cho *et al.*, 1995)(veure FIGURA 9 i 10). Els lligands endògens dels receptors colinèrgics, que no contenen cap anell

aromàtic, presenten una Asn a la posició 6.52 i la mutació d'aquest residu també porta a l'impediment de l'unió d'agonistes i antagonistes (Heitz *et al.*, 1999; Huang *et al.*, 1999; Ward *et al.*, 1999), fet que afirma la interacció amb aquesta posició. El residu $Phe^{6.51}$ interacciona amb l'anell de catecol de l'epinefrina i l'$Asn^{6.55}$ també forma un enllaç d'hidrogen amb l'epinefrina en els receptors β_2-adrenèrgics (Wieland *et al.*, 1996).

A la HTM7, el $Trp^{7.40}$ es troba totalment conservat en tots els receptors de les amines biogèniques i s'ha trobat que en els receptors 5-HT_{2A} i β_1-adrenèrgic interacciona amb antagonistes (Wong *et al.*, 1988; Roth *et al.*, 1997) (veure FIGURA 9 i 10).

El fet que els principals residus implicats en la unió als receptors de les amines biogèniques es trobin conservats, indica que malgrat que els lligands són estructuralment molt diferents, l'evolució ha conservat alguns mecanismes bàsics d'unió dels lligands als receptors i probablement un mecanisme comú d'activació del receptor induïda pels lligands. Tot i així, fins i tot dins de la família de les amines biogèniques caldrà tenir en compte les interaccions específiques de cada tipus de lligand endogen o exogen ja que seran els que aportaran la selectivitat davant dels altres receptors de la família de les amines biogèniques.

1.1.7. ACTIVACIÓ DELS GPCRs

1.1.7.1. Activitat constitutiva dels receptors

Diversos GPCRs quan s'expressen en línies cel·lulars recombinants presenten una resposta cel·lular. Això és degut a que el receptor pot adoptar la conformació activa en absència de l'agonista utilitzant l'energia cinètica per a canviar reversiblement de l'estat inactiu a l'estat actiu (activitat constitutiva). En diversos GPCRs, la mutació d'un sol aminoàcid pot ésser capaç de provocar un augment important d'aquesta activitat constitutiva en absència de l'agonista (Scheer *et al.*, 1996a; Allen *et al.*, 1991; Kjelsberg *et al.*, 1992; Samama *et al.*, 1993). Les mutacions que fan que el receptor sigui constitutivament actiu s'han identificat en gairebé tots els dominis dels receptors. Aquest augment de l'activitat indica que les mutacions que provoquen una activació

constitutiva inadequada poden ser factors etiològics en malalties; moltes d'aquestes mutacions constitutivament actives s'han associat a malalties genètiques (Parma *et al.*, 1993; Parma *et al.*, 1995; Duprez *et al.*, 1997; Rao *et al.*, 1994; Shenker *et al.*, 1993).

Una de les implicacions més importants de l'activitat constitutiva pels farmacòlegs i químics mèdics és la possibilitat de desenvolupar fàrmacs que disminueixin el nivell d'activitat constitutiva. Aquests compostos que s'han anomenat "agonistes inversos", tindrien en teoria efectes fisiològics diferents i possiblement un potencial terapèutic diferent que els efectes dels clàssics antagonistes competitius (antagonistes neutrals).

1.1.7.2. Mecanismes moleculars implicats en l'activació dels receptors

S'ha proposat que el que manté el receptor en l'estat inactiu són les interaccions intermoleculars dins del receptor que restringeixen el moviment de certs dominis. Aquestes restriccions del moviment s'alliberarien quan l'agonista interaccionés amb el receptor. Els canvis mutacionals trenquen les interaccions intramoleculars estabilitzadores de l'estat inactiu, permetent al receptor d'arribar fins a l'estat actiu (Kjelsberg *et al.*, 1992).

Les HTM3, HTM6 i HTM7 es consideren l'estructura del nucli de l'activació dels GPCRs (Okada *et al.*, 2001; Meng and Bourne, 2001; Ballesteros *et al.*, 2001b; Lu *et al.*, 2002). S'ha proposat que l'empaquetament d'aquestes tres hèlixs afavoreix la conformació de l'estat inactiu, mentre que l'alliberament d'aquestes restriccions intrahelicals produeix un estat del receptor relaxat amb tendència a l'activació (Kjelsberg *et al.*, 1992; Porter *et al.*, 1996).

Estudis basats en ressonància paramagnètica electrònica, espectroscopia de fluorescència, alteracions en l'accessibilitat de cisteïnes i enginyeria d'unió de metalls, apunten conjuntament a un paper clau en el canvi de les conformacions de les HTM3 i HTM6 per a l'activació del receptor (Farrens *et al.*, 1996; Sheikh *et al.*, 1996; Gether *et al.*, 1997; Javitch *et al.*, 1997; Rasmussen *et al.*, 1999; Jensen *et al.*, 2001). S'ha proposat que la protonació de l'$Asp^{3.49}$ en el motiu conservat (D/E)RY de la HTM3, que es troba en el costat citoplasmàtic, porta a l'alliberament de les restriccions de les interaccions intramoleculars tot portant al moviment de la HTM3 i HTM6 i a la conversió del receptor a l'estat actiu. Aquesta hipòtesi ha estat recolzada ja que les

mutacions que neutralitzen la càrrega de Asp/Glu$^{3.49}$ a la HTM3 portaven a un increment de l'activació independent de l'agonista d'alguns GPCRs (Rasmussen *et al*., 1999; Arnis *et al.*, 1994; Scheer *et al.*, 1996b). Recentment s'ha proposat que en l'estat inactiu l'Arg$^{3.50}$ a més a més d'interaccionar amb l'Asp$^{3.49}$ també interacciona amb el residu conservat Glu$^{6.30}$ que es troba a l'extrem citoplasmàtic de la HTM6 i que aquesta interacció contribueix a mantenir el receptor en l'estat inactiu; a més a més l'alta conservació d'aquests residus apunta que aquest mecanisme pot ser comú pels GPCRs de la família de la rodopsina (Ballesteros *et al.*, 2001a). També s'ha proposat que un clúster de residus aromàtics a la HTM6, que a més a més està implicat en l'unió d'agonistes d'alguns GPCRs, promouria l'activació del receptor ja que portarien al moviment de l'extrem citoplasmàtic de la HTM3 lluny de la HTM6 (Shi *et al.*, 2002).

A través d'experiments de mutagènsi dirigida i d'estudis de modelització molecular, també s'ha identificat en el receptor TSH una interacció entre Asp$^{6.44}$ i l'Asn$^{7.49}$ que és important per a poder mantenir l'estat inactiu a través d'una restricció en la conformació de la cadena lateral de l'Asn$^{6.44}$. Després de l'activació del receptor la cadena lateral de l'asparagina adoptaria la conformació lliure que implicaria una interacció amb el motiu N$^{1.50}$-D$^{2.50}$. És així, que el trencament d'aquesta interacció porta a l'activació constitutiva del receptor (Govaerts *et al.*, 2001b).

1.1.7.3. Visió clàssica de l'activació dels receptors

La farmacologia clàssica dels receptors emfatitza la necessitat de la interacció d'un agonista amb l'estat inactiu del receptor per a produir l'estimulació del receptor, com per exemple l'estimulació del sistema de transducció de senyal intracel·lular o l'obertura d'un canal iònic. La teoria clàssica de l'estimulació del receptor implica que l'estat inactiu del receptor és favorable termodinàmicament i que la interacció del receptor amb l'agonista proporciona certa quantitat d'energia d'activació, necessària per a vèncer la barrera termodinàmica per a l'activació. Així doncs, el model clàssic del receptor només prediu una conformació termodinàmicament estable que és inactiva i que requereix la interacció d'un agonista per a proporcionar l'energia per a empènyer el receptor a la conformació activa

Tot i així, els receptors són proteïnes en un entorn de membrana dinàmic, i així s'espera que siguin capaces d'adoptar varies conformacions espontàniament. La quantitat de

temps que el receptor passa en aquestes conformacions depèn de la seva estabilitat termodinàmica i de l'energia cinètica disponible per empènyer el receptor a passar d'un estat a un altre.

Si l'activitat constitutiva dels GPCRs és un fenomen comú, tal i com alguns investigadors sospiten, això suggeriria que calen alteracions en el model clàssic de la interacció lligand-receptor.

1.1.7.4. El model del complex ternari estès

Segons el model del complex ternari estès (Samama *et al*., 1993) i el model del complex ternari cúbic (Weiss *et al.,* 1996), el receptor existeix en equilibri entre l'estat inactiu R i l'estat actiu R* en absència del lligand. Aquest equilibri, que serà diferent per a cada receptor, determina l'activitat basal. Pels receptors natius, predomina l'estat R i hi pot haver una certa activitat del receptor en absència de l'agonista degut a la població de receptors en la forma R* (veure FIGURA 11).

Quan l'agonista s'uneix al receptor estabilitza l'estat R* causant l'acoblament de la proteïna G i l'activació de les respostes cel·lulars. Els nivells alts d'expressió del receptor o receptors mutants constitutivament actius augmenten la concentració de R* tot induint certa resposta en absència de l'agonista. En algunes malalties s'hi ha trobat la implicació de les mutacions puntuals que passen naturalment i que donen lloc a l'activació constitutiva dels GPCRs.

L'activitat constitutiva dels GPCRs va suggerir el concepte d'agonista invers (Barker *et al.,* 1994; Chidiac *et al.,* 1994; Bond *et al.,* 1995). Els agonistes inversos són fàrmacs que s'uneixen i estabilitzen R tot inhibint l'activitat basal del receptor. En canvi, els antagonistes s'uneixen igualment a R i R*, i no tenen cap efecte sobre l'activitat basal del receptor, però bloquegen l'efecte dels agonistes i agonistes inversos. De fet, molts fàrmacs que s'havien considerat antagonistes, posteriorment es va trobar que tenien activitat agonista inversa (Chidiac *et al*., 1994). Es creu que els agonistes inversos poden tenir utilitat terapèutica en el marc dels receptors mutants constitutivament actius (Teitler *et al.,* 2002).

1.1.7.5. La interacció amb la proteïna G

En el seu domini intracel·lular els GPCRs poden interaccionar amb una proteïna que es troba a la membrana anomenada proteïna G, que és una proteïna que uneix nucleòtids de guanidina. Aquesta proteïna consisteix en tres subunitats heterotrimèriques: α, β, γ. En funció de la seva homologia de seqüència les subunitats G_α es poden classificar en quatre sugrups principals: α_s, $\alpha_{i/o}$, α_{q11} i α_{12} (Simon *et al.*, 1991). Quan un lligand interacciona amb el receptor, la conformació activa provoca que el receptor interaccioni amb la proteïna G en el seu domini intracel·lular, tot formant el complex ternari lligand-receptor-proteïna G que provoca l'intercanvi de GDP a GTP en la subunitat α de la proteïna G. Aquest intercanvi afavoreix la divisió de la proteïna heterotrimèrica en les subunitats α i $\beta\gamma$; tant el GTP unit a la subunitat α com el dímer $\beta\gamma$ poden modular diferents sistemes efectors que donen lloc a la resposta cel·lular com l'estimulació o inhibició de l'adenilat ciclasa, l'activació de fosfolipases o la regulació de l'activitat de canals de calci i potassi. A continuació, la subunitat α, que té activitat GTP-assa, hidrolitza el GTP a GDP, tot tornant altra vegada a l'estat inactiu (veure FIGURA 12).

1.1.8. DIVERGÈNCIES ESTRUCTURALS ESPECÍFIQUES DELS GPCRS

La gran riquesa de seqüències, lligands i dades de mutacions disponibles contrasta amb la poca quantitat d'informació estructural actual, ja que només es coneix l'estructura de la rodopsina bovina. La manca d'informació estructural ha portat al desenvolupament d'estudis de modelització. La rodopsina bovina és un bon patró per a la modelització per homologia des GPCRs. Tot i així la rodopsina no és el patró perfecte per a tots els GPCRs.

La seqüència de tots els GPCRs es troba conservada en la zona transmembrànica, cosa que ens fa pensar que hi haurà una gran similitud estructural en aquesta regió. Això permet utilitzar l'estructura tridimensional de la regió transmembrànica de la rodopsina bovina per a modelitzar altres GPCRs. Tot i així, la necessitat d'unir de forma específica una gran diversitat de lligands en la regió extracel·lular fa pensar en l'existència de característiques estructurals diferenciades i específiques per a cada

receptor particular. Per a desenvolupar models específics de GPCRs caldrà, doncs, tenir en compte aquestes divergències estructurals característiques de cada GPCR.

1.2 . ELS RECEPTORS DE SEROTONINA

1.2.1. LA SEROTONINA

La serotonina (5-hidroxitriptamina) és un dels principals neurotransmissors en animals, tant en vertebrats com en invertebrats (Tierney, 2001) (veure FIGURA 13). En el sistema nerviós central, la serotonina (5-HT) està implicada en diversos processos, com la regulació del comportament alimentari, l'estat d'ànim, la percepció, l'ansietat, l'agressivitat i el dolor (Roth *et al.*, 2000; Roth and Shapiro, 2001). En teixits no neuronals, la 5-HT també juga diferents papers, com en el creixement i la contractació del múscul llis i en l'agregació de plaquetes (Roth and Shapiro, 2001; Roth *et al*., 2000).

En els mamífers, la funció de la 5-HT està regulada a través de la interacció amb set classes de receptors de serotonina (5-HT_1, 5-HT_2, 5-HT_3, 5-HT_4, 5-HT_5, 5-HT_6 i 5-HT_7). Sis d'aquests receptors són GPCRs i un, el receptor 5-HT_3, és un canal iònic (Roth *et al*., 1997). Els sis GPCRs de serotonina es divideixen en 13 tipus de receptors, basats en la seqüència i la similitud farmacològica. L'eficàcia d'un gran nombre de fàrmacs es basa, almenys parcialment, en la seva habilitat per a interaccionar o modular l'activitat d'aquests receptors de 5-HT. Entre els fàrmacs que interaccionen amb els receptors de serotonina s'hi troben aquells per a tractar l'esquizofrènia, la depressió, la migranya, l'obesitat i l'ansietat (Roth *et al*., 2000; Roth, 1994).

1.2.2. EL RECEPTOR 5-HT_{1A}

En els últims anys les aplicacions d'aquests lligands en processos fisiològics i fisiopatològics dels sistemes nerviós central i perifèric han rebut una particular atenció: el paper que desenvolupa el receptor 5-HT_{1A} en el control de l'ansietat (Menard and Treit, 1999) i de la depressió (Haddjeri *et al.*, 2000), així com la seva acció en el sistema cardiovascular (Yildiz *et al.*, 1998). Per altra banda, s'ha observat que certs

processos degeneratius estan sota el control, entre altres, del receptor 5-HT_{1A}, fet que ha portat a suggerir la utilitat clínica dels compostos amb afinitat pel receptor en el tractament de diverses malalties neurològiques, incloent-hi l'esquizofrènia (Bantick *et al.*, 2001). A més a més, estudis recents indiquen que els agonistes del 5-HT_{1A} podrien exercir efectes neuroprotectors a les neurones hipocampals i corticals, i ser, per tant, útils en el tractament de l'infart cerebral agut (Semkova *et al.*, 1998).

1.2.3. EL RECEPTOR 5-HT_4

El receptor 5-HT_4 es troba al sistema nerviós central (Dumuis *et al.*, 1988), al cor (Kaumann, 1990), a l'intestí (Craig and Clarke, 1990) i a la bufeta (Tonini and Candura, 1996). A través de l'activació d'aquest receptor es modulen processos fisiològics tant importants com l'alliberament de l'acetilcolina a l'hipocamp (Siniscalchi *et al.*, 1999), l'augment de Ca^{+2} i el curs del marcapassos (Ouadid *et al.*, 1992), la iniciació del reflex peristàltic intestinal (Craig and Clarke, 1990) i l'augment de l'alliberació del corticosterol a la glàndula adrenal (Idres *et al.*, 1991). És per això que el mal funcionament del receptor 5-HT_4 està implicat en una gran varietat de desordres patològics i per tant aquesta proteïna és una important diana pel disseny de nous fàrmacs.

1.2.4. EL RECEPTOR 5-HT_7

El receptor $5HT_7$ es troba principalment al sistema nerviós central, encara que també el podem trobar al sistema nerviós perifèric i es troba acoplat positivament a l'adenilat ciclasa (Heidmann *et al.*, 1997). Es creu que el receptor 5-HT_7 està implicat en la regulació del ritme circadià (Lovenberg *et al.*, 1993), la depressió (Yau *et al.*, 1997) i la relaxació del múscul llis (Terron and Falcon-Neri, 1999); tot i així el seu paper patofisològic encara no està del tot resolt. El disseny de lligands selectius agonistes i antagonistes seran d'una gran utilitat per tal d'elucidar en quins mecanismes patològics es troba implicat el receptor 5-HT_7.

El coneixement de l'estructura tridimensional dels diferents GPCRs i la identificació dels llocs d'unió ens permetria fer el disseny racional de fàrmacs a la carta, és a dir, dissenyar agonistes, antagonistes o agonistes parcials que interaccionessin amb un o diversos tipus de receptors en funció de la patologia. És per això que aquesta tesi té com a objectiu principal la construcció de models tridimensionals pels GPCRs i en especial pels receptors de serotonina degut a la seva implicació en diferents patologies d'una gran importància en la nostra societat actual.

- → En aquesta tesi es pretén desenvolupar un model tridimensional pel receptor 5-HT_{1A} utilitzant les eines de modelització molecular i el disseny racional de fàrmacs com a eina de validació, es vol identificar quins són els llocs d'unió dels lligands dins del receptor 5-HT_4 mitjançant la modelització molecular i les dades de mutagènesi dirigida i es vol construir un model d'interacció entre el 5-HT_7 i els seus antagonistes.

Els models desenvolupats en aquest treball van acompanyats d'experiments per tal de validar-los i completar-los. Tot el treball experimental l'ha dut a terme el grup de la Dra. M Luz López-Rodríguez de la Universitat Complutense de Madrid.

1.3. ESTRUCTURA SECUNDÀRIA DELS RECEPTORS ACOBLATS A PROTEÏNA G

1.3.1. LES HÈLIX α

Les hèlixs α són l'element estructural més important de les proteïnes de membrana i com s'ha vist anteriorment, els GPCRs estan formats per set hèlixs α (Fasman, 1989; White and Wimley, 1999). Les hèlixs α presenten uns 3.6 residus a cada volta i una mitjana dels angles diedres Φ_i i Ψ_i de -62 i -41^o respectivament que determinen l'estructura de l'esquelet polipeptídic (Barlow and Thornton, 1988). L'estabilitat de l'hèlix α ve donada per enllaços per pont d'hidrogen entre els grups NH del residu en la posició i i els oxígens carbonílics del residu en la posició i-4 de la volta anterior de l'hèlix (veure FIGURA 15). En proteïnes transmembràniques, com els GPCRs, la formació d'aquesta xarxa d'enllaços d'hidrogen permet que l'esquelet del polipèptid polar s'estengui a través de la bicapa lipídica de la cèl·lula (White and Wimley, 1999).

1.3.2. EFECTE DE L'ENTORN EN LA CONFORMACIÓ DE LES HÈLIXS α

Una anàlisi estadística pionera va revelar que les hèlixs α de proteïnes globulars poden formar un enllaç d'hidrogen addicional entre l'oxigen carbonílic del pèptid i una molècula d'aigua (Blundell *et al.*, 1983); la formació d'aquests enllaços d'hidrogen addicionals produirien un allargament de la distància i una pèrdua de linealitat de l'enllaç d'hidrogen intrahelical, tot produint canvis significatius en els angles diedres Φ_i i Ψ_i i induint una curvatura de l'hèlix. Sembla raonable de suposar que en un entorn hidrofòbic com el que es presenta en proteïnes de membrana, en no haver-hi molècules de solvent hidrofíliques, aquest enllaç d'hidrogen addicional no es podrà formar. En conseqüència s'espera trobar diferències entre les estructures de les hèlixs α de proteïnes globulars i de membrana.

- → Per tal de desenvolupar els models tridimensionals dels GPCRs, en aquest treball s'ha volgut explicitar l'entorn hidrofòbic en el que es troba immersa la seva regió transmembrànica. Així doncs, la primera part de la tesi ha consistit en l'estudi de la influència de l'entorn en la geometria de les hèlixs transmembràniques

- → Per altra banda s'ha volgut esbrinar quines són les diferències estructurals entre les hèlixs α de proteïnes globulars i de membrana com a conseqüència de la modificació d'aquesta xarxa d'enllaços intrahelicals.

1.3.3. RESIDUS QUE INFLUEIXEN EN L'ESTRUCTURA DE LES HÈLIXS α

1.3.3.1. L'efecte de les serines i les treonines en les conformacions de les hèlixs α

Com a conseqüència de la presència d'un grup hidroxil en la seva cadena lateral (veure FIGURA 16), els residus de serina i treonina en hèlixs α formen enllaços d'hidrogen intrahelicals addicionals entre la seva cadena lateral i l'oxigen del carbonil en la posició i-3 o i-4 de la volta anterior (Attwood *et al.*, 2002; Gray and Matthews, 1984) (veure FIGURA 17). Aquest enllaç d'hidrogen intrahelical pot produir canvis en la curvatura de les hèlixs α. De fet la situació és semblant a la distorsió que es produeix en les hèlixs α en un entorn hidrofílic.

1.3.3.2. L'efecte de les prolines en la conformació de les hèlixs α de proteïnes de membrana

La prolina és un altre residu que indueix distorsions en les hèlixs α ja que la seva cadena lateral introdueix una distorsió local, anomenada Pro *kink*, per tal d'evitar el xoc estèric entre l'anell de pirrolidina i l'oxigen del carbonil en i-4 (Barlow and Thornton, 1988; Sankararamakrishnan and Vishveshwara, 1992; Stables *et al.*, 1997; von Heijne, 1991) (veure FIGURA 18 i FIGURA 19). El Pro *kink* dóna flexibilitat a l'esquelet carbonat degut a l'absència de l'enllaç d'hidrogen intrahelical amb l'oxigen del carbonil de la volta anterior. La flexibilitat estructural és un element funcional molt important en les proteïnes de membrana ja que permet la transmissió dels senyals

extracel·lulars a través de canvis conformacionals en les hèlixs transmembràniques (Gether, 2000; Govaerts *et al.*, 2001a; Sansom and Weinstein, 2000).

→ En aquest treball s'ha estudiat l'efecte del Pro *kink* de les hèlixs α de proteïnes de membrana.

2. RESUM GLOBAL DELS RESULTATS

2.1. INTRODUCCIÓ

Els resultats d'aquesta tesi es divideixen en cinc parts que intenten fer un pas més en l'entesa de l'estructura i la funció del GPCRS.

(i) el desenvolupament d'un mètode computacional que permeti reproduir les condicions i característiques de l'entorn hidrofòbic de la regió transmembrànica de les proteïnes de membrana.

(ii) la construcció de models tridimensionals pel receptor 5-HT_{1A} utilitzant el mètode computacional desenvolupat i mitjançant tècniques de modelització per homologia que tinguin en compte els motius estructurals característics del receptor estudiat. Els models teòrics s'han validat mitjançant la el disseny, la síntesi i l'avaluació farmacològica de dos lligands que interaccionen amb el receptor 5-HT_{1A}.

(iii) el disseny de lligands agonistes selectius al receptor 5-HT_{1A} sense afinitat pel receptor α_1-adrenèrgic

(iv) la identificació dels llocs d'unió del lligand GR113808 amb el receptor 5-HT_4 a través de les simulacions de dinàmica molecular i l'estudi dels valors experimentals de mutagènesi dirigida.

(v) la construcció d'un model d'interacció entre el receptor 5-HT_7 i els seus antagonistes.

La síntesi i l'avaluació farmacològica dels lligands l'ha dut a terme el grup de la Dra. M. Luz López-Rodríguez de la Universitat Complutense de Madrid.

2.2. L'EFECTE DE L'ENTORN EN LA CONFORMACIÓ DE LES HÈLIXS α

Els GPCRs són proteïnes de membrana i per tant la seva regió transmembrànica es troba en un entorn hidrofòbic. Un estudi ja havia apuntat que l'aigua era capaç de corbar les hèlixs α en les proteïnes globulars. Per tant era possible que es poguessin

trobar diferències entre la conformació de les hèlixs α de proteïnes de membrana i les hèlixs α de proteïnes globulars.

A partir d'una base de dades d'hèlixs α de proteïnes cristal·litzades globulars i de membrana, es van classificar els residus d'aquestes hèlixs α en tres grups en funció de la polaritat del seu entorn: a) residus de proteïnes globulars exposats a l'aigua, b) residus de proteïnes globulars i residus de proteïnes de membrana que es troben en el cor de la proteïna i c) residus de proteïnes de membrana exposats als lípids.

Si es comparen certs paràmetres geomètrics dels diferents grups obtinguts mitjançant una anàlisi estadística (veure TAULA 1) trobem que:

- ✓ com més polar és l'entorn disminueix el valor de Φ i augmenta i el valor de Ψ (veure article 1)
- ✓ com més polar és l'entorn, augmenta la distància i disminueix l'angle de l'enllaç d'hidrogen intrahelical entre l'O carbonílic i els grup NH de l'esquelet carbonat (veure article 1).

Així doncs, sembla que la polaritat de l'entorn condiciona la conformació de les hèlixs α.

2.3. DESENVOLUPAMENT DE LA CAIXA DE METANS COM A MODEL DEL COR HIDROFÒBIC DE LES MEMBRANES LIPÍDIQUES

Tenint en compte que la polaritat de l'entorn és capaç d'afectar la conformació de les hèlixs α (Blundell *et al*., 1983), s'ha desenvolupat un mètode on s'expliciti l'entorn apolar en el que es troben les proteïnes de membrana per tal de modelitzar i dur a terme simulacions de dinàmica molecular dels GPCRs.

Tradicionalment, moltes simulacions de dinàmica molecular es fan sense tenir en compte un entorn explícit. Això requereix la definició de restriccions artificials de la geometria del sistema que podrien distorsionar els resultats. Per altra banda, els GPCRs es troben atravessant la bicapa lipídica, és a dir, la seva regió transmembrànica es troba en un entorn apolar; per tant si es vol tenir en compte explícitament l'efecte de l'entorn,

les simulacions de dinàmica molecular s'haurien de fer en un model teòric de bicapa lipídica. Degut a que les simulacions de dinàmica molecular en una bicapa lipídica comporta un gran cost computacional i degut a la naturalesa empírica dels models, s'ha optat per usar una metodologia simplificada on les molècules de metà representen l'entorn apolar del cor de la membrana.

Per tal de validar el mètode desenvolupat, es van dur a terme simulacions de dinàmica molecular de 1 nanosegon d'hèlixs α model en un entorn de metans per a simular la regió transmembrànica de les hèlixs α de proteïnes de membrana i també es van dur a terme simulacions de dinàmica molecular d'hèlixs α en un entorn d'aigües per a reproduir l'entorn hidrofílic en el que es troben les hèlixs α de les proteïnes globulars. Els resultats mostren com:

- ✓ les simulacions de dinàmica molecular en un entorn de metans i en un entorn d'aigües reprodueixen els valors trobats (Φ i Ψ i la distància i l'angle de l'enllaç d'hidrogen) d'estructures cristal·lines de proteïnes de membrana i de proteïnes globulars respectivament (veure TAULA 1) (veure article 1).
- ✓ es troba que les hèlixs α de proteïnes de membrana són menys flexibles que les hèlixs α de proteïnes globulars degut a que l'enllaç d'hidrogen intrahelical és més fort (veure article 1).
- ✓ en les simulacions de dinàmica molecular d'hèlixs α en un entorn d'aigües es veu com les molècules d'aigua són capaces de formar un enllaç d'hidrogen entre el seu oxigen i el grup NH de l'esquelet carbonat tot afeblint l'enllaç d'hidrogen intrahelical i produint canvis en Φ i Ψ (veure FIGURA 20) (veure article 1).

La capacitat de les simulacions de dinàmica molecular en un entorn de metans i en un entorn d'aigua per a reproduir els paràmetres de les proteïnes globulars i les proteïnes de membrana mostren la importància de tenir en compte explícitament l'entorn per a fer simulacions de dinàmica molecular i la capacitat d'aquesta metodologia per a reproduir els paràmetres estructurals de les hèlixs α.

2.4. L'EFECTE DE LA PROLINA EN LA CONFORMACIÓ DE LES HÈLIXS α

La prolina indueix distorsions en les hèlixs α ja que introdueix una distorsió local anomenada Pro *kink* . S'ha estudiat si les simulacions de dinàmica molecular d'hèlixs α en un entorn de metans són capaces de reproduir les distorsions estructurals provocades pel Pro *kink*.

Es van comparar els angles diedres Φ i Ψ de la regió dels Pro *kinks* en proteïnes de membrana cristal·litzades i de la regió del Pro *kink* fruit de les simulacions de dinàmica molecular.

- ✓ Les simulacions de dinàmica molecular d'hèlixs α en un entorn de metans amb una prolina en la seva seqüència reprodueixen la geometria del Pro *kink* que trobem a les estructures cristal·lines de proteïnes de membrana, tot indicant que les simulacions de dinàmica molecular en un entorn de metans és capaç de reproduir el comportament conformacional de les deformacions helicals (veure FIGURA 21) (veure article1).

El fet que les simulacions de dinàmica molecular siguin capaces de reproduir les deformacions helicals és important ja que la flexibilitat que aporta el Pro kink es creu que està relacionada amb el procés de tranducció de senyal a través de les hèlixs transmembràniques.

Així doncs, s'ha trobat un model per a reproduir l'entorn hidrofòbic de la regió transmembrànica de les proteïnes de membrana així com les deformacions helicals; aquest mètode es podrà utilitzar per a estudiar d'una manera simplificada els GPCRs en el seu entorn de la bicapa lipídica.

2.5. MODES D'UNIÓ DELS RECEPTORS DE SEROTONINA AMB ELS SEUS LLIGANDS

La gran homologia de seqüència entre els diferents receptors de serotonina, especialment en la seva zona transmembrànica, fa que els receptors de serotonina presentin patrons comuns d'interacció amb els seus lligands, ja que els principals residus responsables de la interacció amb els lligands es troben conservats. Tot i així, petits canvis en aquests residus o en altres residus pròxims al lloc d'unió del lligand causen variacions en el mode d'unió que a la vegada permeten el fet que hi hagi lligands selectius que s'uneixin a uns o altres receptors de serotonina.

Si ens fixem en la seqüència dels receptors de serotonina, en les estructures dels seus lligands i en els modes d'interacció descrits a la Bibliografia, es troben mecanismes d'interacció comuns entre els diferents receptors de serotonina i els seus lligands. A continuació es presenta un esquema on s'intenta relacionar les seqüencies d'aquests receptors amb els grups funcionals dels seus lligands.

2.5.1. Residus de la HTM3 implicats en la unió dels lligands

A la HTM3 hi trobem el residu $Asp^{3.32}$ que és el responsable d'interaccionar amb una càrrega positiva dels lligands, normalment amb una amina protonada. El fet que aquest residu es trobi conservat en tots els receptors de serotonina, preveu que les característiques d'aquesta zona del lligand pugui ser comuna per a tots els receptors de serotonina (veure FIGURA 22).

2.5.2. Residus de la HTM5 implicats en la unió dels lligands

Una altra interacció és entre grups acceptors de pont d'hidrogen dels lligands i residus de Ser i Thr de la HTM5. Si ens fixem en la seqüència de la HTM5 dels receptors de serotonina, veiem com hi ha tres patrons diferents de conservació d'aquests residus amb capacitat de formar ponts d'hidrogen (veure FIGURA 23):

(i) El receptors 5-HT_{1A}, 5-HT_{1B}, 5-HT_{1D}, 5-HT_{1E}, 5-HT_{1F}, 5-HT_{5A}, 5-HT_{5B} i 5-HT_7 presenten un residu de Ser a la posició 5.42 i un residu de Thr a la

posició 5.43. Per a tots aquests receptors, la part del lligand responsable d'interaccionar amb la HTM5 haurà de presentar 1 o 2 grups funcionals amb capacitat acceptora de pont d'hidrogen. És així que trobem grups carbonil i hidroxil en els seus lligands.

(ii) Els receptors 5-HT_{2A} i 5-HT_6 presenten una Ser a la posicó 5.43 i un residu de Ser o Thr a la posicó 5.46, aquests són responsables d'interaccionar amb grups acceptors de pont d'hidrogen. En els seus lligands sovint hi trobem grups sulfonils.

(iii) Els receptors 5-HT_{2B}, 5-HT_{2C} i 5-HT_4 presenten només un residu de Ser a la posició 5.43. Aquesta Ser interaccionarà amb un grup acceptor de pont d'hidrogen. Els seus lligands normalment presenten un grup carbonil.

Les petites diferències en la capacitat del nombre de ponts d'hidrogen possibles així com les petites variacions en la posició d'aquests residus marcarà petites diferències en els requeriments d'aquests grups acceptors de pont d'hidrogen. Altres residus com la $Thr^{3.29}$ en els receptors 5-HT_{2A}, 5-HT_{2B}, 5-HT_{2C}, 5-HT_4 i 5-HT_6 o la $Thr^{3.37}$ en tots els receptors de serotonina podrien col·laborar amb aquesta interacció per pont d'hidrogen si és que la distància entre els grups funcionals ho permet.

A la HTM5 també hi trobem el residu aromàtic totalment conservat $Phe^{5.47}$ (veure FIGURA 23) que serà responsable d'interaccionar amb anells aromàtics adjacents als grups acceptors de l'enllaç per pont d'hidrogen comentats anteriorment.

2.5.3. Residus de la HTM6 implicats en la unió dels lligands

La regió aromàtica que interacciona amb la $Phe^{5.47}$ queda afavorida per la interacció amb la $Phe^{6.52}$ que es troba totalment conservada en tots els receptors de serotonina (veure FIGURA 23 i 24). El residu $Phe^{6.51}$ que es troba totalment conservat interacciona amb l'anell de piperidina, comú en molts lligands de serotonina (veure FIGURA 24).

Una de les posicions que és important de cara a la selectivitat és la posició 6.55, que es troba molt pròxima al lloc d'unió del lligand i que a més a més presenta una gran diversitat (veure FIGURA 24):

(i) En els receptors 5-HT_{2A}, 5-HT_{2B}, 5-HT_{2C}, 5-HT_4 i 5-HT_6 hi trobem el residu $Asn^{6.55}$ que interacciona amb un grup acceptor de pont d'hidrogen com els motius -CONH- o $–NHSO_2$-.

(ii) Els receptors 5-HT_{1B}, 5-HT_{1D} i 5-HT_7 presenten un residu de Ser, és a dir, que també presenten capacitat de formar pont d'hidrogen.

(iii) En aquesta mateixa posició, els receptors $5HT_{1E}$, 5-HT_{1F}, 5-HT_{5A}, $5HT_{5B}$ presenten un residu de glutàmic i per tant els seus lligands podran presentar un motiu amb densitat de càrrega positiva.

2.5.4. Residus de la HTM7 implicats en la unió dels lligands

A la HTM7 hi trobem la $Tyr^{7.43}$ i el $Trp^{7.40}$ que podran interaccionar amb motius aromàtics adjacents a la càrrega positiva dels lligands. Aquest residu es troba totalment conservat en els receptors de serotonina. La presència d'un motiu aromàtic en aquesta zona del lligand quedaria reforçada amb la interacció amb la posició 3.28, on hi trobem un residu aromàtic (Phe o Trp) en tots els receptors de serotonina, excepte en el receptor 5-HT_4 (veure FIGURA 25).

La HTM7 és important perquè s'hi troben molts residus que s'han identificat que estan implicats en la unió a lligands i que a més a més són característics de cada receptor. En el receptor 5-HT_{1A} hi trobem l'$Asn^{7.39}$ que interacciona amb el motiu $NHSO_2Et$ present en lligands agonistes selectius a aquest receptor. La presència d'aquest residu característics del receptor 5-HT_{1A} és molt important per a conferir selectivitat a aquest lligand.

A partir dels residus dels receptors de serotonina descrits responsables d'unir lligands es podrà modelitzar el mode d'unió dels lligands de serotonina. L'entesa del mode d'unió dels lligands així com la identificació de residus característics amb capacitat d'interaccionar amb els lligands permetrà dissenyar lligands agonistes i antagonistes selectius.

2.6. CONSTRUCCIÓ D'UN MODEL TRIDIMENSIONAL PEL RECEPTOR 5-HT_{1A} A PARTIR DELS SEUS LLIGANDS

Malgrat el cert grau de conservació de seqüència entre els diferents GPCRs, cada GPCR té motius de seqüència específics que influiran en la seva conformació i en la seva estructura tridimensional. Les simulacions de dinàmica molecular són un bon mètode per veure les conformacions de les hèlixs α dels GPCRs.

S'ha dut a terme una anàlisi de la conformació de la HTM3 del receptor 5-HT_{1A} de la serotonina respecte a la HTM3 de rodopsina. Les simulacions de dinàmica molecular de la HTM3 del receptor 5-HT_{1A} mostren com

- ✓ La HTM3 tendeix a doblegar-se cap a la HTM5, en contrast amb la HTM3 del receptor de rodopsina que es troba més a prop de la HTM2. Aquesta recol·locació de la HTM3 és conseqüència de la diferent seqüència aminoacída d'aquesta hèlix en rodopsina. En rodopsina, el motiu conservat $Gly^{3.36}Glu^{3.37}$ a la família de les opsines, i en el receptor 5-HT_{1A}, el motiu conservat $Cys^{3.36}Thr^{3.37}$ a la familia dels neurotransmissors, produeix divergències estructurals (veure article 2).

La conformació de la HTM3 en la família dels neurotransmissors condiciona la localització d'un residu d'Asp, que participa en la unió de l'amina protonada dels neurotransmissors, i per tant la posició dels lligands dins del receptor. Per a validar el model del receptor 5-HT_{1A} s'han dissenyat, sintetitzat, i avaluat farmacològicament dos nous lligands 1 i 2 (veure TAULA 2) que interaccionen amb el residu $Asp^{3.32}$ de la HTM3 i el residu $Asn^{7.39}$ de la HTM7. El lligand 1 interaccionaria òptimament amb la conformació de la HTM3 observada per a la família de les opsines (veure FIGURA 26) i el lligand 2 amb la conformació proposada en aquest treball per a la família dels neurotransmissors (veure FIGURA 27).

- ✓ La falta d'afinitat del compost 1 i l'alta afinitat del compost 2 pel receptor 5-HT_{1A} proporciona suport experimental a la conformació de la HTM3 proposada per aquest receptor (veure article 2).

- ✓ Aquest nou lligand 2, caracteritzat farmacològicament com a antagonista del receptor 5-HT_{1A}, és selectiu davant als receptors α_1-adrenèrgic i D_2-dopaminèrgic (veure article 2).

Així doncs, integrant les dades d'unió, tenint en compte els motius estructurals característics de la HTM3 del 5-HT_{1A}, utilitzant la metodologia de dinàmica molecular desenvolupada de l'entorn de metans i validant-ho a través del disseny racional dels lligands, s'ha proposat i validat un model pel receptor 5-HT_{1A}. Aquest model podria utilitzar-se pels altres receptors de serotonina degut a la conservació del motiu de seqüència que introdueix els canvis conformacionals.

2.7. DISSENY DE LLIGANDS AGONISTES SELECTIUS AL RECEPTOR $5HT_{1A}$ SENSE AFINITAT PEL RECEPTOR ADRENÈRGIC

Segons el model del receptor 5-HT_{1A} desenvolupat i el seu model d'interacció amb els compostos de tipus arilpiperazina, el compost 3 (veure TAULA 2) interacciona amb el receptor $5HT_{1A}$ a través de (veure FIGURA 28):

(i) un pont salí entre l'amina protonada de l'anell de piperazina i l'$Asp^{3.32}$

(ii) enllaços per pont d'hidrogen entre els carbonils i $Ser^{5.42}$, $Thr^{5.43}$ i $Thr^{3.37}$

Aquest lligand té afinitat pel receptor 5-HT_{1A} i pel receptor α_1-adrenèrgic degut a l'homologia de seqüència en els residus que interaccionen amb els grups funcionals del lligand ($Asp^{3.32}$, $Thr^{3.37}$, $Ser^{5.42}$ i $Thr^{5.43}$) (veure FIGURA 29). A partir d'aquest model d'interaccó s'ha modificat l'estructura d'aquest lligand per tal que interaccioni amb residus característics del 5-HT_{1A} i no de l'α_1-adrenèrgic. El nou lligand 4 dissenyat (veure TAULA 2) presenta una cadena carbonada escurçada, tot evitant la interacció entre un dels carbonils i la $Thr^{3.37}$ i tot satisfent la seva capacitat de formar pont d'hidrogen amb la $Thr^{5.39}$ (veure FIGURA 30). A la posició 5.39, el receptor α_1-adrenèrgic presenta una Ala, un residu sense capacitat de formació de pont d'hidrogen.

La sola presència d'aquest residu fa que el lligand 4 tingui afinitat pel receptor 5-HT_{1A} i no pel receptor α_1-adrenèrgic, tal com ho confirmen els estudis farmacològics.

- ✓ Així doncs, mitjançant la comparació de les seqüències dels receptors 5-HT_{1A} i α_1-adrenèrgic, s'ha identificat el residu $Thr^{5.39}$ característic del receptor 5-HT_{1A} i s'ha dissenyat un lligand agonista amb afinitat pel receptor 5-HT_{1A} i selectiu respecte al receptor α_1-adrenèrgic (veure article 3).

2.8. ESTUDI DE LA UNIÓ ENTRE EL RECEPTOR 5-HT_4 I EL LLIGAND GR113808

Mitjançant la integració de les dades de mutagènesi dirigida i les simulacions de dinàmica molecular es va construir un model del domini transmembrànic del receptor 5-HT_4 complexat amb l'antagonista GR113808 (veure TAULA 2).

Aquest model es va construir a partir de l'estructura cristal·logràfica de la rodopsina i els residus que estan implicats en la unió amb el lligand, determinats experimentalment per mutagènesi dirigida.

El model teòric fruit de les simulacions de dinàmica molecular mostra que:

- ✓ El mode de reconeixement del GR113808 consisteix en (i) una interacció iònica entre l'amina protonada del lligand i l'$Asp^{3.32}$; (ii) un enllaç d'hidrogen entre l'oxigen carbonílic i la $Ser^{5.43}$; (iii) l'enllaç d'hidrogen entre l'oxigen de l'èter i l'$Asn^{6.55}$; (iv) l'enllaç d'hidrogen entre els grups C-H adjacents al nitrogen de la piperidina protonada i els electrons π de $Phe^{6.51}$; i (v) les interaccions aromàtiques π-σ entre l'anell d'indol i $Phe^{6.52}$ (veure FIGURA 31) (veure article 4).

Aquest model computacional a més a més ofereix indicacions estructurals sobre el paper de l'$Asp^{3.32}$, $Ser^{5.43}$, $Phe^{6.51}$, $Phe^{6.52}$ i $Asn^{6.55}$ en les afinitats d'unió dels experiments:

- ✓ La mutació de $Asp^{3.32}$Asn no afecta la unió de GR113808. La disminució de l'afinitat d'unió del parell iònic al grup NH carregat de l'anell de piperidina

queda compensada degut a (i) la substitució d'una càrrega negativa a la cadena lateral de l'Asp per la cadena lateral neutra de l'Asn provoca una penalització energètica més gran de l'Asp per a trencar l'entorn de la seva cadena lateral en la forma lliure del lligand i (ii) l'augment de la càrrega dels carbonis adjacents a la piperidina protonada augmenta l'energia d'interacció entre Phe$^{6.51}$ i l'anell de piperidina (veure article 4).

- ✓ En el mutant Phe$^{6.52}$Val, l'anell d'indol del lligand substitueix la interacció amb Phe$^{6.52}$ per una interacció intensa similar amb Tyr$^{5.38}$, sense efecte significant en la unió de GR113808 (veure article 4).
- ✓ La mutació Asn$^{6.55}$Leu substitueix l'enllaç d'hidrogen entre l'oxigen de l'éter del lligand i l'Asn$^{6.55}$ per a Cys$^{5.42}$, amb una baixada de l'afinitat del lligand que aproximadament equival a la diferència en energia lliure entre els enllaços d'hidrogen SH···O i NH···O (veure article 4).

Com que aquests residus també es troben presents en altres membres de la família dels neurotransmissors del GPCRs, aquesta troballa també servirà per a la nostra comprensió de la unió de lligands de receptors d'origen similar, tant en altres receptors de serotonina com en altres receptors de la família de les amines biogèniques.

2.9. MODEL D'INTERACCIÓ DELS ANTAGONISTES DEL RECEPTOR 5-HT$_7$

A partir de la metodologia de la caixa de metans desenvolupada, dels models estructurals del receptor 5-HT$_{1A}$ i dels models d'interacció dels lligands dels receptors de serotonina, s'ha proposat un model d'interacció entre el receptor 5-HT$_7$ i el seu lligand antagonista 5 (veure Taula 2).

- ✓ El lligand 5 interacciona amb el receptor a través de (veure FIGURA 32) (veure article 5):

  (i) Un pont salí entre l'amina protonada i l'Asp$^{3.32}$

  (ii) Dos enllaços per pont d'hidrogen entre el carbonil i la Ser$^{5.42}$ i la Thr$^{5.43}$

(iii) Una interacció aromàtica entre l'anell de fenil adjacent a l'anell de piperazina i la $Phe^{3.28}$ i la $Tyr^{7.43}$

(iv) Una interacció aromàtica entre l'anell de naftolactam i $Phe^{6.52}$

A més a més aquest model d'interacció confirma el model de farmacòfor previst pels antagonistes del receptor 5-HT_7 (veure article 5).

La gran homologia de seqüència entre els diferents receptors de serotonina en la seva zona transmebrànica permet a grans trets assimilar tant les característistiques estructurals específiques com els modes d'unió dels seus lligands. És així que es pot definir un patró general d'interació dels lligands amb els receptors de serotonina i incloure-hi les característiques específiques de cada receptor. El fet que molts receptors de les amines biogèniques també presentin aquets motius que tenen un paper estructural o d'unió dels lligands, permet extrapolar els resultats dels receptors de serotonina a tota la subfamília d'amines biogèniques.

3. CONCLUSIONS

Degut a la poca informació sobre l'estructura tridimensional dels GPCRs, la bioinformàtica està esdevenint una eina molt important per a obtenir models de l'estructura d'aquestes proteïnes.

L'estudi de l'estructura i el funcionament dels GPCRs és un trencaclosques de moltes peces. Aquesta tesi mostra com poden encaixar-se algunes d'elles, com la modelització per homologia, les característiques estructurals específiques de cada receptor, les simulacions de dinàmica molecular, els experiments de mutagènesi dirigida, el disseny racional de fàrmacs i les dades d'unió de lligands per tal de proposar i validar models tridimensionals pels receptors de serotonina 5-$HT_{1A,}$ 5-HT_4 i 5-HT_7.

(i) A partir d'una anàlisi estadística de proteïnes globulars i de membrana cristal·litzades i mitjançant les simulacions de dinàmica molecular, s'ha trobat que la polaritat de l'entorn condiciona les conformacions de les hèlixs α. Com més polar és l'entorn, el valor del paràmetre $|\Phi|$ augmenta i $|\Psi|$ disminueix com a conseqüència de la formació d'un segon enllaç d'hidrogen adicional.

(ii) Per tal d'estudiar *in silico* els GPCRS s'ha desenvolupat i validat el mètode de l'entorn de metans que pretén simular de manera senzilla i computacionalment poc costosa les propietats de l'entorn hidrofòbic en el que es troben les proteïnes de membrana.

(iii) S'ha trobat que el mètode computacional desenvolupat és capaç de reproduir les distorsions helicals a causa del Pro *kink*

(iv) Mitjançant el mètode computacional desenvolupat s'ha construit un model tridimensional pel receptor 5-HT_{1A} que a més a més es pot extrapol·lar a tots els receptors de serotonina degut al residu conservat $Thr^{3.37}$. A més a més aquest model tridimensional ha estat validat a través del disseny racional de lligands.

(v) A partir del model tridimensional del 5-HT_{1A} desenvolupat i mitjançant la identificació de motius de seqüència característics del receptor 5-HT_{1A}, s'ha dissenyat dos nous lligands agonistes selectius sense afinitat pel receptor α_1-adrenèrgic.

(vi) Utilitzant com a punt de partida el model tridimensional desenvolupat pels receptors de serotonina, a través de les simulacions de dinàmica molecular i mitjançant

la integració de les dades de mutagènesi dirigida, s'ha identificat el mode d'unió del lligand antagonista GR113808 al receptor 5-HT_4.

(vii) A partir del model tridimenisonal desenvolupat pels receptors de serotonina, de la identificació de motius de seqüència específics, les simulacions de dinàmica molecular i el model del farmacòfor s'han identificat els residus del receptor 5-HT_7 implicats en la unió de lligands antagonistes.

Tot i així, la comprensió total del funcionament dels GPCRs i la validació de la seva estructura tridimensional quedarà en mans dels cristal·lògrafs i de futurs estudis biofísics.

4. BIBLIOGRAFIA

1. Allen LF, Lefkowitz R J, Caron M G and Cotecchia S (1991) G-Protein-Coupled Receptor Genes As Protooncogenes: Constitutively Activating Mutation of the Alpha 1B-Adrenergic Receptor Enhances Mitogenesis and Tumorigenicity. *Proc Natl Acad Sci U S A* **88**: pp 11354-8.

2. Allman K, Page K M, Curtis C A and Hulme E C (2000) Scanning Mutagenesis Identifies Amino Acid Side Chains in Transmembrane Domain 5 of the M(1) Muscarinic Receptor That Participate in Binding the Acetyl Methyl Group of Acetylcholine. *Mol Pharmacol* **58**: pp 175-84.

3. Almaula N, Ebersole B J, Zhang D, Weinstein H and Sealfon S C (1996) Mapping the Binding Site Pocket of the Serotonin 5-Hydroxytryptamine2A Receptor. Ser3.36(159) Provides a Second Interaction Site for the Protonated Amine of Serotonin but Not of Lysergic Acid Diethylamide or Bufotenin. *J Biol Chem* **271**: pp 14672-5.

4. Arnis S, Fahmy K, Hofmann K P and Sakmar T P (1994) A Conserved Carboxylic Acid Group Mediates Light-Dependent Proton Uptake and Signaling by Rhodopsin. *J Biol Chem* **269**: pp 23879-81.

5. Attwood TK, Blythe M J, Flower D R, Gaulton A, Mabey J E, Maudling N, McGregor L, Mitchell A L, Moulton G, Paine K and Scordis P (2002) PRINTS and PRINTS-S Shed Light on Protein Ancestry. *Nucleic Acids Res* **30**: pp 239-41.

6. Attwood TK and Findlay J B (1994) Fingerprinting G-Protein-Coupled Receptors. *Protein Eng* **7**: pp 195-203.

7. Baldwin JM, Schertler G F and Unger V M (1997) An Alpha-Carbon Template for the Transmembrane Helices in the Rhodopsin Family of G-Protein-Coupled Receptors. *J Mol Biol* **272**: pp 144-64.

8. Ballesteros JA, Jensen A D, Liapakis G, Rasmussen S G, Shi L, Gether U and Javitch J A (2001a) Activation of the Beta 2-Adrenergic Receptor Involves Disruption of an Ionic Lock Between the Cytoplasmic Ends of Transmembrane Segments 3 and 6. *J Biol Chem* **276**: pp 29171-7.

9. Ballesteros JA, Shi L and Javitch J A (2001b) Structural Mimicry in G Protein-Coupled Receptors: Implications of the High-Resolution Structure of Rhodopsin for Structure-Function Analysis of Rhodopsin-Like Receptors. *Mol Pharmacol* **60**: pp 1-19.

10. Ballesteros, J. A. and Weinstein, H. *Methods in Neuroscience*. **25**: pp 366-428.

11. Bantick RA, Deakin J F and Grasby P M (2001) The 5-HT1A Receptor in Schizophrenia: a Promising Target for Novel Atypical Neuroleptics? *J Psychopharmacol* **15**: pp 37-46.

12. Barker EL, Westphal R S, Schmidt D and Sanders-Bush E (1994) Constitutively Active 5-Hydroxytryptamine2C Receptors Reveal Novel Inverse Agonist Activity of Receptor Ligands. *J Biol Chem* **269**: pp 11687-90.

13. Barlow DJ and Thornton J M (1988) Helix Geometry in Proteins. *J Mol Biol* **201**: pp 601-19.

14. Blundell T, Barlow D, Borkakoti N and Thornton J (1983) Solvent-Induced Distortions and the Curvature of Alpha-Helices. *Nature* **306**: pp 281-3.

15. Bond RA, Leff P, Johnson T D, Milano C A, Rockman H A, McMinn T R, Apparsundaram S, Hyek M F, Kenakin T P, Allen L F and et a l (1995) Physiological Effects of Inverse Agonists in Transgenic Mice With Myocardial Overexpression of the Beta 2-Adrenoceptor. *Nature* **374**: pp 272-6.

16. Cavalli A, Fanelli F, Taddei C, De Benedetti P G and Cotecchia S (1996) Amino Acids of the Alpha1B-Adrenergic Receptor Involved in Agonist Binding: Differences in Docking Catecholamines to Receptor Subtypes. *FEBS Lett* **399**: pp 9-13.

17. Chidiac P, Hebert T E, Valiquette M, Dennis M and Bouvier M (1994) Inverse Agonist Activity of Beta-Adrenergic Antagonists. *Mol Pharmacol* **45**: pp 490-9.

18. Cho W, Taylor L P, Mansour A and Akil H (1995) Hydrophobic Residues of the D2 Dopamine Receptor Are Important for Binding and Signal Transduction. *J Neurochem* **65**: pp 2105-15.

19. Choudhary MS, Craigo S and Roth B L (1993) A Single Point Mutation (Phe340-->Leu340) of a Conserved Phenylalanine Abolishes 4-[125I]Iodo-(2,5-Dimethoxy)Phenylisopropylamine and. *Mol Pharmacol* **43**: pp 755-61.

20. Cox BA, Henningsen R A, Spanoyannis A, Neve R L and Neve K A (1992) Contributions of Conserved Serine Residues to the Interactions of Ligands With Dopamine D2 Receptors. *J Neurochem* **59**: pp 627-35.

21. Craig DA and Clarke D E (1990) Pharmacological Characterization of a Neuronal Receptor for 5-Hydroxytryptamine in Guinea Pig Ileum With Properties Similar to the 5-Hydroxytryptamine Receptor. *J Pharmacol Exp Ther* **252**: pp 1378-86.

22. Dumuis A, Bouhelal R, Sebben M, Cory R and Bockaert J (1988) A Nonclassical 5-Hydroxytryptamine Receptor Positively Coupled With Adenylate Cyclase in the Central Nervous System. *Mol Pharmacol* **34**: pp 880-7.

23. Duprez L, Parma J, Costagliola S, Hermans J, Van Sande J, Dumont J E and Vassart G (1997) Constitutive Activation of the TSH Receptor by Spontaneous Mutations Affecting the N-Terminal Extracellular Domain. *FEBS Lett* **409**: pp 469-74.

24. Farrens DL, Altenbach C, Yang K, Hubbell W L and Khorana H G (1996) Requirement of Rigid-Body Motion of Transmembrane Helices for Light Activation of Rhodopsin. *Science* **274**: pp 768-70.

25. Fasman GD (1989) Protein Conformational Prediction. *Trends Biochem Sci* **14**: pp 295-9.

26. Flower DR (1999) Modelling G-Protein-Coupled Receptors for Drug Design. *Biochim Biophys Acta* **1422**: pp 207-34.

27. Fredriksson R, Lagerstrom M C, Lundin L G and Schioth H B (2003) The G-Protein-Coupled Receptors in the Human Genome Form Five Main Families. Phylogenetic Analysis, Paralogon Groups, and Fingerprints. *Mol Pharmacol* **63**: pp 1256-72. Rec #: 2270

28. Gantz I, DelValle J, Wang L D, Tashiro T, Munzert G, Guo Y J, Konda Y and Yamada T (1992) Molecular Basis for the Interaction of Histamine With the Histamine H2 Receptor. *J Biol Chem* **267**: pp 20840-3.

29. Gether U (2000) Uncovering Molecular Mechanisms Involved in Activation of G Protein-Coupled Receptors. *Endocr Rev* **21**: pp 90-113.

30. Gether U, Lin S, Ghanouni P, Ballesteros J A, Weinstein H and Kobilka B K (1997) Agonists Induce Conformational Changes in Transmembrane Domains III and VI of the Beta2 Adrenoceptor. *EMBO J* **16**: pp 6737-47.

31. Govaerts C, Blanpain C, Deupi X, Ballet S, Ballesteros J A, Wodak S J, Vassart G, Pardo L and Parmentier M (2001a) The TXP Motif in the Second Transmembrane Helix of CCR5. A Structural Determinant of Chemokine-Induced Activation. *J Biol Chem* **276**: pp 13217-25.

32. Govaerts C, Lefort A, Costagliola S, Wodak S J, Ballesteros J A, Van Sande J, Pardo L and Vassart G (2001b) A Conserved Asn in Transmembrane Helix 7 Is an on/Off Switch in the Activation of the Thyrotropin Receptor. *J Biol Chem* **276**: pp 22991-9.

33. Gray TM and Matthews B W (1984) Intrahelical Hydrogen Bonding of Serine, Threonine and Cysteine Residues Within Alpha-Helices and Its Relevance to Membrane-Bound Proteins. *Journal of Molecular Biology* **175**: pp 75-81.

34. Haddjeri N, Szabo S T, de Montigny C and Blier P (2000) Increased Tonic Activation of Rat Forebrain 5-HT(1A) Receptors by Lithium Addition to Antidepressant Treatments. *Neuropsychopharmacology* **22**: pp 346-56.

35. Harmar AJ (2001) Family-B G-Protein-Coupled Receptors. *Genome Biol* **2**: pp REVIEWS3013.

36. Heidmann DE, Metcalf M A, Kohen R and Hamblin M W (1997) Four 5-Hydroxytryptamine7 (5-HT7) Receptor Isoforms in Human and Rat Produced by Alternative Splicing: Species Differences Due to Altered Intron-Exon Organization. *J Neurochem* **68**: pp 1372-81.

37. Heitz F, Holzwarth J A, Gies J P, Pruss R M, Trumpp-Kallmeyer S, Hibert M F and Guenet C (1999) Site-Directed Mutagenesis of the Putative Human Muscarinic M2 Receptor Binding Site. *Eur J Pharmacol* **380**: pp 183-95.

38. Ho BY, Karschin A, Branchek T, Davidson N and Lester H A (1992) The Role of Conserved Aspartate and Serine Residues in Ligand Binding and in Function of the 5-HT1A Receptor: a Site-Directed Mutation Study. *FEBS Lett* **312**: pp 259-62.

39. Howard AD, McAllister G, Feighner S D, Liu Q, Nargund R P, Van der Ploeg L H and Patchett A A (2001) Orphan G-Protein-Coupled Receptors and Natural Ligand Discovery. *Trends Pharmacol Sci* **22**: pp 132-40.

40. Huang XP, Nagy P I, Williams F E, Peseckis S M and Messer W S Jr (1999) Roles of Threonine 192 and Asparagine 382 in Agonist and Antagonist Interactions With M1 Muscarinic Receptors. *Br J Pharmacol* **126**: pp 735-45.

41. Idres S, Delarue C, Lefebvre H and Vaudry H (1991) Benzamide Derivatives Provide Evidence for the Involvement of a 5-HT4 Receptor Type in the Mechanism of Action of Serotonin in Frog Adrenocortical Cells. *Brain Res Mol Brain Res* **10**: pp 251-8.

42. Javitch JA, Ballesteros J A, Weinstein H and Chen J (1998) A Cluster of Aromatic Residues in the Sixth Membrane-Spanning Segment of the Dopamine D2 Receptor Is Accessible in the Binding-Site Crevice. *Biochemistry* **37**: pp 998-1006.

43. Javitch JA, Fu D, Liapakis G and Chen J (1997) Constitutive Activation of the Beta2 Adrenergic Receptor Alters the Orientation of Its Sixth Membrane-Spanning Segment. *J Biol Chem* **272**: pp 18546-9.

44. Jensen AD, Guarnieri F, Rasmussen S G, Asmar F, Ballesteros J A and Gether U (2001) Agonist-Induced Conformational Changes at the Cytoplasmic Side of Transmembrane Segment 6 in the Beta 2 Adrenergic Receptor Mapped by Site-Selective Fluorescent Labeling. *J Biol Chem* **276**: pp 9279-90.

45. Ji TH, Grossmann M and Ji I (1998) G Protein-Coupled Receptors. I. Diversity of Receptor-Ligand Interactions. *J Biol Chem* **273**: pp 17299-302.

46. Johnson MP, Wainscott D B, Lucaites V L, Baez M and Nelson D L (1997) Mutations of Transmembrane IV and V Serines Indicate That All Tryptamines Do Not Bind to the Rat 5-HT2A Receptor in the Same Manner. *Brain Res Mol Brain Res* **49**: pp 1-6.

47. Kao HT, Adham N, Olsen M A, Weinshank R L, Branchek T A and Hartig P R (1992) Site-Directed Mutagenesis of a Single Residue Changes the Binding Properties of the Serotonin 5-HT2 Receptor From a Human to a Rat Pharmacology. *FEBS Lett* **307**: pp 324-8.

48. Kaumann AJ (1990) Piglet Sinoatrial 5-HT Receptors Resemble Human Atrial 5-HT4-Like Receptors. *Naunyn Schmiedebergs Arch Pharmacol* **342** : pp 619-22.

49. Kjelsberg MA, Cotecchia S, Ostrowski J, Caron M G and Lefkowitz R J (1992) Constitutive Activation of the Alpha 1B-Adrenergic Receptor by All Amino Acid Substitutions at a Single Site. Evidence for a Region Which Constrains Receptor Activation. *J Biol Chem* **267**: pp 1430-3.

50. Kobilka B (1992) Adrenergic Receptors As Models for G Protein-Coupled Receptors. *Annu Rev Neurosci* **15**: pp 87-114.

51. Kolakowski LF Jr (1994) GCRDb: a G-Protein-Coupled Receptor Database. *Receptors Channels* **2**: pp 1-7.

52. Lander ES et al. (2001) Initial Sequencing and Analysis of the Human Genome. *Nature* **409**: pp 860-921.

53. Leurs R, Smit M J, Tensen C P, Ter Laak A M and Timmerman H (1994) Site-Directed Mutagenesis of the Histamine H1-Receptor Reveals a Selective Interaction of Asparagine207 With Subclasses of H1-Receptor Agonists. *Biochem Biophys Res Commun* **201**: pp 295-301.

54. Liapakis G, Ballesteros J A, Papachristou S, Chan W C, Chen X and Javitch J A (2000) The Forgotten Serine. A Critical Role for Ser-2035.42 in Ligans Binding to and Activation of the Beta 2-Adrenergic Receptor. *J Biol Chem* **275**: pp 37779-88.

55. Ligneau X, Morisset S, Tardivel-Lacombe J, Gbahou F, Ganellin C R, Stark H, Schunack W, Schwartz J C and Arrang J M (2000) Distinct Pharmacology of Rat and Human Histamine H(3) Receptors: Role of Two Amino Acids in the Third Transmembrane Domain. *Br J Pharmacol* **131**: pp 1247-50.

56. Lovenberg TW, Baron B M, de Lecea L, Miller J D, Prosser R A, Rea M A, Foye P E, Racke M, Slone A L, Siegel B W and et a l (1993) A Novel Adenylyl Cyclase-Activating Serotonin Receptor (5-HT7) Implicated in the Regulation of Mammalian Circadian Rhythms. *Neuron* **11**: pp 449-58.

57. Lu ZL and Hulme E C (1999) The Functional Topography of Transmembrane Domain 3 of the M1 Muscarinic Acetylcholine Receptor, Revealed by Scanning Mutagenesis. *J Biol Chem* **274**: pp 7309-15.

58. Lu ZL, Saldanha J W and Hulme E C (2002) Seven-Transmembrane Receptors: Crystals Clarify. *Trends Pharmacol Sci* **23**: pp 140-6.

59. Mansour A, Meng F, Meador-Woodruff J H, Taylor L P, Civelli O and Akil H (1992) Site-Directed Mutagenesis of the Human Dopamine D2 Receptor. *Eur J Pharmacol* **227**: pp 205-14.

60. Marinissen MJ and Gutkind J S (2001) G-Protein-Coupled Receptors and Signaling Networks: Emerging Paradigms. *Trends Pharmacol Sci* **22**: pp 368-76.

61. Menard J and Treit D (1999) Effects of Centrally Administered Anxiolytic Compounds in Animal Models of Anxiety. *Neurosci Biobehav Rev* **23**: pp 591-613.

62. Meng EC and Bourne H R (2001) Receptor Activation: What Does the Rhodopsin Structure Tell Us? *Trends Pharmacol Sci* **22**: pp 587-93.

63. Mirzadegan T, Benko G, Filipek S and Palczewski K (2003) Sequence Analyses of G-Protein-Coupled Receptors: Similarities to Rhodopsin. *Biochemistry* **42**: pp 2759-67.

64. Moguilevsky N, Varsalona F, Guillaume J P, Noyer M, Gillard M, Daliers J, Henichart J P and Bollen A (1995) Pharmacological and Functional Characterisation of the Wild-Type and Site-Directed Mutants of the Human H1 Histamine Receptor Stably Expressed in CHO Cells. *J Recept Signal Transduct Res* **15**: pp 91-102.

65. Ohta K, Hayashi H, Mizuguchi H, Kagamiyama H, Fujimoto K and Fukui H (1994) Site-Directed Mutagenesis of the Histamine H1 Receptor: Roles of Aspartic Acid107, Asparagine198 and Threonine194. *Biochem Biophys Res Commun* **203**: pp 1096-101.

66. Okada T, Ernst O P, Palczewski K and Hofmann K P (2001) Activation of Rhodopsin: New Insights From Structural and Biochemical Studies. *Trends Biochem Sci* **26**: pp 318-24.

67. Okada T, Fujiyoshi Y, Silow M, Navarro J, Landau E M and Shichida Y (2002) Functional Role of Internal Water Molecules in Rhodopsin Revealed by X-Ray Crystallography. *Proc Natl Acad Sci U S A* **99**: pp 5982-7.

68. Ouadid H, Seguin J, Dumuis A, Bockaert J and Nargeot J (1992) Serotonin Increases Calcium Current in Human Atrial Myocytes Via the Newly Described 5-Hydroxytryptamine4 Receptors. *Mol Pharmacol* **41**: pp 346-51.

69. Palczewski K, Kumasaka T, Hori T, Behnke C A, Motoshima H, Fox B A, Le Trong I, Teller D C, Okada T, Stenkamp R E, Yamamoto M and Miyano M (2000) Crystal Structure of Rhodopsin: A G Protein-Coupled Receptor. *Science* **289**: pp 739-45.

70. Parma J, Duprez L, Van Sande J, Cochaux P, Gervy C, Mockel J, Dumont J and Vassart G (1993) Somatic Mutations in the Thyrotropin Receptor Gene Cause Hyperfunctioning Thyroid Adenomas. *Nature* **365**: pp 649-51.

71. Parma J, Van Sande J, Swillens S, Tonacchera M, Dumont J and Vassart G (1995) Somatic Mutations Causing Constitutive Activity of the Thyrotropin Receptor Are the Major Cause of Hyperfunctioning Thyroid Adenomas: Identification of Additional Mutations Activating Both the Cyclic Adenosine 3',5'-Monophosphate and Inositol Phosphate-Ca2+ Cascades. *Mol Endocrinol* **9**: pp 725-33.

72. Perez DM, Hwa J, Zhao M M and Porter J (1998) Molecular Mechanisms of Ligand Binding and Activation in Alpha 1-Adrenergic Receptors. *Adv Pharmacol* **42**: pp 398-

403.

73. Pollock NJ, Manelli A M, Hutchins C W, Steffey M E, MacKenzie R G and Frail D E (1992) Serine Mutations in Transmembrane V of the Dopamine D1 Receptor Affect Ligand Interactions and Receptor Activation. *J Biol Chem* **267**: pp 17780-6.

74. Porter JE, Hwa J and Perez D M (1996) Activation of the Alpha1b-Adrenergic Receptor Is Initiated by Disruption of an Interhelical Salt Bridge Constraint. *J Biol Chem* **271**: pp 28318-23.

75. Rao VR, Cohen G B and Oprian D D (1994) Rhodopsin Mutation G90D and a Molecular Mechanism for Congenital Night Blindness. *Nature* **367**: pp 639-42.

76. Rasmussen SG, Jensen A D, Liapakis G, Ghanouni P, Javitch J A and Gether U (1999) Mutation of a Highly Conserved Aspartic Acid in the Beta2 Adrenergic Receptor: Constitutive Activation, Structural Instability, and Conformational Rearrangement of Transmembrane Segment 6. *Mol Pharmacol* **56**: pp 175-84.

77. Roth BL (1994) Multiple Serotonin Receptors: Clinical and Experimental Aspects. *Ann Clin Psychiatry* **6**: pp 67-78.

78. Roth, B. L., Kroeze, W. K., Patel, S., and Lopez, E. The Multiplicity of Serotonin Receptors: Uselessly diverse molecules or an embarrasment of riches? The Neuroscientist 6, 252-262. 2000.

79. Roth BL and Shapiro D A (2001) Insights into the Structure and Function of 5-HT(2) Family Serotonin Receptors Reveal Novel Strategies for Therapeutic Target Development. *Expert Opin Ther Targets* **5**: pp 685-695.

80. Roth BL, Shoham M, Choudhary M S and Khan N (1997) Identification of Conserved Aromatic Residues Essential for Agonist Binding and Second Messenger Production at 5-Hydroxytryptamine2A Receptors. *Mol Pharmacol* **52**: pp 259-66.

81. Samama P, Cotecchia S, Costa T and Lefkowitz R J (1993) A Mutation-Induced Activated State of the Beta 2-Adrenergic Receptor. Extending the Ternary Complex Model. *J Biol Chem* **268**: pp 4625-36.

82. Sankararamakrishnan R and Vishveshwara S (1992) Geometry of Proline-Containing Alpha-Helices in Proteins. *Int J Pept Protein Res* **39**: pp 356-63.

83. Sansom MS and Weinstein H (2000) Hinges, Swivels and Switches: the Role of Prolines in Signalling Via Transmembrane Alpha-Helices. *Trends Pharmacol Sci* **21**: pp 445-51.

84. Savarese TM and Fraser C M (1992) In Vitro Mutagenesis and the Search for Structure-Function Relationships Among G Protein-Coupled Receptors. *Biochem J* **283 (Pt 1)**: pp 1-19.

85. Scheer A, Fanelli F, Costa T, De Benedetti P G and Cotecchia S (1996a) Constitutively Active Mutants of the Alpha 1B-Adrenergic Receptor: Role of Highly Conserved Polar Amino Acids in Receptor Activation. *EMBO J* **15**: pp 3566-78.

86. Scheer A, Fanelli F, Costa T, De Benedetti P G and Cotecchia S (1996b) Constitutively Active Mutants of the Alpha 1B-Adrenergic Receptor: Role of Highly Conserved Polar Amino Acids in Receptor Activation. *EMBO J* **15**: pp 3566-78.

87. Semkova I, Wolz P and Krieglstein J (1998) Neuroprotective Effect of 5-HT1A Receptor Agonist, Bay X 3702, Demonstrated in Vitro and in Vivo. *Eur J Pharmacol* **359**: pp 251-60.

88. Shacham S, Topf M, Avisar N, Glaser F, Marantz Y, Bar-Haim S, Noiman S, Naor Z and Becker O M (2001) Modeling the 3D Structure of GPCRs From Sequence. *Med Res Rev* **21**: pp 472-83.

89. Sheikh SP, Zvyaga T A, Lichtarge O, Sakmar T P and Bourne H R (1996) Rhodopsin Activation Blocked by Metal-Ion-Binding Sites Linking Transmembrane Helices C and F. *Nature* **383**: pp 347-50.

90. Shenker A, Laue L, Kosugi S, Merendino J J Jr, Minegishi T and Cutler G B Jr (1993) A Constitutively Activating Mutation of the Luteinizing Hormone Receptor in Familial Male Precocious Puberty. *Nature* **365**: pp 652-4.

91. Shi L, Liapakis G, Xu R, Guarnieri F, Ballesteros J A and Javitch J A (2002) Beta2 Adrenergic Receptor Activation. Modulation of the Proline Kink in Transmembrane 6 by a Rotamer Toggle Switch. *J Biol Chem* **277**: pp 40989-96.

92. Simon MI, Strathmann M P and Gautam N (1991) Diversity of G Proteins in Signal Transduction. *Science* **252**: pp 802-8.

93. Siniscalchi A, Badini I, Beani L and Bianchi C (1999) 5-HT4 Receptor Modulation of Acetylcholine Outflow in Guinea Pig Brain Slices. *Neuroreport* **10**: pp 547-51.

94. Spalding TA, Birdsall N J, Curtis C A and Hulme E C (1994) Acetylcholine Mustard Labels the Binding Site Aspartate in Muscarinic Acetylcholine Receptors. *J Biol Chem* **269**: pp 4092-7.

95. Stables J, Green A, Marshall F, Fraser N, Knight E, Sautel M, Milligan G, Lee M and Rees S (1997) A Bioluminescent Assay for Agonist Activity at Potentially Any G-Protein-Coupled Receptor. *Anal Biochem* **252**: pp 115-26.

96. Strader CD, Candelore M R, Hill W S, Sigal I S and Dixon R A (1989) Identification of Two Serine Residues Involved in Agonist Activation of the Beta-Adrenergic Receptor. *J Biol Chem* **264**: pp 13572-8.

97. Strader CD, Fong T M, Graziano M P and Tota M R (1995) The Family of G-Protein-Coupled Receptors. *FASEB J* **9**: pp 745-54.

98. Strader CD, Gaffney T, Sugg E E, Candelore M R, Keys R, Patchett A A and Dixon R A (1991) Allele-Specific Activation of Genetically Engineered Receptors. *J Biol Chem* **266**: pp 5-8.

99. Teitler M, Herrick-Davis K and Purohit A (2002) Constitutive Activity of G-Protein Coupled Receptors: Emphasis on Serotonin Receptors. *Curr Top Med Chem* **2**: pp 529-38.

100. Teller DC, Okada T, Behnke C A, Palczewski K and Stenkamp R E (2001) Advances in Determination of a High-Resolution Three-Dimensional Structure of Rhodopsin, a Model of G-Protein-Coupled Receptors (GPCRs). *Biochemistry* **40**: pp 7761-72.

101. Terron JA and Falcon-Neri A (1999) Pharmacological Evidence for the 5-HT7 Receptor Mediating Smooth Muscle Relaxation in Canine Cerebral Arteries. *Br J Pharmacol* **127**: pp 609-16.

102. Tierney AJ (2001) Structure and Function of Invertebrate 5-HT Receptors: a Review. *Comp Biochem Physiol A Mol Integr Physiol* **128**: pp 791-804.

103. Tonini M and Candura S M (1996) 5-HT4 Receptor Agonists and Bladder Disorders. *Trends Pharmacol Sci* **17**: pp 314-6.

104. Unger VM, Hargrave P A, Baldwin J M and Schertler G F (1997) Arrangement of Rhodopsin Transmembrane Alpha-Helices. *Nature* **389**: pp 203-6.

105. Venter JC et al. (2001) The Sequence of the Human Genome. *Science* **291** : pp 1304-51. Rec #: 720

106. von Heijne G (1991) Proline Kinks in Transmembrane Alpha-Helices. *J Mol Biol* **218**: pp 499-503.

107. Wang CD, Gallaher T K and Shih J C (1993) Site-Directed Mutagenesis of the Serotonin 5-Hydroxytrypamine2 Receptor: Identification of Amino Acids Necessary for Ligand Binding and Receptor Activation. *Mol Pharmacol* **43**: pp 931-40.

108. Ward SD, Curtis C A and Hulme E C (1999) Alanine-Scanning Mutagenesis of Transmembrane Domain 6 of the M(1) Muscarinic Acetylcholine Receptor Suggests That Tyr381 Plays Key Roles in Receptor Function. *Mol Pharmacol* **56**: pp 1031-41.

109. Weiss JM, Morgan P H, Lutz M W and Kenakin T P (1996) The Cubic Ternary Complex Receptor-Occupancy Model. III. Resurrecting Efficacy. *J Theor Biol* **181**: pp 381-97.

110. Wess J, Gdula D and Brann M R (1991) Site-Directed Mutagenesis of the M3 Muscarinic Receptor: Identification of a Series of Threonine and Tyrosine Residues Involved in Agonist but Not Antagonist Binding. *EMBO J* **10**: pp 3729-34.

111. White SH and Wimley W C (1999) Membrane Protein Folding and Stability: Physical Principles. *Annu Rev Biophys Biomol Struct* **28**: pp 319-65.

112. Whitehead IP, Zohn I E and Der C J (2001) Rho GTPase-Dependent Transformation by G Protein-Coupled Receptors. *Oncogene* **20**: pp 1547-55.

113. Wieland K, Zuurmond H M, Krasel C, Ijzerman A P and Lohse M J (1996) Involvement of Asn-293 in Stereospecific Agonist Recognition and in Activation of the Beta 2-Adrenergic Receptor. *Proc Natl Acad Sci U S A* **93**: pp 9276-81.

114. Wong SK, Slaughter C, Ruoho A E and Ross E M (1988) The Catecholamine Binding Site of the Beta-Adrenergic Receptor Is Formed by Juxtaposed Membrane-Spanning Domains. *J Biol Chem* **263**: pp 7925-8.

115. Yau JL, Noble J, Widdowson J and Seckl J R (1997) Impact of Adrenalectomy on 5-HT6 and 5-HT7 Receptor Gene Expression in the Rat Hippocampus. *Brain Res Mol Brain Res* **45**: pp 182-6.

116. Yildiz O, Smith J R and Purdy R E (1998) Serotonin and Vasoconstrictor Synergism. *Life Sci* **62**: pp 1723-32.

5. COMPENDI DE PUBLICACIONS

Influence of the Environment in the Conformation of α-Helices Studied by Protein Database Search and Molecular Dynamics Simulations

Mireia Olivella,* Xavier Deupi,* Cedric Govaerts,†‡ and Leonardo Pardo*

*Laboratori de Medicina Computacional, Unitat de Bioestadística, Facultat de Medicina, Universitat Autònoma de Barcelona, 08193 Bellaterra, Spain; †Institut de Recherche Interdisciplinaire en Biologie Humaine et Nucléaire, Université Libre de Bruxelles, Campus Erasme, B-1070 Bruxelles, Belgium; and ‡Service de Conformation des Macromolécules Biologiques, Université Libre de Bruxelles, 1050 Bruxelles, Belgium

ABSTRACT The influence of the solvent on the main-chain conformation (ϕ and Ψ dihedral angles) of α-helices has been studied by complementary approaches. A first approach consisted in surveying crystal structures of both soluble and membrane proteins. The residues of analysis were further classified as exposed to either the water (polar solvent) or the lipid (apolar solvent) environment or buried to the core of the protein (intermediate polarity). The statistical results show that the more polar the environment, the lower the value of ϕ_i and the higher the value of Ψ_i are. The intrahelical hydrogen bond distance increases in water-exposed residues due to the additional hydrogen bond between the peptide carbonyl oxygen and the aqueous environment. A second approach involved nanosecond molecular dynamics simulations of poly-Ala α-helices in environments of different polarity: water to mimic hydrophilic environments that can form hydrogen bonds with the peptide carbonyl oxygen and methane to mimic hydrophobic environments without this hydrogen bond capabilities. These simulations reproduce similar effects in ϕ and Ψ angles and intrahelical hydrogen bond distance and angle as observed in the protein survey analysis. The magnitude of the intrahelical hydrogen bond in the methane environment is stronger than in the water environment, suggesting that α-helices in membrane-embedded proteins are less flexible than in soluble proteins. There is a remarkable coincidence between the ϕ and Ψ angles obtained in the analysis of residues exposed to the lipid in membrane proteins and the results from computer simulations in methane, which suggests that this simulation protocol properly mimic the lipidic cell membrane and reproduce several structural characteristics of membrane-embedded proteins. Finally, we have compared the ϕ and Ψ torsional angles of Pro kinks in membrane protein crystal structures and in computer simulations.

INTRODUCTION

α-Helices are major structural elements in both soluble and membrane proteins (Fasman, 1989; White and Wimley, 1999). The stability of α-helices is basically achieved by the hydrogen bonds between the N—H atoms of residue i to the carbonyl oxygen of residue $i - 4$ in the preceding turn of the helix. Importantly, in transmembrane proteins, the formation of this hydrogen bond network allows the polar polypeptide backbone to expand the hydrophobic lipid bilayer of the cell membrane. Thus, the helical bundle motif frequently builds the three-dimensional structure of membrane proteins along with the β-barrel motif also observed in membrane-spanning proteins (White and Wimley, 1999).

An early statistical analysis of the conformation of α-helices in crystal structures of mostly soluble proteins (Barlow and Thornton, 1988) showed average main-chain torsion ϕ and Ψ angles of $-62°$ and $-41°$, respectively. However, additional hydrogen bonds between the peptide carbonyl oxygen to a solvent molecule (Blundell et al., 1983) or to a protein side-chain (Ballesteros et al., 2000) produce a significant change in ϕ and Ψ angles and in the curvature of the helix. Thus, it seems reasonable to assume that the conformation of α-helices located in hydrophilic environments, such as water, will differ from the conformation of α-helices located in hydrophobic environments, such as the cell membrane.

To assess the influence of the environment on the conformation of α-helices, complementary approaches were used in this study. A first approach consisted in surveying known protein structures. The results are presented for crystal structures of both soluble and membrane proteins. Despite the limited availability of membrane protein structures in the Brookhaven protein data bank (PDB), the significant increase in the number of deposited structures during the last years yields to an acceptable number of transmembrane helices for statistical analysis. Moreover, the residues of analysis are further classified as exposed, to either the water or the lipid environment, or buried to the core of the protein. A second approach involved nanosecond molecular dynamics simulations of poly-Ala α-helices in environments of different polarity: water and methane. The main-chain ϕ and Ψ torsional angles and intrahelical hydrogen bond parameters obtained in the analysis of protein crystal structures are compared with those obtained in computer simulations. Moreover, we have compared the ϕ and Ψ torsional angles of Pro kinks in membrane protein crystal structures and in computer simulations.

Submitted July 19, 2001, and accepted for publication February 28, 2002.

Address reprint requests to Dr. Leonardo Pardo, Laboratori de Medicina Computacional, Unitat de Bioestadística, Facultat de Medicina, Universitat Autònoma de Barcelona, 08193 Bellaterra, Spain. Tel.: 3493-581-2797; Fax: 3493-581-2344; E-mail: leonardo.pardo@uab.es.

0006-3495/02/06/3207/07 $2.00

MATERIALS AND METHODS

Membrane protein structures

The atomic coordinates of bacteriorhodopsin (PDB access number 1c3w, 1.55-Å resolution), aa3 (1occ, 2.8 Å), and ba3 (1ehk, 2.4 Å) cytochrome *c* oxidases, photosyntethic reaction center (1prc, 2.3 Å), potassium channel (1bl8, 3.2 Å), mechanosensitive ion channel (1msl, 3.5 Å), rhodopsin (1f88, 2.8 Å), halorhodopsin (1el2, 1.8 Å), sensory rhodopsin (1h68, 2.1 Å), light harvesting complex (1lgh, 2.4 Å), photosystem I (1jbo, 2.5 Å), AQP1 (1hwo, 3.7 Å), and GlpF (1fx8, 2.2 Å) channels, P-type ATPasa (1eul, 2.6 Å), and fumerate reductase respiratory complex (1qla, 2.2 Å) were obtained from the Brookhaven PDB. The coordinates of the residues in the HELIX annotation of the PDB files, corresponding to transmembrane helices 1–7 of 1c3w; 2–3, 7, 9, 12, 14–15, 19–20, 23, 28–30, 32–35, 41, 54, 59–60, and 63–66 of 1occ; 1, 3–9, 13–14, 16, 18–19, and 22 of 1ehk; 6, 8–10, and 13–14 of 1prc; 1 and 3 of 1bl8; 2–4 of 1msl; 1–7 of 1f88; 1–6, 8–9, 13–14, and 16 of 1e12; 1–8 of 1h68; 2 and 5 of 1lgh; 4, 8, 10, 16, 20, 27, 34–36, 40, 44, 48, 53, 57, 59, 68, 71, 77, 80, 85, 94, 103, 105, 109, 113, and 115–116 of 1jbo; 1 of 1hwo; 1–6, 9, 11–12, and 15 of 1fx8; 2, 4–5, 10–12, 15–16, 20, 25, 28, 31, 36, 38, and 41–43 of 1eul; and 1, 13, 16–20, 22, 25, 28, 29, 32, 26, 38, 40–41, 43–44, 47–48, and 81 of 1qla, were extracted for analysis. This results in a total of 160 transmembrane helices. These helices were split into amino acid stretches of 12 residues long with 1) Ala (349 structures) or 2) Pro (27 structures) at the eighth position. Stretches with other Pro residues in the sequence were removed from the database.

Soluble protein structures

Iditis 3.1 (Oxford Molecular, Oxford, U.K.) was used for the selection of protein structures in the Brookhaven PDB. The chosen α-helices possess: 1) a resolution of 2.0 Å or better; 2) 12 residues length with Ala at the eighth position; and 3) no Pro residues in the sequence. If two α-helical segments have more than 80% sequence identity (if 10 or more than 10 residues of 12 are identical) only the structure with best resolution was considered.

Accessible surface

The accessible surface of the residues in the survey of protein crystal structures at the fourth ($i - 4$) and the eighth (i) positions, was obtained with the Naccess program (Hubbart and Thornton, 1993). The sum of the accessible surface of residues i and $i - 4$ was used to classify the helices as exposed (>60) or buried (<40). These cutoffs were chosen by visual inspection of the crystal structures. The structures between these values could not be visually assigned to either group and were not included in the analysis.

Molecular dynamics simulations

The model peptides Ace-Ala_{25}-Nme and Ace-Ala_{12}-Pro-Ala_{12}-Nme were built in the standard α-helical conformation (backbone dihedral angles ϕ and Ψ of -58 and $-47°$) using the SYBYL 6.5 program (Tripos Inc., St. Louis, MO). The Ace-Ala_{25}-Nme structure was placed in a rectangular box containing 808 water or 1532 methane molecules, and the Ace-Ala_{12}-Pro-Ala_{12}-Nme structure was placed in a rectangular box containing 1689 methane molecules. The sizes of the boxes were approximately $52 \times 23 \times 23$ Å for the α-helix in water, and $60 \times 36 \times 36$ Å for the α-helices in methane, resulting in a density of 1.0 g cm^{-3} and 0.5 g cm^{-3}, respectively. It is important to note that the density of the methane box is not the density observed in the hydrophobic core of the membrane (White and Wimley, 1999). This is due to the different equilibrium distance between carbons in the methane box and in the polycarbon chain of the lipid. The density of the methane box was chosen to equal the first peak of the radial distribution function for the $H_4C\cdot\cdot CH_4$ distance obtained in the molecular dynamics simulations with the interatomic distance between two methane molecules obtained by full geometry optimization with ab initio quantum mechanical calculations at the MP2/6-31G** level of theory (Fig. 1 *a*). An increase of the density of the methane box leads to short contacts between molecules and thus extreme behavior of the system.

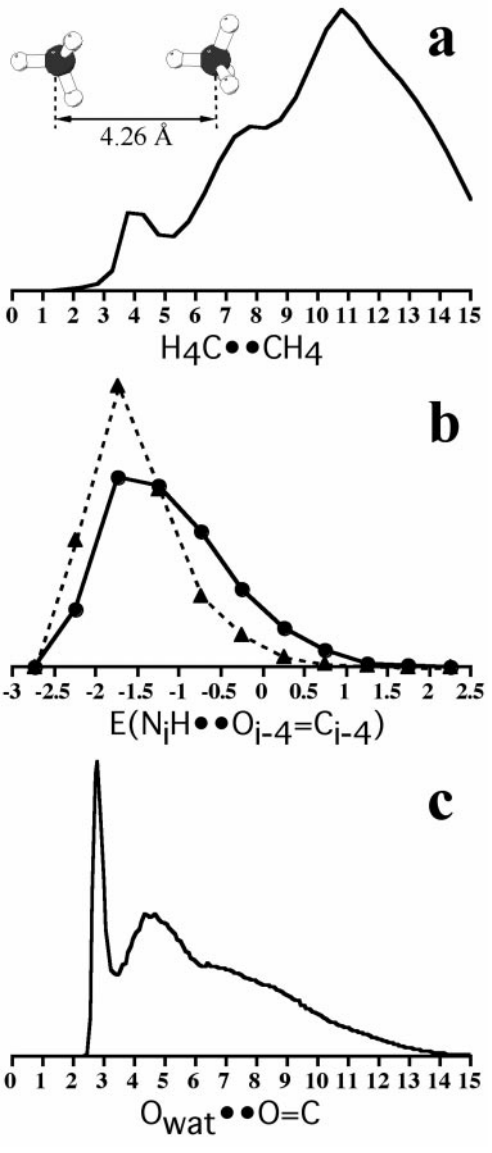

FIGURE 1 (*a*) Radial distribution function for the $H_4C\cdot\cdot CH_4$ distance (Å) obtained in molecular dynamics simulations of methane and the structure of $H_4C\cdot\cdot CH_4$ obtained by full geometry optimization with ab initio quantum mechanical calculations at the MP2/6-31G** level of theory. (*b*) Distribution of the energy of interaction (kcal/mol) between the N—H atoms of residue i and the carbonyl group of residue $i - 4$ obtained from the molecular dynamics simulations of a poly-Ala α-helix in water (*circles*, *solid line*) and methane (*triangles*, *broken line*). (*c*) Radial distribution function for the distance (Å) between the peptide carbonyl oxygen and the oxygen of the water molecules obtained in the molecular dynamics simulations of a poly-Ala α-helix in water.

Initially, the atoms of the model peptides were kept fixed, whereas the solvent molecules were energy minimized (500 steps), heated (from 0–300

TABLE 1 Means/standard deviations of the backbone torsion angles (ϕ_i and ψ_i, in degrees) of the residue at the eighth position (denoted as *i*) in the survey of α-helices containing Ala in protein crystal structures or at the 13th position (denoted as *i*) in the molecular dynamics simulations of poly-Ala α-helix, intrahelical hydrogen bond distance ($N_i \cdot\cdot O_{i-4}$, in Å), and angle ($N_i \cdot\cdot O_{i-4} = C_{i-4}$, in degrees) between the N atom of residue *i* to the carbonyl of residue *i* − 4, the energy of interaction between the N–H atoms of residue *i* and the carbonyl group of residue *i* − 4 ($E(N_i \cdot\cdot O_{i-4} = C_{i-4})$, in kcal/mol), and the intermolecular hydrogen bond distance ($O_{wat} \cdot\cdot O_{i-4}$, in Å) and angle ($O_{wat} \cdot\cdot O_{i-4} = C_{i-4}$, in degrees) between the peptide carbonyl oxygen and the oxygen of the water molecules obtained in the molecular dynamics simulations of the poly-Ala α-helix in water

	Protein database search			Molecular dynamics	
	$SOL_{hydrophilic}$	$SOL\text{-}MEM_{core}$	$MEM_{hydrophobic}$	Water	Methane
n	252	510	97	1000	1000
ϕ_i	−63.5/5.6	−62.9/5.3	−61.8/6.7	−65.9/10.0	−61.2/8.3
ψ_i	−40.9/5.4	−41.6/6.1	−43.1/7.0	−39.3/9.7	−44.1/8.5
$N_i \cdot\cdot O_{i-4}$	3.04/0.14	2.98/0.15	2.96/0.17	3.10/0.25	2.93/0.13
$N_i \cdot\cdot O_{i-4} = C_{i-4}$	151.5/6.0	153.3/7.1	153.5/7.5	148.9/10.5	154.4/8.3
$E(N_i \cdot\cdot O_{i-4}) = C_{i-4}$				−1.1/0.7	−1.5/0.6
$O_{wat} \cdot\cdot O_{i-4}$				2.94/0.2	
$O_{wat} \cdot\cdot O_{i-4} = C_{i-4}$				116.6/15.3	

K in 15 ps), and equilibrated (from 15–50 ps). Subsequently, the entire system was subjected to 500 iterations of energy minimization and then heated to 300 K in 15 ps. This was followed by an equilibration period (15–500 ps for Ace-Ala_{25}-Nme, and from 15–1000 ps for Ace-Ala_{12}-Pro-Ala_{12}-Nme) and a production run (from 500–1000 ps for Ace-Ala_{25}-Nme, and from 1000–1500 ps for Ace-Ala_{12}-Pro-Ala_{12}-Nme) at constant volume using the particle mesh Ewald method to evaluate electrostatic interactions (Darden et al., 1993). The equilibration time was chosen so that root mean square deviations relative to the first structure in the simulations remained constant (results not shown). The longer equilibration period of the Pro-containing structure is necessary to account for the flexibility of Pro kinks. Structures were collected for analysis every 0.5 ps during the last 500 ps of simulation (1000 structures). The energy of interaction between the N—H atoms of residue 13 and the carbonyl group of residue 9 was calculated with the Anal program of AMBER 5 (Case et al., 1997). The molecular dynamics simulations were run with the Sander module of AMBER 5, the all-atom force field (Cornell et al., 1995), SHAKE bond constraints in all bonds, a 2-fs integration time step, and constant temperature of 300 K coupled to a heat bath.

Statistical analysis

One-way analysis of variance for independent samples plus a posteriori one-sided Tukey's test was used for contrasting the backbone torsion angles at position 8 (ϕ_i and Ψ_i) and intrahelical hydrogen bond distance ($N_i \cdot\cdot O_{i-4}$) and angle ($N_i \cdot\cdot O_{i-4} = C_{i-4}$) between residues in soluble proteins that are exposed to the hydrophilic aqueous solvent, in membrane proteins that are exposed to the hydrophobic lipid bilayer, and in both soluble and membrane proteins that are exposed to the core of the protein. Averages and standard deviations of ϕ_i, Ψ_i, $N_i \cdot\cdot O_{i-4}$, and $N_i \cdot\cdot O_{i-4} = C_{i-4}$ obtained in the molecular dynamics simulations were calculated from all the geometries in the production phase. The data obtained in molecular dynamics simulations are not independent, thus it is not possible to perform statistical tests as in the protein survey analysis. The statistical analysis was performed with the SPSS 10 program (SPSS Inc. Chicago, IL).

RESULTS AND DISCUSSION

Survey of helices in known protein structures

Table 1 summarizes the means and standard deviations for the backbone torsion angles of the residue at position 8 (ϕ_i and Ψ_i), populated by Ala, of α-helices (see Materials and Methods) in soluble proteins that are exposed to the hydrophilic aqueous solvent ($SOL_{hydrophilic}$, 252 entries), in membrane proteins that are exposed to the hydrophobic lipid bilayer ($MEM_{hydrophobic}$, 97 entries), and in both soluble and membrane proteins that are exposed to the core of the protein ($SOL\text{-}MEM_{core}$, 510 entries). It has recently been proposed that, in contrast to previous hypothesis, the hydrophobicities of interior residues of both membrane and water-soluble proteins are comparable (Rees and Eisenberg, 2000; Stevens and Arkin, 1999). In consequence, the residues of α-helices pointing toward the core of soluble and membrane proteins have been grouped ($SOL\text{-}MEM_{core}$). Thus, the expected rank order of hydrophobicity, from hydrophobic to hydrophilic, of the environment to which the analyzed residues are exposed is: $MEM_{hydrophobic} > SOL\text{-}MEM_{core} > SOL_{hydrophilic}$. Besides, ϕ and Ψ angles vary depending on both side-chain type and side-chain conformation (Ballesteros et al., 2000; Chakrabarti and Pal, 1998). We limited the survey to alanine to avoid any direct or indirect effect of the side-chain in the conformation of the helix. In addition, Ala is the most helix-favoring residue in water (O'Neil and DeGrado, 1990), and it has one of the lowest turn propensities in transmembrane helices (Monne et al., 1999). Ala was favored over Gly because the lack of side chain in Gly provides additional flexibility (Kumar and Bansal, 1998). As shown in Table 1, the values of the backbone ϕ_i dihedral are found in the following rank order: $MEM_{hydrophobic}$ (−61.8°) > $SOL\text{-}MEM_{core}$ (−62.9°) > $SOL_{hydrophilic}$ (−63.5°). Thus, there is a positive correlation between hydrophobicity and ϕ_i: the more hydrophobic the environment, the higher the value of ϕ_i is. The values of the backbone Ψ_i dihedral are found in the following rank order: $MEM_{hydrophobic}$ (−43.1°) < $SOL\text{-}MEM_{core}$ (−41.6°) < $SOL_{hydrophilic}$ (−40.9°). Thus, in the case of Ψ_i the correlation is negative: the more hydrophobic the environment, the lower the value of Ψ_i is. It is important to remark that the difference between the conformation of an α-helix ex-

posed to either the hydrophilic aqueous solvent or the hydrophobic lipid bilayer is in average 1.7° for ϕ_i and 2.2° for Ψ_i. These differences in ϕ_i ($p = 0.016$) and Ψ_i ($p = 0.003$) are significant from a statistical point of view (see Materials and Methods). However, there are not statistical differences in ϕ_i and Ψ_i between SOL-MEM$_{core}$ and MEM$_{hydrophobic}$ or between SOL-MEM$_{core}$ and SOL$_{hydrophilic}$. Considering the small amplitudes of the difference, the influence of the lipidic or aqueous environment in the conformation of the α-helix will only be noticeable for long helices. The deviation between C-terminal positions of helices constructed with the ϕ_i and Ψ_i angles reported in Table 1 for SOL$_{hydrophilic}$ (−63.5° and −40.9°) and MEM$_{hydrophobic}$ (−61.8° and −43.1°), is 0.9 Å or 1.4 Å or 1.7 Å if helices 20 or 25 or 30 residues long are considered, respectively.

Table 1 also shows the means and standard deviations of the intrahelical hydrogen bond distance $N_i \cdot\cdot O_{i-4}$, and angle $N_i \cdot\cdot O_{i-4} = C_{i-4}$. The $N_i \cdot\cdot O_{i-4}$ distance increases as the environment becomes more hydrophilic: MEM$_{hydrophobic}$ (2.96 Å) > SOL-MEM$_{core}$ (2.98 Å) > SOL$_{hydrophilic}$ (3.04 Å). There are statistical differences between SOL$_{hydrophilic}$ and both SOL-MEM$_{core}$ ($p < 0.0005$) and MEM$_{hydrophobic}$ ($p < 0.0005$). Clearly, the additional hydrogen bond between the peptide carbonyl oxygen to a solvent molecule, in water-exposed residues (SOL$_{hydrophilic}$), increases the intrahelical hydrogen bond distance. Correspondingly, the $N_i \cdot\cdot O_{i-4} = C_{i-4}$ angle decreases in linearity in water exposed residues: MEM$_{hydrophobic}$ (153.5°) > SOL-MEM$_{core}$ (153.3°) > SOL$_{hydrophilic}$ (151.5°). Similarly to the $N_i \cdot\cdot O_{i-4}$ hydrogen bond distance, there are statistical differences between SOL$_{hydrophilic}$ and both SOL-MEM$_{core}$ ($p = 0.001$) and MEM$_{hydrophobic}$ ($p = 0.025$). Following the argument put forward by Blundell et al. (1983), the presence of a second hydrogen bond donor (i.e., a solvent molecule: O_{wat}) to the peptide carbonyl oxygen tends to bifurcate the $N_i \cdot\cdot O_{i-4} = C_{i-4}$ and the $O_{wat} \cdot\cdot O_{i-4} = C_{i-4}$ angles toward 120° (see below).

Molecular dynamics simulations of poly-Ala α-helices

We have performed nanosecond molecular dynamics simulations of poly-Ala α-helices (see Materials and Methods) in two different environments: water to mimic hydrophilic environments that can form hydrogen bonds with the peptide carbonyl oxygen of the α-helix and methane to mimic hydrophobic environments without this hydrogen bond capabilities. Table 1 shows the obtained values of ϕ_i and Ψ_i and the intrahelical hydrogen bond parameters $N_i \cdot\cdot O_{i-4}$ and $N_i \cdot\cdot O_{i-4} = C_{i-4}$ (in which i denotes residue number 13 in the poly-Ala α-helix). Notably, the effect of the environment observed in molecular dynamics simulations is the same in both magnitude and direction as the observed in the protein survey analysis. The polar environment formed by the water molecules tends to decrease ϕ_i (−61.2° vs. −65.9°), increase Ψ_i (−44.1° vs. −39.3°), increase $N_i \cdot\cdot O_{i-4}$ (2.93 Å vs. 3.10 Å), and decrease $N_i \cdot\cdot O_{i-4} = C_{i-4}$ (154.4° vs. 148.9°), relative to the apolar environment formed by the methane molecules. Thus, the presence or the absence of additional hydrogen bonds from the environment to the peptide carbonyl oxygen modifies the conformation of α-helices.

It is important to note that there is a remarkable coincidence between the values obtained in the analysis of exposed residues in membrane proteins (MEM$_{hydrophobic}$) and the results from computer simulations in the methane environment (ϕ_i: −61.8° vs.−61.2°; Ψ_i: −43.1° vs. −44.1°; $N_i \cdot\cdot O_{i-4}$: 2.96 Å vs. 2.93 Å; $N_i \cdot\cdot O_{i-4} = C_{i-4}$: 153.5° vs. 154.4°; see Table 1). Thus, we suggest, based on this analysis, that explicit methane molecules in molecular dynamics simulations properly mimic the lipidic cell membrane and reproduce several structural characteristics of membrane-embedded proteins.

The fact that the intrahelical hydrogen bond distance ($N_i \cdot\cdot O_{i-4}$) in water (3.10 Å) is longer than in methane (2.93 Å) suggests that this hydrogen bond in water is weaker than in methane. To corroborate this hypothesis we have calculated the mean and standard deviation (Table 1) and the distribution (Fig. 1 *b*) of the energy of interaction between the N—H atoms of residue i and the carbonyl group of residue $i - 4$ obtained from the molecular dynamics simulations in water (circles, solid line) and methane (triangles, broken line). The magnitude of the intrahelical hydrogen bond in water is smaller than in methane (−1.1 vs. −1.5 kcal/mol). The formation of a second hydrogen bond between the peptide carbonyl oxygen and the aqueous solvent enfeebles the intrahelical hydrogen bond that stabilize α-helices. This destabilization of the intrahelical hydrogen bond in water suggests that α-helices are more flexible in polar environments. The larger standard deviation (Table 1) of the dihedral angles that define the conformation of the helix, ϕ_i (10.0° vs. 8.3°) and Ψ_i (9.7° vs. 8.5°), in water than in methane reinforces this proposal. However, it is important to note that the standard deviations of ϕ_i and Ψ_i in the protein survey analysis of exposed soluble and membrane proteins do not follow this trend. We attribute this to the different number of structures in each category and the better resolution of soluble proteins compared with membrane proteins.

Fig. 1 *c* shows the radial distribution function for the distance between the peptide carbonyl oxygen and the oxygen of the water molecules obtained in the molecular dynamics simulations of a poly-Ala α-helix in water. The first peak in the distribution occurs at distances up to 3.3 Å, which implies an explicit hydrogen bond between the carbonyl oxygen of the α-helix and water. To characterize the geometric parameters of this hydrogen bond ($O_{wat} \cdot\cdot O_{i-4}$ and $O_{wat} \cdot\cdot O_{i-4} = C_{i-4}$), we selected the

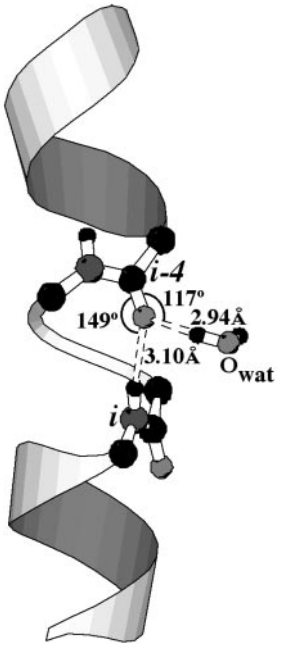

FIGURE 2 Representative structure obtained in the molecular dynamics simulations of the poly-Ala α-helices in water (see Materials and Methods). Distances (Å) and angles (degrees) are shown relative to the heavy atoms.

bound water molecules ($O_{wat}\cdot\cdot O_{i-4} < 3.3$ Å) to the carbonyl oxygen from the 1000 structures computed during the last 500 ps of simulation (see Materials and Methods) for statistical analysis. Fig. 2 shows a representative structure of the interaction between the water molecule and the carbonyl group that occurs at a $O_{wat}\cdot\cdot O_{i-4}$ distance of 2.94 Å and at a $O_{wat}\cdot\cdot O_{i-4} = C_{i-4}$ angle of 116.6° (see Table 1). The electronic nature of the carbonyl oxygen allows the formation of a hydrogen bond with both the N—H group of the residue in the following turn of the helix and a water molecule.

Structural analysis of Pro-containing α-helices in hydrophobic environments

Pro induce distorsion in α-helices as their cyclic side-chains introduce a local break, denoted Pro kink, to avoid a steric clash between the pyrrolidine ring and the carbonyl oxygen of residue $i - 4$ (Barlow and Thornton, 1988; Milner-White et al., 1992; Sankararamakrishnan and Vishveshwara, 1992; Von Heijne, 1991). Pro kinks impart backbone flexibility, due to the absence of the hydrogen bond with the carbonyl oxygen in the preceding turn of the helix. This structural flexibility is an important functional element in membrane proteins that transduce extracellular signals across the membrane through conformational changes in the transmembrane α-helices (Gether et al., 1997; Govaerts et al., 2001a; Ri et al., 1999; Sansom and Weinstein, 2000). We have studied the main-chain ϕ and Ψ torsional angles of Pro kinks in membrane protein crystal structures and in computer simulations. Pro kinks alter the conformation of a complete turn of the helix, from the Pro residue i to $i - 4$. Thus, the ϕ and Ψ angles of all these residues must be taken into account in the conformational analysis. In the protein survey analysis some of these residues forming the Pro kink will be exposed to the lipidic membrane and others to the core of the protein. In contrast, in the molecular dynamics simulation all these residues will be exposed to the hydrophobic environment made of methane molecules. Moreover, we have searched for Pro kinks with the xxxxP sequence in the crystal structures, where x is any residue except Pro, whereas we have run the AAAAP sequence in the molecular dynamics simulation (see Materials and Methods). Therefore, some divergences between crystal structures and computer simulations are expected due to the effect of the environment and the different residues forming the Pro kink. However, the effect of the environment (see above and Table 1) and the type of residue (Ballesteros et al., 2000; Chakrabarti and Pal, 1998) in the ϕ and Ψ torsional angles are much lower than the influence of the Pro residue in the conformation of the helix (Fig. 3). Fig. 3 shows the evolution of ϕ (squares) and Ψ (circles) torsional angles along the α-helix as observed during the molecular dynamics simulations (black line) and in the crystal structures of membrane proteins (broken line). The helical distortion induced by the Pro residue is clearly seen at the level of the dihedral angles up to residue four positions upstream. Clearly the simulation in the methane environment reproduces the dihedral angles profile of the Pro kink observed in the analysis of crystal structures (see Table 2), indicating that the methane box can reliably reproduce the conformational behavior of helical deformations as well.

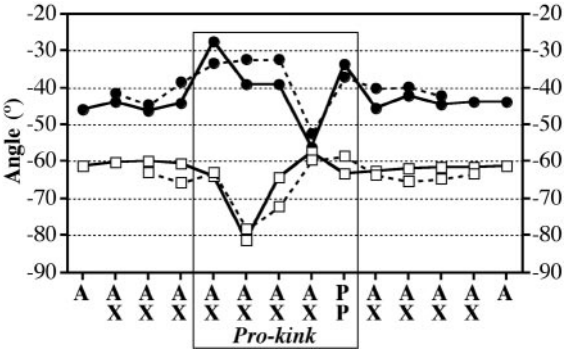

FIGURE 3 Mean values of the ϕ (*squares*) and Ψ (*circles*) torsional angles (degrees) along the α-helix containing the Pro kink as observed during the molecular dynamics simulations (*black line*) and in the crystal structures of membrane proteins (*broken line*). The *x* axis shows the sequence of the helix in the molecular dynamics simulations (*top*) and in the membrane protein survey (*bottom*). A, Ala; P, Pro; X, any residue except Pro.

TABLE 2 Means/standard deviations of the backbone torsion angles (ϕ and ψ, in degrees) of α-helices containing Pro in membrane crystal structures (27 entries) or in molecular dynamics simulations of Pro-containing α-helix in a methane environment (1000 entries)

	Membrane proteins		Molecular dynamics	
Position	ϕ_i	ψ_i	ϕ_i	ψ_i
$i-8$			−61.1/8.2	−46.0/8.3
$i-7$		−41.5/6.6	−60.3/8.2	−43.7/8.2
$i-6$	−62.9/5.9	−44.5/9.5	−59.8/8.0	−46.2/8.3
$i-5$	−65.7/7.7	−38.4/10.7	−60.6/7.9	−44.2/7.5
$i-4$	−62.9/6.7	−33.4/9.1	−63.9/8.2	−27.5/12.0
$i-3$	−78.3/13.1	−32.4/11.3	−81.2/12.6	−38.9/9.5
$i-2$	−72.1/14.3	−32.1/9.2	−64.3/9.2	−39.2/9.9
$i-1$	−59.3/9.2	−52.4/8.7	−57.5/8.7	−56.2/7.3
Pro	−58.5/7.7	−37.0/11.5	−63.1/9.5	−33.7/9.6
$i+1$	−63.7/7.3	−40.2/8.7	−62.4/7.8	−45.6/8.4
$i+2$	−65.3/6.3	−39.8/7.3	−62.0/8.2	−42.0/8.0
$i+3$	−64.7/6.5	−42.2/9.5	−61.4/7.5	−44.4/8.1
$i+4$	−63.1/7.3		−61.6/8.0	−43.8/8.2
$i+5$			−61.2/7.9	−44.0/7.8

The residues that constitute the Pro kink are highlighted.

CONCLUSIONS

The influence of the environment in the conformation of α-helices has been studied by surveying crystal structures of both soluble and membrane proteins and by molecular dynamics simulations of poly-Ala α-helices in water and methane. The results of both approaches show that polar environments tend to decrease ϕ_i and increase Ψ_i, relative to hydrophobic environments. Thus, there is a significant change in the conformation of the α-helix depending whether the peptide bond is exposed to bulk water or to the lipidic membrane. This effect is produced by an additional hydrogen bond between the peptide carbonyl oxygen to a water molecule (Blundell et al., 1983), which is not possible in membrane-embedded α-helices. Moreover, the participation of the carbonyl oxygen in the hydrogen bond with both the N—H group of the residue in the following turn of the helix and the water molecule increases the intramolecular $N_i \cdot\cdot O_{i-4}$ hydrogen bond distance and decreases the $N_i \cdot\cdot O_{i-4} = C_{i-4}$ angle. The fact that the intrahelical hydrogen bond in apolar environments is stronger suggests that α-helices in membrane-embedded proteins are more rigid than in soluble proteins. However, conformational changes in the transmembrane α-helices are necessary to transduce extracellular signals across the membrane (Sansom and Weinstein, 2000). Thus, membrane proteins incorporate in the sequence of their transmembrane helices specific residues like Pro, Gly, Ser, and Thr (Senes et al., 2000), which add flexibility and assist in the conformational change (Ballesteros et al., 2000; Gether et al., 1997; Govaerts et al., 2001a; Palczewski et al., 2000; Ri et al., 1999). Notably, in soluble proteins, these residues are mostly located in loop regions and acts as helix breaker (O'Neil and DeGrado, 1990).

Membrane proteins are particularly difficult to crystallize, yielding to only a few available structures (White and Wimley, 1999). Thus, molecular dynamics simulations are becoming a powerful tool to study the structure and dynamics of membrane proteins (Forrest and Sansom, 2000). We have observed a remarkable coincidence between the ϕ and Ψ angles obtained in the analysis of residues exposed to the lipid in membrane proteins and the results from computer simulations in methane. Thus, the simulation technique described here, where the membrane environment is replaced by explicit methane molecules, is a fast and reliable method that appears to reproduce several important characteristics of membrane-embedded proteins. Similar procedure has been recently used to mimic the membrane in molecular dynamics simulations of the potassium channel (Åqvist and Luzhkov, 2000). This approach is therefore well suited to study, in a reasonable amount of time, conformational arrangements and dynamic behavior of membrane proteins, and study the structural effects of specific mutations in their transmembrane domain (Govaerts et al., 2001b).

This work was supported in part by grants from CICYT (SAF99-073), Fundació La Marató TV3 (0014/97), and the Improving Human Potential of the European Community (HPRI-CT-1999-00071). Computer facilities were provided by the Center de Computació i Comunicacions de Catalunya.

REFERENCES

Åqvist, J., and V. Luzhkov. 2000. Ion permeation mechanism of the potassium channel. *Nature.* 404:881–884.

Ballesteros, J. A., X. Deupi, M. Olivella, E. E. J. Haaksma, and L. Pardo. 2000. Serine and threonine residues bend α-helices in the $\chi1$ = g- conformation. *Biophys. J.* 79:2754–2760.

Barlow, D. J., and J. M. Thornton. 1988. Helix geometry in proteins. *J. Mol. Biol.* 201:601–619.

Blundell, T., D. Barlow, N. Borkakoti, and J. Thornton. 1983. Solvent-induced distortions and the curvature of alpha-helices. *Nature.* 306: 281–283.

Case, D. A., D. A. Pearlman, J. W. Caldwell, T. E. Cheatham, III, W. S. Ross, C. L. Simmerling, T. A. Darden, K. M. Merz, R. V. Stanton, A. L. Cheng, J. J. Vincent, M. Crowley, D. M. Ferguson, R. J. Radmer, G. L. Seibel, U. C. Sing, P. K. Weiner, and P. A. Kollman. 1997. AMBER 5. University of California, San Francisco, CA.

Chakrabarti, P., and D. Pal. 1998. Main-chain conformational features at different conformations of the side-chains in proteins. *Prot. Eng.* 11: 631–647.

Cornell, W. D., P. Cieplak, C. I. Bayly, I. R. Gould, K. M. Merz, Jr., D. M. Ferguson, D. C. Spellmeyer, T. Fox, J. W. Caldwell, and P. A. Kollman. 1995. A second-generation force field for the simulation of proteins, nucleic acids, and organic molecules. *J. Am. Chem. Soc.* 117: 5179–5197.

Darden, T. A., D. York, and L. Pedersen. 1993. Particle mesh Ewald: an N log(N) method for Ewald sums in large systems. *J. Chem. Phys.* 98: 10089–10092.

Fasman, G. D., editor. 1989. Prediction of Protein Structure and the Principles of Protein Conformation. Plenum Press, New York.

Forrest, L. R., and M. S. P. Sansom. 2000. Membrane simulations: bigger and better? *Curr. Opin. Struct. Biol.* 10:174–181.

Gether, U., S. Lin, P. Ghanouni, J. A. Ballesteros, H. Weinstein, and B. K. Kobilka. 1997. Agonists induce conformational changes in transmembrane domains III and VI of the β2 adrenergic receptor. *EMBO J.* 16:6737–6747.

Govaerts, C., C. Blanpain, X. Deupi, S. Ballet, J. A. Ballesteros, S. J. Wodak, G. Vassart, L. Pardo, and M. Parmentier. 2001a. The TxP motif in the second transmembrane helix of CCR5: a structural determinant in chemokine-induced activation. *J. Biol. Chem.* 276:13217–13225.

Govaerts, C., A. Lefort, S. Costagliola, S. Wodak, J. A. Ballesteros, L. Pardo, and G. Vassart. 2001b. A conserved Asn in transmembrane helix 7 is an on/off switch in the activation of the thyrotropin receptor. *J. Biol. Chem.* 276:22991–22999.

Hubbart, S. J., and J. M. Thornton. 1993. NACCESS. Department of Biochemistry and Molecular Biology, University College London.

Kumar, S., and M. Bansal. 1998. Geometrical and Sequence Characteristics of α-helices in globular proteins. *Biophys. J.* 75:1935–1944.

Milner-White, E. J., L. H. Bell, and P. H. Maccallum. 1992. Pyrrolidine ring puckering in *cis* and *trans*-proline residues in proteins and polypeptides. *J. Mol. Biol.* 228:725–724.

Monne, M., M. Hermansson, and G. von Heijne. 1999. A turn propensity scale for transmembrane helices. *J. Mol. Biol.* 288:141–145.

O'Neil, K. T., and W. F. DeGrado. 1990. A thermodynamic scale for the helix-forming tendencies of the commonly occurring amino acids. *Science.* 250:646–651.

Palczewski, K., T. Kumasaka, T. Hori, C. A. Behnke, H. Motoshima, B. A. Fox, I. L. Trong, D. C. Teller, T. Okada, R. E. Stenkamp, M. Yamamoto, and M. Miyano. 2000. Crystal structure of rhodopsin: a G protein-coupled receptor. *Science.* 289:739–745.

Rees, D. C., and D. Eisenberg. 2000. Turning a reference inside-out: commentary on an article by Stenvens and Arkin entitled "Are membrane proteins 'inside-out' proteins?" *Proteins Struct. Funct. Genet.* 38:121–122.

Ri, Y., J. A. Ballesteros, C. K. Abrams, S. Oh, V. K. Verselis, H. Weinstein, and T. A. Bargiello. 1999. The role of a conserved proline residue in mediating conformational changes associated with voltage gating of Cx32 gap junctions. *Biophys. J.* 76:2887–2898.

Sankararamakrishnan, R., and S. Vishveshwara. 1992. Geometry of proline-containing alpha-helices in proteins. *Int. J. Pept. Protein Res.* 39: 356–363.

Sansom, M. S. P., and H. Weinstein. 2000. Hinges, swivels and switches: the role of prolines in signalling via transmembrane α-helices. *Trends Pharmacol. Sci.* 21:445–451.

Senes, A., M. Gerstein, and D. M. Engelman. 2000. Statistical analysis of amino acid patterns in transmembrane helices: the GxxxG motif occurs frequently and in association with β-branched residues at neighboring positions. *J. Mol. Biol.* 296:921–936.

Stevens, T. J., and I. T. Arkin. 1999. Are membrane proteins "inside-out" proteins? *Proteins Struct. Funct. Genet.* 36:135–143.

Von Heijne, G. 1991. Proline kinks in transmembrane alpha-helices. *J. Mol. Biol.* 218:499–503.

White, S. H., and W. C. Wimley. 1999. Membrane protein folding and stability: physical principles. *Ann. Rev. Biophys. Biomol. Struct.* 28: 319–365.

0026-895X/02/6201-15–21$7.00
MOLECULAR PHARMACOLOGY
Vol. 62, No. 1
1395/989397
Mol Pharmacol 62:15–21, 2002
Printed in U.S.A.

Design, Synthesis and Pharmacological Evaluation of 5-Hydroxytryptamine$_{1a}$ Receptor Ligands to Explore the Three-Dimensional Structure of the Receptor

MARÍA L. LÓPEZ-RODRÍGUEZ, BRUNO VICENTE, XAVIER DEUPI, SERGIO BARRONDO, MIREIA OLIVELLA, M. JOSÉ MORCILLO, BELLINDA BEHAMÚ, JUAN A. BALLESTEROS, JOAN SALLÉS, and LEONARDO PARDO

Departamento de Química Orgánica I, Facultad de Ciencias Químicas, Universidad Complutense, Madrid, Spain (M.L.L.-R., B.V., B.B.); Laboratori de Medicina Computacional, Unitat de Bioestadística, Facultat de Medicina, Universitat Autònoma de Barcelona, Barcelona, Spain (X.D., M.O., L.P.); Departamento de Farmacología, Universidad del Pais Vasco, Vitoria, Spain (S.B., J.S.); Facultad de Ciencias, Universidad Nacional de Educación a Distancia, Madrid, Spain (M.J.M.); and Novasite Pharmaceuticals, Inc., San Diego, California (J.A.B.)

Received September 27, 2001; accepted March 21, 2002

This article is available online at http://molpharm.aspetjournals.org

ABSTRACT

In this work, we evaluate the structural differences of transmembrane helix 3 in rhodopsin and the 5-hydroxytryptamine 1A (5-HT$_{1A}$) receptor caused by their different amino acid sequence. Molecular dynamics simulations of helix 3 in the 5-HT$_{1A}$ receptor tends to bend toward helix 5, in sharp contrast to helix 3 in rhodopsin, which is properly located within the position observed in the crystal structure. The relocation of the central helix 3 in the helical bundle facilitates the experimentally derived interactions between the neurotransmitters and the Asp residue in helix 3 and the Ser/Thr residues in helix 5. The different amino acid sequence that forms helix 3 in rhodopsin (basically the conserved Gly$^{3.36}$Glu$^{3.37}$ motif in the opsin family) and the 5-HT$_{1A}$ receptor (the conserved Cys$^{3.36}$Thr$^{3.37}$ motif in the neurotransmitter family) produces these structural divergences. These structural differences were experimentally checked by designing and testing ligands that contain comparable functional groups but at different interatomic distance. We have estimated the position of helix 3 relative to the other helices by systematically changing the distance between the functional groups of the ligands (**1** and **2**) that interact with the residues in the receptor. Thus, ligand **1** optimally interacts with a model of the 5-HT$_{1A}$ receptor that matches rhodopsin template, whereas ligand **2** optimally interacts with a model that possesses the proposed conformation of helix 3. The lack of affinity of **1** ($K_i > 10{,}000$ nM) and the high affinity of **2** ($K_i = 24$ nM) for the 5-HT$_{1A}$ receptor binding sites, provide experimental support to the proposed structural divergences of helix 3 between the 5-HT$_{1A}$ receptor and rhodopsin.

G protein-coupled receptors (GPCRs) are membrane proteins that transmit extracellular signals of neurotransmitters, peptides, and glycoproteins through heterotrimeric G proteins bound in the interior of the cell (Ji et al., 1998). The GPCR family possesses highly conserved motifs in the transmembrane region (Ballesteros and Weinstein, 1995; Horn et al., 1998), which suggests a common transmembrane structure. Recently, the detailed three-dimensional (3-D) structure of the GPCR rhodopsin (RHO) was determined at 2.8-Å resolution (Palczewski et al., 2000). This structure has confirmed that RHO and probably the RHO family of GPCRs are formed by a highly organized heptahelical transmembrane bundle. This structural homology between RHO and the other GPCRs probably does not extend to the extracellular domain, for which there is very little homology, and is highly structured in RHO, blocking the access of the extracellular ligand to the core of the receptor (Bourne and Meng, 2000).

The amino acid residues involved in ligand binding have been primarily identified by pharmacological and mutagenesis studies [for review, see van Rhee and Jacobson (1996)]. In particular, agonists and antagonists of the neurotransmitter subfamily of GPCRs bind with their protonated amine to the conserved Asp$^{3.32}$ (see *Materials and Methods* for the receptor-numbering scheme), in transmembrane helix (TMH) 3 (Strader et al., 1988). The hydroxyl groups present in the chemical structure of many neurotransmitters seem to hydrogen bond (Strader et al., 1989; Liapakis et al., 2000) a series of conserved Ser/Thr residues (5.42, 5.43, and 5.46), in TMH 5. Moreover, mutagenesis experiments on the α_2- (Suryanarayana et al., 1991), β_2- (Suryanarayana and Kobilka, 1993), 5-HT$_{1A}$ (Guan et al., 1992), and 5-HT$_{1B}$ (Glennon et al., 1996) receptors have shown that Asn$^{7.39}$, in TMH

This work was supported in part by grants from Dirección General de Investigación Científica y Tecnológica (PB97-0282), Comisión Interministerial de Ciencia y Tecnologica (SAF98–0064-C02 and SAF99-0073), Comunidad de Madrid (08.5/0079/2000), Universidad del Pais Vasco (G15/98), and Fundació La Marató TV3 (0014/97).

ABBREVIATIONS: GPCRs, G protein coupled receptors; 3-D, three-dimensional; RHO, rhodopsin; TMH, transmembrane helix; 5-HT$_{1A}$R, 5-hydroxytryptamine$_{1A}$ receptor; EF-7412, 2-[4-[4(*m*-ethylsulfonamido)-phenyl)piperazin-1-yl[butyl]-1,3-dioxoperhydropyrrolo[1,2-*c*]imidazole.

7, is important in conferring specificity to a series of ligands such as pindolol and propanolol.

The publication of the crystal structure of RHO has provided the arrangement of the TMHs in the cell membrane (Palczewski et al., 2000). The central TMH 3 is near TMH 5 in its cytoplasmic end and far from TMH 5 in its extracellular end, which hinders the binding of the small neurotransmitter molecules between $Asp^{3.32}$ and the implicated $Ser/Thr^{5.42,5.43,5.46}$ residues, located at the extracellular side. This finding was previously noted in the translation of the electron density maps of frog RHO (Unger et al., 1997) into an α-carbon template (Baldwin et al., 1997). Thus, the following factor should be taken into account. Wide ranges of extracellular ligands, from small neurotransmitters to large peptides and hormones, are recognized by the different GPCR subfamilies. Each subfamily has probably developed specific structural motifs that allow the receptor to accommodate the different extracellular ligands. Interestingly, RHO possesses two nonconserved successive Gly residues at positions 89 ($Gly^{2.56}$) and 90 ($Gly^{2.57}$). This specific motif of the opsin family induces a significant distortion of TMH 2, which bends strongly toward TMH 1 (Palczewski et al., 2000). In contrast, the chemokine family of GPCR possesses in this region of TMH 2 a conserved $Thr^{2.56}XPro^{2.58}$ motif, where X is any amino acid. We have recently shown that this TxP motif in CCR5 bends TMH 2 toward the center of the bundle and away from TMH 1 (Govaerts et al., 2001a). Moreover, this structural singularity is important for chemokine-induced functional response (Govaerts et al., 2001a). Thus, the presence of specific and conserved residues among the families of GPCR may result in structural differences among them. The similarities and differences between RHO and other GPCRs have recently been reviewed in detail (Ballesteros et al., 2001).

In this work, we aim to evaluate the structural differences of TMH 3 in RHO and the 5-HT_{1A} receptor (5-HT_{1A}R) caused by their different amino acid sequence. The conformation of TMH 3 in the neurotransmitter family of GPCR changes the location of $Asp^{3.32}$ and in consequence where the extracellular ligand is placed. Thus, we aim to estimate the position of TMH 3 relative to the other helices, primarily TMH 5 and 7 where ligands bind, in the inactive conformation of the 5-HT_{1A}R. Several approaches have been developed to elucidate intermolecular distances between helices: double revertant mutant constructs (Zhou et al., 1994), spin labeling (Yang et al., 1996), zinc site engineering (Elling et al., 1995, 1999), and Cys crosslinking (Yu et al., 1995). We have developed a new approach in which the distance between the functional groups of the ligand that interact with the residues in the receptor is systematically varied. This procedure has allowed us to discern between conformations of the receptor obtained computationally. Antagonists are preferred over agonists to explore the inactive form of the receptor. Recently, we have reported the pharmacological characterization of EF-7412 as an antagonist in vivo in pre- and postsynaptic 5-HT_{1A}R sites (Lopez-Rodriguez et al., 2001a,b). We have designed, synthesized, and pharmacologically evaluated a new set of compounds, using EF-7412 as a template, to discern between computer models of the 5-HT_{1A}R.

Materials and Methods

Residue Numbering Scheme. Each transmembrane residue is numbered with the helix number (from 1 to 7) in which it is located plus its relative position to the most conserved residue in the helix, arbitrarily labeled 50 (Ballesteros and Weinstein, 1995). Therefore, the most conserved TMH 3 residue is designated with the index number 3.50 ($Arg^{3.50}$). The Asp preceding the Arg in the (D/E)RY motif is designated $Asp^{3.49}$, and the Tyr after the Arg is designated $Tyr^{3.51}$.

Molecular Dynamics Simulations of TMH 3 in RHO and the 5-HT_{1A}R. The peptide corresponding to the residues from 3.22 to 3.54 in TMH 3 of RHO (Ace-PTGCYFEGFFATLGGEIALWSLVV-LAIERYVVV-NMe), and the 5-HT_{1A}R (Ace-QVTCDLFIALDVL-CCTSSILHLCAIALDRYWAI-NMe), were built in the standard α-helix conformation (backbone dihedral angles ϕ and ψ of -58 and -47 degrees). All ionizable residues in the helices were considered uncharged. The structures obtained were placed in a rectangular box containing methane molecules (2693 and 3095 for RHO and 5-HT_{1A}R, respectively) to mimic the hydrophobic environment of the TMHs. A similar procedure has recently been employed to mimic the membrane in molecular dynamics simulations of the thyrotropin receptor (Govaerts et al., 2001b) and TMH 2 of the CCR5 receptor (Govaerts et al., 2001a). The sizes of the boxes were $74.5 \times 43.5 \times 41.0$ Å for RHO, and $76.5 \times 45.5 \times 41.5$ Å for 5-HT_{1A}R. The systems were energy-minimized (500 steps), heated (from 0 to 300°K in 15 ps), equilibrated (from 15 to 500 ps) and the production run (from 500 to 1000 ps) was carried out at constant volume using the particle mesh Ewald method to evaluate electrostatic interactions. Structures were collected every 5 ps during the last 500 ps of simulation (100 structures per simulation). The molecular dynamics simulations were run with the Sander module of AMBER 5 (http://www.amber.ucsf.edu/amber/amber.html), the all-atom force field (Cornell et al., 1995), SHAKE bond constraints in all bonds, a 2-fs integration time step, and constant temperature of 300°K coupled to a heat bath.

The logistic regression model (Hosmer and Lemeshow, 1989) was used to fit the binary dependent variable (RHO, 5-HT_{1A}R) to the independent variables: the torsional angles (ϕ and Ψ) of the residues spanning from 3.33 to 3.48 (32 variables) obtained during the molecular dynamics trajectory (a total of 200 structures). In contrast to the standard regression analysis, the dependent variable in the logistic regression is discrete, taking only two possible values (RHO and 5-HT_{1A}R). The stepwise method was employed to select the independent variables in the model. Thus, only the torsional angles ϕ and Ψ that better classify the structures as RHO or 5-HT_{1A}R are included in the regression equation. The odds ratio is a function of the coefficient of the independent variable in the regression equation and measures how many times it is more likely to be RHO or 5-HT_{1A}R with a decrease or an increase of 1° in the torsional angles (independent variables). The larger the value of the odds ratio, the more predictive the independent variable is. Independent variables with odds ratio of 1 indicates no predictive power. Calculations were performed with SAS 6.11 (SAS Institute, Cary, NC).

A Molecular Model of the 5-HT_{1A}R. The 3-D model of the transmembrane domain of the 5-HT_{1A}R was constructed by computer-aided model building techniques from the crystal structure of RHO (Palczewski et al., 2000) (PDB access number 1F88). Conserved residues Asn^{55} (residue number in the PDB file of RHO) and Asn^{54} (residue number in the human 5-HT_{1A}R sequence) [$Asn^{1.50}$ in the generalized numbering scheme (Ballesteros and Weinstein, 1995)]; Asp^{83} and Asp^{82} ($Asp^{2.50}$); Arg^{135} and Arg^{134} ($Arg^{3.50}$); Trp^{161} and Trp^{161} ($Trp^{4.50}$); Pro^{215} and Pro^{207} ($Pro^{5.50}$); Pro^{267} and Pro^{360} ($Pro^{6.50}$); and Pro^{303} and Pro^{397} ($Pro^{7.50}$) were employed in the alignment of RHO and human 5-HT_{1A}R transmembrane sequences. All ionizable residues in the helices were considered uncharged with the exception of $Asp^{2.50}$, $Asp^{3.32}$, $Asp^{3.49}$, $Arg^{3.50}$, and $Glu^{6.30}$. SCWRL-2.1 was employed to add the side chains of the nonconserved residues based on a backbone-dependent rotamer library (Dunbrack and Co-

hen, 1997). This computer model, which maintains the position of the TMHs as in RHO, is denoted 5-HT$_{1A}$R^{RHO}. TMH 3 was then replaced by the most representative structure of the geometries obtained during the molecular dynamics trajectory of TMH 3 in 5-HT$_{1A}$R (see above). This representative structure was selected by automatically clustering the collected geometries into conformationally related subfamilies with the program NMRCLUST (Kelley et al., 1996). The backbone of the highly conserved E/DR$^{3.50}$Y motif superimposed the structures. This computer model, which changes relative to 5-HT$_{1A}$R^{RHO} the position of TMH 3 at the extracellular side, is denoted 5-HT$_{1A}$R^{MD}.

The initial structure of the complex between (±)-2-[4-[4-(6-hydroxy-2-pyridyl)piperazin-1-yl]butyl]-1,3-dioxoperhydropyrrolo[1,2-*c*]imidazole (**1**) and (±)-2-[4-[4-(*m*-(acetylamino)phenyl)piperazin-1-yl]butyl]-1,3-dioxoperhydropyrrolo[1,2-*c*]imidazole (**2**) and the 5-HT$_{1A}$R was obtained from the previously reported structure of the complex between EF-7412 and the 5-HT$_{1A}$R (Lopez-Rodriguez et al., 2001b). Subsequently, the complete systems were energy-minimized (5000 steps). Energy minimizations were run with the Sander module of AMBER 5 (http://www.amber.ucsf.edu/amber/amber.html), the all-atom force field (Cornell et al., 1995), and a 13-Å cutoff for nonbonded interactions. Parameters for ligands **1** and **2** were adapted from the force field of Cornell et al. (1995) using RESP point charges (Cieplak et al., 1995).

Chemistry. Derivative **1** was synthesized by the following procedure: 2.0 ml of triethylamine (1.5 g, 14.6 mmol) was added to a suspension of 2.5 g (9 mmol) of 2-(4-bromobutyl)-1,3-dioxoperhydropyrrolo[1,2-*c*]imidazole (Lopez-Rodriguez et al., 1996) and 2.7 g (15 mmol) of 1-(6-hydroxy-2-pyridyl)piperazine (Pavia et al., 1987) in 19 ml of acetonitrile. The mixture was refluxed for 20 to 24 h (thin-layer chromatography). Then, the solvent was evaporated under reduced pressure and the residue was resuspended in water and extracted with dichloromethane (3 × 100 ml). The combined organic layers were washed with water and dried over $MgSO_4$. After evaporation of the solvent, the crude oil was purified by column chromatography (dichloromethane) to afford 1.1 g (33%) of **1**, which was converted into the hydrochloride salt. Derivative **2** was synthesized by the following procedure: 0.11 ml (1.6 mmol) of acetyl chloride was added dropwise to a solution of 600 mg (1.6 mmol) of 2-[4-[4-(*m*-aminophenyl)piperazin-1-yl]butyl]-1,3-dioxoperhydropyrrolo[1,2-*c*]imidazole (Lopez-Rodriguez et al., 2001a) in 20 ml of pyridine at 0°C. After stirring at room temperature for 1.5 h (thin-layer chromatography), the mixture was diluted with 50 ml of methylene chloride and washed with a saturated aqueous solution of $CuSO_4$, water, and brine (25 ml). The organic layer was dried (Na_2SO_4) and the solvent evaporated under reduced pressure to afford 668 mg (67%) of **2**, which was converted to the hydrochloride salt. The new compounds were characterized by IR and ^{1}H- and ^{13}C-NMR spectroscopy and gave satisfactory combustion analyses (C, H, N).

Radioligand Binding Assays. The 5-HT$_{1A}$ receptor binding studies were performed by a modification of a procedure described previously (Clark et al., 1990). The cerebral cortices of male Sprague-Dawley rats (*Rattus norvegicus albinus*) weighing 180 to 200 g were homogenized in 10 volumes of ice-cold Tris buffer (50 mM Tris-HCl, pH 7.7 at 25°C) and centrifuged at 28,000*g* for 15 min. The membrane pellet was washed twice by resuspension and centrifugation. After the second wash, the resuspended pellet was incubated at 37°C for 10 min. Membranes were then collected by centrifugation and the final pellet was resuspended in 50 mM Tris-HCl, 5 mM $MgSO_4$, and 0.5 mM EDTA buffer, pH 7.4 at 37°C. Fractions of the final membrane suspension (about 1 mg of protein) were incubated at 37°C for 15 min with 0.6 nM [^{3}H]8-hydroxy-2-dipropylaminotetralin (133 Ci/mmol), in the presence or absence of several concentrations of the competing drug, in a final volume of 1.1 ml of assay buffer (50 mM Tris-HCl, 10 nM clonidine, 30 nM prazosin, pH 7.4 at 37°C). Incubation was terminated by rapid vacuum filtration through Whatman GF/B filters, presoaked in 0.05% poly(ethylenimine), using a Brandel cell harvester. The filters were then washed with the assay buffer and dried. The filters were placed in poly(ethylene) vials to which 4 ml of a scintillation cocktail (Aquasol) was added, and the radioactivity bound to the filters was measured by liquid scintillation spectrometry. The data were analyzed by an iterative curve-fitting procedure (Prism; GraphPad Software, San Diego, CA), which provided IC_{50}, K_i, and r^2 values for test compounds; K_i values were calculated from the Cheng and Prusoff equation (Cheng and Prusoff, 1973). The protein concentrations of the rat cerebral cortex were determined by the method of Lowry et al. (1951) using bovine serum albumin as the standard. Nonspecific binding was determined with 10 μM 5-HT. Competing drug, nonspecific, total and radioligand bindings were defined in triplicate.

Results and Discussion

Amino Acid Composition of TMH 3 in the Opsin and Neurotransmitter Families of GPCR. We analyze in this section the amino acid sequence of TMH 3 in the opsin and neurotransmitter families that might cause structural differences in the helix. These differences are relevant because the crystal structure of RHO (Palczewski et al., 2000) is an appropriate template to model the 3-D structure of receptors for neurotransmitters and the conformation of TMH 3 in the neurotransmitter family changes the location of Asp$^{3.32}$, the anchoring point of both agonists and antagonists (Strader et al., 1988; van Rhee and Jacobson, 1996). The intracellular side of TMH 3 contains in both cases the highly conserved E/DR$^{3.50}$Y motif. The protonation of E/D$^{3.49}$ is thought to be important in G-protein coupling (Arnis et al., 1994; Oliveira et al., 1994; Scheer et al., 1996). We assume that this common E/DR$^{3.50}$Y motif, in the compact cytoplasmatic surface, is hold in similar position in both families. Thus, the location of the amino acid 3.32 in the opsin and the neurotransmitter families, relative to the E/DR$^{3.50}$Y motif, will depend on the amino acid composition of the residues spanning from 3.33 to 3.48.

Table 1 shows the statistical analysis of the conservation pattern in this continuous stretch of residues from 3.33 to 3.48 of all GPCR sequences denoted as (Rhod)opsin (245 entries) and Amine (288 entries) in GPCRDB (Horn et al., 1998), as of December 2001. Ser or Thr or Cys residues are present in 6 of 16 positions (3.35, 3.36, 3.37, 3.39, 3.44, and

TABLE 1

Statistical analysis of the conservation pattern in a continuous stretch of residues from 3.33 to 3.48 in TMH 3 of all GPCR sequences denoted as (Rhod)opsin and Amine in GPCRDB.

The position in the helix, the amino acid most often present at this position, and the population of this amino acid in the family are shown.

Position	(Rhod)opsin	Amine
	%	
3.33	Thr 51.4	Val 64.6
3.34	Leu 65.7	Leu 51.0
3.35	Gly 50.0	Cys 53.1
3.36	Gly 98.8	Cys 56.9
3.37	Glu 34.3	Thr 85.1
3.38	Ile 33.1	Ala 82.6
3.39	Ala 41.2	Ser 100.0
3.40	Leu 66.9	Ile 85.8
3.41	Trp 85.3	Leu 43.4
3.42	Ser 77.1	Asn 42.4
3.43	Leu 80.4	Leu 89.9
3.44	Val 40.8	Cys 72.6
3.45	Val 55.5	Ala 41.7
3.46	Leu 54.3	Ile 92.1
3.47	Ala 75.9	Ser 65.3
3.48	Ile 33.5	Leu 42.0

3.47) more than 50% of the time in the neurotransmitter family, in sharp contrast to the opsin family, which contains only two positions (3.33 and 3.42). Ser, Thr, and Cys residues play a special role in α-helices because they can form an intrahelical hydrogen bond between the side chain OH_γ (or SH_γ) and the i-3 or i-4 carbonyl oxygen of the preceding turn (Gray and Matthews, 1984). This additional hydrogen bond to the peptide carbonyl oxygen can produce significant changes in the curvature of the helix (Ballesteros et al., 2000; Govaerts et al., 2001a). It is important to note that Ser, Thr, and Cys are not present simultaneously in the opsin and the neurotransmitter families in the 3.33–3.48 range (Table 1). Besides, there are two amino acid sites in the TMH 3 domain of the opsin family at which a Gly is present in more than 50% of the receptors: $Gly^{3.35}$ (50.0%) and $Gly^{3.36}$ (98.8%). Gly is most often located in loop regions and acts as helix-breaker in soluble proteins (O'Neil and DeGrado, 1990). In contrast, Gly residues are frequently detected in the transmembrane segments of membrane proteins (Senes et al., 2000) which suggests a structural role. The absence of the side chain in Gly probably adds flexibility to Gly-containing helices (Kumar and Bansal, 1998). The neurotransmitter family possesses Cys residues at these 3.35 and 3.36 positions. Thus, the different attributes of the amino acids forming TMH 3 in the opsin and the neurotransmitter families can produce significant structural deviations among them.

Molecular Dynamics Simulations of TMH 3 in RHO and the 5-HT_{1A}R. To obtain a rough idea of the possible consequences that the different amino acid sequences that form TMH 3 in rhodopsin and the 5-HT_{1A}R might have on the structure, we performed a molecular modeling exercise using the 3-D structure of rhodopsin as the template (Palczewski et al., 2000). Figure 1, a (view parallel to the membrane with the extracellular side at the top) and b (perpendicular to the membrane from the extracellular side), show the result of superimposing the structures computed during the molecular dynamics trajectory (see *Materials and Methods* for computational details) of the amino acid sequence that form TMH 3 in RHO (orange) and the 5-HT_{1A}R (green) on TMH 3 of RHO. The backbone of the highly conserved $E/DR^{3.50}Y$ motif superimposed the computed structures and the helix bundle of RHO. This procedure hypothesizes that the common $E/DR^{3.50}Y$ motif is located in similar positions in rhodopsin and the 5-HT_{1A}R. Visual inspection of the helix axes of the computed structures in Fig. 1, a and b, reveal that TMH 3 in RHO and the 5-HT_{1A}R behaves differently. The conformational space explored by the extracellular part of TMH 3 in the 5-HT_{1A}R is precisely toward TMH 5. In contrast, the energetically available structures of RHO are distant to TMH 5, basically within the position of TMH 3 in the crystal structure.

The logistic regression model (see *Materials and Methods* for computational details) was employed to characterize the amino acid positions in RHO and the 5-HT_{1A}R that most influence the structural differences observed in TMH 3. The binary dependent variable (RHO, 5-HT_{1A}R) was fitted to the torsional angles (Φ and Ψ) of the residues spanning from 3.33 to 3.48. Table 2 shows the torsional angles selected in the stepwise procedure and the odds ratio of the included variables. The torsional angles Φ of the residue at position 3.35 ($\Phi_{3.35}$); Φ and Ψ at positions 3.36 and 3.37 ($\Phi_{3.36}$, $\Phi_{3.37}$, $\Psi_{3.36}$, and $\Psi_{3.37}$); and Ψ at positions 3.39, 3.43, and 3.46 ($\Psi_{3.39}$, $\Psi_{3.43}$, and $\Psi_{3.46}$), properly classify 100% of the input conformations of RHO and the 5-HT_{1A}R. However, the predictive power of the selected torsions is not the same. The variables $\Phi_{3.36}$, $\Phi_{3.37}$, $\Psi_{3.36}$, and $\Psi_{3.37}$ possess the highest odds ratio (Table 2) and thus the highest classification power. A logistic regression model with only these four independent variables

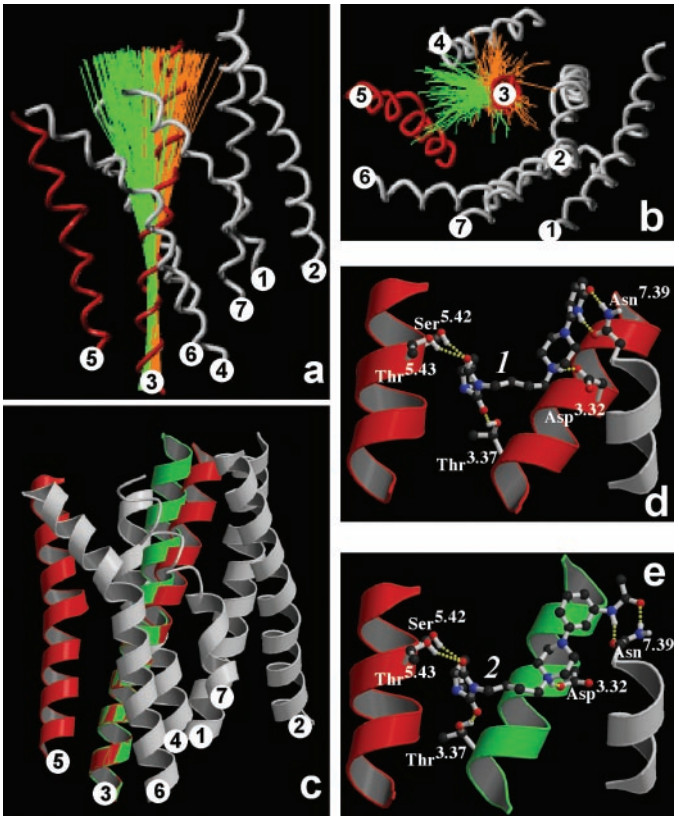

Fig. 1. a and b, the α-carbon traces of the transmembrane helix bundle of RHO (Palczewski et al., 2000) are depicted as tube ribbons in red for TMHs 3 and 5 and white for the other TMHs. The views are parallel to the membrane with the extracellular side at the top (a) and perpendicular to the membrane from the extracellular side (b). The helix axes of the structures computed during the molecular dynamics trajectory of the amino acid sequence that form TMH 3 in RHO (orange) and the 5-HT_{1A}R (green) are displayed. c, the representative structure of the geometries obtained during the molecular dynamics trajectory of TMH 3 in the 5-HT_{1A}R (green helix axes) is shown in green. d and e, detailed view of the transmembrane helix bundle of 5-$HT_{1A}R^{RHO}$ complexed with ligand **1** (d) and 5-$HT_{1A}R^{MD}$ complexed with ligand **2** (e). The C_α traces of the extracellular part (top) of TM 3, 5, and 7 are only shown. Nonpolar hydrogens are not depicted to offer a better view of the recognition pocket. Figures were created using MolScript ver. 2.1.1 (Kraulis, 1991) and Raster3D ver. 2.5 (Merritt and Bacon, 1997).

TABLE 2

Torsional angles and its odds ratio of the selected variables in the stepwise logistic regression between the binary dependent variable (RHO, 5-HT_{1A}R) and the torsional angles (Φ and Ψ) obtained during the molecular dynamics trajectory of the residues spanning from 3.33 to 3.48.

$Torsion_{Position}$	Odds ratio
$\Phi_{3.35}$	2.0
$\Phi_{3.36}$	4.5
$\Psi_{3.36}$	5.0
$\Phi_{3.37}$	2.3
$\Psi_{3.37}$	2.9
$\Psi_{3.39}$	1.7
$\Psi_{3.43}$	1.4
$\Psi_{3.46}$	1.7

already classifies 93% of the input conformations. Remarkably, Gly$^{3.36}$ is highly conserved in the opsin family (98.8%) but not in the neurotransmitter family that contains Cys (56.9%). Substitution of Gly$^{3.36}$ in RHO with more bulky residues promotes partial agonist activity of 11-*cis*-retinal (Han et al., 1997). Thr$^{3.37}$ is present 85.1% of the time in the neurotransmitter family and is absent in the opsin family (Glu 34.3%, Ile 21.8%). It is important to note that Thr$^{3.37}$ is not present in the 5-HT$_6$ and muscarinic receptor subfamilies (see *Conclusions*). Substitution of Thr$^{3.37}$ in the α_{1B}-adrenergic receptor by Ala produces epinephrine and norepinephrine to behave as partial agonists (Cavalli et al., 1996). The same authors concluded that Thr$^{3.37}$ might play a role in preserving the receptor structure and function rather than directly interacting with the agonist (Cavalli et al., 1996).

We propose that the different structural properties of Gly$^{3.36}$Glu$^{3.37}$ in the opsin family and Cys$^{3.36}$Thr$^{3.37}$ in the neurotransmitter family produce different TMH 3 orientations. This results in structural divergences between the neurotransmitter family of GPCR and RHO template (Palczewski et al., 2000). The absence of Thr$^{3.37}$ in the muscarinic receptors also suggests structural divergences relative to the other members of the neurotransmitter family. Incorporation into the RHO template (white and red transmembrane helix bundle in Fig. 1c) of a representative conformation of TMH 3 (green transmembrane helix in Fig. 1c; see *Materials and Methods* for computational details) results in a significant displacement of Asp$^{3.32}$ toward TMH 5, without modifying the more compact cytoplasmatic surface. This relocation facilitates the experimentally derived interactions between the neurotransmitters and the Ser/Thr residues in TMH 5. In particular, Ser$^{5.42}$ and Thr$^{5.43}$ are important in the binding of agonists to the 5-HT$_{1A}$R (Ho et al., 1992). The magnitude of the relocation might be estimated from the structures depicted in Fig. 1c. Thus, the distances between the α-carbon positions of the implicated Asp$^{3.32}$ and Ser$^{5.42}$ and Thr$^{5.43}$ residues in the RHO template (5-HT$_{1A}$R^{RHO}, see methods) are 14.6 and 15.9 Å, respectively. These distances decrease to 12.6 and 14.1 Å if the obtained conformation of TMH 3 from the 5HT$_{1A}$R is incorporated into the RHO template (5-HT$_{1A}$R^{MD}).

It must be stressed that there may be other structural variations that could facilitate the binding of neurotransmitter to their receptors. We must be open to the possibility that the different sequence of the other transmembrane helices might also cause structural differences as well. However, the conservation of functionally important sequence motifs within the rhodopsin-like GPCR family has been interpreted to mean that the basic characteristics of the rhodopsin fold are similar in the different receptor subtypes. We propose that structural adaptation of a receptor to its cognate ligand is necessary in some domains of the transmembrane region while still maintaining a similar overall rhodopsin fold. We hypothesize structural differences only in TMH 3, whereas the other transmembrane helices remain unchanged relative to the RHO template.

Design and Test of 5-HT$_{1A}$R Ligands That Interact with Asp$^{3.32}$ and Asn$^{7.39}$ to Discern between the Conformation of TMH 3. We aim to provide experimental support to the proposed conformation of TMH 3 by designing and testing 5-HT$_{1A}$R ligands that contain comparable functional groups but differ in the interatomic distance between them. The rationale behind this approach is that by varying the distance between the functional groups of the ligand that interact with the side chains of the receptor, we will be able to discern between the computer models of TMH 3. EF-7412 (see Table 3), a recent pharmacologically characterized antagonist in vivo in pre- and postsynaptic 5-HT$_{1A}$R sites (Lopez-Rodriguez et al., 2001a), will be used as a template. It was proposed that EF-7412 forms an ionic interaction with Asp$^{3.32}$ throughout the protonated amine of the piperazine ring, hydrogen bonds with Asn$^{7.39}$ throughout the *m*-NHSO$_2$Et group, and hydrogen bonds with Thr$^{3.37}$, Ser$^{5.42}$, and Thr$^{5.43}$ throughout the hydantoin moiety of the ligand (Lopez-Rodriguez et al., 2001b). A first approach would be to change the distance between the protonated amine of the piperazine ring and the hydantoin moiety of the ligand to assess the conformation of TMH 3 relative to TMH 5. However, the flexibility of the –CH$_2$ chain connecting both groups would impede to obtain any reliable conclusion. Nevertheless, the bending of TMH 3 toward TMH 5 also modifies the position of TMH 3 relative to TMH 7 at the extracellular site. Thus, we have designed 5-HT$_{1A}$R ligands that intended to interact with Asp$^{3.32}$ and Asn$^{7.39}$, to discriminate the conformation of TMH 3 relative to TMH 7. Remarkably, these two positions have also been used to elucidate intermolecular distances by zinc site engineering experiments: substitution of Asp$^{3.32}$ for His and Asn$^{7.39}$ for Cys in the β_2-adrenergic receptor results in a mutant that is activated by free zinc ions (Elling et al., 1999).

Table 3 shows the chemical structures of compounds **1** and **2**. These ligands replace the *m*-NHSO$_2$Et group of EF-7412 with a common –NHCO group that optimally interacts with the side chain of Asn$^{7.39}$. This –NHCO group is located at different positions in the structure relative to the protonated amine. The interatomic distance between the nitrogen of the protonated amine and the centroid of the –NHCO group for compounds **1** and **2** are 6.4 and 8.5 Å, respectively. Structures **1** and **2** were optimized (see *Materials and Methods* for computational details) inside 5-HT$_{1A}$R^{RHO} and 5-HT$_{1A}$R^{MD} models, respectively. Figure 1, d and e, show **1** and **2**, respectively, in the binding pocket. The unique N-H group of the protonated amine of both ligands interacts with one of the O$_\delta$ atoms of Asp at the optimized distance between heteroatoms

TABLE 3
In vitro binding data of compounds EF-7412, 1, and 2
All values are the mean ± S.E.M. of two to four experiments performed in triplicate.

Compound		5-HT$_{1A}$ [^{3}H]8-OH-DPAT
		nM
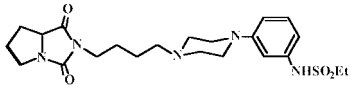	**EF-7412**	27 ± 8
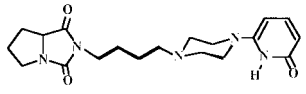	**1**	> 10,000
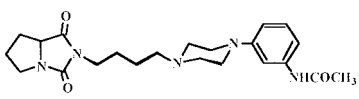	**2**	24 ± 2

From Lopez-Rodriguez et al. (2001a, b).
8-OH-DPAT, 8-hydroxy-2-dipropylaminotetralin.

of 2.5 Å in both cases. Moreover, the N-H moiety of the common –NHCO group acts as a hydrogen bond donor in the hydrogen bond interaction with the $O_{\delta 1}$ atom of Asn, at the optimized distances between heteroatoms of 2.8 Å in both ligands, and the C═O moiety of –NHCO group acts as a hydrogen bond acceptor in the hydrogen bond interaction with the $N_{\delta 2}$-H moiety of Asn, at the optimized distances between heteroatoms of 2.8 or 2.9 Å for ligands **1** or **2**, respectively. Moreover, the proposed recognition of the extracellular ligands involves the hydrogen bonds between both C═O groups of the hydantoin moiety of the ligand and $Thr^{3.37}$ (2.9 Å in both ligands), $Ser^{5.42}$ (3.5 Å) and $Thr^{5.43}$ (3.5 Å). Thus, **1** interacts optimally with 5-$HT_{1A}R^{RHO}$, which matches RHO template, whereas **2** optimally interacts with 5-$HT_{1A}R^{MD}$, which possesses the proposed conformation of TMH 3. It is important to note that the interaction of the –NHCO group of ligand **2** with $Asn^{7.39}$ would benefit from a more bent conformation of TMH 3, which located the helix closer to TMH 5 and farther from TMH 7 at the extracellular part. This more extreme conformation was energetically accessible during the molecular dynamics trajectory of TMH 3 (see above). However, this conformational subfamily was not selected as the most representative in the automatic clustering procedure with the program NMRCLUST and was not used in the construction of 5-$HT_{1A}R^{MD}$ (see *Materials and Methods*).

Table 3 shows the in vitro affinity of compounds **1** (K_i > 10,000 nM) and **2** (K_i = 24 nM) for the 5-HT_{1A}R binding sites. The lack of affinity of **1**, which was designed to match RHO template (5-$HT_{1A}R^{RHO}$), and the high affinity of **2**, which was designed to interact with a modified template of RHO (5-$HT_{1A}R^{MD}$), provides experimental support to the proposed structural divergences of TMH 3 between the 5-HT_{1A}R and RHO.

Conclusions

We have presented in this study a structural analysis of the conformation of TMH 3 in RHO and the 5-HT_{1A}R in the context of the crystal structure of RHO (Palczewski et al., 2000). This analysis is relevant because the structure of RHO is normally used as a template to model the class A family of GPCRs and the conformation of TMH 3 in the neurotransmitter family changes the location of $Asp^{3.32}$, the anchoring point of both agonists and antagonists (Strader et al., 1988; van Rhee and Jacobson, 1996). The different amino acid sequence of TMH 3 in RHO (basically the conserved $Gly^{3.36}Glu^{3.37}$ motif in the opsin family) and the 5-HT_{1A}R (the conserved $Cys^{3.36}Thr^{3.37}$ motif in the neurotransmitter family) produces significant structural divergences. Molecular dynamics simulations of the amino acid sequence that forms TMH 3 in the 5-HT_{1A}R tends to bend toward TMH 5, in sharp contrast to the amino acid sequence that forms TMH 3 in RHO, which is properly located within the position observed in the crystal structure. The relocation of the central TMH 3 facilitates the experimentally derived interactions between the neurotransmitters and the Asp residue in TMH 3 and the Ser/Thr residues in TMH 5.

We have designed two new ligands (**1** and **2**) that are thought to interact, in addition to other residues in the 5-HT_{1A}R, with $Asp^{3.32}$ in TMH 3 and $Asn^{7.39}$ in TMH 7. Ligand **1** interacts optimally with a model of the 5-HT_{1A} receptor that matches rhodopsin template, whereas ligand **2** interacts optimally with a model that possesses the proposed conformation of helix 3. The lack of affinity of **1** (K_i > 10,000 nM) and the high affinity of **2** (K_i = 24 nM) for the 5-HT_{1A}R binding sites provides experimental support to the proposed structural divergences of helix 3 between the 5-HT_{1A}R and RHO. The significant difference in affinity (K_i > 10000 nM versus K_i = 24 nM) between these similar compounds that contain comparable functional groups led us to suggest that the 5-HT_{1A}R binding sites are not flexible and the extracellular ligand must be accommodated in the binding site in an optimal manner.

Statistical analysis of the conservation pattern at the 3.37 position shows that Thr (85.1%) is present in all the neurotransmitter family of GPCRs apart from the 5-HT_6 receptor which contains Ser (2.4%) and the muscarinic receptors which contains Asn (10.8%). All these polar side chains can form intrahelical hydrogen bonds with the backbone and bend helices (Ballesteros et al., 2000). There is more degree of variability across neurotransmitter receptors at the 3.36 locus. Cys (56.9%) is present in the α-adrenergic, dopamine (with the exception of D_1), histamine (with the exception of H_1), and serotonin (with the exception of 5-HT_2 and 5-HT_4) subfamilies of receptors; Ser (28.5%) is present in the D_1, H_1, 5-HT_2, and muscarinic receptors; Thr (1.7%) is present in the 5-HT_4 receptor; and Val (12.1%) is present in the β-adrenergic subfamily of receptors. The side chains of both Ser and Thr can form hydrogen bonds with the backbone (Ballesteros et al., 2000), the side chain of Cys can also form hydrogen bonds with the backbone but of less strength, and the nonpolar side chain of Val cannot form hydrogen bonds. We have shown recently that the impairment of CCR5 receptor activation caused by the T82V, T82C, and T82S mutations parallels with the bending of the α-helix caused by these residues (Govaerts et al., 2001a). Thus, the presence of Thr, Ser, Cys, or Val alters to a greater or lesser degree the conformation of the helix. The wide range of bending and twisting that can result from the presence of these residues in TMH 3 has recently been illustrated (Ballesteros et al., 2001). These findings suggest that there might be some degree of variability in TMH 3 across the neurotransmitter family. Importantly, there are conservation patterns among subfamilies at the 3.36 and 3.37 positions. D_1, H_1, and 5-HT_2 receptors contain SerThr, 5-HT_4 receptors contain ThrThr, β-adrenergic receptors contain ValThr, 5-HT_6 receptors contain CysSer, muscarinic receptors contain SerAsn, and all the others contain CysThr. These findings might serve to model the complexes between the neurotransmitter family and their ligands. These models are important because they provide the tools for guiding the design and synthesis of new ligands with predetermined affinities and selectivity.

Acknowledgments

Computer facilities were provided by the Centre de Computació i Comunicacions de Catalunya.

References

Arnis S, Fahmy K, Hofmann KP, and Sakmar TP (1994) A conserved carboxylic acid group mediates light-dependent proton uptake and signaling by rhodopsin. *J Biol Chem* **269:**23879–23881.

Baldwin JM, Schertler GFX, and Unger VM (1997) An alpha-carbon template for the transmembrane helices in the rhodopsin family of G-protein-coupled receptors. *J Mol Biol* **272:**144–164.

Ballesteros JA, Deupi X, Olivella M, Haaksma EEJ, and Pardo L (2000) Serine and

threonine residues bend α-helices in the $\chi_1 = g_-$ conformation. *Biophys J* **79:**2754–2760.
Ballesteros JA, Shi L, and Javitch JA (2001) Structural mimicry in G protein-coupled receptors: implications of the high-resolution structure of rhodopsin for structure-function analysis of rhodopsin-like receptors. *Mol Pharmacol* **60:**1–19.
Ballesteros JA and Weinstein H (1995) Integrated methods for modeling G-protein coupled receptors. *Methods Neurosci* **25:**366–428.
Bourne HR and Meng EC (2000) Structure. Rhodopsin sees the light. *Science (Wash DC)* **289:**733–734.
Cavalli A, Fanelli F, Taddei C, De Benedetti PG, and Cotecchia S (1996) Amino acids of the alpha$_{1B}$-adrenergic receptor involved in agonist binding: differences in docking catecholamines to receptor subtypes. *FEBS Lett* **399:**9–13.
Cheng YC and Prusoff WH (1973) Relationship between the inhibition constant (K_i) and the concentration of inhibitor which causes 50 per cent inhibition (IC_{50}) of an enzymatic reaction. *Biochem Pharmacol* **22:**3099–3108.
Cieplak P, Cornell WD, Bayly C, and Kollman PA (1995) Application of the multimolecule and multiconformational RESP methodology to biopolymers: charge derivation for DNA, RNA and proteins. *J Comput Chem* **16:**1357–1377.
Clark RD, Weinhardt KK, Berger J, Fischer LE, Brown CM, MacKinnon A, Kilpatrick AT, and Spedding M (1990) 1,9-Alkano-bridged 2,3,4,5-tetrahydro-1*H*-3-benzazepines with affinity for the α_2-adrenoceptor and the 5-HT$_{1A}$ receptor. *J Med Chem* **33:**633–641.
Cornell WD, Cieplak P, Bayly CI, Gould IR, Merz KM Jr, Ferguson DM, Spellmeyer DC, Fox T, Caldwell JW, and Kollman PA (1995) A second generation force field for the simulation of proteins, nucleic acids and organic molecules. *J Am Chem Soc* **117:**5179–5197.
Dunbrack RLJ and Cohen FE (1997) Bayesian statistical analysis of protein sidechain rotamer preferences. *Protein Sci* **6:**1661–1681.
Elling CE, Nielsen SM, and Schwartz TW (1995) Conversion of antagonist-binding site to metal-ion site in the tachykinin NK-1 receptor. *Nature (Lond)* **374:**74–77.
Elling CE, Thirstrup K, Holst B, and Schwartz TW (1999) Conversion of agonist site to metal-ion chelator site in the β_2-adrenergic receptor. *Proc Natl Acad Sci USA* **96:**12322–12327.
Glennon RA, Dukat M, Westkaemper RB, Ismaiel AM, Izzarelli DG, and Parker EM (1996) The binding of propanolol at 5-hydroxytryptamine$_{1D\beta}$ T355N mutant receptors may involve formation of two hydrogen bonds to asparagine. *Mol Pharmacol* **49:**198–206.
Govaerts C, Blanpain C, Deupi X, Ballet S, Ballesteros JA, Wodak S, Vassart G, Pardo L, and Parmentier M (2001a) The TxP motif in the second transmembrane helix of CCR5: a structural determinant in chemokine-induced activation. *J Biol Chem* **276:**13217–13225.
Govaerts C, Lefort A, Costagliola S, Wodak S, Ballesteros JA, Pardo L, and Vassart G (2001b) A conserved Asn in TM7 is a on/off switch in the activation of the TSH receptor. *J Biol Chem* **276:**22991–22999.
Gray TM and Matthews BW (1984) Intrahelical hydrogen bonding of serine, threonine and cysteine residues within alpha-helices and its relevance to membrane-bound proteins. *J Mol Biol* **175:**75–81.
Guan X-M, Peroutka SJ, and Kobilka BK (1992) Identification of a single amino acid residue responsible for the binding of a class of β-adrenergic receptor antagonists to 5-HT$_{1A}$ receptors. *Mol Pharmacol* **41:**695–698.
Han M, Lou J, Nakanishi K, Sakmar TP, and Smith SO (1997) Partial agonist activity of 11-cis-retinal in rhodopsin mutants. *J Biol Chem* **272:**23081–23085.
Ho BY, Karschin A, Branchek T, Davidson N, and Lester HA (1992) The role of conserved aspartate and serine residues in ligand binding and in function of the 5-HT$_{1A}$ receptor: a site-directed mutation study. *FEBS Lett* **312:**259–262.
Horn F, Weare J, Beukers MW, Hörsch S, Bairoch A, Chen W, Edvardsen Ø, Campagne F, and Vriend G (1998) GPCRDB: an information system for G protein coupled receptors. *Nucleic Acids Res* **26:**277–281.
Hosmer DW and Lemeshow S (1989) *Applied Logistic Regression*. John Wiley & Sons, Inc., New York,
Ji TH, Grossmann M, and Ji I (1998) G protein-coupled receptors. I. Diversity of receptor-ligand interactions. *J Biol Chem* **273:**17299–17302.
Kelley LA, Gardner SP, and Sutcliffe MJ (1996) An automated approach for clustering an ensemble of NMR-derived protein structures into conformationally-related subfamilies. *Protein Eng* **9:**1063–1065.
Kraulis J (1991) MOLSCRIPT: a program to produce both detailed and schematic plots of protein structure. *J Appl Cryst* **24:**946–950.
Kumar S and Bansal M (1998) Geometrical and sequence characteristics of α-helices in globular proteins. *Biophys J* **75:**1935–1944.
Liapakis G, Ballesteros JA, Papachristou S, Chan WC, Chen X, and Javitch JA (2000) The forgotten serine. A critical role for Ser-203$^{5.42}$ in ligand binding to and activation of the β2-adrenergic receptor. *J Biol Chem* **275:**37779–37788.
Lopez-Rodriguez ML, Morcillo MJ, Fernandez E, Porras E, Orensanz L, Beneytez ME, Manzanares J, and Fuentes JA (2001a) Synthesis and structure-activity relationships of a new model of arylpiperazines. 5. Study of the physicochemical influence of the pharmacophore on 5-HT$_{1A}$/α_1-adrenergic receptor affinity: synthesis of a new derivative with mixed 5-HT$_{1A}$/D$_2$ antagonist properties. *J Med Chem* **44:**186–197.
Lopez-Rodriguez ML, Morcillo MJ, Fernandez E, Rosado ML, Pardo L, and Schaper K-J (2001b) Synthesis and structure-activity relationships of a new model of arylpiperazines. 6. Study of the 5-HT$_{1A}$/α_1-adrenergic receptor affinity by classical Hansch analysis, artificial neural networks and computational simulation of ligand recognition. *J Med Chem* **44**:198–207.
Lopez-Rodriguez ML, Rosado ML, Benhamú B, Morcillo MJ, Sanz AM, Orensanz L, Beneytez ME, Fuentes JA, and Manzanares J (1996) Synthesis and structure-activity relationships of a new model of arylpiperazines. 1. 2-[[4-(*o*-Methoxyphenyl)piperazin-1-yl]methyl]-1,3-dioxoperhydroimidazo[1,5-*a*]pyridine: a selective 5-HT$_{1A}$ receptor agonist. *J Med Chem* **39:**4439–4450.
Lowry OH, Rosebrough NJ, Farr AL, and Randall RJ (1951) Protein measurement with the folin phenol reagent. *J Biol Chem* **193:**265–275.
Merritt EA and Bacon DJ (1997) Raster3D: photorealistic molecular graphics. *Methods Enzymol* **277:**505–524.
O'Neil KT and DeGrado WF (1990) A thermodynamic scale for the helix-forming tendencies of the commonly occurring amino acids. *Science (Wash DC)* **250:**646–651.
Oliveira L, Paiva ACM, Sander C, and Vriend G (1994) A common step for signal transduction in G-protein coupled receptors. *Trends Pharmacol Sci* **15:**170–172.
Palczewski K, Kumasaka T, Hori T, Behnke CA, Motoshima H, Fox BA, LeTrong I, Teller DC, Okada T, Stenkamp RE, et al. (2000) Crystal structure of rhodopsin: a G protein-coupled receptor. *Science (Wash DC)* **289:**739–745.
Pavia ML, Taylor CP, Hershenson FM, and Lobbestael SJ (1987) 6-Alkoxy-N,N-disubstituted-2-pyridinamines as anticonvulsant agents. *J Med Chem* **30:**1210–1214.
Scheer A, Fanelli F, Costa T, De Benedetti PG, and Cotecchia S (1996) Constitutively active mutants of the alpha 1B-adrenergic receptor: role of highly conserved polar amino acids in receptor activation. *EMBO (Eur Mol Biol Organ) J* **15:**3566–3578.
Senes A, Gerstein M, and Engelman DM (2000) Statistical analysis of amino acid patterns in transmembrane helices: the GxxxG motif occurs frequently and in association with β-branched residues at neighboring positions. *J Mol Biol* **296:**921–936.
Strader CD, Candelore MR, Hill WS, Dixon RA, and Sigal IS (1989) A single amino acid substitution in the beta-adrenergic receptor promotes partial agonist activity from antagonists. *J Biol Chem* **264:**16470–16477.
Strader CD, Sigal IS, Candelore MR, Rands MR, Hill WS, and Dixon RAF (1988) Conserved aspartic acid residues 79 and 113 of the β-adrenergic receptor have different roles in receptor function. *J Biol Chem* **263:**10267–10271.
Suryanarayana S, Daunt DA, Zastrow MV, and Kobilka BK (1991) A point mutation in the seventh hydrophobic domain of the α_2-adrenergic receptor increases its affinity for a family of β receptor antagonists. *J Biol Chem* **266:**15488–15492.
Suryanarayana S and Kobilka BK (1993) Amino acid substitutions at position 312 in the seventh hydrophobic segment of the β_2-adrenergic receptor modify ligand-binding specificity. *Mol Pharmacol* **44:**111–114.
Unger VM, Hargrave PA, Baldwin JM, and Schertler GF (1997) Arrangement of rhodopsin transmembrane alpha-helices. *Nature (Lond)* **389:**203–206.
van Rhee AM and Jacobson KA (1996) Molecular architecture of G protein-coupled receptors. *Drug Devel Res* **37:**1–38.
Yang K, Farrens DL, Attenbach C, Farahbakhsh ZT, Hubbell WL, and Khorana HG (1996) Structure and function in rhodopsin. Cysteines 65 and 316 are in proximity in a rhodopsin mutant as indicated by disulfide formation and interactions between attached spin labels. *Biochemistry* **35:**14040–14046.
Yu H, Kono M, McKee TD, and Oprian DD (1995) A general method for mapping tertiary contacts between amino acid residues in membrane-embedded proteins. *Biochemistry* **34:**14963–14969.
Zhou W, Flanagan C, Ballesteros JA, Konvicka K, Davidson JS, Weinstein H, Millar RP, and Sealfon SC (1994) A reciprocal mutation supports helix 2 and helix 7 proximity in the gonadotropin-releasing hormone receptor. *Mol Pharmacol* **45:**165–170.

Address correspondence to: Dr. Leonardo Pardo, Unitat de Bioestadística, Facultat de Medicina, Universitat Autònoma de Barcelona, 08193 Bellaterra (Barcelona), Spain. E-mail: leonardo.pardo@uab.es

Pergamon

SCIENCE DIRECT®

Bioorganic & Medicinal Chemistry Letters 13 (2003) 1429–1432

BIOORGANIC & MEDICINAL CHEMISTRY LETTERS

Design and Synthesis of *S*-(−)-2-[[4-(napht-1-yl)piperazin-1-yl]-methyl]-1,4-dioxoperhydropyrrolo[1,2-*a*]pyrazine (CSP-2503) Using Computational Simulation. A 5-HT_{1A} Receptor Agonist

María L. López-Rodríguez,[a,*] Mª José Morcillo,[b] Esther Fernández,[a] Bellinda Benhamú,[a] Ignacio Tejada,[a] David Ayala,[a] Alma Viso,[a] Mireia Olivella,[c] Leonardo Pardo,[c] Mercedes Delgado,[d] Jorge Manzanares[d] and José A. Fuentes[d]

[a]*Departamento de Química Orgánica I, Facultad de Ciencias Químicas, Universidad Complutense, E-28040 Madrid, Spain*
[b]*Sección de Química, Facultad de Ciencias, Universidad Nacional de Educación a Distancia, E-28040 Madrid, Spain*
[c]*Unitat Bioestadística, Institut de Neurociències, Universitat Autònoma, E-08913 Cerdanyola del Vallès, Barcelona, Spain*
[d]*Unidad de Cartografía Cerebral, Instituto Pluridisciplinar, Universidad Complutense, E-28040 Madrid, Spain*

Received 12 November 2002; revised 20 January 2003; accepted 10 February 2003

Abstract—Based on a computational model for 5-HT_{1A}R-ligand interaction and QSAR studies, we have designed and synthesized a new series of arylpiperazines **2**–**8** which exhibit high 5-HT_{1A}R affinity and selectivity over α_1-adrenergic receptors. Among them, compound CSP-2503 (**4**) has been pharmacologically characterized as a 5-HT_{1A}R agonist at somatodendritic and postsynaptic sites, endowed with anxiolytic properties.

Introduction

The identification of multiple serotonin (5-HT) receptor subtypes in recent years has been accompanied by a parallel explosion in the development of drugs that alter 5-HT neurotransmission.[1,2] Specially, the 5-HT_{1A} receptor (5-HT_{1A}R) is a major target for neurobiological research and drug development, due to its implication in many (patho)physiological processes.[3–5] Agonists and partial agonists have been proven to be effective in anxiety and depression.[6–9] In addition to therapeutic applications in the field of psychiatry, more recent preclinical studies have suggested that 5-HT_{1A}R agonists have also pronounced neuroprotective properties.[10–12]

In the course of a program aimed at the discovery of new 5-HT_{1A}R agents, we have synthesized a series of arylpiperazines of general structure **I** ($n=3$, 4),[13–19] which showed affinity for both 5-HT_{1A} and α_1-adrenergic receptors due to the high degree of homology in both their transmembrane amino acid sequence and structure. It is widely accepted that the rhodopsin family of G protein-coupled receptors (GPCRs), including receptors for biogenic amines, share a comparable transmembrane structure formed by a highly organized heptahelical transmembrane bundle.[20] In the present work, we have used a computational model between the 5-HT_{1A}R and arylpiperazines of formula **I** (X = –$(CH_2)_3$–, $m=0$, $n=4$, Ar = *m*-(ethylsulfonamido)phenyl;[21] X = –$(CH_2)_3$–, $m=0$, $n=4$, Ar = *m*-(acetylamino)phenyl)[22] and previous 3-D-QSAR studies[23] for the synthesis of a new series of arylpiperazines **I** ($n=1$) which exhibit high 5-HT_{1A}R affinity and selectivity over α_1-adrenoceptors. Among them, compound CSP-2503 (**4**) has been pharmacologically characterized as a 5-HT_{1A}R agonist endowed with anxiolytic properties.

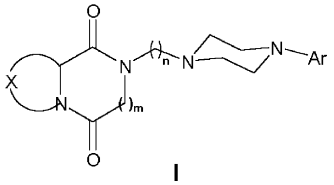

I

Computational simulation

Figure 1a shows compound **1** (X = –$(CH_2)_3$–, $m=0$, $n=4$, Ar = naphth-1-yl) in the binding pocket of the 5-HT_{1A}R. This type of arylpiperazine, with a chain length of $n=4$ connecting both rings, was predicted[21,22]

*Corresponding author. Tel.: +34-91-3944239; fax: +34-91-3944103; e-mail: mluzir@quim.ucm.es

0960-894X/03/$ - see front matter © 2003 Elsevier Science Ltd. All rights reserved.
doi:10.1016/S0960-894X(03)00160-4

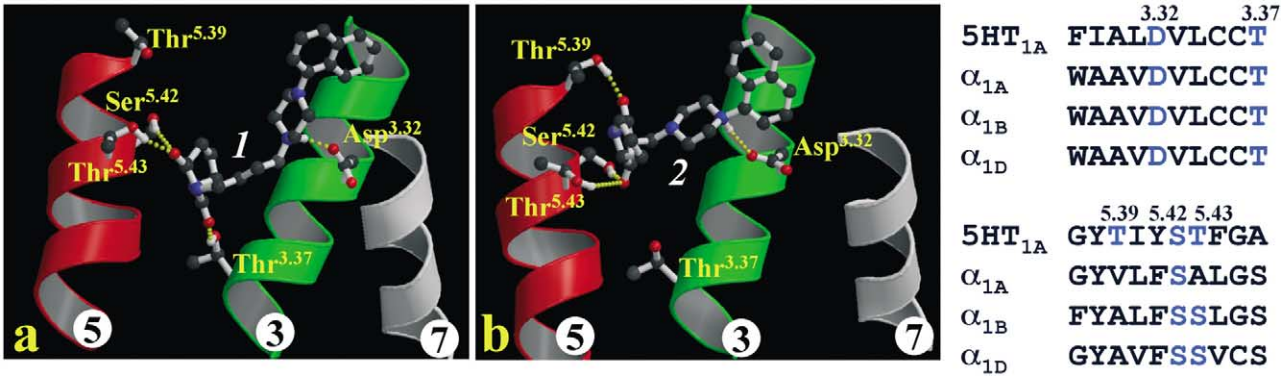

Figure 1. Interactions of compounds **1** and **2** with a model of the 5-HT_{1A}R. Hypothesis for 5-HT_{1A}/α_1 selectivity.

to interact with $Asp^{3.32}$ throughout the protonated NH group of the piperazine ring, and with $Thr^{3.37}$, $Ser^{5.42}$, and $Thr^{5.43}$ throughout the hydantoin moiety. This model reproduces the suggested interaction of Ser/Thr at positions 5.42 and 5.43 with the hydroxyl/carbonyl moiety of the ligand.[24] The presence of $Asp^{3.32}$, $Thr^{3.37}$, $Ser^{5.42}$, and Thr/$Ser^{5.43}$ in both 5-HT_{1A} and α_1-adrenergic receptors (Fig. 1) explains the lack of selectivity of arylpiperazine derivatives with $n=4$. Notably, $Thr^{5.39}$, located in helix 5, is pointing inside the bundle and is present only in the 5-HT_{1A}R (Fig. 1). Thus, the interaction of the ligand with the side chain of $Thr^{5.39}$ would provide the desired selectivity. This interaction is achieved by shortening the chain length to $n=1$ and avoiding the ligand to expand deep in the bundle as compound **1**. Figure 1b shows compound **2** (X = $-(CH_2)_3-$, m = 0, n = 1, Ar = naphth-1-yl) interacting with $Asp^{3.32}$ throughout the protonated NH group of the piperazine ring, and with $Thr^{5.39}$, $Ser^{5.42}$, and $Thr^{5.43}$ throughout the hydantoin moiety. Table 1 shows the binding affinity of these compounds. Clearly, compound **2** is selective versus the α_1-adrenoceptor while **1** binds both receptors, as predicted by the computer models.

Chemistry

Based on the proposed hypothesis for 5-HT_{1A}/α_1 selectivity, we have synthesized a new series of arylpiperazines **I** ($n=1$), in which the volume of the pharmacophore is increased in positions *ortho* and *meta* of the aromatic ring. Previous QSAR studies[23] showed that this is an additional structural feature that accounts for 5-HT_{1A}/α_1 selectivity. Compounds **2–8** were obtained by Mannich reaction of bicyclohydantoins **9**,**10**[25,26] or diketopiperazines **11**,**12**[27,28] with the appropriate bicycloarylpiperazines **13–16**[29–31] in the presence of formaldehyde (Scheme 1).

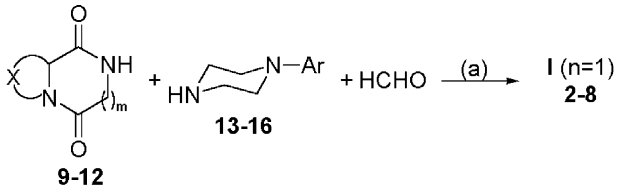

Scheme 1. (a) See Tables 1 and 2 for chemical structures of compounds **2–8**.

Table 1. Binding data of compounds I[a]

Compd	X	*m*	*n*	Ar	$K_i \pm$SEM (5-HT_{1A})	$K_i \pm$SEM (α_1)
1	$(CH_2)_3$	0	4	Naphth-1-yl	2.4 ± 0.1	64.9 ± 1.5
2	$(CH_2)_3$	0	1	Naphth-1-yl	10.4 ± 0.8	> 1000

[a]Values are means of 2–4 experiments performed in triplicate.

Pharmacology

Affinity data

Target compounds were assessed for in vitro binding affinity at serotoninergic 5-HT_{1A} and α_1-adrenergic receptors by radioligand binding assays, using [^{3}H]-8-OH-DPAT[32] and [^{3}H]prazosin,[33] respectively, in rat cerebral cortex membranes. All the synthesized compounds **2–8** exhibited high 5-HT_{1A}R affinity and selectivity over α_1-adrenergic receptors (Table 2), confirming our hypotheses for 5-HT_{1A}/α_1 selectivity in this class of arylpiperazine ligands. Compound **4** (CSP-2503) was also evaluated for affinity at serotonin 5-HT_{2A} ($K_i = 13.5 \pm 2.5$ nM), 5-HT_3 ($K_i = 8.9 \pm 1.4$ nM), 5-HT_4 ($K_i > 10{,}000$ nM) and 5-HT_7 ($K_i = 100.9 \pm 1.4$ nM) receptors, serotonin transporter ($K_i = 976.3 \pm 42.8$ nM), dopamine D_2 receptors ($K_i = 192.1 \pm 20.1$ nM), and benzodiazepine receptors ($K_i > 10{,}000$ nM). The following specific ligands and tissue sources were used: 5-HT_{2A}, [^{3}H]ketanserin, rat cerebral frontal cortex membranes;[34] 5-HT_3, [^{3}H]LY278584, rat cerebral cortex membranes;[35] 5-HT_4, [^{3}H]GR113808, rat striatum membranes;[36] 5-HT_7, [^{3}H]-5-CT, rat hypothalamus

Table 2. Binding data of compounds I[a]

Compd	X	*m*	Ar	$K_i \pm$SEM (5-HT_{1A})	$K_i \pm$SEM (α_1)
3	$(CH_2)_4$	0	Naphth-1-yl	5.6 ± 0.3	> 1000
4 (CSP-2503)	$(CH_2)_3$	1	Naphth-1-yl	4.1 ± 1.2	> 1000
5	$(CH_2)_4$	0	Benzodioxan-5-yl	9.3 ± 0.4	> 1000
6	$(CH_2)_4$	0	Benzodioxepin-6-yl	6.1 ± 0.4	> 1000
7	$(CH_2)_3$	1	Benzodioxepin-6-yl	12.3 ± 2.1	> 1000
8	$(CH_2)_3$	0	Benzimidazol-4-yl	4.1 ± 0.2	> 10,000

[a]Values are means of 2–4 experiments performed in triplicate.

membranes;[37] 5-HT transporter, [^{3}H]paroxetine, rat cerebral cortex membranes;[38] D_2, [^{3}H]raclopride, rat striatum membranes;[39] benzodiazepine, [^{3}H]flunitrazepam, rat cerebral cortex membranes.[40]

Pharmacological characterization of CSP-2503 (4)

Presynaptic 5-HT_{1A}R activity was assessed by measuring mouse rectal temperature.[41] The administration of CSP-2503 provoked a dose related decrease in mice rectal temperature (Fig. 2). This induced hypothermia suggests that CSP-2503 acts on 5-HT_{1A} somatodendritic autoreceptors.

The transduction mechanism of CSP-2503 was determined by using HeLa cells expressing human 5-HT_{1A}Rs.[42] CSP-2503 inhibited in a dose dependent manner the cAMP increase induced by forskolin. The half maximal effect (EC_{50}) observed was 0.15 μM and the maximal inhibitory effect was 90.3±1.3%. This negative control of CSP-2503 on adenylate cyclase activity indicates a transduction system coupled to 5-HT_{1A}R stimulation.

Functional activity of CSP-2503 on 5-HT_{1A}Rs was further assessed by evaluating its ability to decrease 5-HT neuronal activity.[43] The administration of CSP-2503 induced a decrease in 5-hydroxyindoleacetic acid (5-HIAA)/5-HT ratio in whole hypothalamus of mice (Fig. 3). These results further indicate that CSP-2503 behaves as a 5-HT_{1A}R agonist acting at the somatodendritic site.

Furthermore, we have evaluated the potential anxiolytic activity of CSP-2503 by using the light/dark box test.[44] Indeed, the administration of CSP-2503 (10 mg/kg) caused an increase in the time that mice spent in the lit area (155.4±9.3 vs 83±13 s, $P<0.05$). The 5-HT_{1A}R agonist 8-OH-DPAT was tested in the same test as reference compound, at a dose of 2.5 mg/kg (time spent in the lit area: 188.8±26 vs 105±14.7 s). These measurements were performed thirty min after the *sc* administration of the drug or vehicle and for the period of 5 min.

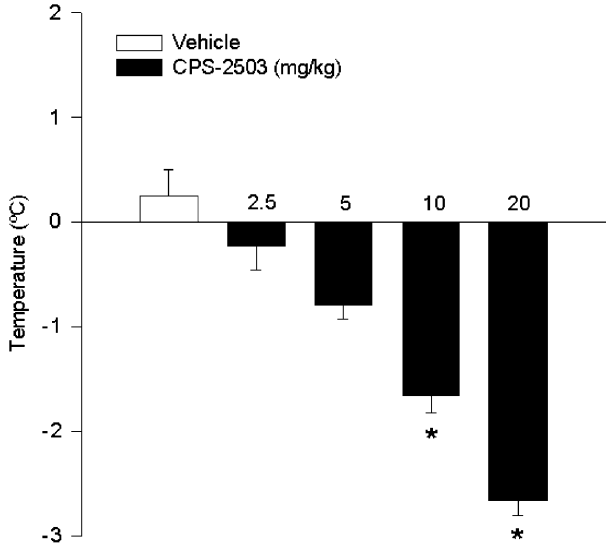

Figure 2. Dose–response effect of CSP-2503 on rectal temperature. *Values of CSP-2503 that decrease more than 1.1 °C and are significantly different ($P<0.05$) from their respective basal rectal temperature before *sc* drug administration.

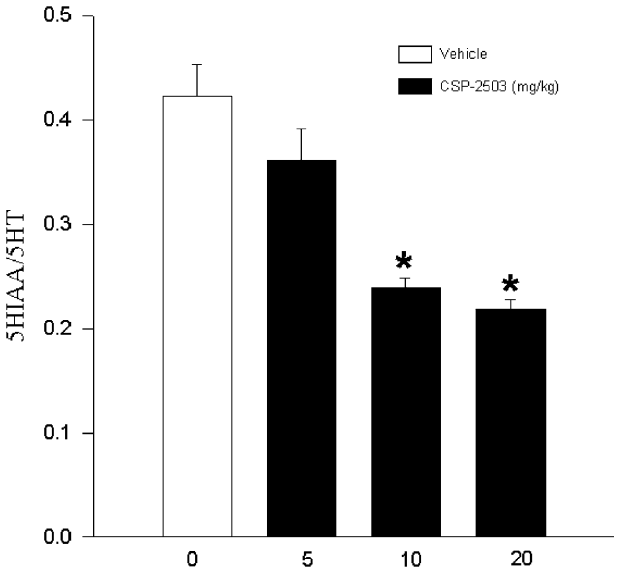

Figure 3. Dose–response effect of CSP-2503 on hypothalamic 5-HT activity. *Values of CSP-2503 treated mice that are significantly different ($P<0.05$) from vehicle group.

These results indicate that CSP-2503 is an agonist of the 5-HT_{1A}R at the somatodendritic and postsynaptic sites, with anxiolytic potential. In order to complete its pharmacological profile, further behavioural and neurochemical evaluation are currently in progress, though the present data suggest that CSP-2503 may be therapeutically useful in the treatment of anxiety-related disorders.

Conclusions

Based on our recently proposed computational model for 5-HT_{1A}R-ligand interaction, we have synthesized a new series of arylpiperazines **I** ($n=1$) which exhibit high 5-HT_{1A}R affinity and selectivity over α_1-adrenergic receptors. Among them, compound CSP-2503 (**4**) has been pharmacologically characterized as a 5-HT_{1A}R agonist at somatodendritic and postsynaptic sites, endowed with anxiolytic properties.

Acknowledgements

This work was supported by Ministerio de Ciencia y Tecnología (BQU2001-1459), Comunidad Autónoma de Madrid (08.5/0079/2000), and CEPA-SCHWARZ-PHARMA. E. Fernández and I. Tejada are also grateful to U.N.E.D. for a predoctoral grant. Computer facilities were provided by the Centre de Computació i Comunicacions de Catalunya.

References and Notes

1. Baumgarten, H. G.; Göthert, M. *Serotoninergic Neurons and 5-HT Receptors in the CNS; Handb. Exp. Pharm. Vol. 129*; Springer Verlag: Berlin, 1997.
2. *Advances in Serotonin Receptor Research: Molecular Biology, Signal Transmission, and Therapeutics*; Martin, G. R., Eglen, R. M., Hoyer, D., Hamblin, M. W., Yocca, F., Eds. Ann. N.Y. Acad. Sci.: New York, 1998.
3. Olivier, B.; van Wijngaarden, I.; Soudjin, W. *Serotonin Receptors and their Ligands*; Elsevier: The Nederlands, 1997.
4. Olivier, B.; Soudjin, W.; van Wijngaarden, I. *Prog. Drug Res.* **1999**, *52*, 103.
5. López-Rodríguez, M. L.; Ayala, D.; Benhamú, B.; Morcillo, M. J.; Viso, A. *Curr. Med. Chem.* **2002**, *9*, 443.
6. Rickels, K.; Derivan, A.; Kunz, N.; Pallay, A.; Schweizer, E. *J. Clin. Psychopharmacol.* **1996**, *16*, 212.
7. Lee, C. H.; Oh, J. I.; Park, H. D.; Kim, H. J.; Park, T. K.; Kim, J. S.; Hong, C. Y.; Lee, S. J.; Ahn, K. H.; Kim, Y. Z. *Arch. Pharm. Res.* **1999**, *22*, 157.
8. Schwartz, P. J.; Turner, E. H.; García-Borreguero, D.; Sedway, J.; Vetticad, R. G.; Wehr, T. A.; Murphy, D. L.; Rosenthal, N. E. *Psychiatry Res.* **1999**, *86*, 9.
9. Peglion, J. L.; Goument, B.; Despaux, N.; Charlot, V.; Giraud, H.; Nisole, C.; Newman-Tancredi, A.; Dekeyne, A.; Bertrand, M.; Genissel, P.; Millan, M. J. *J. Med. Chem.* **2002**, *45*, 165.
10. Alessandri, B.; Tsuchida, E.; Bullock, R. M. *Brain Res.* **1999**, *845*, 232.
11. Kamei, K.; Maeda, N.; Ogino, R.; Koyama, M.; Nakajima, M.; Tatsuoka, T.; Ohno, T.; Inoue, T. *Bioorg. Med. Chem. Lett.* **2001**, *11*, 595.
12. Harkany, T.; Mulder, J.; Horvath, K. M.; Keijser, J.; van der Meeberg, E. K.; Nyakas, C.; Luiten, P. G. M. *Neuroscience* **2001**, *108*, 629.
13. López-Rodríguez, M. L.; Rosado, M. L.; Benhamú, B.; Fernández, E.; Morcillo, M. J. Patent PCT/ES95/00094, 1995.
14. López-Rodríguez, M. L.; Rosado, M. L.; Benhamú, B.; Morcillo, M. J.; Sanz, A. M.; Orensanz, L.; Beneitez, M. E.; Fuentes, J. A.; Manzanares, J. *J. Med. Chem.* **1996**, *39*, 4439.
15. López-Rodríguez, M. L.; Morcillo, M. J.; Fernández, E.; Porras, E.; Murcia, M.; Sanz, A. M.; Orensanz, L. *J. Med. Chem.* **1997**, *40*, 2653.
16. López-Rodríguez, M. L.; Morcillo, M. J.; Fernández, E. Patent PCT/ES98/00250, 1998.
17. López-Rodríguez, M. L.; Morcillo, M. J.; Rovat, T. K.; Fernández, E.; Vicente, B.; Sanz, A. M.; Hernández, M.; Orensanz, L. *J. Med. Chem.* **1999**, *42*, 36.
18. López-Rodríguez, M. L.; Viso, A.; Benhamú, B.; Rominguera, J. L.; Murcia, M. *Bioorg. Med. Chem. Lett.* **1999**, *9*, 2339.
19. López-Rodríguez, M. L.; Morcillo, M. J.; Fernández, E.; Porras, E.; Orensanz, L.; Beneytez, M. E.; Manzanares, J.; Fuentes, J. A. *J. Med. Chem.* **2001**, *44*, 186.
20. Palczewski, K.; Kumasaka, T.; Hori, T.; Behnke, C. A.; Motoshima, H.; Fox, B. A.; LeTrong, I.; Teller, D. C.; Okada, T.; Stenkamp, R. E. *Science* **2000**, *289*, 739.
21. López-Rodríguez, M. L.; Morcillo, M. J.; Fernández, E.; Rosado, M. L.; Pardo, L.; Schaper, K.-J. *J. Med. Chem.* **2001**, *44*, 198.
22. López-Rodríguez, M. L.; Vicente, B.; Deupi, X.; Barrondo, S.; Olivella, M.; Morcillo, M. J.; Benhamú, B.; Ballesteros, J. A.; Sallés, J.; Pardo, L. *Mol. Pharmacol.* **2002**, *62*, 15.
23. López-Rodríguez, M. L.; Rosado, M. L.; Benhamú, B.; Morcillo, M. J.; Fernández, E.; Schaper, K.-J. *J. Med. Chem.* **1997**, *40*, 1648.
24. Liapakis, G.; Ballesteros, J. A.; Papachristou, S.; Chan, W. C.; Chen, X.; Javitch, J. A. *J. Biol. Chem.* **2000**, *275*, 37779.
25. Dakin, H. D. *J. Biol. Chem.* **1920**, *44*, 499.
26. Freed, M. E.; Day, A. R. *J. Org. Chem.* **1960**, *25*, 2108.
27. Vicar, J.; Smolíková, J.; Blahá, K. *Collect. Czech. Chem. Commun.* **1972**, *37*, 4060.
28. Bláha, K.; Budesinský, M.; Fric, I.; Smolíková, J.; Vicar, J. *Tetrahedron Lett.* **1972**, *15*, 1437.
29. Glennon, R. A.; Slusher, R. M.; Lyon, R. A.; Titeler, M.; McKenney, J. D. *J. Med. Chem.* **1986**, *29*, 2375.
30. van Wijngaarden, I.; Kruse, C. G.; van der Heyden, J. A. M.; Tulp, M. T. M. *J. Med. Chem.* **1988**, *31*, 1934.
31. López-Rodríguez, M. L.; Benhamú, B.; Ayala, D.; Rominguera, J. L.; Murcia, M.; Ramos, J. A.; Viso, A. *Tetrahedron* **2000**, *56*, 3245.
32. Clark, R. D.; Weinhardt, K. K.; Berger, J.; Fischer, L. E.; Brown, C. M.; MacKinnon, A. C.; Kilpatrick, A. T.; Spedding, M. *J. Med. Chem.* **1990**, *33*, 633.
33. Ambrosio, E.; Montero, M. T.; Fernández, I.; Azuara, M. C.; Orensanz, L. M. *Neurosci. Lett.* **1984**, *49*, 193.
34. Titeler, M.; Lyon, R. A.; Davis, K. H.; Glennon, R. A. *Biochem. Pharmacol.* **1987**, *36*, 3265.
35. Wong, D. T.; Robertson, D. W.; Reid, L. R. *Eur. J. Pharmacol.* **1989**, *166*, 107.
36. Grossman, C. J.; Kilpatrick, G. J.; Bunce, K. T. *Br. J. Pharmacol.* **1993**, *109*, 618.
37. Aguirre, N.; Ballaz, S.; Lasheras, B.; del Río, J. *Eur. J. Pharmacol.* **1998**, *346*, 181.
38. Hadert, E.; Graham, D.; Tahraoui, L.; Claustre, Y.; Langer, S. Z. *Eur. J. Pharmacol.* **1985**, *118*, 107.
39. Hall, H.; Wedel, I.; Sällemark, M. *Pharmacol. Toxicol.* **1988**, *63*, 118.
40. Orensanz, L. M.; Córdoba, C.; Fernández, I. *Neurosci. Lett.* **1990**, *111*, 241.
41. Goodwin, G. M.; Green, A. R. *Br. J. Pharmacol.* **1985**, *84*, 743.
42. Boddeke, H. W.; Fargin, A.; Raymond, J. R.; Schoeffter, P.; Hoyer, D. *Arch. Pharmacol.* **1992**, *345*, 257.
43. Chapin, D. S.; Lookingland, K. J.; Moore, K. E. *Currents Separations* **1986**, *7*, 68.
44. Crawley, J. N. *Neurosci. Biobehav. Rev.* **1985**, *9*, 37.

Journal of Computer-Aided Molecular Design, **15:** 1025–1033, 2001.
KLUWER/ESCOM

Computational Model of the Complex between GR113808 and the 5-HT$_4$ Receptor Guided by Site-Directed Mutagenesis and the Crystal Structure of Rhodopsin *

María L. López-Rodríguez[b], Marta Murcia[b], Bellinda Benhamú[b], Mireia Olivella[a], Mercedes Campillo[a] & Leonardo Pardo[a,*]
[a]*Laboratori de Medicina Computacional, Unitat de Bioestadística, Facultat de Medicina, Universitat Autònoma de Barcelona, E-08193 Bellaterra, Spain;* [b]*Departamento de Química Orgánica I, Facultad de Ciencias Químicas, Universidad Complutense, E-28040 Madrid, Spain*

Accepted 22 November 2001

Key words: 5-HT$_4$ receptor, antagonist binding, drug design, G protein-coupled receptors, molecular modeling, serotonin, transmembrane helices

Summary

A computational model of the transmembrane domain of the human 5-HT$_4$ receptor complexed with the GR113808 antagonist was constructed from the crystal structure of rhodopsin and the putative residues of the ligand-binding site, experimentally determined by site-directed mutagenesis. The recognition mode of GR113808 consist of: (i) the ionic interaction between the protonated amine and Asp$^{3.32}$; (ii) the hydrogen bond between the carbonylic oxygen and Ser$^{5.43}$; (iii) the hydrogen bond between the ether oxygen and Asn$^{6.55}$; (iv) the hydrogen bond between the C-H groups adjacent to the protonated piperidine nitrogen and the π electrons of Phe$^{6.51}$; and (v) the π-σ aromatic-aromatic interaction between the indole ring and Phe$^{6.52}$.

This computational model offers structural indications about the role of Asp$^{3.32}$, Ser$^{5.43}$, Phe$^{6.51}$, Phe$^{6.52}$, and Asn$^{6.55}$ in the experimental binding affinities. Asp$^{3.32}$Asn mutation does not affect the binding of GR113808 because the loss of binding affinity from an ion pair to a charged hydrogen bond is compensated by the larger energetical penalty of Asp to disrupt its side chain environment in the ligand-free form, and the larger interaction between Phe$^{6.51}$ and the piperidine ring of the ligand in the mutant receptor. In the Phe$^{6.52}$Val mutant the indole ring of the ligand replaces the interaction with Phe$^{6.52}$ by a similarly intense interaction with Tyr$^{5.38}$, with no significant effect in the binding of GR113808. The mutation of Asn$^{6.55}$ to Leu replaces the hydrogen bond of the ether oxygen of the ligand from Asn$^{6.55}$ to Cys$^{5.42}$, with a decrease of binding affinity that approximately equals the free energy difference between the SH$\cdots$O and NH$\cdots$O hydrogen bonds.

Because these residues are also present in the other members of the neurotransmitter family of G protein-coupled receptors, these findings will also serve for our understanding of the binding of related ligands to their cognate receptors.

Abbreviations: 5-HT$_4$R, 5-HT$_4$ receptor; GPCR, G protein-coupled receptor; TM, transmembrane helix; RHO, rhodopsin

*To whom correspondence should be addressed. E-mail: Leonardo.Pardo@uab.es

Introduction

The 5-HT_4 receptor (5-HT_4R) belongs to the G protein-coupled receptor (GPCR) superfamily that transmit extracellular signals of neurotransmitters, peptides and glycoproteins through heterotrimeric G proteins bound in the interior of the cell [1]. The 5-HT_4R is of considerable interest because it is involved in (patho)physiological processes both in peripheral and central nervous systems [2]. A major advance in search for more potent and selective 5-HT_4R antagonists came with the identification of GR113808 [[1-[2-(methylsulphonylamino)ethyl]-4-piperidinyl]methyl-1-methyl-1H-indole-3-carboxylate], a highly potent and competitive antagonist of the 5-HT_4R [3]. GR113808 behaved as an antagonist of serotonin in guinea pig ascending colon ($pA_2 = 9.2$), rat oesophagus ($pA_2 = 9.5$), and human atrium ($pK_b = 8.8$). GR113808 is also highly selective with only weak affinity at 5-HT_3 receptors ($pK_i = 6.0$) and no activity at other 5-HT receptors (up to 10 μM). GR113808 was subsequently tritiated and it is normally used in both binding assays and radiographic analysis [2, 4].

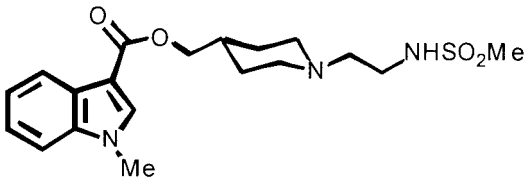

GR113808

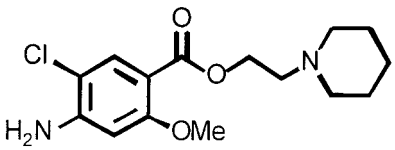

ML10302

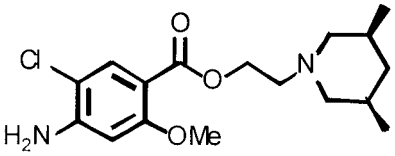

ML10375

The modification of the amino acid sequence of members of the GPCR family of receptors, using methods of molecular biology, is a common procedure to define the amino acid side chains of the receptor that form the ligand binding pocket [5]. Recently, the binding site of serotonin, GR113808, ML10302 [6], and ML10375 [6, 7] to the human 5-HT_4R has been explored by site-directed mutagenesis [8]. Serotonin anchors the completely conserved $Asp^{3.32}$ (see Methods for receptor-numbering scheme), in transmembrane helix 3 (TM 3), throughout its protonated amine, as revealed by the lack of binding affinity of serotonin to the $Asp^{3.32}$Asn point mutation [8]. Surprisingly, the antagonist GR113808 is not influenced by this mutation, the agonist ML10302 is only weakly affected, and the antagonist ML10375 is moderately affected; despite all these compounds contain a protonated amine moiety. These results are in contrast to the observation that $Asp^{3.32}$ binds both agonists and antagonists (see [5] for a review), in the other members of the neurotransmitter family of receptors. On the other hand, substitution of $Ser^{5.43}$, in TM 5, by Ala avoids the binding of GR113808 [8]. TM 5 possesses, in the neurotransmitter family of receptors, a series of conserved Ser/Thr residues, at positions 5.43 and 5.46, that appear to hydrogen bond the hydroxyl groups present in the chemical structure of many neurotransmitters [9]. Thus, it was reasonably hypothesized that the hydroxyl group of serotonin and the carbonyl oxygen of the ester group of GR113808 are involved in the hydrogen bond to $Ser^{5.43}$. It has recently been shown that another Ser residue at position 5.42 in the β_2-adrenergic receptor is also involved in the binding of catecholamine ligands [10]. Both $Ser^{5.42}$ and $Ser^{5.43}$ of the β_2-adrenergic receptor interact with the meta-hydroxyl group of catecholamine ligands [10]. The 5-HT_4R contains a Cys residue at this 5.42 position. Substitution of $Cys^{5.42}$ by Ala in the 5-HT_4R increases the binding of GR113808 and ML10302 [8]. Thus, in contrast to the β_2-adrenergic receptor, $Cys^{5.42}$ in the 5-HT_4R does not seem an additional site for ligand binding. It has also been shown for the β_2-adrenergic receptor that the $Asn^{6.55}$Leu point mutation, in TM 6, produces a substantial loss of stereospecificity for isoproterenol [11]. The β-OH-group of the ligand, which defines the chiral center, was proposed to hydrogen bond $Asn^{6.55}$. Substitution of the analogous $Asn^{6.55}$ in the 5-HT_4R by Leu abolishes the binding of serotonin [8]. However, the influence of this mutation in the binding of the GR113808 antagonist is not clear. Despite the single $Asn^{6.55}$Leu or $Phe^{6.52}$Val mutation moderately reduces the affinity for GR113808, the double $Phe^{6.52}$Ala/$Asn^{6.55}$Leu

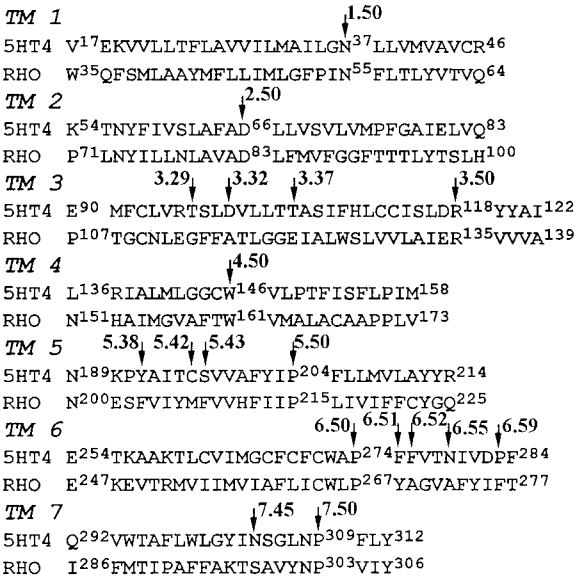

Figure 1. Alignment of the transmembrane sequences from bovine RHO and human 5-HT_4R. Numbers at the top define the general numbering scheme to identify residues in the transmembrane segments of different receptors [21]. Superscript numbers give the corresponding positions of the amino acids in the sequences of the receptor proteins.

mutation totally avoids the binding of GR113808 to the 5-HT_4R. TM 6 possesses the $Pro^{6.50}$PhePhe motif in both the adrenergic and serotoninergic subfamilies of receptors. The role of these conserved aromatic residues in ligand binding appears to be depending on the receptor family. $Phe^{6.52}$ stabilizes the interaction of the aromatic catechol-containing ring with the β_2-adrenergic receptor [12] and the interaction with certain 5-HT_{2A}R ligands [13-15]. Substitution of the adjacent $Phe^{6.51}$ has minimal effects on ligand binding in these receptors. In contrast, $Phe^{6.51}$, and not $Phe^{6.52}$, is a key residue involved in the interaction of the aromatic catechol ring with the α_{1B}-adrenergic receptor [16]. The role of these aromatic residues in the 5-HT_4R have been studied throughout the $Phe^{6.51}$Ala and $Phe^{6.52}$Leu mutations [8]. Replacement of $Phe^{6.51}$ by Ala abolishes the binding of the GR113808 antagonist, suggesting a direct interaction. $Phe^{6.52}$ substituion does not have a significant effect in either serotonin or GR113808. It is only the double $Phe^{6.52}$Ala/$Asn^{6.55}$Leu mutation (see above) that totally avoids the binding of GR113808 to the receptor. Thus, the role of $Phe^{6.52}$ and $Asn^{6.55}$ in the binding of the GR113808 antagonist remains unclear.

The structural interpretation of these experiments, investigating the structure-function relationships of GPCRs, were accomplished with molecular models of the complex between the ligands and the transmembrane domain of the receptor [8, 10, 11]. These 3-D models were derived from the high-resolution structure of bacteriorhodopsin [17] or the low-resolution structure of rhodopsin (RHO) [18, 19]. Recently, the 3-D structure of RHO was determined at 2.8 Å resolution [20]. It provides a detailed view of a GPCR in the inactive conformation of the receptor. In this work we aim to model the complex between the GR113808 antagonist and the transmembrane domain of the 5-HT_4R derived from the recent crystal structure of RHO [20]. This structure represents an appropriate template to model the 3-D structure of the 5-HT_4R because of the large number of conserved sequence patterns in the transmembrane segments [21, 22]. This computational model must offer additional structural indications about the experimentally determined role of $Asp^{3.32}$, $Ser^{5.43}$, $Phe^{6.51}$, $Phe^{6.52}$, and $Asn^{6.55}$ in the binding of GR113808 [8]. Because these residues are also present in the other members of the neurotransmitter family of 7-TM receptors, these findings will also serve for our understanding of the binding of related ligands to their cognate receptors. Moreover, the model will provide the tools for predicting the affinity of related compounds, and for guiding the design and synthesis of new ligands with predetermined affinities and selectivity.

Methods

Residue numbering scheme

We use a general numbering scheme to identify residues in the transmembrane segments of different receptors [21]. Each residue is numbered according to the helix (1 through 7) in which it is located and to the position relative to the most conserved residue in that helix, arbitrarily assigned to 50 (see Figure 1). For instance, the most conserved residue in helix 3 is designated with the index number 3.50 ($Arg^{3.50}$), the Asp preceeding the Arg is designated $Asp^{3.49}$, and the Tyr following the Arg is designated $Tyr^{3.51}$.

Molecular modeling of the transmembrane region of the 5-HT_4 receptor

The 3-D model of the transmembrane domain of the 5-HT_4R was constructed by computer-aided model building techniques from the transmembrane domain (HELIX annotation in the 1F88 PDB file) of the crystal

structure of RHO [20]. Figure 1 shows the alignment of bovine RHO and human 5-HT$_4$R (Genbank accession number Q13639) transmembrane sequences. All ionizable residues in the helices were considered uncharged with the exception of Asp$^{2.50}$, Asp$^{3.32}$, Asp$^{3.49}$, Arg$^{3.50}$ and Glu$^{6.30}$. SCWRL-2.1 was employed to add the side chains of the non-conserved residues based on a backbone-dependent rotamer library [23]. It is important to note that Thr$^{3.37}$ adopts the *gauche*-conformation. This is the only allowed conformation of Thr$^{3.37}$ due to the steric clash between the methyl group and the carbonyl oxygen of residue i-3 in the *trans* conformation [24] and the steric clash between the methyl group and the C_α (interatomic distance between heavy atoms of 2.8 Å) or C_β (3.2 Å) atoms of Pro$^{4.53}$ in the *gauche*+ conformation. Ser and Thr residues in this *gauche*− conformation induces a small bending angle in transmembrane helices because of the additional hydrogen bond formed between the O_γ atom of Ser and Thr and the i-3 or i-4 peptide carbonyl oxygen [25]. It has recently been shown that this effect is important in the 3-D conformation of the receptor [26]. Thus, a bending angle of 4° [25] has been incorporated in TM 3 at Thr$^{3.37}$. This induces the displacement of the residues located at the extracellular part of TM 3 towards TM 5, facilitating the experimentally derived interactions between the ligand and Asp$^{3.32}$ and Ser$^{5.43}$ [8].

Model of the 5-HT$_4$ receptor complexed with GR113808

The mode of recognition of GR113808 was first determined by *ab-initio* geometry optimization with the 3-21G basis set. The model system consisted on Asp$^{3.32}$, Ser$^{5.43}$ and Asn$^{6.55}$ (only the $C_\alpha$atom of the backbone is included) of the 5-HT$_4$R and the ligand GR113808 (the sulphonamide side chain attached to the piperidine nitrogen were replaced by a methyl group). All free valences were capped with hydrogen atoms. The C_α atoms of the residues were kept fixed at the positions previously obtained (see above). These optimized reduce model was used to position GR113808 inside the previously equilibrated transmembrane domain of the 5-HT$_4$R. Subsequently, the complete system was energy minimized (5000 steps). Similar procedure has been used in our recent 3-D model of the 5-HT$_{1A}$ receptor [27]. The interaction between the side chain of Asp$^{3.32}$ and the protonated piperidine ring with the side chain of Phe$^{6.51}$ was also modeled by full geometry optimization at the MP2 level of theory with the 6-31G* basis set. This procedure is capable, in principle, of describing C-H$\cdots\pi$ bonds [28].

Models of the mutant 5-HT$_4$ receptor complexed with GR113808

The helix bundles of the Asp$^{3.32}$Asn, Phe$^{6.52}$Val, Asn$^{6.55}$Leu, and Phe$^{6.52}$Ala/Asn$^{6.55}$Leu mutant receptors bound with GR113808 were constructed from the structure of the 5-HT$_4$R$\cdots$GR113808 complex, and changing the atoms implicated in the aminoacid substitutions and the conformation of GR113808 by interactive computer graphics. Subsequently, the complete systems were energy minimized (5000 steps). The interaction between Asn$^{3.32}$, in the Asp$^{3.32}$Asn mutant, and the protonated piperidine ring with Phe$^{6.51}$ was modeled by full geometry optimization at the MP2 level of theory with the 6-31G* basis set.

Quantum mechanical calculations were performed with the GAUSSIAN-98 system of programs [29]. Energy minimizations and molecular dynamics simulations were run with the Sander module of AMBER5 [30], the all-atom force field [31], SHAKE bond constraints in all bonds, a 2 fs integration time step, and a 13 Å cutoff for non-bonded interactions. Parameters for GR113808 were adapted from Cornell et al. [31] force field using RESP point charges [32].

Results and discussion

Model of the 5-HT$_4$ receptor complexed with GR113808

To identify the arragement in space of the essential determinants for recognition of the GR113808 ligand, we performed *ab-initio* geometry optimization of the ligand inside the side chains of Asp$^{3.32}$, Ser$^{5.43}$ and Asn$^{6.55}$, experimentally determined to form the ligand binding pocket [8]. Figure 2a depicts the energy-optimized structure. The complex is formed through (i) the ionic interaction between the N-H group of the protonated piperidine and the O_δ atom of Asp$^{3.32}$ at the optimized distance between heteroatoms of 2.65 Å; (ii) the hydrogen bond between the carbonylic oxygen of the ligand and the hydroxyl group of Ser$^{5.43}$ (3.00 Å); and (iii) hydrogen bond between the ether oxygen of the ligand and the amide group of Asn$^{6.55}$ (2.99 Å).

This optimized reduced model was used to position the ligand inside the transmembrane domain of

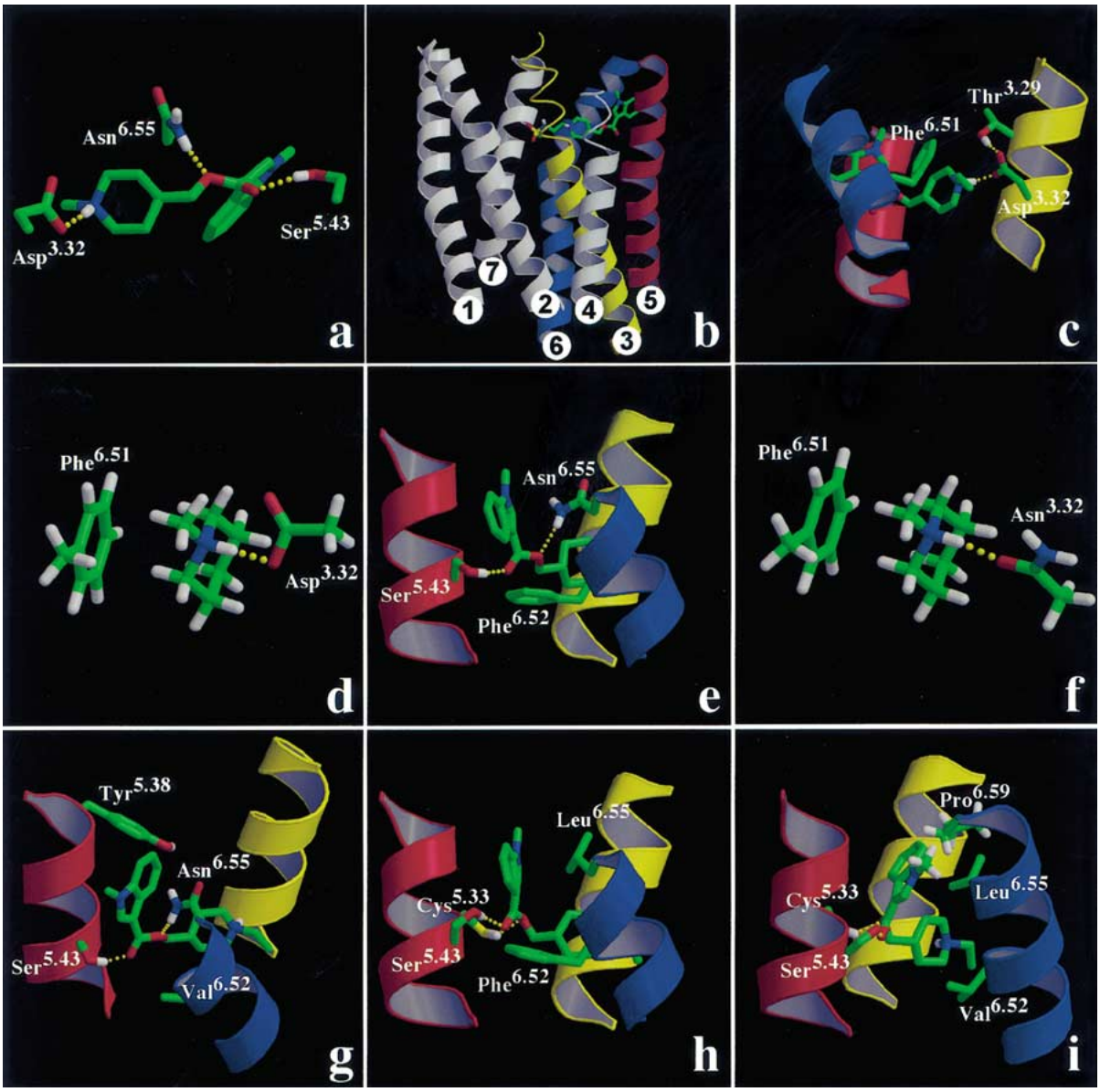

Figure 2. (a) *Ab-initio* geometry optimization, at the HF/3-21G level of theory, of GR113808 inside the side chains of $Asp^{3.32}$, $Ser^{5.43}$ and $Asn^{6.55}$. Only polar hydrogens are depicted to offer a better view. (b) Molecular model of the complex between GR113808 and the transmembrane helix bundle of the human 5-HT_4R constructed from the crystal structure of bovine RHO [20], in a view parallel to the membrane. (c, e, g, h, i) Detailed view of the transmembrane helix bundle of the 5-HT_4R (c, e) and the $Phe^{6.52}$Val (g), $Asn^{6.55}$Leu (h), and $Phe^{6.52}$Val/$Asn^{6.55}$Leu (i) mutant receptors complexed with GR113808 (the sulphonamide side chain is not depicted for clarity). The C_α traces of the extracellular part (top) of TM 3 (yellow), 5 (red), and 6 (blue) are shown. The protonated piperidine of the ligand forms an ionic interaction with $Asp^{3.32}$ and a C-H$\cdots\pi$ hydrogen bond with $Phe^{6.51}$ (c). The side chain of $Asp^{3.32}$ also forms a hydrogen bond with the neighboring side chain of $Thr^{3.29}$ (c). The carbonylic oxygen, the ether oxygen and the indole ring of the ligand hydrogen bond $Ser^{5.43}$, $Asn^{6.55}$ and $Phe^{6.52}$ (aromatic-aromatic interaction), respectively (e). The indole ring of the ligand replaces the interaction with $Phe^{6.52}$ by a similarly intense interaction with $Tyr^{5.38}$ in the $Phe^{6.52}$Val mutant (g). The mutation of $Asn^{6.55}$ to Leu replaces the hydrogen bond of the ether oxygen of the ligand from $Asn^{6.55}$ to $Cys^{5.42}$ (h). The change of orientation of the indole ring caused by the double $Phe^{6.52}$Val/$Asn^{6.55}$Leu mutant makes its N-methyl group to crash with $Pro^{6.59}$ (i). (d, f) Ab-initio geometry optimization, at the MP2/6-31G* level of theory, of $Asp^{3.32}$ in wild type receptor (d) or $Asn^{3.32}$ in the $Asp^{3.32}$Asn mutant receptor (f), the piperidine moiety of the ligand, and $Phe^{6.51}$.

the 5-HT_4R (see Figure 2b and methods for computational details). The protonated piperidine of the ligand is located between (i) $Asp^{3.32}$ and (iv) $Phe^{6.51}$ (see Figure 2c). The electron-rich clouds of the aromatic ring of $Phe^{6.51}$ interact with the electron-poor hydrogens of the carbon atoms adjacent to the protonated piperidine nitrogen of the ligand. Probably, the -CH_2- group in the side chain attached to the piperidine nitrogen achieves the larger interaction with $Phe^{6.51}$ (see Figure 2c). This type of C-H$\cdots\pi$ interaction plays a significant role in stabilizing local 3-D structures of proteins [33]. This mode of binding explains why substitution of $Phe^{6.51}$ by Ala abolishes the binding of GR113808 to the 5-HT_4R [8]. To evaluate the magnitude of this C-H$\cdots\pi$ interaction a model complex formed by the side chain of $Asp^{3.32}$, the protonated piperidine ring of the ligand, and the side chain of $Phe^{6.51}$ was optimized at the MP2 level of theory with the 6-31G* basis set (see methods for computational details). Despite the system was fully optimized with no constraints, the relative orientation of $Asp^{3.32}$, the piperidine ring of the ligand, and $Phe^{6.51}$ resembles the model of the ligand inside the 5-HT_4R (see Figures 2c and 2d). The energy of interaction (see methods for computational details) defined as the difference in energy between the optimized complex and the sum of the energies of the $Asp^{3.32}$/piperidine moieties and $Phe^{6.51}$ side chain, calculated in the conformation obtained in the complex, is -6.9 kcal/mol. Thus, there is a significant interaction of the aromatic side chain of $Phe^{6.51}$ with the $Asp^{3.32}$/piperidine fragment, despite the presence of the negatively charged Asp side chain. The importance of this C-H$\cdots\pi$ interaction is also reflected in the crystal structure of the enzyme acetylcholinesterase [34, 35], that catalyzes the hydrolysis of the neurotransmitter acetylcholine into choline. The complexes with different inhibitors, that contain trimethyl substituted amine nitrogen, revealed that the cationic side chain interact primarily with aromatic residues and not with negatively charged residues also present in the active site. Moreover, the side chain of $Asp^{3.32}$ also forms a hydrogen bond with the neighboring side chain of $Thr^{3.29}$ (Figure 2c).

The indole ring of GR113808 is pointing towards (v) $Phe^{6.52}$ (see Figure 2e). The Phe side chain is positioned in the face-to-edge orientation (T-shaped) to the indole ring. This type of π-σ aromatic-aromatic interaction has been described as a protein structure stabilization [36]. $Phe^{6.52}$ act as hydrogen bond acceptor (π electrons) and the indole ring of GR113808 act as hydrogen bond donor (the C-H bond). Finally, the sulphonamide side chain attached to the piperidine nitrogen is pointing towards TM 7 and interacting with $Asn^{7.45}$ (results not shown).

Model of the $Asp^{3.32}$Asn mutant receptor

In the $Asp^{3.32}$Asn mutant receptor the N-H group of the protonated piperidine moiety of the ligand (i) forms a charged hydrogen bond with the O_δ atom of $Asn^{3.32}$ (see Figure 2f) replacing the ionic interaction with the O_δ atom of $Asp^{3.32}$ in the wild type receptor (see above). However, this significant modification of the mode of binding of the ligand does not decrease the affinity of GR113808 for the receptor [8].

The affinity constant is function of the interaction energy between the ligand and the receptor, the energy required to displace the ligand from the extracellular aqueous environment to the binding pocket of the receptor, and the energy required to change the conformation of the receptor from the unbound to the bound state. Thus, the following factors must be taken into account. First, the $Asp^{3.32}$Asn mutation decreases the binding of the N-H moiety of the protonated piperidine, from an ion pair ($Asp^{3.32}$) to a charged hydrogen bond ($Asn^{3.32}$). However, substitution of a negatively charged side chain (Asp) by a neutral side chain (Asn) increases the explicit charge in the hydrogens of the carbon atoms adjacent to the protonated piperidine nitrogen and accordingly the interaction with $Phe^{6.51}$. Thus, in order to estimate this effect we evaluated the interaction between $Phe^{6.51}$ and the protonated piperidine ring of the ligand hydrogen bonded to $Asn^{3.32}$, in a similar manner to the interaction of $Phe^{6.51}$ with the $Asp^{3.32}$/piperidine fragment in the wild type receptor (see above and methods). The fully optimized complex is depicted in Figure 2f. The calculated interaction energies confirm the previous hypothesis that the interaction of $Phe^{6.51}$ with the $Asn^{3.32}$/piperidine fragment (-11.0 kcal/mol) is stronger than with the $Asp^{3.32}$/piperidine fragment (-6.9 kcal/mol), partially compensating the decrease of binding energy due to the substitution of $Asp^{3.32}$ by Asn. The absence in serotonin of the piperidine ring or more importantly the $-CH_2$ group in the side chain attached to the piperidine nitrogen explains why the $Asp^{3.32}$Asn mutation has a significant effect in the binding of serotonin [8]. Notably, both ML10302 and ML10375 ligands possess the piperidine ring and the effect of the $Asp^{3.32}$Asn mutation is only partial. The magnitude of the $Asp^{3.32}$Asn mutation in piperidine-containing ligands will depend in the mode of binding

and the relative orientation of Phe$^{6.51}$ to stabilize the complex through the proposed C-H$\cdots\pi$ interaction.

Second, in the absence of the ligand the side chain at position 3.32 (Asp$^{3.32}$ in wild type or Asn$^{3.32}$ in the mutant receptor) is coordinated with other side chains of the receptor. For example, it has been shown for the α_{1B}-adrenergic receptor that Asp$^{3.32}$ interacts in the ligand-free form with a Lys residue in TM 7 [37, 38]. Thus, the process of ligand binding requires the partial or total disruption of the side chain environment at position 3.32. Clearly, this side chain reorganization will require a larger energetical cost for Asp than for Asn.

This data suggests that GR113808 possess similar affinity for the Asp$^{3.32}$Asn mutant receptor than for wild type receptor [8], because the loss of binding affinity from an ion pair (Asp) to a charged hydrogen bond (Asn) is compensated by the larger energetical penalty of Asp to disrupt its side chain environment, and the larger interaction between Phe$^{6.51}$ and the piperidine ring of the ligand in the Asp$^{3.32}$Asn mutant.

Model of the Phe$^{6.52}$Val mutant receptor

In the Phe$^{6.52}$Val mutant the indole ring of GR113808 modifies the conformation observed in the binding mode to wild type receptor (see Figure 2e) and replaces the π-σ aromatic-aromatic interaction with (v) Phe$^{6.52}$ by a similarly intense π-σ interaction with Tyr$^{5.38}$ (see Figure 2g). The Tyr side chain is also positioned in the face-to-edge orientation to the indole ring. In this mode of binding the indole ring of GR113808 act as hydrogen bond acceptor (π electrons) and Tyr$^{5.38}$ act as hydrogen bond donor (the C-H bond). Phe$^{6.52}$Val substitution does not have a significant effect in the binding of GR113808 [8], because the Phe$\cdots$indole interaction is similar in magnitude to the indole$\cdots$Tyr interaction.

Model of the Asn$^{6.55}$Leu mutant receptor

Substitution of Asn$^{6.55}$ by Leu does not allow the ether oxygen of GR113808 to hydrogen bond (iii) the amide group of Asn$^{6.55}$ as in wild type receptor (see above). Thus, the absence of Asn$^{6.55}$ drives the ether oxygen of the ligand to hydrogen bond Cys$^{5.42}$ while the carbonylic oxygen remains hydrogen bonded to Ser$^{5.43}$ (see Figure 2h). This hydrogen bond network resembles the suggested binding of the meta-hydroxyl group of catecholamine ligands to Ser$^{5.42}$ and Ser$^{5.43}$ in the β_2-adrenergic receptor [10]. It is important to note that the indole ring of GR113808 is pointing towards the intracellular side to achieve the π-σ aromatic-aromatic interaction with (v) Phe$^{6.52}$ as in wild type receptor (see above). This mode of binding orients the N-methyl substituent of the indole ring towards the extracellular side (see Figure 2h).

Clearly, the $-$SH moiety of Cys$^{5.42}$ cannot hydrogen bond the ether oxygen of the ligand with the same strength as the $-NH_2$ moiety of Asn$^{6.55}$. Thus, the Asn$^{6.55}$Leu mutation reduces the affinity of GR113808 by a factor of 5.2 [8] that represents a free energy change of 1.0 kcal/mol. This approximately equals the free energy difference between the SH$\cdots$O and NH$\cdots$O hydrogen bonds.

In contrast, the Asn$^{6.55}$ to Leu substitution abolishes the binding of serotonin [8]. Thus, the mode of binding of serotonin to Asn$^{6.55}$ differs from GR113808. The absence of the second hydrogen bond acceptor group in serotonin (the ether oxygen in GR113808) makes the indole ring of serotonin to hydrogen bond Asn$^{6.55}$ (results not shown). The hydrogen bond is formed between the π electron-rich clouds of the aromatic ring and the electron-poor $-NH_2$ hydrogens of Asn$^{6.55}$ in a similar manner to the proposed hydrogen bond between benzene and water [39]. Clearly, in the Asn$^{6.55}$Leu mutant receptor the indole ring of serotonin cannot hydrogen bond Cys$^{5.42}$ as the ether oxygen of GR113808 does with the observed loss of binding affinity.

Model of the Phe$^{6.52}$Val/Asn$^{6.55}$Leu double mutant receptor

Surprisingly, the double Phe$^{6.52}$Val/Asn$^{6.55}$Leu mutant avoids the binding of GR113808, despite the single Phe$^{6.52}$Val or Asn$^{6.55}$Leu mutations have none or small effect [8]. In this double mutant receptor the absence of Asn$^{6.55}$ forces the ether/carbonylic oxygens of the ligand to hydrogen bond Cys$^{5.42}$ and Ser$^{5.43}$, as in the Asn$^{6.55}$Leu mutant receptor (see above); and the absence of Phe$^{6.52}$ forces the indole ring of the ligand to point towards the extracellular, as in the Phe$^{6.52}$Val mutant (see above). However, in the Phe$^{6.52}$Val single mutant receptor the hydrogen bond to Ser$^{5.43}$ and Asn$^{6.55}$ places the indole ring between TM 5 and 6 (see Figure 2g), whereas in the Phe$^{6.52}$Val/Asn$^{6.55}$Leu double mutant the hydrogen bond to Cys$^{5.42}$ and Ser$^{5.43}$ places the indole ring towards TM 6 (see Figure 2i). This small change in the orientation of the indole ring makes its N-methyl group to crash with Pro$^{6.59}$ in TM 6 (see Figure 2i). This mode of binding explains the lack of affinity

of GR113808 for the double Phe$^{6.52}$Val/Asn$^{6.55}$Leu mutant receptor [8].

Conclusions

The recognition of the GR113808 antagonist by the transmembrane domain of the human 5-HT$_4$R consist of: (i) the ionic interaction between the N-H group of the protonated piperidine of the ligand and Asp$^{3.32}$; (ii) the hydrogen bond between the carbonylic oxygen of the ligand and Ser$^{5.43}$; (iii) the hydrogen bond between the ether oxygen of the ligand and Asn$^{6.55}$; (iv) the hydrogen bond between the C-H groups adjacent to the protonated piperidine nitrogen and the π electrons of Phe$^{6.51}$; and (v) the π-σ aromatic-aromatic interaction between the indole ring of the ligand and Phe$^{6.52}$. This derived computational model has provided additional structural interpretation of the mutagenesis experiments aimed to test the role of Asp$^{3.32}$, Ser$^{5.43}$, Phe$^{6.51}$, Phe$^{6.52}$, and Asn$^{6.55}$ on the binding affinity of GR113808 to the 5-HT$_4$R [8]. This recognition model, together with the postulated pharmacophore model for the binding of 5-HT$_4$R antagonists [40], will be used to guide the design of new antagonists with predetermined affinities and selectivity. These studies are now in progress and the results will be reported in due course.

Acknowledgements

This work has been supported by the DGESIC (PB97-0282), the CICYT (SAF99-073), the Universidad Complutense (PR486/97-7483) and Fundació La Mataró TV3 (0014/97). Some of the simulations were run at the Centre de Computació i Comunicacions de Catalunya. The authors are grateful to Universidad Complutense for a predoctoral grant to M. Murcia.

References

1. Ji, T.H., Grossmann, M. and Ji, I., J. Biol. Chem., 273 (1998) 17299.
2. Eglen, R.M., Wong, E.H., Dumuis, A. and Bockaert, J., Trends Pharmacol. Sci., 16 (1995) 391.
3. Grossman, C.J., Gale, J.D., Bunce, K.T., Kilpatrick, G.J., Whitehead, J.W.F., Oxford, A.W. and Humphrey, P.P.A., Br. J. Pharmacol., 108 (1993) 106P.
4. Grossman, C.J., Kilpatrick, G.J. and Bunce, K.T., Br. J. Pharmacol., 109 (1993) 618.
5. Rhee, A.M.v. and Jacobson, K.A., Drug Devel. Res., 37 (1996) 1.
6. Yang, D., Soulier, J.L., Sicsic, S., Mathe-Allainmat, M., Bremont, B., Croci, T., Cardamone, R., Aureggi, G. and Langlois, M., J. Med. Chem., 40 (1997) 608.
7. Blondel, O., Gastineau, M., Langlois, M. and Fischmeister, R., Br. J. Pharmacol., 125 (1998) 595.
8. Mialet, J., Dahmoune, Y., Lezoualc'h, F., Berque-Bestel, I., Eftekhari, P., Hoebeke, J., Sicsic, S., Langlois, M. and Fischmeister, R., Br. J. Pharmacol., 130 (2000) 527.
9. Strader, C.D., Candelore, M.R., Hill, W.S., Sigal, I.S. and Dixon, R.A.F., J. Biol. Chem., 264 (1989) 13572.
10. Liapakis, G., Ballesteros, J.A., Papachristou, S., Chan, W.C., Chen, X. and Javitch, J.A., J. Biol. Chem., 275 (2000) 37779.
11. Wieland, K., Zuurmond, H.M., Krasel, C., Ijzerman, A.P. and Lohse, M.J., Proc. Natl. Acad. Sci. USA, 93 (1996) 9276.
12. Strader, C.D., Fong, T.M., Tota, M.R., Underwood, D. and Dixon, R.A.F., Annu. Rev. Biochem., 63 (1994) 101.
13. Choudhary, M.S., Craigo, S. and Roth, B.L., Mol. Pharmacol., 43 (1993) 755.
14. Choudhary, M.S., Sachs, N., Uluer, A., Glennon, R.A., Westkaemper, R.B. and Roth, B.L., Mol. Pharmacol., 47 (1995) 450.
15. Roth, B.L., Shoham, M., Choudhary, M.S. and Khan, N., Mol. Pharmacol., 52 (1997) 259.
16. Chen, S., Xu, M., Lin, F., Lee, D., Riek, P. and Graham, R.M., J. Biol. Chem., 274 (1999) 16320.
17. Henderson, R., Baldwin, J.M., Ceska, T.A., Zemlin, F., Beckmann, E. and Downing, K.H., J. Mol. Biol., 213 (1990) 899–929.
18. Unger, V.M., Hargrave, P.A., Baldwin, J.M. and Schertler, G.F.X., Nature, 389 (1997) 203.
19. Baldwin, J.M., Schertler, G.F.X. and Unger, V.M., J. Mol. Biol., 272 (1997) 144.
20. Palczewski, K., Kumasaka, T., Hori, T., Behnke, C.A., Motoshima, H., Fox, B.A., Trong, I.L., Teller, D.C., Okada, T., Stenkamp, R.E., Yamamoto, M. and Miyano, M., Science, 289 (2000) 739.
21. Ballesteros, J.A. and Weinstein, H., Methods in Neurosciences, 25 (1995) 366.
22. Horn, F., Weare, J., Beukers, M.W., Hörsch, S., Bairoch, A., Chen, W., Edvardsen, Ø., Campagne, F. and Vriend, G., Nucl. Acids Res., 26 (1998) 277.
23. Dunbrack, R.L.J. and Cohen, F.E., Protein Sci., 6 (1997) 1661.
24. Gray, T.M. and Matthews, B.W., J. Mol. Biol., 175 (1984) 75.
25. Ballesteros, J.A., Deupi, X., Olivella, M., Haaksma, E.E.J. and Pardo, L., Biophys. J., 79 (2000) 2754.
26. Govaerts, C., Blanpain, C., Deupi, X., Ballet, S., Ballesteros, J.A., Wodak, S.J., Vassart, G., Pardo, L. and Parmentier, M., J. Biol. Chem., 276 (2001) 13217.
27. López-Rodriguez, M.L., Morcillo, M.J., Fernández, E., Rosado, M.L., Pardo, L. and Schaper, K.-J., J. Med. Chem., 44 (2001) 198.
28. Novoa, J.J. and Mota, F., Chem. Phys. Lett., 318 (2000) 345.
29. Frisch, M.J., Trucks, G.W., Schlegel, H.B., Scuseria, G.E., Robb, M.A., Cheeseman, J.R., Zakrzewski, V.G., Montgomery, J.A., Keith, T.A., Petersson, G.A., Raghavachari, K., Al-Laham, A., Stratmann, R.E., Burant, J.C., Dapprich, S., Millam, J.M., Daniels, A.D., Kudin, K.N., Strain, M.C., Farkas, O., Tomasi, J., Barone, V., Cossi, M., Cammi, R., Mennucci, B., Pomelli, C., Adamo, C., Clifford, S., Ochterski, J., Petersson, G.A., Ayala, P.Y., Cui, Q., Morokuma, K., Malick, D.K., Rabuck, A.D., Raghavachari, K., Foresman, J.B., Cioslowski, J., Ortiz, J.V., Stefanov, B.B., Liu, G., Liashenko, A., Piskorz, P., Komaromi, I., Gomperts, R., Martin, R.L., Fox, D.J., Keith, T., Al-Laham, M.A., Peng,

C.Y., Nanayakkara, A., Gonzalez, C., Challacombe, M., Gill, P.M.W., Johnson, B.G., Chen, W., Wong, W., Andres, J.L., Head–Gordon, M., Replogle, E.S. and Pople, J.A. (1998) GAUSSIAN-98.
30. Case, D.A., Pearlman, D.A., Caldwell, J.W., Cheatham III, T.E., Ross, W.S., Simmerling, C.L., Darden, T.A., Merz, K.M., Stanton, R.V., Cheng, A.L., Vicent, J.J., Crowley, M., Ferguson, D.M., Radmer, R.J., Seibel, G.L., Singh, U.C., Weiner, P.K. and Kollman, P.A. (1997) AMBER5, University of California, San Francisco.
31. Cornell, W.D., Cieplak, P., Bayly, C.I., Gould, I.R., Merz Jr., K.M., Ferguson, D.M., Spellmeyer, D.C., Fox, T., Caldwell, J.W. and Kollman, P.A., J. Am. Chem. Soc., 117 (1995) 5179.
32. Cieplak, P., Cornell, W.D., Bayly, C. and Kollman, P.A., J. Comput. Chem., 16 (1995) 1357.
33. Steiner, T. and Koellner, G., J. Mol. Biol., 305 (2001) 535.
34. Kryger, G., Silman, I. and Sussman, J.L., Structure, 7 (1999) 297.
35. Harel, M., Shalk, I., Ehret-Sabatier, L., Bouet, L., Goeldner, M., Hirth, C., Axelsen, P.H., Silman, I. and Sussman, J.L., Proc. Natl. Acad. Sci. USA, 90 (1993) 9031.
36. Burley, S.K. and Petsko, G.A., Science, 229 (1985) 23.
37. Porter, J.E., Hwa, J. and Perez, D.M., J. Biol. Chem., 271 (1996) 28318.
38. Porter, J.E. and Perez, D.M., J. Biol. Chem., 274 (1999) 34535.
39. Suzuki, S., Green, P.G., Bumgarner, R.E., Dasgupta, S., Goddard III, W.A. and Blake, G.A., Science, 257 (1992) 942.
40. López-Rodriguez, M.L., Morcillo, M.J., Benhamú, B. and Rosado, M.L., J. Comput. Aid. Mol. Des., 11 (1997) 589.
41. Kraulis, J., J. Appl. Cryst., 24 (1991) 946.
42. Merritt, E.A. and Bacon, D.J., Meth. Enzymol., 277 (1997) 505.

Optimization of the Pharmacophore Model for 5-HT$_7$R Antagonism. Design and Synthesis of New Naphtholactam and Naphthosultam Derivatives

María L. López-Rodríguez,*,† Esther Porras,† M. José Morcillo,‡ Bellinda Benhamú,† Luis J. Soto,† José L. Lavandera,† José A. Ramos,§ Mireia Olivella,|| Mercedes Campillo,|| and Leonardo Pardo||

Departamento de Química Orgánica I, Facultad de Ciencias Químicas, and Departamento de Bioquímica y Biología Molecular III, Facultad de Medicina, Universidad Complutense, E-28040 Madrid, Spain, Facultad de Ciencias, Universidad Nacional de Educación a Distancia, E-28040 Madrid, Spain, and Laboratori de Medicina Computacional, Unitat de Bioestadística and Institut de Neurociències, Universitat Autònoma de Barcelona, E-08193 Cerdanyola del Vallès, Barcelona, Spain

Received March 13, 2003

We present in this study an optimization of a preliminary pharmacophore model for 5-HT$_7$R antagonism, with the incorporation of recently reported ligands and using an efficient procedure with the CATALYST program. The model consists of five features: a positive ionizable atom (PI), a H-bonding acceptor group (HBA), and three hydrophobic regions (HYD). This model has been supported by the design, synthesis, and biological evaluation of new naphtholactam and naphthosultam derivatives of general structure **I** (**39**−**72**). A systematic structure−affinity relationship (SAFIR) study on these analogues has allowed us to confirm that the model incorporates the essential structural features for 5-HT$_7$R antagonism. In addition, computational simulation of the complex between compound **56** and a rhodopsin-based 3D model of the 5-HT$_7$R transmembrane domain has permitted us to define the molecular details of the ligand−receptor interaction and gives additional support to the proposed pharmacophore model for 5-HT$_7$R antagonism: (i) the HBA feature of the pharmacophore model binds Ser$^{5.42}$ and Thr$^{5.43}$, (ii) the HYD1 feature interacts with Phe$^{6.52}$, (iii) the PI feature forms an ionic interaction with Asp$^{3.32}$, and (iv) the HYD3 (AR) feature interacts with a set of aromatic residues (Phe$^{3.28}$, Tyr$^{7.43}$). These results provide the tools for the design and synthesis of new ligands with predetermined affinities and pharmacological properties.

Introduction

Serotonin (5-hydroxytryptamine, 5-HT) is an important neurotransmitter discovered over 50 years ago and, at present, it continues to generate interest as one of the most attractive targets for medicinal chemists. Molecular cloning and gene expression techniques have led to the characterization of 14 serotonin receptor subtypes, which can be classified in seven subfamilies (5-HT$_{1-7}$)[1−4] based on pharmacological properties, second messenger coupling, and sequence data. These receptors belong to the seven transmembrane G protein-coupled receptor superfamily (GPCRs),[5,6] except the 5-HT$_3$ receptor, which is a ligand-gated ion channel. 5-HT$_7$ is the most recent addition to the burgeoning family of 5-HT receptors that was identified from cloning studies before the corresponding endogenous receptor was found.[7,8] This receptor is positively coupled to adenylyl cyclase through G_s when expressed in cell lines.[9] The 5-HT$_7$ receptor (5-HT$_7$R) has been cloned from mouse,[10] rat,[11,12] guinea pig,[13] and human[14] and exhibits a low sequence homology with other 5-HT receptors. The binding profile appears consistent across species and between cloned and native 5-HT$_7$Rs. Splice variants have been identified[15−17] in rat and human that display similar tissue distribution and pharmacological and functional characteristics. Although the biological functions of the 5-HT$_7$R have not been fully clarified, early pharmacological data suggest that this subtype may be involved in disturbance of circadian rhythms,[18,19] such as jet lag and delayed sleep-phase syndrome. Therefore, a 5-HT$_7$R antagonist might be a useful therapeutic agent for the treatment of sleep disorders. It is also believed that a deregulated circadian rhythm could lead to mental fatigue and depression. Thus, one of the consequent mechanisms of antidepressant treatment could be the modulation of a possible dysrhythmic circadian function in depression, in which the 5-HT$_7$R might be one of the key players.[20] The fact that antipsychotic agents exhibit a high affinity for the 5-HT$_7$R leads to the speculation that this receptor might provide a target for the treatment of psychotic disorders.[21−24] In the periphery, the 5-HT$_7$R plays a role in smooth muscle relaxation in a variety of tissues[25−30] and so it might be involved in diseases such as irritable bowel syndrome[31] or migraine.[32] Nevertheless, the therapeutic utility of 5-HT$_7$R agents awaits the development of selective ligands. Despite intense research efforts in this area, very few compounds with significant 5-HT$_7$R antagonist activity have been reported and, to date, only five selective antagonists belonging to two structural classes of compounds (SB-258719,[33] DR4004,[34] SB-269970,[35] DR4365,[36] and DR4485[37]) have been discovered by high-throughput screening. Information on the structural properties of the 5-HT$_7$R agents remains unknown and its determi-

* To whom correspondence should be addressed. Phone: 34-91-3944239. Fax: 34-91-3944103. E-mail: mluzlr@quim.ucm.es.
† Departamento de Química Orgánica I, Facultad de Ciencias Químicas, Universidad Complutense.
‡ Universidad Nacional de Educación a Distancia.
§ Departamento de Bioquímica y Biología Molecular III, Facultad de Medicina, Universidad Complutense.
|| Universitat Autònoma de Barcelona.

10.1021/jm030841r CCC: $25.00
Published on Web 11/08/2003

nation represents a critical step for developing specific compounds.

In this context it is important to derive putative 3D pharmacophore models, and we have recently postulated a pharmacophore model for 5-HT_7R antagonism,[38] as an initial step in the course of an extensive program targeted at the discovery of new serotonin 5-HT_7R ligands.

In the present work, with the aim of gaining insight into the pharmacophoric patterns responsible for 5-HT_7R affinity, we have carried out an optimization of this preliminary hypothesis with the incorporation of recently reported antagonists and using a systematic and efficient procedure with the CATALYST program.[39] Subsequently, the identified 3D pharmacophore was used to search flexible 3D databases to discover novel chemical entities that could provide knowledge for the design of new lead compounds. On the basis of these results and in order to give support to our model, new designed analogues of general structure **I** (**39**−**72**) were synthesized and evaluated for affinity at the 5-HT_7R. The analysis of the influence of some structural variations of the different pharmacophoric elements on the affinity for the 5-HT_7R of this class of compounds led us to confirm the essential requirements postulated for 5-HT_7R antagonism. Moreover, computational simulations of the complex between compound **56** and a 3D model of the transmembrane domain of the receptor have permitted the identification of the molecular determinants of recognition of these ligands by the 5-HT_7R.

Computational Methods

Pharmacophore Model for 5-HT_7R Antagonists. Compounds **1**−**38** were built de novo using standard options within the 2D/3D editor sketcher of the CATALYST 4.5[39] program. In cases where the chirality of the active form is not known, all possible stereoisomers were generated and considered. Each compound is treated as a collection of conformers covering the accessible conformational space within an energy range.[40,41] The BEST conformational analysis procedure was applied. The number of conformers was limited to a maximum of 250 and with 25 kcal/mol energy threshold above the calculated global minimum as estimated with the CHARMm-like force field.[40,42,43]

CATALYST 4.5[39] software supports the HypoGen algorithm, which is able to generate pharmacophoric hypotheses from a set of compounds known to be active at a specific target, by means of identification of common features present in the active but absent in the inactive molecules of the training set. Previously reported models developed by HypoGen have been successfully used to suggest new directions in lead discovery[44−49] and for searching databases to identify new structural classes of potential lead candidates.[50] The following values were chosen: spacing (1.00−2.95 Å), weight variation (1.0), tolerance variation (1.0), mapping coefficient (0), and activity uncertainty (3). Hypothesis selection is done by a cost analysis procedure. The cost function consists on three terms: the weight cost, which increases in a Gaussian form as the feature weight in a model deviates from an idealized value of 2.0; the error cost, which penalizes the deviation between the estimated activities of the training set and their experimentally determined values; and the configuration cost, which penalizes the complexity of the hypothesis. Of these three, the error cost contributes the most in determining the overall cost of a hypothesis. The 10 lowest energy cost hypotheses are extracted and analyzed. Moreover, the cost of two theoretical hypotheses [the ideal hypothesis, which is the simplest possible hypothesis that fits the data with minimal cost (fixed cost), and the null hypothesis, where the error cost is high (null cost)] are computed. These fixed and null cost values represent the minimum and maximum energy cost values, respectively. The greater their difference, the higher the probability of finding predictive models (>60 bits, >90%; 40−60 bits, 75−90%; <40 bits, <75%).

3D-Database Searching. A database search has been performed using the "best flexible search" method provided by CATALYST 4.5.[39] The defined pharmacophore model was built into a 3D query, which included pharmacophoric features (HBA, PI, HYD1, HYD2, and HYD3) and distance ranges between the crucial components of the pharmacophore. The conformational models stored in the databases are allowed to flex in order to map the 3D query. The NCI (National Cancer Institute), Maybridge, MiniBioByte, and Sample databases (provided with CATALYST 4.5), containing a total of approximately 178 600 compounds, were searched.

Model of the Complex between Compound 56 and the 5-HT_7R. The construction of the 3D model of the transmembrane domain of the 5-HT_7R was performed in a manner similar to the recently described model of the 5-HT_4R.[51] This computer model maintains the position of the transmembrane helices (TMHs) as in rhodopsin[52] with the exception of TMH 3. TMH 3 is slightly bent toward TMH 5, at position 3.37 (receptor-numbering scheme of Ballesteros and Weinstein[53]), to facilitate the experimentally derived interactions between the ligand and the conserved $Asp^{3.32}$, in TMH 3, and a series of conserved Ser/Thr residues (5.42 and 5.43), in TMH 5. This structural effect is due to the gauche-conformation of the $Thr^{3.37}$ side chain.[54] We have recently provided experimental evidence for this structural difference of TMH 3 in rhodopsin and the serotonin family by designing and testing ligands that contain comparable functional groups but at different interatomic distances.[55]

The mode of recognition of the naphtholactam moiety of the ligand was first determined by ab initio geometry optimization with the ONIOM procedure.[56] The model system consisted of $Val^{3.33}$, $Ile^{4.56}$, $Ser^{5.42}$, $Thr^{5.43}$, and $Phe^{6.52}$ (only the C_α atom of the backbone is included) of the 5-HT_7R and the ligand **56** [the $-(CH_2)_5-$ chain plus the piperazine and phenyl rings were replaced by a methyl group]. All free valences were capped with hydrogen atoms. The C_α atoms of the residues were kept fixed at the positions obtained in the 5-HT_7R model. The ONIOM procedure allows the molecular system to be divided into three layers that are treated at different levels of theory: ligand **56** and $Phe^{6.52}$ at the MP2/6-31G* level of theory, which is capable of describing the proposed C−H$\cdots\pi$ interactions;[57] $Ser^{5.42}$ and $Thr^{5.43}$ at the B3LYP/6-31G level of theory; and $Val^{3.33}$ and $Ile^{4.56}$ at the semiempirical AM-1 level of theory.

This optimized reduced model of the ligand−receptor complex was used to position compound **56** inside the

Table 1. Training Set Used in the Generation of the Pharmacophore for Selective 5-HT$_7$R Antagonists

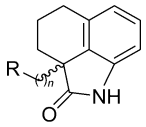

no.	*n*	R	pK_i expl.[a]	pK_i est.
1	2	4-phenylpiperazin-1-yl	7.0	7.7
2	3	4-phenylpiperazin-1-yl	8.3	7.4
3	4	4-phenylpiperazin-1-yl	8.5	8.0
4	4	4-(2-methoxyphenyl)piperazin-1-yl	8.3	8.4
5	4	4-(2-cyanophenyl)piperazin-1-yl	8.4	8.1
6	4	4-(2-pyridyl)piperazin-1-yl	8.7	8.4
7 (DR4004)	4	4-phenyl-1,2,3,6-tetrahydropyridyl	8.7	8.7
8	4	4-cyclohexylpiperazin-1-yl	4	5.2

[a] Values reported in ref 34.

entire transmembrane domain of the 5-HT$_7$R. Subsequently, the ligand−receptor complex was placed in a rectangular box (∼76 Å × 77 Å × 64 Å in size) containing methane molecules (7312 molecules in addition to the transmembrane domain) to mimic the hydrophobic environment of the transmembrane helices. It has been shown that this procedure reproduces several structural characteristics of membrane-embedded proteins.[58] Finally, the complete system was energy-minimized using the particle mesh Ewald method to evaluate electrostatic interactions and a 13 Å cutoff for nonbonded interactions. Parameters for the system were obtained from the Cornell et al. force field[59] and the "general Amber force field" using RESP point charges.[60]

Quantum mechanical calculations were performed with the GAUSSIAN-98 system of programs.[61] Energy minimizations were run with the Sander module of AMBER7.[62]

Results and Discussion

Conformational Analysis with Catalyst. A total of 38 reported compounds were selected[10−12,14,33−35,63−65] as a training set in the generation of a pharmacophoric model for 5-HT$_7$R antagonists. Their 2D chemical structure and binding affinities are represented in Tables 1−5 and Chart 1. The structural diversity and wide range of affinities, spanning 5 orders of magnitude, from 1.3 nM to 100 μM, are necessary to obtain meaningful results. A conformational analysis was performed, as described in the Computational Methods section, for the compounds in the training set. In our case, an almost balanced distribution of axial and equatorial substituents on the piperazine ring (representing the most favorable conformations) was highlighted. In addition, twisted or even orthogonal conformations of the piperazine with respect to the phenyl ring of the arylpiperazine moiety of the ligands were also found. These results were compared with Molecular Dynamics and Monte Carlo conformational searches carried out on these piperazine derivatives.

The library of the chemical descriptors in the program[66] was used to map the chemical functionalities of each molecule. The following kinds of surface-accessible functions were considered for pharmacophore generation: hydrogen bond acceptor (HBA), hydrophobic group (HYD), positively ionizable center (PI), and aromatic ring (AR). The obtained conformations of each compound were used to align these chemically important functional groups, and pharmacophoric models were then generated from the aligned structures.

As an initial approach, a training set of 38 compounds from different chemical series, described in the literature as selective and nonselective 5-HT$_7$R antagonists, were used to generate pharmacophore models with CATALYST. The best hypothesis obtained (hypothesis 1 in Table 6), with one hydrogen-bond acceptor (HBA), two hydrophobic (HYD) features, one positive ionizable (PI) group, and one aromatic ring (AR) feature, presented a low correlation coefficient (0.7396). Thus, to improve this poor statistic, we removed the nonselective compounds (**25**−**38**) from the training set, with the aim of identifying a statistically significant 3D arrangement of chemical functions that explains the selective affinity for the 5-HT$_7$R. It is important to note that attempts to obtain a pharmacophore model using the nonselective set (**25**−**38**) leads to models with a low predictive power (the difference between null and fixed cost is lower than 35; results not shown).

Pharmacophore Model for Selective 5-HT$_7$R Antagonists. Sets of 10 hypotheses were generated with compounds **1**−**24**. Table 6 shows the best hypotheses obtained, listed as 2−6, with different cost values, correlation coefficients, and pharmacophore features. Hypotheses 2 and 3 have five chemical features in a similar spatial location, their only difference being the replacement of one of the hydrophobic features found

Table 2. Training Set Used in the Generation of the Pharmacophore for Selective 5-HT$_7$R Antagonists

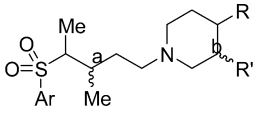

no.	Ar	R	R	stereochemistry a	stereochemistry b	pK_i expl[a]	pK_i est.
9	1-naphthyl	H	Me	*R*	*R*	6.9	6.8
10	1-naphthyl	H	Me	*R*	*S*	6.2	6.5
11	1-naphthyl	H	Me	*S*	*R*	5.8	6.1
12	1-naphthyl	H	Me	*S*	*S*	4	6.0
13 (SB-258719)	3-methylphenyl	Me	H	*R*		7.5	7.7
14	1-naphthyl	Me	H	*R*		7.5	6.6
15	3,4-dichlorophenyl	Me	H	*R*		7.5	7.4
16	3,4-dibromophenyl	Me	H	*R*		7.7	7.7
17	4,5-dibromo-2-thienyl	Me	H	*R*		7.8	7.2

[a] Values reported in ref 33.

Table 3. Training Set Used in the Generation of the Pharmacophore for Selective 5-HT$_7$R Antagonists

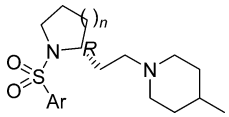

no.	Ar	*n*	pK_i expl[a]	pK_i est.
18	1-naphthyl	2	7.8	7.5
19	1-naphthyl	1	8.0	7.7
20	3,4-dichlorophenyl	1	8.4	8.7
21	3-bromophenyl	1	8.7	8.2
22 (SB-258741)	3-methylphenyl	1	8.5	8.0
23	3-methoxyphenyl	1	8.0	8.3
24 (SB-269970)	3-hydroxyphenyl	1	8.9	8.6

[a] Values reported in ref 35.

Table 4. Training Set Used in the Generation of the Pharmacophore for Nonselective 5-HT$_7$R Antagonists

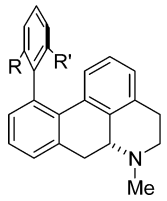

no.	R	R	pK_i(5-HT$_7$)[a]
25	OMe	OMe	7.9
26	CN	Me	8.4
27	OH	Me	7.6

[a] Values reported in ref 63.

Table 5. Training Set Used in the Generation of the Pharmacophore for Nonselective 5-HT$_7$R Antagonists

no.	compd	pK_i(5-HT$_7$)	refs
28	metergoline	8.2	12, 14, 64
29	mesulergine	8.1	12
30	2-Br-LSD	8.0	10
31	methylsergide	7.9	12
32	clozapine	7.9	12
33	(*S*)-methiothepine	9.0	12
34	cyproheptadine	7.3	12
35	mianserin	7.2	11
36	(+)-butaclamol	7.2[a]	10, 11
37	ritanserin	7.8	12
38	spiperone	7.7	11, 65

[a] This value represents the mean of different pK_i values reported in refs 10 and 11.

in hypothesis 2 with a more specific aromatic ring in hypothesis 3 (Figure 1a,b). On the basis of the very similar composition of the two hypotheses, hypothesis 2, characterized by the best statistical parameters (Table 6), has been chosen to represent the best candidate as a pharmacophore for 5-HT$_7$R selective compounds, which consist of a basic nitrogen atom (PI), a H-bonding acceptor group (HBA), and three hydrophobic regions (HYD) at the distances represented in Figure 1a. The HYD (blue) and PI (red) features are drawn as globes, whereas HBA (green) and AR (orange) features are shown as two globes due to the directional nature of these chemical functions.

The total cost of hypothesis 2 was 154.15. With a cost difference between fixed and null hypotheses of 48.95 bits, the probability that a true correlation exists in the data is high. On this hypothesis, all the compounds mapped the PI feature and at least one of the three HYD

Chart 1. 2D Chemical Structures of the Molecules of the Nonselective Training Set (**28**−**38**)

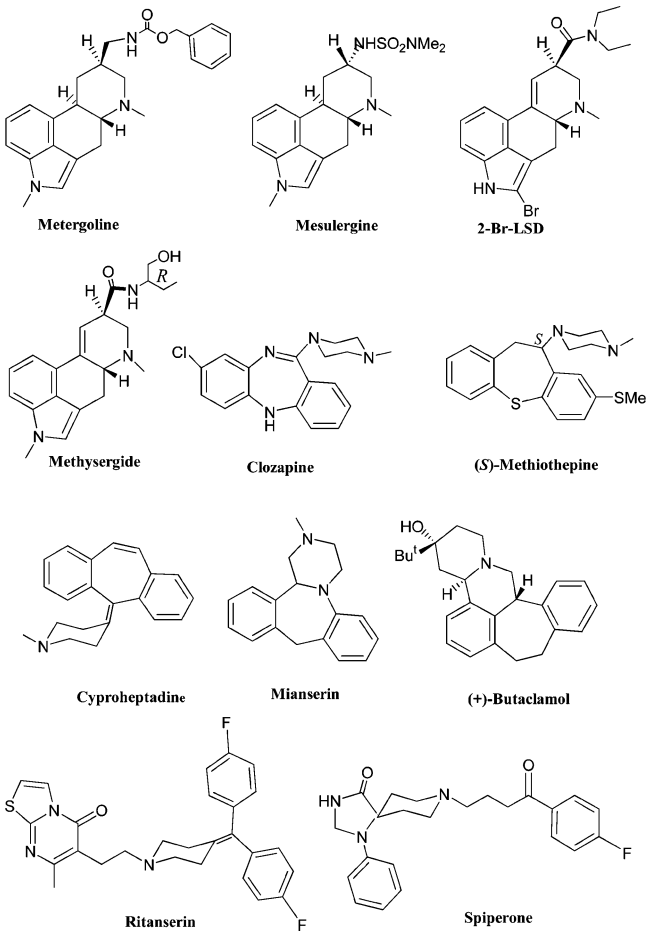

features, while the HBA was fitted by 62.5% of compounds. In Figure 2, the good predictive power of this model is indicated by the high correlation coefficient between experimental and estimated affinity values (r = 0.9123). As shown in Tables 1−3, for all the molecules in the training set this model is able to predict the affinity of compounds with reasonable precision. In this case a predicted pK_i value within 1 log unit of the experimental pK_i value was considered to be a valid prediction of fit. From these data in Tables 1−3 we can see that out of 10 highly active compounds (pK_i > 8), nine were accurately predicted as highly active and only one (compound **2**) was predicted as moderately active. Out of nine moderately active compounds (8 ≤ pK_i ≤ 7), one compound (**23**) was predicted as highly active and another one (**14**) was predicted as poorly active (pK_i < 7). Those compounds with low 5-HT$_7$R affinity (pK_i < 7) were correctly predicted.

Figure 1c,d shows DR4004 (**7**) and SB-269970 (**24**), the most active and selective compounds in the training set, placed into the pharmacophore model for selective 5-HT$_7$R antagonists. In detail, SB-269970 (**24**) fulfills HYD features through aliphatic regions, the HBA with the sulfonamide group, and the PI feature through the protonated nitrogen of the piperidine ring.

3D-Database Searching and Design. We have selected hypothesis 2 for selective 5-HT$_7$R antagonists as a better pharmacophore model (Figure 1a) to design and synthesize new 5-HT$_7$R ligands as a *test set* in order to evaluate the predictive power of the model. This

Table 6. Summary of All the Most Important Generated Hypotheses

hypothesis	training set[a]	features in the hypothesis[b]	cost			compd mappings
			fixed	total (correl)	null	
1	A = 38 compds	HBA, 2xHYD, PI, AR	166.906	215.294 (0.7396)	227.741	11 HBA; 14 HYD1; 29 HYD2; 36 PI; 38 AR
2	B = 24 selective compds	HBA, 3xHYD, PI	122.888	154.15 (0.9123)	171.836	15 HBA; 24 HYD1; 14 HYD2; 24 HYD3; 24 PI
3	B = 24 selective compds	HBA, 2xHYD, PI, AR	122.888	162.003 (0.8617)	171.836	19HBA; 23 HYD1; 24 HYD2; 24 PI; 6 AR
4	B = 24 selective compds	HBA, 2xHYD, PI, AR	122.888	164.424 (0.8857)	171.836	18HBA; 24 HYD1; 23 HYD2; 23 PI; 7 AR
5	B = 24 selective compds	HBA, 3xHYD, PI	123.158	154.788 (0.9043)	171.836	15 HBA; 24 HYD1; 13 HYD2; 23 HYD3; 24 PI
6	B = 24 selective compds	HBA, 2xHYD, PI, AR	123.158	162.537 (0.8539)	171.836	16 HBA; 24 HYD1; 24 HYD2; 24 PI; 7 AR

[a] 38 compds = whole set of compounds selective + nonselective. [b] HBA, hydrogen bond acceptor; HYD, hydrophobic; PI, positive ionizable; AR, aromatic ring.

pharmacophore model was used as a 3D query to perform a database search to find other structural motifs that fulfill the functional and spatial constraints imposed by the model itself. Several databases (see Computational Methods), containing approximately 178 600 compounds, were searched.

On the basis of the analysis of these results, a new series of derivatives of general structure **I** with synthetic accessibility were designed as *test set* (Figure 3a). Conformational analysis reveals that compounds with an optimum length of four or five methylene units for the spacer map fit in an efficient way the hypothesis 2. For example, in compound **51** (X = CO, n = 4, Y = N, R = phenyl) an aromatic ring of the naphtholactam system fits within HYD1, the carbonyl group acts as HBA, the basic nitrogen atom fits within the PI, the piperazine ring fits within HYD2, and the phenyl ring is HYD3 (Figure 3b). Thus, we have considered the synthesis, biological evaluation, and initial SAR investigations of compounds **39**−**72** (Table 7) with the aim of giving support to the proposed pharmacophore model and confirming the optimum spacer length.

Chemistry. The synthetic routes used in the preparation of **39**−**72** are outlined in Scheme 1. Compounds **39** and **40** (n = 1) were obtained by Mannich reaction of benzo[*cd*]indol-2(1*H*)-one (naphtholactam) with formaldehyde and the appropriate arylpiperazines (method A). Treatment of 1-aryl-4-(3-chloropropyl)piperazines **73** and **74** with naphtholactam, in the presence of sodium hydride and *N*,*N*-dimethylformamide (DMF), gave **41** and **42** (method B). Desired compounds **43**−**71** (n = 4−6) were obtained by reaction of intermediates **75**−**80** with the appropriate amines in the presence of triethylamine in acetonitrile as solvent (method C). Preparation of compound **72** was performed by reaction of **75** with 1-methyl-1*H*-imidazole-2-thiol in the presence of sodium methoxide and methanol as solvent (method D). Treatment of 1-arylpiperazines with 1-bromo-3-chloropropane, in the presence of potassium carbonate and DMF, gave the corresponding intermediates **73** and **74**. The key derivatives **75**−**80** were prepared by reaction of naphtholactam or naphthosultam with the appropriate dibromoalkane in the presence of sodium hydride and DMF. Amines **81**−**83** were obtained by catalytic hydrogenation of corresponding pyridines. Respective hydrochloride salts were prepared as samples for biological assays. All new compounds were characterized by IR and ^{1}H and ^{13}C NMR spectroscopy and gave satisfactory combustion analyses (C, H, N).

Biochemistry. The 5-HT$_7$R binding affinity of synthesized compounds **39**−**72** was determined by measurement of the displacement of [^{3}H]-5-CT binding in rat hypothalamus membranes.[68] All the compounds were used in form of hydrochloride salts and were methanol-soluble. The inhibition constant K_i was calculated from the IC_{50} by the Cheng−Prusoff equation.[69] The results of these assays are illustrated in Table 7. Additionally, compound **56** was evaluated in a previously described functional model of 5-HT$_7$ receptor activation,[70] blocking 5-carboxamidotryptamine (5-CT)-stimulated adenylyl cyclase activity, indicating its antagonist profile.

Structure−**Affinity Relationship Studies.** One of the most important facts observed in the analysis of the results presented in Table 7 is that all the synthesized compounds that possess a significant affinity for the 5-HT$_7$R share all the chemical features of our pharmacophore model [e.g., pK_i(**52**) = 7.2, pK_i(**56**) = 7.1, and

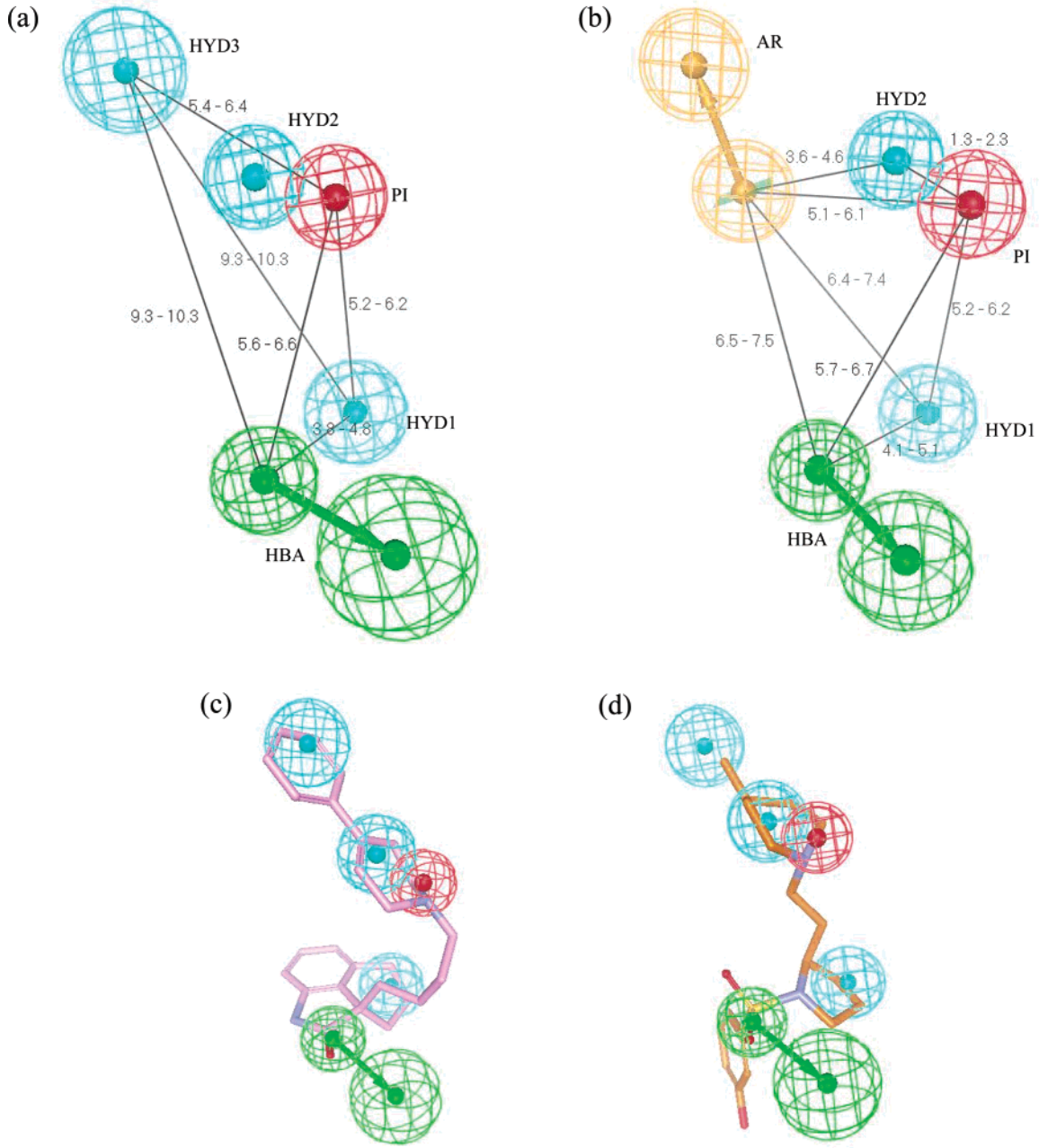

Figure 1. Pharmacophore models for selective 5-HT$_7$R antagonists: (a) hypothesis 2 and (b) hypothesis 3. Most active compounds in the selective training set, mapped onto hypothesis 2: (c) DR4004 (**7**) and (d) SB-269970 (**24**).

pK_i(**57**) = 7.0]. In contrast, derivatives that lack any of the pharmacophoric features required for 5-HT$_7$R antagonism are inactive; for instance, inactive compounds **39**−**42** lack the appropriate distance of 5.6−6.6 Å between HBA and PI. In this series the hydrophobic region (HYD3) situated at a distance of 5.4−6.4 Å from the nitrogen atom (PI) should be a more specific aromatic ring. Thus compounds with a nonaromatic moiety fitting within HYD3 are inactive [e.g. compounds **49** and **62** (R = methyl) and **50** and **55** (R = cyclohexyl)].

Study of the relationship between the structure and affinity of this class of compounds has given support to the pharmacophoric requirements postulated and has led to the following conclusions: (i) It can be observed that the optimum spacer length is four or five methylene units, since compounds with $n = 1$ or 3 are inactive [e.g. analogues **39** ($n = 1$) and **41** ($n = 3$): pK_i < 5]. An exception is represented by derivative **42** with a 3-carbon chain in the spacer (pK_i(**42**) = 6.4), but this compound has less affinity than **52** ($n = 4$, pK_i(**52**) = 7.2). An increase in the size of the alkyl chain to $n = 6$ causes a retention or moderate decrease in the binding affinity [e.g., pK_i(**64**) = 6.7 vs pK_i(**71**) = 6.7]. These results are in agreement with our pharmacophore model, which defines the optimum distance between the HBA and the basic center as 5.6−6.6 Å. Analogues with a shorter spacer than 5.6 Å ($n = 1$, 3) are inactive. The length of the spacer of derivatives bearing a 6-carbon chain may allow them to adopt a folded conformation with the appropriate distance to interact with the receptor. (ii) On the other hand, an examination of the binding data shows that naphtholactam derivatives are more potent at 5-HT$_7$R sites than naphthosultam analogues [e.g., pK_i(**52**) = 7.2 vs pK_i(**64**) = 6.7; pK_i(**57**) =

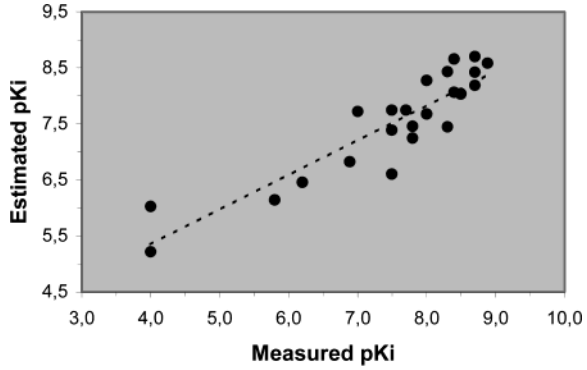

Figure 2. Correlation line displaying the experimental vs estimated affinity values by using the statistical most significant hypothesis of the selective training set (hypothesis 2), $r = 0.9123$.

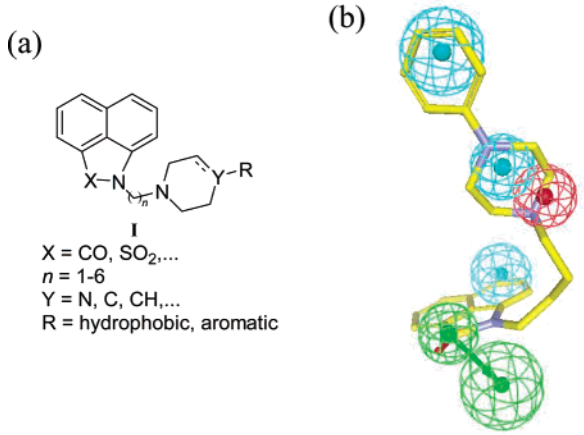

Figure 3. (a) Designed compounds of general structure **I**. (b) Compound **51** mapped on the pharmacophore model generated for selective 5-HT$_7$R antagonists (hypothesis 2).

7.0 vs pK_i(**68**) = 6.6)]. (iii) In general, replacement of the piperazine with a piperidine or tetrahydropyridine ring causes a dramatic loss in affinity. Thus, compound **51** (Y = N) shows 5-HT$_7$R affinity (pK_i = 6.2), while analogues **47** (Y = CH) and **48** (Y = C) are inactive (pK_i < 6). These findings clearly suggest that the nitrogen in position 4 of the piperazine ring plays an important role on 5-HT$_7$R affinity, in this kind of ligand. (iv) Our data indicate that the hydrophobic region HYD3 must be aromatic, since only compounds of general structure **I** with this *hydrophobic−aromatic* region show affinity for the 5-HT$_7$R. Thus, substitution of the phenyl moiety by a methyl or cyclohexyl group, as in compounds **51** vs **49** and **50**, led to a loss of affinity at the 5-HT$_7$R [pK_i(**51**) = 6.2 vs pK_i(**49**) < 5 and pK_i(**50**) < 5]. The only exception to this trend is analogue **45** (R = isopropyl), which is moderately active at the 5-HT$_7$R [pK_i(**45**) = 6.7]. (v) The isosteric change of basic piperazine moiety for an imidazole seems to have a negative influence on the 5-HT$_7$R affinity [e.g. pK_i(**56**) = 7.1 vs pK_i(**72**) < 5). These data might suggest that the interaction between the protonated nitrogen of the piperazine and the receptor is electrostatic, and it is not due to prototropic equilibrium.

These findings have allowed us to conclude that the resulting model provides significant correlation between the chemical structures of the synthesized compounds and their biological data, and confirms that the proposed pharmacophore model for 5-HT$_7$R antagonism incorporates the essential structural features. Further synthesis and biological evaluation of new derivatives are currently in progress.

Table 7. Binding Affinity of Synthesized Compounds at 5-HT$_7$Rs

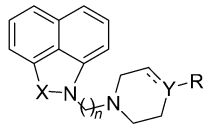

I

Comp.	X	*n*	Y	R	pK_i±SEM[a]
39	CO	1	N	phenyl	<5
40	CO	1	N	*o*-methoxyphenyl	<5
41	CO	3	N	phenyl	<5
42	CO	3	N	*o*-methoxyphenyl	6.4±0.06
43	CO	4	CH	H	<5
44	CO	4	CH	methyl	<6
45	CO	4	CH	isopropyl	6.7±0.05
46	CO	4	CH	cyclohexyl	<6
47	CO	4	CH	phenyl	<6
48	CO	4	C	phenyl	<6
49	CO	4	N	methyl	<5
50	CO	4	N	cyclohexyl	<5
51	CO	4	N	phenyl	6.2±0.003
52	CO	4	N	*o*-methoxyphenyl	7.2±0.005
53	CO	5	CH	isopropyl	<6
54	CO	5	C	phenyl	<6
55	CO	5	N	cyclohexyl	<5
56	CO	5	N	phenyl	7.1±0.02
57	CO	5	N	*o*-methoxyphenyl	7.0±0.05
58	CO	6	N	phenyl	<6
59	CO	6	N	*o*-methoxyphenyl	<6
60	SO_2	4	CH	H	<5
61	SO_2	4	CH	methyl	<5
62	SO_2	4	N	methyl	<5
63	SO_2	4	N	phenyl	6.0±0.06
64	SO_2	4	N	*o*-methoxyphenyl	6.7±0.004
65	SO_2	5	CH	methyl	<5
66	SO_2	5	CH	cyclohexyl	<5
67	SO_2	5	N	phenyl	6.7±0.06
68	SO_2	5	N	*o*-methoxyphenyl	6.6±0.02
69	SO_2	6	CH	methyl	<5
70	SO_2	6	N	phenyl	<6
71	SO_2	6	N	*o*-methoxyphenyl	6.7±0.03
72	CO	4			<5
			DR4004		7.3[b]
			SB-256719		7.1[b]
			SB-269970		7.5[b]

[a] pK_i = −log K_i. K_i (M) values are means of two to four assays, performed in triplicate. Inhibition curves were analyzed by a computer-assisted-curve-fitting program (Prism GraphPad). [b] Data from ref 67 (in rat hypothalamus).

Model of the Complex between Compound 56 and the 5-HT$_7$R. Mutagenesis experiments on several GPCRs that bind biogenic amines have identified a series of conserved Ser/Thr residues (5.42 and 5.43), in TMH 5, which act as hydrogen-bonding sites for the hydroxyl groups present in the chemical structure of many neurotransmitters.[71,72] Thus, it seems reasonable to assume that the carbonyl group (X = CO) of the naphtholactam moiety of compound **56** interacts with the side chain of these Ser/Thr residues. Figure 4a shows the energy-minimized structure of the complex between this naphtholactam moiety and the side chains of Val$^{3.33}$, Ile$^{4.56}$, Ser$^{5.42}$, Thr$^{5.43}$, and Phe$^{6.52}$ that are forming its binding site in the 3D model of the transmembrane domain of the 5-HT$_7$R (see Computational

Scheme 1[a]

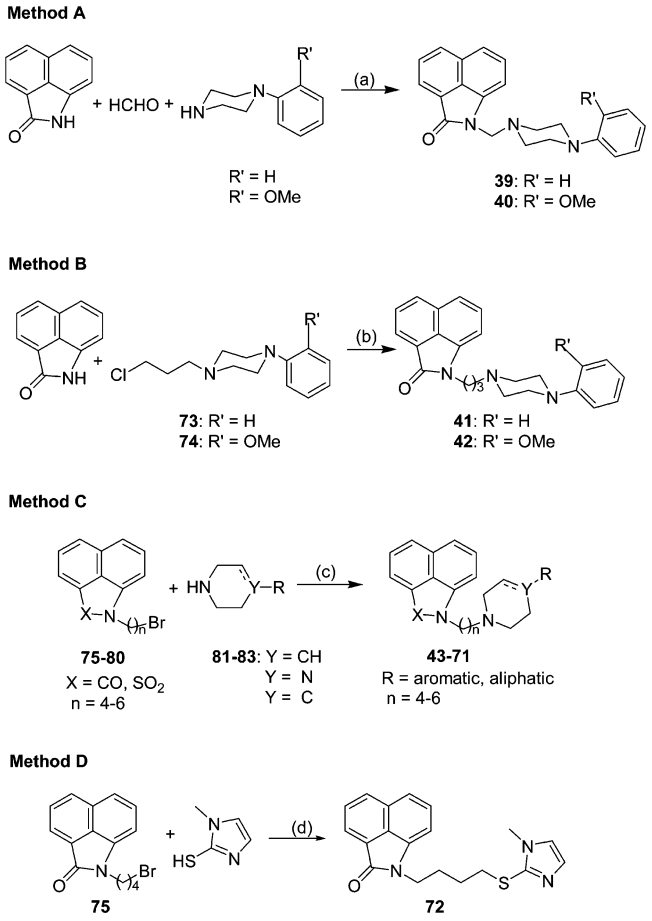

[a] Reagents: (a) EtOH; (b) NaH, DMF anh.; (c) Et_3N, CH_3CN; (d) MeONa, MeOH.

Methods for details). The carbonylic oxygen of the ligand is interacting with the hydroxyl groups of Ser$^{5.42}$ and Thr$^{5.43}$. It is important to note that the interaction of the ligand with these Ser/Thr residues would benefit from a less bulky aromatic ring. However, this extensive naphtholactam ring favors the $\pi-\sigma$ aromatic−aromatic interaction with the side chain of Phe$^{6.52}$ in the face-to-edge orientation (T-shaped). TMH 6 possesses the conserved Pro$^{6.50}$-Phe-Phe motif in both the adrenergic and serotoninergic subfamilies of GPCRs. It has been suggested that Phe$^{6.52}$ stabilizes the interaction of the aromatic catechol-containing ring with the β_2-adrenergic receptor[73] and the interaction with certain 5-HT$_{2A}$R ligands.[74] Near this recognition cavity are located two bulky residues: Val$^{3.33}$ and Ile$^{4.56}$. These residues are oriented toward the aromatic ring and thus limit the size of the recognition site. Thus, an interaction between the electron-rich clouds of the aromatic ring and the electron-poor hydrogens of the carbon atoms of Val$^{3.33}$ and Ile$^{4.56}$ is suggested. This type of C−H$\cdots\pi$ interaction plays a significant role in stabilizing local 3D structures of proteins.[75]

This optimized reduced model was used to position compound **56** inside the transmembrane domain of the 5-HT$_7$R (see Figure 4b). In addition to the described interactions, the NH group of the protonated piperazine ring of the ligand forms the frequently proposed ionic interaction with the O_δ atom of Asp$^{3.32}$ in the gauche+ side chain rotamer conformation (see Figure 4c). It is

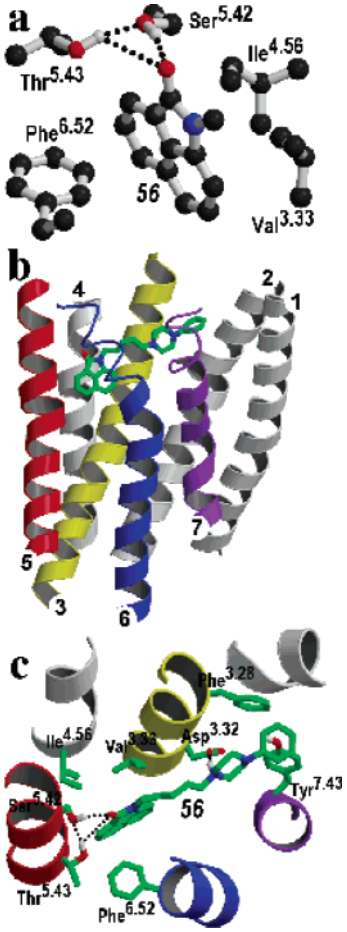

Figure 4. (a) Ab initio geometry optimization, with the ONIOM procedure, of compound **56** (the $-(CH_2)_5-$ chain plus the piperazine and phenyl rings were replaced by a methyl group) inside the side chains of Val$^{3.33}$, Ile$^{4.56}$, Ser$^{5.42}$, Thr$^{5.43}$, and Phe$^{6.52}$. Only polar hydrogens are depicted to offer a better view. (b) Molecular model of the complex between compound **56** and the transmembrane helix bundle of the 5-HT$_7$R constructed from the crystal structure of bovine rhodopsin, in a view parallel to the membrane. (c) Detailed view of the transmembrane helix bundle of the 5-HT$_7$R complexed with compound **56**. The carbonylic oxygen of the ligand is interacting with the hydroxyl groups of Ser$^{5.42}$ and Thr$^{5.43}$, the naphtholactam ring with Phe$^{6.52}$, the protonated piperazine ring with Asp$^{3.32}$, and the phenyl ring with Phe$^{3.28}$ and Tyr$^{7.43}$. Figures were created using MolScript v2.1.1[76] and Raster3D v2.5.[77]

important to remark that this gauche+ conformation differs from the trans conformation observed in our previous model of the 5-HT$_{1A}$R complexed with a piperazine derivative containing four methylene units as a spacer.[55] Thus, it seems reasonable to conclude that while the larger compound **56**, with five methylene units ($n = 5$), optimally interacts with Asp$^{3.32}$ pointing toward TMH 7 (*gauche*+), the shorter compound **51**, with four methylene units ($n = 4$), would optimally interact with Asp$^{3.32}$ pointing toward TMH 5 (trans). This finding provides a molecular explanation for the previous conclusion that the optimum spacer length is four or five methylene units. Finally, the phenyl ring attached to the piperazine ring expands between TMHs 3 and 7 and interacts with the aromatic side chains of Phe$^{3.28}$ and Tyr$^{7.43}$ (see Figure 4c).

Remarkably, the independent generation of a pharmacophore model and a 3D model of the transmembrane

domain of the 5-HT_7R complexed with ligand **56** have provided similar conclusions: (i) the HBA feature of the pharmacophore model binds $Ser^{5.42}$ and $Thr^{5.43}$; (ii) the HYD1 feature interacts with $Phe^{6.52}$; (iii) the PI feature forms an ionic interaction with $Asp^{3.32}$; and (iv) the HYD3 feature interacts with a set of aromatic residues ($Phe^{3.28}$, $Tyr^{7.43}$).

Conclusion

We present here an optimization of our postulated pharmacophore model for 5-HT_7R antagonism, by analyzing a variety of recently reported 5-HT_7R antagonists with the CATALYST program. The pharmacophore model consists of five features: a positive ionizable atom (PI), a H-bonding acceptor group (HBA), and three hydrophobic regions (HYD). To give support to the model, a series of new naphtholactam and naphthosultam derivatives of general structure **I** (**39**−**72**) were designed to interact with any or all pharmacophoric features simultaneously. This pharmacophore model was able to rationalize the relationships between the chemical features of synthesized compounds and their 5-HT_7R binding affinity data and confirmed that it incorporates the essential structural features for 5-HT_7R antagonism, thereby illustrating how the model can be used in the discovery of new classes of 5-HT_7R ligands. In addition, the independent generation of a 3D model of the transmembrane domain of the 5-HT_7R complexed with ligand **56** have provided similar conclusions: (i) the HBA feature of the pharmacophore model binds $Ser^{5.42}$ and $Thr^{5.43}$; (ii) the HYD1 feature interacts with $Phe^{6.52}$; (iii) the PI feature forms an ionic interaction with $Asp^{3.32}$; and (iv) the HYD3 (AR) feature interacts with a set of aromatic residues ($Phe^{3.28}$, $Tyr^{7.43}$). These results provide the tools for the design and synthesis of new ligands with predetermined affinities and pharmacological properties. Further synthesis and biological evaluation of new derivatives are currently in progress, and the results will be reported in due course.

Experimental Section

Chemistry. Melting points (uncorrected) were determined on a Gallenkamp electrothermal apparatus. Infrared (IR) spectra were obtained on a Perkin-Elmer 781 infrared spectrophotometer. ^1H and ^{13}C NMR spectra were recorded on a Varian VXR-300S, Bruker Avance 300, or Bruker AC-200 instrument. Chemical shifts (δ) are expressed in parts per million relative to internal tetramethylsilane; coupling constants (J) are in hertz. The following abbreviations are used to describe peak patterns when appropriate: s (singlet), d (doublet), t (triplet), q (quartet), qt (quintet), m (multiplet), br (broad). Elemental analyses (C, H, N) were determined at the UCM's analysis services and were within (±0.4% of the theoretical values. Analytical thin-layer chromatography (TLC) was run on Merck silica gel 60 F-254 plates with detection by UV light, iodine, acidic vanillin solution, or 10% phosphomolybdic acid solution in ethanol. For normal pressure and flash chromatography, Merck silica gel type 60 (size 70−230 and 230−400 mesh, respectively) was used. Unless stated otherwise, starting materials and reagents used were high-grade commercial products purchased from Aldrich, Fluka, or Merck. All solvents were distilled prior to use. Dry DMF was obtained by stirring with CaH_2 followed by distillation under argon. All final compounds (**39**−**72**) were prepared as hydrochloride salts for biological assays, and spectral data refer to free bases.

The following intermediates were synthesized according to described procedures: 1-(3-chloropropyl)-4-phenylpiperazine (**73**),[78] 1-(3-chloropropyl)-4-(2-methoxyphenyl)piperazine (**74**),[78] 4-isopropylpiperidine (**81**),[79] 4-cyclohexylpiperidine (**82**),[80] and 4-phenylpiperidine (**83**).[81] Spectral data of all described compounds were consistent with the proposed structures for series **75**−**80** and **39**−**72**; here we include the data of compounds **75**, **78**, **39**, **42**, **45**, **48**, **50**, **56**, **58**, **63** and **72**.

Synthesis of 1-(ω-Bromoalkyl)benzo[*cd*]indol-2(1*H*)-ones and 2-(ω-Bromoalkyl)-2*H*-naphtho[1,8-*cd*]isothiazole 1,1-Dioxides 75−80. General Procedure. To a solution of benzo[*cd*]indol-2(1*H*)-one or 2*H*-naphtho[1,8-*cd*]isothiazole 1,1-dioxide (26 mmol) in anhydrous DMF (30 mL) was added NaH 60% (1.0 g, 26 mmol). After stirring for 1 h at 60 °C under an argon atmosphere, a solution of the corresponding dibromoalkyl derivative (52 mmol) in anhydrous DMF (25 mL) was added. The mixture was refluxed under argon at 110 °C for 3 h (TLC). Then, the solvent was evaporated under reduced pressure, and the residue was resuspended in water (50 mL) and extracted with dichloromethane (3 × 50 mL). The combined organic layers were washed with water and dried over anhydrous $MgSO_4$. After evaporation of the solvent, the crude oil was purified by column chromatography to afford the desired derivatives **75**−**80** as pure compounds (eluents, hexane/ethyl acetate; relative proportions depending upon the compound). In all cases, small amounts of the dialkylated compound (25−35%) and starting material (5−10%) were observed in the ^1H NMR spectra of the reaction crudes.

1-(4-Bromobutyl)benzo[*cd*]indol-2(1*H*)-one (75): yield 5.2 g (65%); chromatography hexane/ethyl acetate, from 13:1 to 1:1; mp 80−82 °C (chloroform/ hexane); ^1H NMR ($CDCl_3$) δ 1.96 (qt, J = 7.2, 4H), 3.46 (t, J = 6.6, 2H), 3.96 (t, J = 6.2, 2H), 6.92 (d, J = 6.8, 1H), 7.46 (dd, J = 8.4, 6.9, 1H), 7.53 (d, J = 8.4, 1H), 7.70 (dd, J = 8.1, 6.9, 1H), 8.00 (d, J = 8.2, 1H), 8.05 (d, J = 6.9, 1H); ^{13}C NMR ($CDCl_3$) δ 27.4, 29.9, 33.9, 39.3, 105.1, 120.5, 124.4, 125.2, 126.6, 128.6, 128.8, 129.2, 130.9, 139.3, 168.2.

1-(5-Bromopentyl)benzo[*cd*]indol-2(1*H*)-one (76): yield 4.4 g (53%); chromatography hexane/ethyl acetate, from 13:1 to 1:1; bp 289−292 °C/0.06 mmHg.

1-(6-Bromohexyl)benzo[*cd*]indol-2(1*H*)-one (77): yield 4.4 g (50%); chromatography hexane/ethyl acetate, from 13:1 to 1:1; bp 177−180 °C/0.06 mmHg.

2-(4-Bromobutyl)-2*H*-naphtho[1,8-*cd*]isothiazole 1,1-dioxide (78): yield 5.4 g (61%); chromatography hexane/ethyl acetate, 8.5:1.5; mp 67−69 °C (chloroform/hexane); ^1H NMR ($CDCl_3$) δ 2.06−2.12 (m, 4H), 3.49 (t, J = 7.6, 2H), 3.88 (t, J = 6.8, 2H), 6.76 (dd, J = 7.1, 1.0, 1H), 7.46 (dd, J = 8.5, 1.0, 1H), 7.55 (dd, J = 8.5, 7.1, 1H), 7.75 (dd, J = 8.1, 7.3, 1H), 7.97 (dd, J = 7.3, 0.7, 1H), 8.07 (dd, J = 8.1, 0.7, 1H); ^{13}C NMR ($CDCl_3$) δ 26.6, 29.7, 32.9, 41.1, 102.8, 118.1, 119.1, 119.7, 128.0, 129.2, 130.1, 130.6, 131.1, 136.3.

2-(5-Bromopentyl)-2*H*-naphtho[1,8-*cd*]isothiazole 1,1-dioxide (79): yield 5.3 g (58%); chromatography hexane/ethyl acetate, 9:1; mp 62−64 °C (chloroform/hexane).

2-(6-Bromohexyl)-2*H*-naphtho[1,8-*cd*]isothiazole 1,1-dioxide (80): yield 4.2 g (44%); chromatography hexane/ethyl acetate, from 9:1 to 8:2; mp 67−69 °C (chloroform/hexane).

General Method A. Preparation of Derivatives 39, 40. To a suspension of benzo[*cd*]indol-2(1*H*)-one (0.5 g, 3 mmol) and 0.23 mL (3 mmol) of 35% formaldehyde in 7 mL of ethanol was added the corresponding 1-arylpiperazine (3 mmol) and was refluxed for 1−4 h (TLC). The reaction mixture was allowed to cool, then the solvent was evaporated under reduced pressure, and the residue was resuspended in water (20 mL) and extracted with chloroform (3 × 20 mL). The combined organic layers were dried over anhydrous Na_2SO_4. After evaporation of the solvent, the crude oil was purified by column chromatography (eluent, hexane/ethyl acetate; relative proportions depending upon the compound).

1-[(4-Phenylpiperazin-1-yl)methyl]benzo[*cd*]indol-2(1*H*)-one (39): yield 0.7 g (69%); chromatography hexane/ethyl acetate, from 8:2 to 1:1; mp 153−155 °C (chloroform/hexane); ^1H NMR ($CDCl_3$) δ 2.88 (t, J = 5.1, 4H), 3.18 (t, J = 5.1, 4H), 4.79 (s, 2H), 6.80 (t, J = 7.2, 1H), 6.86 (d, J = 7.8, 2H), 7.07 (d, J = 6.9, 1H), 7.18−7.26 (m, 2H), 7.46 (dd, J = 8.4, 6.9, 1H), 7.55 (d, J = 8.4, 1H), 7.72 (dd, J = 8.7, 7.2, 1H),

8.03 (d, $J = 7.8$, 1H), 8.08 (d, $J = 6.9$, 1H); ^{13}C NMR ($CDCl_3$) δ 49.0, 50.6, 61.9, 106.0, 116.1, 119.6, 120.2, 124.6, 125.1, 126.1, 128.3, 128.5, 128.9, 129.0, 130.9, 139.9, 151.1, 168.7. Anal. ($C_{22}H_{21}N_3O\cdot 2HCl\cdot {}^3/_2H_2O$) C, H, N.

1-{[4-(2-Methoxyphenyl)piperazin-1-yl]methyl}benzo[*cd*]indol-2(1*H*)-one (40): yield 1.0 g (88%); chromatography hexane/ethyl acetate, 1:1; mp 160−163 °C (chloroform/hexane). Anal. ($C_{23}H_{23}N_3O_2\cdot 2HCl\cdot 3H_2O$) C, H, N.

General Method B. Preparation of Derivatives 41, 42. To a solution of benzo[*cd*]indol-2(1*H*)-one (1.0 g, 6 mmol) in anhydrous DMF (3.3 mL) was added slowly 60% NaH (0.25 g, 6 mmol), and the mixture was warmed at 60 °C for 1 h under an argon atmosphere. Then, a solution of the corresponding 1-aryl-4-(3-chloropropyl)piperazine **73**, **74** (6 mmol) in anhydrous DMF (3.3 mL) was added dropwise and the mixture was refluxed at 110 °C under argon for 1−3 h (TLC). The solvent was evaporated under reduced pressure, the residue was resuspended in water (50 mL) and extracted with dichloromethane (3 × 50 mL). The combined organic layers were dried over anhydrous Na_2SO_4. After evaporation of the solvent, the crude oil was purified by column chromatography (eluent, hexane/ethyl acetate; relative proportions depending upon the compound).

1-[3-(4-Phenylpiperazin-1-yl)propyl]benzo[*cd*]indol-2(1*H*)-one (41): yield 1.4 g (64%); chromatography hexane/ethyl acetate, 2:8; mp 192−195 °C (chloroform/diethyl ether). Anal. ($C_{24}H_{25}N_3O\cdot 2HCl\cdot {}^5/_2H_2O$) C, H, N.

1-{3-[4-(2-Methoxyphenyl)piperazin-1-yl]propyl}benzo[*cd*]indol-2(1*H*)-one (42): yield 1.7 g (72%); chromatography hexane/ethyl acetate, 7:3; mp 200−202 °C (chloroform/diethyl ether); ^{1}H NMR ($CDCl_3$) δ 1.26 (qt, $J = 7.1$, 2H), 2.52 (t, $J = 7.1$, 2H), 2.62 (br s, 4H), 3.05 (br s, 4H), 3.85 (s, 3H), 4.02 (t, $J = 6.8$, 2H), 6.83−7.05 (m, 5H), 7.44 (dd, $J = 8.5$, 6.6, 1H), 7.55 (dd, $J = 8.5$, 1.0, 1H), 7.71 (dd, $J = 8.4$, 6.8, 1H), 8.00 (d, $J = 8.0$, 1H), 8.04 (d, $J = 6.8$, 1H); ^{13}C NMR ($CDCl_3$) δ 25.9, 38.4, 50.6, 53.3, 55.3, 55.5, 105.1, 111.2, 118.0, 120.1, 120.9, 122.8, 124.1, 125.9, 126.7, 128.4, 128.6, 129.1, 130.7, 139.7, 141.3, 152.2, 168.9. Anal. ($C_{25}H_{27}N_3O_2\cdot 2HCl\cdot {}^7/_2H_2O$) C, H, N.

General Method C. Preparation of Derivatives 43−71. To a suspension of the corresponding derivatives **75**−**80** (9 mmol) and the appropriate amine (15 mmol) in acetonitrile (19 mL) was added 2.0 mL of triethylamine (1.5 g, 15 mmol), and the mixture was stirred at 60 °C for 18−24 h (TLC). Then, the solvent was evaporated under reduced pressure and the residue was resuspended in water and extracted with dichloromethane (3 × 100 mL). The combined organic layers were dried over anhydrous Na_2SO_4. After evaporation of the solvent, the crude oil was purified by column chromatography (eluent, hexane/ethyl acetate, ethyl acetate/ethanol, or chloroform/methanol; relative proportions depending upon the compound).

1-(4-Piperidinobutyl)benzo[*cd*]indol-2(1*H*)-one (43): yield 2.5 g (89%); chromatography chloroform/methanol, 9:1; mp 198−200 °C (chloroform/hexane). Anal. ($C_{20}H_{24}N_2O\cdot HCl\cdot 2H_2O$) C, H, N.

1-[4-(4-Methylpiperidino)butyl]benzo[*cd*]indol-2(1*H*)-one (44): yield 1.7 g (60%); chromatography ethyl acetate/ethanol, 7:3; mp 204−207 °C (chloroform/hexane). Anal. ($C_{21}H_{26}N_2O\cdot HCl\cdot 2H_2O$) C, H, N.

1-[4-(4-Isopropylpiperidino)butyl]benzo[*cd*]indol-2(1*H*)-one (45): yield 2.7 g (84%); chromatography ethyl acetate/ethanol, 8:2; mp 173−175 °C (chloroform/diethyl ether); ^{1}H NMR ($CDCl_3$) δ 0.79 (d, $J = 6.7$, 6H), 0.85−1.00 (m, 1H), 1.12−1.45 (m, 3H), 1.51−1.91 (m, 8H), 2.34 (t, $J = 7.5$, 2H), 2.91 (d, $J = 11.4$, 2H), 3.88 (t, $J = 7.1$, 2H), 6.86 (d, $J = 6.6$, 1H), 7.39 (dd, $J = 8.5$, 6.6, 1H), 7.47 (d, $J = 8.4$, 1H), 7.64 (dd, $J = 8.1$, 7.1, 1H), 7.95 (d, $J = 8.5$, 1H), 7.98 (d, $J = 7.2$, 1H); ^{13}C NMR ($CDCl_3$) δ 19.8, 24.1, 26.8, 29.0, 32.4, 40.0, 42.3, 54.3, 58.3, 105.1, 120.2, 124.2, 125.4, 126.9, 128.5, 128.6, 129.2, 130.8, 139.5, 168.2. Anal. ($C_{23}H_{30}N_2O\cdot HCl\cdot {}^1/_2H_2O$) C, H, N.

1-[4-(4-Cyclohexylpiperidino)butyl]benzo[*cd*]indol-2(1*H*)-one (46): yield 2.7 g (78%); chromatography ethyl acetate/ethanol, 9:1; mp 217−219 °C (chloroform/hexane). Anal. ($C_{26}H_{34}N_2O\cdot HCl\cdot {}^1/_2H_2O$) C, H, N.

1-[4-(4-Phenylpiperidino)butyl]benzo[*cd*]indol-2(1*H*)-one (47): yield 2.3 g (66%); chromatography hexane/ethyl acetate, from 1:1 to ethyl acetate; mp 215−217 °C (chloroform/diethyl ether). Anal. ($C_{26}H_{28}N_2O\cdot HCl\cdot 2H_2O$) C, H, N.

1-[4-(4-Phenyl-3,6-dihydropyridin-1(2*H*)-yl)butyl]benzo[*cd*]indol-2(1*H*)-one (48): yield 1.6 g (54%); chromatography hexane/ethyl acetate, from 3:7 to ethyl acetate; mp 222−224 °C (dec) (chloroform/hexane); ^{1}H NMR ($CDCl_3$) δ 1.68 (qt, $J = 8.4$, 2H), 1.86 (qt, $J = 7.5$, 2H), 2.46−2.54 (m, 4H), 2.67 (t, $J = 7.5$, 2H), 3.12 (d, $J = 3.3$, 2H), 3.97 (t, $J = 7.2$, 2H), 6.03 (t, $J = 1.8$, 1H), 6.93 (d, $J = 6.9$, 1H), 7.21−7.34 (m, 5H), 7.46 (td, $J = 8.4$, 1.8, 1H), 7.52 (d, $J = 8.1$, 1H), 7.70 (ddd, $J = 8.1$, 6.9, 1.8, 1H), 8.00 (d, $J = 8.1$, 1H), 8.04 (d, $J = 6.9$, 1H); ^{13}C NMR ($CDCl_3$) δ 24.5, 26.8, 28.1, 40.1, 50.4, 53.3, 57.8, 105.1, 120.3, 121.8, 124.3, 125.0, 125.3, 126.8, 127.0, 128.3, 128.5, 128.7, 129.6, 130.8, 135.0, 139.5, 140.9, 168.2. Anal. ($C_{26}H_{26}N_2O\cdot HCl\cdot {}^1/_2H_2O$) C, H, N.

1-[4-(4-Methylpiperazin-1-yl)butyl]benzo[*cd*]indol-2(1*H*)-one (49): yield 2.2 g (76%); chromatography chloroform/methanol, 6:4; mp 268−270 °C (dec) (chloroform/hexane). Anal. ($C_{20}H_{25}N_3O\cdot 2HCl\cdot {}^1/_2H_2O$) C, H, N.

1-[4-(4-Cyclohexylpiperazin-1-yl)butyl]benzo[*cd*]indol-2(1*H*)-one (50): yield 3.2 g (90%); chromatography ethyl acetate; mp 290−292 °C (dec) (chloroform/diethyl ether); ^{1}H NMR ($CDCl_3$) δ 1.00−1.27 (m, 5H), 1.55−1.62 (m, 3H), 1.75−1.83 (m, 4H), 1.90−1.92 (m, 2H), 2.30−2.41 (m, 3H), 2.54 (br s, 4H), 2.66 (br s, 4H), 3.91 (t, $J = 6.9$, 2H), 6.88 (d, $J = 6.9$, 1H), 7.42 (dd, $J = 8.4$, 6.9, 1H), 7.50 (d, $J = 8.4$, 1H), 7.67 (dd, $J = 8.1$, 7.2, 1H), 7.98 (d, $J = 8.4$, 1H), 8.02 (d, $J = 6.9$, 1H); ^{13}C NMR ($CDCl_3$) δ 24.3, 26.0, 26.3, 26.9, 28.9, 40.2, 48.9, 53.3, 58.1, 63.9, 105.2, 120.3, 124.4, 125.3, 126.9, 128.6, 128.8, 129.3, 130.9, 139.6, 168.2. Anal. ($C_{25}H_{33}N_3O\cdot 2HCl\cdot {}^5/_2H_2O$) C, H, N.

1-[4-(4-Phenylpiperazin-1-yl)butyl]benzo[*cd*]indol-2(1*H*)-one (51): yield 3.0 g (86%); chromatography ethyl acetate; mp 255−257 °C (dec) (dichloromethane/hexane). Anal. ($C_{25}H_{27}N_3O\cdot 2HCl\cdot H_2O$) C, H, N.

1-{4-[4-(2-Methoxyphenyl)piperazin-1-yl]butyl}benzo[*cd*]indol-2(1*H*)-one (52): yield 3.0 g (80%); chromatography ethyl acetate; mp 219−221 °C (dec) (chloroform/hexane). Anal. ($C_{26}H_{29}N_3O_2\cdot 2HCl$) C, H, N.

1-[5-(4-Isopropylpiperidino)pentyl]benzo[*cd*]indol-2(1*H*)-one (53): yield 2.7 g (83%); chromatography ethyl acetate/ethanol, 8:2; mp 212−215 °C (acetone/ diethyl ether). Anal. ($C_{24}H_{32}N_2O\cdot HCl$) C, H, N.

1-[5-(4-Phenyl-3,6-dihydropyridin-1(2*H*)-yl)pentyl]benzo[*cd*]indol-2(1*H*)-one (54): yield 1.9 g (53%); chromatography hexane/ethyl acetate, 1:1; bp 230−232 °C/0.06 mmHg. Anal. ($C_{27}H_{28}N_2O\cdot HCl\cdot {}^3/_2H_2O$) C, H, N.

1-[5-(4-Cyclohexylpiperazin-1-yl)pentyl]benzo[*cd*]indol-2(1*H*)-one (55): yield 3.3 g (91%); chromatography ethyl acetate; mp 259−261 °C (dec) (chloroform/diethyl ether). Anal. ($C_{26}H_{35}N_3O\cdot 2HCl\cdot {}^3/_2H_2O$) C, H, N.

1-[5-(4-Phenylpiperazin-1-yl)pentyl]benzo[*cd*]indol-2(1*H*)-one (56): yield 3.3 g (93%); chromatography ethyl acetate; mp 211−213 °C (dichloromethane/hexane); ^{1}H NMR ($CDCl_3$) δ 1.43 (qt, $J = 7.2$, 2H), 1.58 (qt, $J = 7.5$, 2H), 1.82 (qt, $J = 7.5$, 2H), 2.35 (t, $J = 7.5$, 2H), 2.55 (t, $J = 5.1$, 4H), 3.15 (t, $J = 5.1$, 4H), 3.92 (t, $J = 7.5$, 2H), 6.83 (t, $J = 7.2$, 1H), 6.87−6.93 (m, 3H), 7.24 (t, $J = 6.9$, 2H), 7.45 (dd, $J = 8.4$, 6.9, 1H), 7.52 (d, $J = 8.4$, 1H), 7.69 (dd, $J = 8.1$, 6.9, 1H), 7.99 (d, $J = 6.9$, 1H), 8.04 (d, $J = 7.2$, 1H); ^{13}C NMR ($CDCl_3$) δ 24.8, 26.5, 28.6, 40.1, 49.0, 53.2, 58.4, 104.8, 115.9, 119.5, 120.1, 124.1, 125.1, 126.7, 128.4, 128.6, 129.0, 129.6, 130.6, 139.5, 151.2, 168.0. Anal. ($C_{26}H_{29}N_3O\cdot 2HCl$) C, H, N.

1-{5-[4-(2-Methoxyphenyl)piperazin-1-yl]pentyl}benzo[*cd*]indol-2(1*H*)-one (57): yield 2.9 g (75%); chromatography ethyl acetate; mp 209−211 °C (chloroform/hexane). Anal. ($C_{27}H_{31}N_3O_2\cdot 2HCl\cdot {}^1/_2H_2O$) C, H, N.

1-[6-(4-Phenylpiperazin-1-yl)hexyl]benzo[*cd*]indol-2(1*H*)-one (58): yield 3.0 g (80%); chromatography ethyl acetate; mp 183−185 °C (chloroform/diethyl ether); ^{1}H NMR ($CDCl_3$) δ 1.30−1.61 (m, 6H), 1.81 (qt, $J = 7.1$, 2H), 2.39 (t, $J = 6.8$, 2H), 2.60 (t, $J = 5.1$, 4H), 3.20 (t, $J = 5.1$, 4H), 3.93 (t, $J = 7.3$, 2H), 6.81−6.97 (m, 4H), 7.26 (t, $J = 7.3$, 2H), 7.46

(dd, J = 8.5, 6.6, 1H), 7.54 (dd, J = 8.3, 1.0, 1H), 7.71 (dd, J = 8.3, 6.8, 1H), 8.02 (dd, J = 8.3, 0.7, 1H), 8.06 (dd, J = 6.8, 0.7, 1H); ^{13}C NMR ($CDCl_3$) δ 26.8, 27.0, 27.4, 28.9, 40.4, 49.1, 53.3, 58.7, 105.1, 116.2, 119.8, 120.3, 124.4, 125.3, 126.9, 128.6, 128.8, 129.2, 129.4, 130.9, 139.7, 151.4, 168.2. Anal. ($C_{27}H_{31}N_3O\cdot 2HCl\cdot 2H_2O$) C, H, N.

1-{6-[4-(2-Methoxyphenyl)piperazin-1-yl]hexyl}benzo[*cd*]indol-2(1*H*)-one (59): yield 3.8 g (94%); chromatography ethyl acetate; mp 188−190 °C (chloroform/hexane). Anal. ($C_{28}H_{33}N_3O_2\cdot HCl\cdot H_2O$) C, H, N.

2-(4-Piperidinobutyl)-2*H*-naphtho[1,8-*cd*]isothiazole 1,1-dioxide (60): yield 2.8 g (89%); chromatography chloroform/methanol, 9:1; mp 217−219 °C (chloroform/hexane). Anal. ($C_{19}H_{24}N_2O_2S\cdot HCl$) C, H, N.

2-[4-(4-Methylpiperidino)butyl]-2*H*-naphtho[1,8-*cd*]isothiazole 1,1-dioxide (61): yield 2.8 g (87%); chromatography chloroform/methanol, 9:1; mp 219−221 °C (dec) (chloroform/hexane). Anal. ($C_{20}H_{26}N_2O_2S\cdot HCl$) C, H, N.

2-[4-(4-Methylpiperazin-1-yl)butyl]-2*H*-naphtho[1,8-*cd*]isothiazole 1,1-dioxide (62): yield 2.6 g (81%); chromatography chloroform/methanol, from 9.5:0.5 to 9:1; mp 265−268 °C (dec) (chloroform/hexane). Anal. ($C_{19}H_{25}N_3O_2S\cdot 2HCl\cdot {}^1/_2H_2O$) C, H, N.

2-[4-(4-Phenylpiperazin-1-yl)butyl]-2*H*-naphtho[1,8-*cd*]isothiazole 1,1-dioxide (63): yield 3.1 g (81%); chromatography hexane/ethyl acetate, from 1:1 to ethyl acetate; mp 213-215 °C (dichloromethane/hexane); ^{1}H NMR ($CDCl_3$) δ 1.72 (qt, J = 7.5, 2H), 1.98 (qt, J = 7.5, 2H), 2.47 (t, J = 7.5, 2H), 2.59 (t, J = 4.8, 4H), 3.18 (t, J = 4.8, 4H), 3.86 (t, J = 7.5, 2H), 6.75 (d, J = 6.9, 1H), 6.83 (t, J = 7.5, 1H), 6.90 (d, J = 7.8, 2H), 7.25 (t, J = 7.2, 2H), 7.43 (d, J = 8.4, 1H), 7.52 (dd, J = 8.4, 7.2, 1H), 7.73 (dd, J = 8.1, 7.2, 1H), 7.94 (d, J = 7.2, 1H), 8.05 (d, J = 8.4, 1H); ^{13}C NMR ($CDCl_3$) δ 24.1, 26.1, 42.0, 49.1, 53.2, 57.8, 102.9, 116.0, 118.1, 119.3, 119.6, 119.7, 128.0, 129.0, 129.3, 130.4, 130.7, 131.1, 136.6, 151.3. Anal. ($C_{24}H_{27}N_3O_2S\cdot 2HCl\cdot {}^1/_2H_2O$) C, H, N.

2-{4-[4-(2-Methoxyphenyl)piperazin-1-yl]butyl}-2*H*-naphtho[1,8-*cd*]isothiazole 1,1-dioxide (64): yield 3.3 g (82%); chromatography ethyl acetate; mp 211−213 °C (dichloromethane/diethyl ether). Anal. ($C_{25}H_{29}N_3O_3S\cdot 2HCl$) C, H, N.

2-[5-(4-Methylpiperidino)pentyl]-2*H*-naphtho[1,8-*cd*]isothiazole 1,1-dioxide (65): yield 3.3 g (98%); chromatography chloroform/methanol, 9:1; mp 187−189 °C (chloroform). Anal. ($C_{21}H_{28}N_2O_2S\cdot 2HCl\cdot {}^5/_2H_2O$) C, H, N.

2-[5-(4-Cyclohexylpiperidino)pentyl]-2*H*-naphtho[1,8-*cd*]isothiazole 1,1-dioxide (66): yield 3.9 g (98%); chromatography ethyl acetate/ethanol, 9:1; mp 163−165 °C (methanol/diethyl ether). Anal. ($C_{26}H_{36}N_2O_2S\cdot HCl\cdot H_2O$) C, H, N.

2-[5-(4-Phenylpiperazin-1-yl)pentyl]-2*H*-naphtho[1,8-*cd*]isothiazole 1,1-dioxide (67): yield 3.7 g (94%); chromatography hexane/ethyl acetate, from 3:7 to 1:9; mp 216−218 °C (dichloromethane/hexane). Anal. ($C_{25}H_{29}N_3O_2S\cdot 2HCl$) C, H, N.

2-{5-[4-(2-Methoxyphenyl)piperazin-1-yl]pentyl}-2*H*-naphtho[1,8-*cd*]isothiazole 1,1-dioxide (68): yield 3.7 g (87%); chromatography ethyl acetate/ethanol, 8:2; mp 210−212 °C (methanol/diethyl ether). Anal. ($C_{26}H_{31}N_3O_3S\cdot 2HCl$) C, H, N.

2-[6-(4-Methylpiperidino)hexyl]-2*H*-naphtho[1,8-*cd*]isothiazole 1,1-dioxide (69): yield 3.2 g (93%); chromatography ethyl acetate/ethanol, from 8.5:1.5 to 8:2; mp 168−170 °C (chloroform/hexane). Anal. ($C_{22}H_{30}N_2O_2S\cdot HCl\cdot 3H_2O$) C, H, N.

2-[6-(4-Phenylpiperazin-1-yl)hexyl]-2*H*-naphtho[1,8-*cd*]isothiazole 1,1-dioxide (70): yield 3.4 g (84%); chromatography hexane/ethyl acetate, from 4:6 to ethyl acetate; mp 205−207 °C (chloroform/diethyl ether). Anal. ($C_{26}H_{31}N_3O_2S\cdot 2HCl$) C, H, N.

2-{6-[4-(2-Methoxyphenyl)piperazin-1-yl]hexyl}-2*H*-naphtho[1,8-*cd*]isothiazole 1,1-dioxide (71): yield 3.5 g (80%); chromatography ethyl acetate; mp 203−205 °C (chloroform/hexane). Anal. ($C_{27}H_{33}N_3O_3S\cdot 2HCl$) C, H, N.

Synthesis of 1-{4-[(1-Methyl-1*H*-imidazol-2-yl)thio]butyl}benzo[*cd*]indol-2(1*H*)-one (72). To a solution of sodium methoxide (0.7 g, 13 mmol) in 20 mL of methanol chilled to 0 °C was added 1-methyl-1*H*-imidazole-2-thiol (1.5 g, 13 mmol). After 5 min, compound **75** (4.0 g, 13 mmol) was added in one portion, and the mixture was stirred and allowed to come to room temperature overnight. The solution was diluted with 30 mL of water and extracted with diethyl ether (3 × 50 mL). The combined organic extracts were washed with 10% NaOH, water, and brine and dried over anhydrous Na_2SO_4. After evaporation of the solvent, the crude oil was purified by column chromatography (hexane/ethyl acetate, from 1:1 to 0.5:9.5) to afford 3.4 g (77%) of **72**: mp 181−183 °C; ^{1}H NMR ($CDCl_3$) δ 1.72−2.00 (m, 4H), 3.09 (t, J = 6.8, 2H), 3.57 (s, 3H), 3.93 (t, J = 6.8, 2H), 6.87 (d, J = 1.5, 1H), 6.91 (dd, J = 6.6, 0.7, 1H), 7.01 (d, J = 1.2, 1H), 7.45 (dd, J = 8.5, 6.6, 1H), 7.53 (dd, J = 8.5, 0.7, 1H), 7.70 (dd, J = 8.3, 6.8, 1H), 8.01 (d, J = 7.6, 1H), 8.05 (d, J = 7.1, 1H); ^{13}C NMR ($CDCl_3$) δ 27.3, 27.8, 33.3, 34.0, 39.8, 105.2, 120.4, 122.3, 124.4, 125.3, 126.8, 128.7, 128.8, 129.3, 129.4, 130.9, 139.5, 141.7, 168.2. Anal. ($C_{19}H_{19}N_3OS\cdot HCl$) C, H, N.

Radioligand Binding Assays at 5-HT$_7$R. Male Sprague−Dawley rats (*Rattus norvegicus albinus*), weighing 180−200 g, were killed by decapitation and the brains rapidly removed and dissected. The receptor binding studies were performed by a modification of a previously described procedure.[68] The hypothalamus was homogenized in 5 mL of ice-cold Tris buffer (50 mM Tris-HCl, pH 7.4 at 25 °C) and centrifuged at 48 000*g* for 10 min. The membrane pellet was washed by resuspension and centrifugation, and then the resuspended pellet was incubated at 37 °C for 10 min. Membranes were then collected by centrifugation, and the final pellet was resuspended in 100 volumes of ice-cold 50 mM Tris-HCl, 4 mM $CaCl_2$, 1 mg/mL ascorbic acid, 0.01 mM pargyline, and 3 μM pindolol[82] buffer (pH 7.4 at 25 °C). Fractions of 400 μL of the final membrane suspension were incubated at 23 °C for 120 min. with 0.5 nM [^{3}H]-5-CT (88 Ci/mmol), in the presence or absence of several concentrations of the competing drug, in a final volume of 0.5 mL of assay buffer (50 mM Tris-HCl, 4 mM $CaCl_2$, 1 mg/mL ascorbic acid, 0.01 mM pargyline, and 3 μM pindolol buffer (pH 7.4 at 25 °C)). Nonspecific binding was determined with 10 μM 5-HT. Competing drug, nonspecific, total, and radioligand bindings were defined in triplicate. Incubation was terminated by rapid vacuum filtration through Whatman GF/C filters, presoaked in 0.01% poly(ethylenimine), using a Brandel cell harvester. The filters were then washed with the assay buffer and were placed in vials to which were added 4 mL of a scintillation cocktail (Ecolite), and the radioactivity bound to the filters was measured by liquid scintillation spectrometry. The data were analyzed by an iterative curve-fitting procedure (program Prism Graph Pad), which provided IC_{50}, K_i, and r^2 values for test compounds, K_i values being calculated from the Cheng−Prusoff equation.[69] The protein concentrations of the rat hypothalamus were determined by the method of Lowry,[83] using bovine serum albumin as the standard.

Acknowledgment. This work was supported by Ministerio de Ciencia y Tecnología (BQU2001-1457). The authors are grateful to U.N.E.D. for a predoctoral grant to E. Porras.

Supporting Information Available: Spectral data of new intermediates **76**, **77**, **79**, and **80** and final compounds **40**, **41**, **43**, **44**, **46**, **47**, **49**, **51**−**55**, **57**, **59**−**62**, and **64**−**71**. This material is available free of charge via the Internet at http://pubs.acs.org.

References

(1) *Serotoninergic Neurons and 5-HT Receptors in the CNS*; Baumgarten, H. G., Göthert, M., Eds.; Springer-Verlag: Berlin, 1997.
(2) Olivier, B.; van Wijngaarden, I.; Soudijn, W. *Serotonin Receptors and their Ligands*; Olivier, B., van Wijngaarden, I., Soudijn, W., Eds.; Elsevier: The Netherlands, 1997.
(3) Barnes, N. M.; Sharp, T. A Review of Central 5-HT Receptors and their Function. *Neuropharmacology* **1999**, *38*, 1083−1152.
(4) Hoyer, D.; Hannon, J. P.; Martin, G. R. Molecular, Pharmacological and Functional Diversity of 5-HT Receptors. *Pharmacol. Biochem. Behav.* **2002**, *71*, 533−554.

(5) Bikker, J. A.; Trumpp-Kallmeyer, S.; Humblet, C. G-Protein Coupled Receptors: Models, Mutagenesis, and Drug Design. *J. Med. Chem.* **1998**, *41*, 2911−2927.
(6) Klabunde, T.; Hessler, G. Drug Design Strategies for Targeting G-Protein-Coupled Receptors. *ChemBioChem.* **2002**, *3*, 928−944.
(7) Eglen, R. M.; Jasper, J. R.; Chang, D. J.; Martin, G. R. The 5-HT_7 Receptor: Orphan Found. *Trends Pharmacol. Sci.* **1997**, *18*, 104−107.
(8) Vanhoenacker, P.; Haegeman, G.; Leysen, J. E. 5-HT_7 Receptors: Current Knowledge and Future Prospects. *Trends Pharmacol. Sci.* **2000**, *21*, 70−77.
(9) Lovenberg, T. W.; Baron, B. M.; de Lecea, L.; Miller, J. D.; Prosser, R. A.; Rea, M. A.; Foye, P. E.; Racke, M.; Slone, A. L.; Siegel, B. W.; Danielson, P. E.; Sutcliffe, J. G.; Erlander, M. G. A Novel Adenylyl Cyclase-Activating Serotonin Receptor (5-HT_7) Implicated in the Regulation of Mammalian Circadian Rhythms. *Neuron* **1993**, *11*, 449−458.
(10) Plassat, J.-L.; Amlaiky, N.; Hen, R. Molecular Cloning of a Mammalian Serotonin Receptor that Activates Adenylate Cyclase. *Mol. Pharmacol.* **1993**, *44*, 229−236.
(11) Ruat, M.; Traiffort, E.; Leurs, R.; Tardivel-Lacombe, J.; Diaz, J.; Arrang, J.-M.; Schwartz, J.-C. Molecular Cloning, Characterization, and Localization of a High-Affinity Serotonin Receptor (5-HT_7) Activating cAMP Formation. *Proc. Natl. Acad. Sci. U.S.A.* **1993**, *90*, 8547−8551.
(12) Shen, Y.; Monsma, F. J., Jr.; Metcalf, M. A.; Jose, P. A.; Hamblin, M. W.; Sibley, D. R. Molecular Cloning and Expression of a 5-Hydroxytryptamine$_7$ Serotonin Receptor Subtype. *J. Biol. Chem.* **1993**, *268*, 18200−18204.
(13) Tsou, A.-P.; Kosaka, A.; Bach, C.; Zuppan, P.; Yee, C.; Tom, L.; Alvarez, R.; Ramsey, S.; Bonhaus, D. W.; Stefanich, E.; Jakeman, L.; Eglen, R. M.; Chan, H. W. Cloning and Expression of a 5-Hydroxytryptamine$_7$ Receptor Positively Coupled to Adenylyl Cyclase. *J. Neurochem.* **1994**, *63*, 456−464.
(14) Bard, J. A.; Zgombick, J.; Adham, N.; Vaysse, P.; Branchek, T. A.; Weinshank, R. L. Cloning of a Novel Human Serotonin Receptor (5-HT_7) Positively Linked to Adenylate Cyclase. *J. Biol. Chem.* **1993**, *268*, 23422−23426.
(15) Heidmann, D. E. A.; Metcalf, M. A.; Kohen, R.; Hamblin, M. W. Four 5-Hydroxytryptamine$_7$ (5-HT_7) Receptor Isoforms in Human and Rat Produced by Alternative Splicing: Species Differences Due to Altered Intron-Exon Organization. *J. Neurochem.* **1997**, *68*, 1372−1381.
(16) Liu, H.; Irving, R. H.; Coupar, I. M. Expression Patterns of 5-HT_7 Receptor Isoforms in the Rat Digestive Tract. *Life Sci.* **2001**, *69*, 2467−2475.
(17) Krobert, K. A.; Levy, F. O. The Human 5-HT_7 Serotonin Receptor Splice Variants: Constitutive Activity and Inverse Agonist Effects. *Br. J. Pharmacol.* **2002**, *135*, 1563−1571.
(18) Ehlen, J. C.; Grossman, G. H.; Glass, J. D. In Vivo Resetting of the Hamster Circadian Clock by 5-HT_7 Receptors in the Suprachiasmatic Nucleus. *J. Neurosci.* **2001**, *21*, 5351−5357.
(19) Smith, B. N.; Sollars, P. J.; Dudek, E. E.; Pickard, G. E. Serotonergic Modulation of Retinal Input to the Mouse Suprachiasmatic Nucleus Mediated by 5-HT_{1B} and 5-HT_7 Receptors. *J. Biol. Rhythms* **2001**, *16*, 25−38.
(20) Neumaier, J. F.; Sexton, T. J.; Yracheta, J.; Diaz, A. M.; Brownfield, M. Localization of 5-HT_7 Receptor in Rat Brain by Inmunocytochemistry, in situ Hybridization, and Agonist Stimulated cFos Expression. *J. Chem. Neuroanat.* **2001**, *21*, 63−73.
(21) Roth, B. L.; Meltzer, H. Y.; Khan,N. Binding of Typical and Atypical Antipsychotic Drugs to Multiple Neurotransmitter Receptors. *Adv. Pharmacol. (San Diego)* **1998**, *42*, 482−485.
(22) Mullins, U. L.; Gianutsos, G.; Eison, A. S. Effects of Antidepressants on 5-HT_7 Receptor Regulation in the Rat Hypothalamus. *Neuropsychopharmacology* **1999**, *21*, 352−367.
(23) Errico, M.; Crozier, R. A.; Plummer, M. R.; Cowen, D. S. 5-HT_7 Receptors Activate the Mitogen Activated Protein Kinase Extracellular Signal Related Kinase in Cultured Rat Hippocampal Neurons. *Neuroscience* **2001**, *102*, 361−367.
(24) Gill, C. H.; Soffin, E. M.; Hagan, J. J.; Davies, C. H. 5-HT_7 Receptors Modulate Synchronized Network Activity in Rat Hippocampus. *Neuropharmacology* **2002**, *42*, 82−92.
(25) Leung, E.; Walsh, L. K. M.; Pulido-Rios, M. T.; Eglen, R. M. Characterization of Putative 5-ht$_7$ Receptors Mediating Direct Relaxation in *Cynomolgus* Monkey Isolated Jugular Vein. *Br. J. Pharmacol.* **1996**, *117*, 926−930.
(26) Morecroft, I.; MacLean, M. R. 5-Hydroxytryptamine Receptors Mediating Vasoconstriction and Vasodilation in Perinatal and Adult Rabbit Small Pulmonary Arteries. *Br. J. Pharmacol.* **1998**, *125*, 69−78.
(27) Terrón, J. A.; Falcón-Neri, A. Pharmacological Evidence for the 5-HT_7 Receptor Mediating Smooth Muscle Relaxation in Canine Cerebral Arteries. *Br. J. Pharmacol.* **1999**, *127*, 609−616.
(28) Prins, N. H.; Briejer, M. R.; van Bergen, P. J. E.; Akkermans, L. M. A.; Schuurkes, J. A. J. Evidence for 5-HT_7 Receptors Mediating Relaxation of Human Colonic Circular Smooth Muscle. *Br. J. Pharmacol.* **1999**, *128*, 849−852.
(29) Centurión, D.; Sánchez-López, A.; Ortiz, M. I.; De Vries, P.; Saxena, P. R.; Villalón, C. M. Mediation of 5-HT-Induced Internal Carotid Vasodilatation in GR127935 and Ritanserin-Pretreated Dogs by 5-HT_7 Receptors. *Naunyn-Schmiedeberg's Arch. Pharmacol.* **2000**, *362*, 169−176.
(30) Howarth, C. J.; Prince, R. I.; Dyker, H.; Lösel, P. M.; Seinsche, A.; Osborne, R. H. Pharmacological Characterization of 5-Hydroxytryptamine-Induced Contractile Effects in the Isolated Gut of the Lepidopteran Caterpillar Spodoptera Frugiperda. *J. Insect Physiol.* **2002**, *48*, 43−52.
(31) De Ponti, F.; Tonini, M. Irritable Bowel Syndrome. New Agents Targeting Serotonin Receptor Subtypes. *Drugs* **2001**, *61*, 317−332.
(32) Terrón, J. A. Is the 5-HT_7 Receptor Involved in the Pathogenesis and Prophylactic Treatment of Migraine? *Eur. J. Pharmacol.* **2002**, *439*, 1−11.
(33) Forbes, I. T.; Dabbs, S.; Duckworth, D. M.; Jennings, A. J.; King, F. D.; Lovell, P. J.; Brown, A. M.; Collin, L.; Hagan, J. J.; Middlemiss, D. N.; Riley, G. J.; Thomas, D. R.; Upton, N. (*R*)-3,*N*-Dimethyl-*N*-[1-methyl-3-(4-methylpiperidin-1-yl)propyl]benzenesulfonamide: The First Selective 5-HT_7 Receptor Antagonist. *J. Med. Chem.* **1998**, *41*, 655−657.
(34) Kikuchi, C.; Nagaso, H.; Hiranuma, T.; Koyama, M. Tetrahydrobenzindoles: Selective Antagonists of the 5-HT_7 Receptor. *J. Med. Chem.* **1999**, *42*, 533−535.
(35) Lovell, P. J.; Bromidge, S. M.; Dabbs, S.; Duckworth, D. M.; Forbes, I. T.; Jennings, A. J.; King, F. D.; Middlemiss, D. N.; Rahman, S. K.; Saunders: D. V.; Collin, L. L.; Hagan, J. J.; Riley, G. J.; Thomas, D. R. A Novel, Potent, and Selective 5-HT_7 Antagonist: (*R*)-3-(2-(2-(4-Methylpiperidin-1-yl)ethyl)pyrrolidine-1-sulfonyl)phenol (SB-269970). *J. Med. Chem.* **2000**, *43*, 342−345.
(36) Kikuchi, C.; Ando, T.; Watanabe, T.; Nagaso, H.; Okuno, M.; Hiranuma, T.; Koyama, M. 2a-[4-(Tetrahydropyridoindol-2-yl)-butyl]tetrahydrobenzoindole Derivatives: New Selective Antagonists of the 5-Hydroxytryptamine7 Receptor. *J. Med. Chem.* **2002**, *45*, 2197−2206.
(37) Kikuchi, C.; Suzuki, H.; Hiranuma, T.; Koyama, M. New Tetrahydrobenzoindoles as Potent and Selective 5-HT_7 Antagonists with Increased In Vitro Metabolic Stability. *Bioorg. Med. Chem. Lett.* **2003**, *13*, 61−64.
(38) López-Rodríguez, M. L.; Porras, E.; Benhamú, B.; Ramos, J. A.; Morcillo, M. J.; Lavandera, J. L. First Pharmacophoric Hyphothesis for 5-HT_7 Antagonism. *Bioorg. Med. Chem. Lett.* **2000**, *10*, 1097−1100.
(39) *CATALYST 4.5*; Molecular Simulations Inc.: San Diego, CA 92121-3752.
(40) Smellie, A.; Kahn, S. D.; Teig, S. An Analysis of Conformational Coverage 1. Validation and Estimation of Coverage. *J. Chem. Inf. Comput. Sci.* **1995**, *35*, 285−294.
(41) Smellie, A.; Kahn, S. D.; Teig, S. An Analysis of Conformational Coverage 2. Applications of Conformational Models. *J. Chem. Inf. Comput. Sci.* **1995**, *35*, 295−304.
(42) Smellie, A.; Teig, S.; Towbin, P. Poling: Promoting Conformational Coverage. *J. Comput. Chem.* **1995**, *16*, 171−187.
(43) Brooks, B. R.; Bruccoleri, R. E.; Olafson, B. D.; States, D. J.; Swaminathan, S.; Karplus, M. CHARMm: A Program for Macromolecular Energy, Minimization, and Dynamics Calculations. *J. Comput. Chem.* **1983**, *4*, 187−217.
(44) Duffy, J. C.; Dearden, J. C.; Green, D. S. V. Use of Catalyst in the Design of Novel Non-Steroidal Anti-Inflamatory Analgesic Drugs. In *QSAR and Molecular Modeling: Concepts, Computational Tools and Biological Applications*; Sanz, F.; Giraldo, J.; Manaut, J., Eds.; Prous Science Publishers: Barcelona, 1995; pp 289−291.
(45) Halova, J.; Zak, P.; Strouf, O.; Uchida, N.; Yuzuri, T.; Sakakibara, K.; Hirota, M. Multicriteria Methodology Validation Using Catalyst Software System. A Case Study on SAR of Cathecol Analogues against Malignant Melanoma. *Org. React.* **1997**, *31*, 31−43.
(46) Daveu, C.; Bureau, R.; Baglin, I.; Prunier, H.; Lancelot, J.-C.; Rault, S. Definition of a Pharmacophore for Partial Agonists of Serotonin 5-HT_3 Receptors. *J. Chem. Inf. Comput. Sci.* **1999**, *39*, 362−369.
(47) Ekins, S.; Durst, G. L.; Stratford, R. E.; Thorner, D. A.; Lewis, R.; Loncharich, R. J.; Wikel, J. H. Three-Dimensional Quantitative Structure-Permeability Relationship Analysis for a Series of Inhibitors of Rhinovirus Replication. *J. Chem. Inf. Comput. Sci.* **2001**, *41*, 1578−1586.
(48) Saladino, R.; Crestini, C.; Palamara, A. T.; Danti, M. C.; Manetti, F.; Corelli, F.; Garaci, E.; Botta, M. Synthesis, Biological Evaluation, and Pharmacophore Generation of Uracil, 4(3*H*)-Pyrimidinone, and Uridine Derivatives as Potent and Selective Inhibitors of Parainfluenza 1 (Sendai) Virus. *J. Med. Chem.* **2001**, *44*, 4554−4562.

(49) Hirashima, A.; Morimoto, M.; Kuwano, E.; Taniguchi, E.; Eto, M. Three-Dimensional Common-Feature Hypotheses for Octopamine Agonist 2-(Arylimino)imidazolidines. *Bioorg. Med. Chem.* **2002**, *10*, 117−123.
(50) Sprague, P. W.; Hoffmann, R. Catalyst Pharmacophore Models and Their Utility as Queries for Searching 3D Databases. In *Computer Assisted Lead Finding and Optimization-Current Tools for Medicinal Chemistry*; Van de Waterbeemd H., Testa, B., Folkers, G., Eds.; VHCA: Basel, 1997; pp 230−240.
(51) López-Rodríguez, M. L.; Murcia, M.; Benhamú, B.; Viso, A.; Campillo, M.; Pardo, L. Benzimidazole Derivatives. 3. 3D-QSAR/CoMFA Model and Computational Simulation for the Recognition of 5-HT_4 Receptor Antagonists. *J. Med. Chem.* **2002**, *45*, 4806−4815.
(52) Palczewski, K.; Kumasaka, T.; Hori, T.; Behnke, C. A.; Motoshima, H.; Fox, B. A.; Le Trong, I.; Teller, D. C.; Okada, T.; Stenkamp, R. E.; Yamamoto, M.; Miyano, M. Crystal Structure of Rhodopsin: A G Protein-Coupled Receptor. *Science* **2000**, *289*, 739−745.
(53) Ballesteros, J. A.; Weinstein, H. Integrated Methods for the Construction of Three-Dimensional Models and Computational Probing of Structure−Function Relations in G-Protein Coupled Receptors. *Methods Neurosci.* **1995**, *25*, 366−428.
(54) Ballesteros, J. A.; Deupi, X.; Olivella, M.; Haaksma, E. E.; Pardo, L. Serine and Threonine Residues Bend Alpha-Helices in the chi(1) = g(−) Conformation. *Biophys. J.* **2000**, *79*, 2754−2760.
(55) López-Rodríguez, M. L.; Vicente, B.; Deupi, X.; Barrondo, S.; Olivella, M.; Morcillo, M. J.; Benhamú, B.; Ballesteros, J. A.; Salles, J.; Pardo, L. Design, Synthesis and Pharmacological Evaluation of 5-Hydroxytryptamine (1a) Receptor Ligands to Explore the Three-Dimensional Structure of the Receptor. *Mol. Pharmacol.* **2002**, *62*, 15−21.
(56) Maseras, F.; Morokuma, K. IMOMM: a New Integrated ab initio + Molecular Mechanics Geometry Optimization Scheme of Equilibrium Structures and Transition States. *J. Comput. Chem.* **1995**, *16*, 1170−1179.
(57) Tsuzuki, S.; Honda, K.; Uchimaru, T.; Mikami, M.; Tanabe, K. The Magnitude of the CH/π Interaction Between Benzene and Some Model Hydrocarbons. *J. Am. Chem. Soc.* **2000**, *122*, 3746−3753.
(58) Olivella, M.; Deupi, X.; Govaerts, C.; Pardo, L. Influence of the Environment in the Conformation of Alpha-Helices Studied by Protein Database Search and Molecular Dynamics Simulations. *Biophys. J.* **2002**, *82*, 3207−3213.
(59) Cornell, W. D.; Cieplak, P.; Bayly, C. I.; Gould, I. R.; Merz, K. M., Jr.; Ferguson, D. M.; Spellmeyer, D. C.; Fox, T.; Caldwell, J. W.; Kollman, P. A. A Second Generation Force Field for the Simulation of Proteins, Nucleic Acids, and Organic Molecules. *J. Am. Chem. Soc.* **1995**, *117*, 5179−5197.
(60) Cieplak, P.; Cornell, W. D.; Bayly, C.; Kollman, P. A. Application of the Multimolecule and Multiconformational RESP Methodology Biopolymers: Charge Derivation for the DNA, RNA and Proteins. *J. Comput. Chem.* **1995**, *16*, 1357−1377.
(61) Frisch, M. J.; Trucks, G. W.; Schlegel, H. B.; Scuseria, G. E.; Robb, M. A.; Cheeseman, J. R.; Zakrzewski, V. G.; Montgomery, J. A., Jr.; Stratmann, R. E.; Burant, J. C.; Dapprich, S.; Millam, J. M.; Daniels, A. D.; Kudin, K. N.; Strain, M. C.; Farkas, O.; Tomasi, J.; Barone, V.; Cossi, M.; Cammi, R.; Mennucci, B.; Pomelli, C.; Adamo, C.; Clifford, S.; Ochterski, J.; Petersson, G. A.; Ayala, P. Y.; Cui, Q.; Morokuma, K.; Malick, D. K.; Rabuck, A. D.; Raghavachari, K.; Foresman, J. B.; Cioslowski, J.; Ortiz, J. V.; Stefanov, B. B.; Liu, G.; Liashenko, A.; Piskorz, P.; Komaromi, I.; Gomperts, R.; Martin, R. L.; Fox, D. J.; Keith, T.; Al-Laham, M. A.; Peng, C. Y.; Nanayakkara, A.; Gonzalez, C.; Challacombe, M.; Gill, P. M. W.; Johnson, B. G.; Chen, W.; Wong, M. W.; Andres, J. L.; Head-Gordon, M.; Replogle, E. S.; Pople, J. A. *Gaussian 98*; Gaussian, Inc.: Pittsburgh, PA, 1998.
(62) Case, D. A.; Pearlman, D. A.; Caldwell, J. W.; Cheatham, T. E., III; Wang, J.; Ross, W. S.; Simmerling, C. L.; Darden, T. A.; Merz, K. M.; Stanton, R. V.; Cheng, A. L.; Vicent, J. J.; Crowley, M.; Tsui, V.; Gohlke, H.; Radmer, R. J.; Duan, Y.; Pitera, J.; Masova, I.; Seibel, G. L.; Singh, U. C.; Weiner, P. K.; Kollman, P. A. AMBER7; University of California, San Francisco, 2002.
(63) Linnanen, T.; Brisander, M.; Unelius, L.; Rosqvist, S.; Nordvall, G.; Hacksell, U.; Johansson, A. M. Atropisomeric Derivatives of 2′,6′-Disubstituted (*R*)-11-Phenylaporphine: Selective Serotonin 5-HT_7 Receptor Antagonists. *J. Med. Chem.* **2001**, *44*, 1337−1340.
(64) To, Z. P.; Bonhaus, D. W.; Eglen, R. M.; Jakeman, L. B. Characterization and Distribution of Putative 5-ht_7 Receptors in Guinea-Pig Brain. *Br. J. Pharmacol.* **1995**, *115*, 107−116.
(65) Jasper, J. R.; Kosaka, A.; To, Z. P.; Chang, D. J.; Eglen, R. M. Cloning, Expression and Pharmacology of a Truncated Splice Variant of the Human 5-HT_7 Receptor (h5-$HT_{7(b)}$). *Br. J. Pharmacol.* **1997**, *122*, 126−132.
(66) Greene, J.; Kahn, S.; Savoj, H.; Sprague, S.; Teig, S. Chemical Function Queries for 3D Database Search. *J. Chem. Inf. Comput. Sci.* **1994**, *34*, 1297−1308.
(67) Kogan, H. A.; Marsden, C. A.; Fone, K. C. F. DR4004, a Putative 5-HT_7 Receptor Antagonist, Also Has Functional Activity at the Dopamine D2 Receptor. *Eur. J. Pharmacol.* **2002**, *449*, 105−111.
(68) Aguirre, N.; Ballaz, S.; Lasheras, B.; del Río, J. MDMA ('Ecstasy') Enhances 5-HT_{1A} Receptor Density and 8-OH-DPAT-Induced Hypothermia: Blockade by Drugs Preventing 5-Hydroxytryptamine Depletion. *Eur. J. Pharmacol.* **1998**, *346*, 181−188.
(69) Cheng, Y. C.; Prusoff, W. H. Relationship Between the Inhibition Constant (K_i) and the Concentration of Inhibitor which Causes 50 Per Cent Inhibition (IC_{50}) of an Enzymatic Reaction. *Biochem. Pharmacol.* **1973**, *22*, 3099−3108.
(70) Hagan, J. J.; Price, G. W.; Jeffrey, P.; Deeks, N. J.; Stean, T.; Piper, D.; Smith, M. I.; Upton, N.; Medhurst, A. D.; Middlemiss, D. N.; Riley, G. J.; Lovell, P. J.; Bromidge, S. M.; Thomas, D. R. Characterization of SB-269970-A, a Selective 5-HT(7) Receptor Antagonist. *Br. J. Pharmacol.* **2000**, *130(3)*, 539−548.
(71) Strader, C. D.; Candelore, M. R.; Hill, W. S.; Sigal, I. S.; Dixon, R. A. F. Identification of Two Serine Residues Involved in Agonist Activation of the α-Adrenergic Receptor. *J. Biol. Chem.* **1989**, *264*, 13572−13578.
(72) Liapakis, G.; Ballesteros, J. A.; Papachristou, S.; Chan, W. C.; Chen, X.; Javitch, J. A. The Forgotten Serine. A Critical Role For Ser-$203^{5.42}$ in Ligand Binding to and Activation of the Beta 2-Adrenergic Receptor. *J. Biol. Chem.* **2000**, *275*, 37779−37788.
(73) Strader, C. D.; Fong, T. M.; Tota, M. R.; Underwood, D.; Dixon, R. A. F. Structure and Function of G Protein-Coupled Receptors. *Annu. Rev. Biochem.* **1994**, *63*, 101−132.
(74) Choudhary, M. S.; Craigo, S.; Roth, B. L. A Single Point Mutation (Phe^{340}/ Leu^{340}) of a Conserved Phenylalanine Abolishes 4-[^{125}I]-Iodo-(2,5-dimethoxy)phenylisopropylamine and [^{3}H]Mesulergine but Not [^{3}H]Ketanserin Binding to 5-Hydroxytryptamine$_2$ Receptors. *Mol. Pharmacol.* **1993**, *43*, 755−761.
(75) Steiner, T.; Koellner, G. Hydrogen Bonds with π-Acceptors in Proteins: Frequencies and Role in Stabilizing Local 3D Structures. *J. Mol. Biol.* **2001**, *305*, 535−557.
(76) Kraulis, P. J. MOLSCRIPT: A Program to Produce both Detailed and Schematic Plots of Protein Structures. *J. Appl. Crystallogr.* **1991**, *24*, 945−950.
(77) Merritt, E. A.; Bacon, D. J. Raster3D: Photorealistic Molecular Graphics. *Methods Enzymol.* **1997**, *277*, 505−524.
(78) López-Rodríguez, M. L.; Morcillo, M. J.; Fernández, E.; Porras, E.; Orensanz, L.; Beneytez, M. E.; Manzanares, J.; Fuentes, J. A. Synthesis and Structure−Activity Relationships of a New Model of Arylpiperazines. 5. Study of the Physicochemical Influence of the Pharmacophore on 5-HT_{1A}/α_1-Adrenergic Receptor Affinity: Synthesis of a New Derivative with Mixed 5-HT_{1A}/D_2 Antagonist Properties. *J. Med. Chem.* **2000**, *44*, 186−197.
(79) Lakomý, J.; Silhankova, A.; Ferles, M.; Exner, O. Studies in the Pyridine Series. XXV. Dissociation Constants of some Piperidine and Piperideine Bases. *Collect. Czech. Chem. Commun.* **1968**, *33*, 1700−1708.
(80) Bright, C.; Brown, T. J.; Cox, P.; Halley, F.; Lockey, P.; McLay, I. M.; Moore, U.; Porter, B.; Williams, R. J. Identification of a Non Peptidic RANTES Antagonist. *Bioorg. Med. Chem. Lett.* **1998**, *8*, 771−774.
(81) Pelz, K.; Protiva, M. Neurotrope und Psychotrope Substanzen XIV. 3-(4-Phenylpiperidino)propylderivative. *Collect. Czech. Chem.* **1967**, *32*, 2840−2853.
(82) Fone, K. C. F.; Marsden, C. A. Serotonin 5-HT_7 Receptors Binding to Rat Hypothalamic Membranes-Reply. *J. Neurochem.* **1999**, *72*, 883−884.
(83) Lowry, O. H.; Rosebrough, N. J.; Farr, A. L.; Randall, R. J. Protein Measurement with the Folin Phenol Reagent. *J. Biol. Chem.* **1951**, *193*, 265−275.

JM030841R

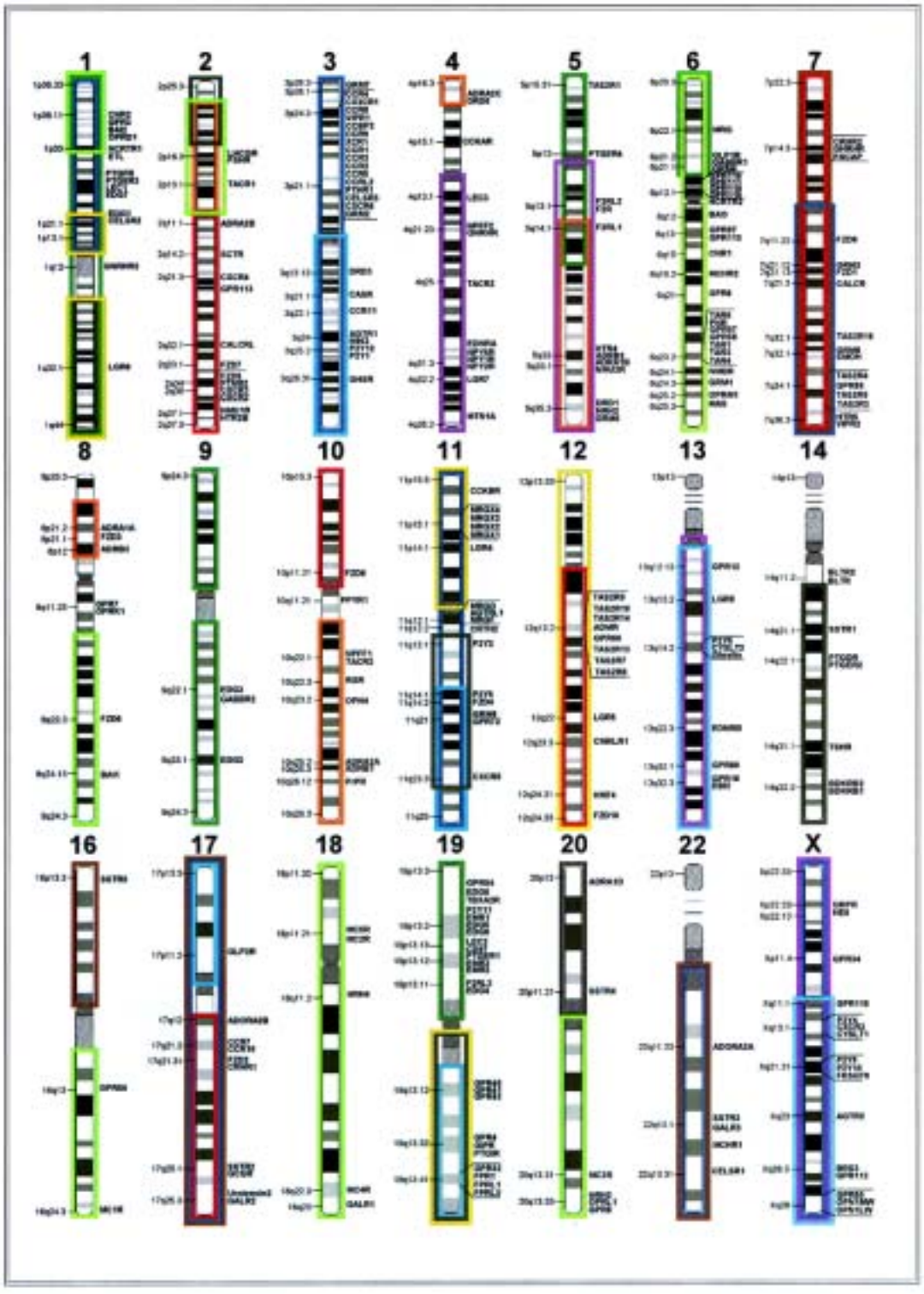

FIGURA 1. Posició dels GPCRs en els grups paralogon del genoma humà.

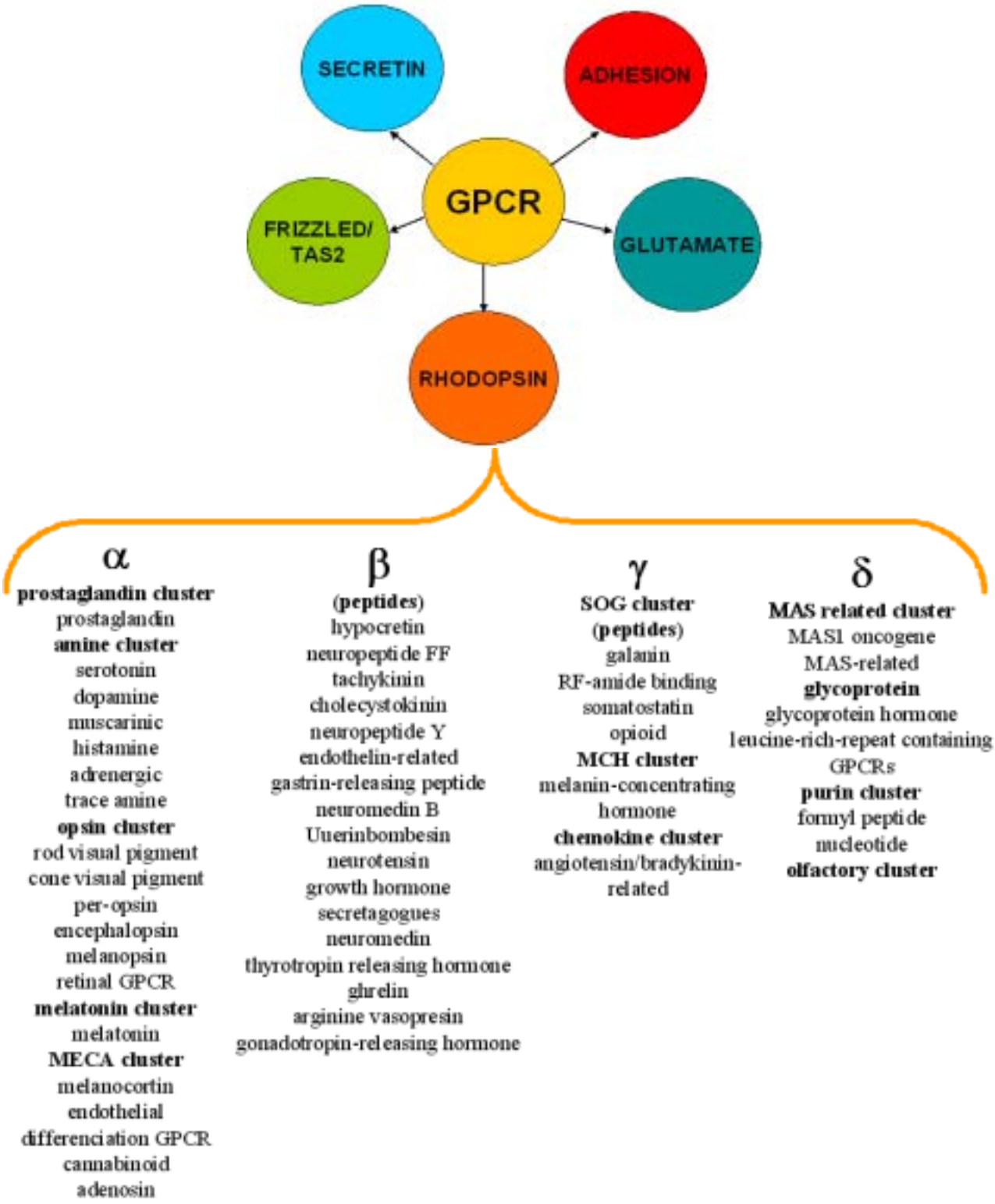

FIGURA 2. Classificació dels GPCRs del genoma humà a partir d'una anàlisi filogenètica. Dins de la família de la rodopsina, hi trobem 4 subgrups (α, β, γ, δ) que a la vegada es divideixen en 13 subclasses.

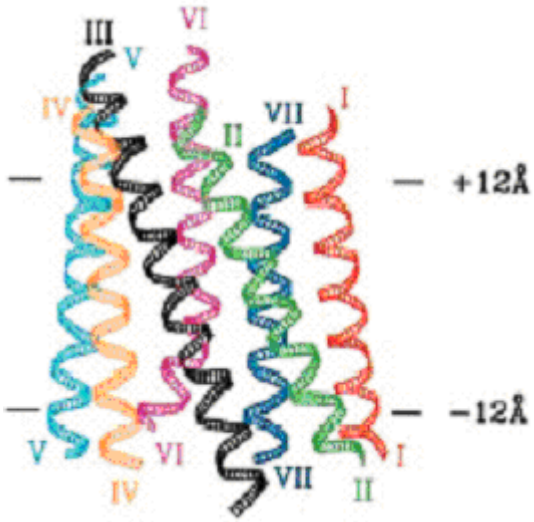

FIGURA 3. Model tridimensional per a les posicions dels carbonis alfa de les set hèlixs transmembràniques de la rodopsina. El model incorpora informació estructural a partir de l'anàlisi de 500 seqüències de GPCRs. L'empaquetament de les hèlixs es deriva dels mapes de densitat electrònica de la rodopsina determinats per microscopia electrònica. A més a més aquest model proposa quins residus que es troben altament conservats entre els GPCRs interaccionen entre ells. En el model també s'hi inclouen i s'hi discuteixen els resultats de tècniques com la creació de llocs d'unió de metalls i de ponts disulfurs, estudis de *site-directed spin-labelling*, mètodes d'accessibilitat de cisteïnes substituïdes i estudis de mutagènesi dirigida.

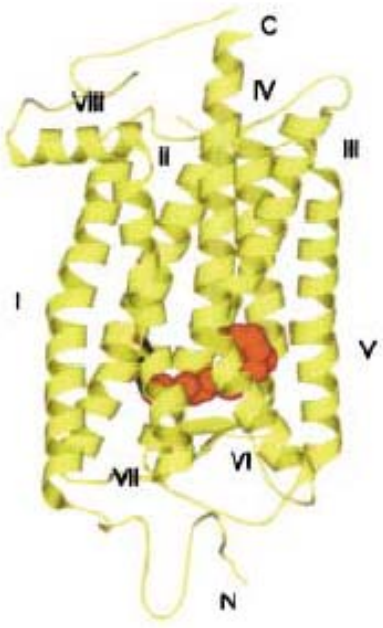

FIGURA 4. Visió paral·lela a la membrana cel·lular de l'estructura de la rodopsina bovina a partir dels cristalls tridimensionals (codi d'accés 1HZX). El polipèptid presenta set hèlixs transmembràniques paral·leles a la membrana cel·lular i s'hi identifiquen els llaços extracel·lulars i intracel·lulars, l'hèlix 8 perpendiculars a la membrana cel·lular així com les regions N i C terminals. El cromofor retinal es mostra en vermell.

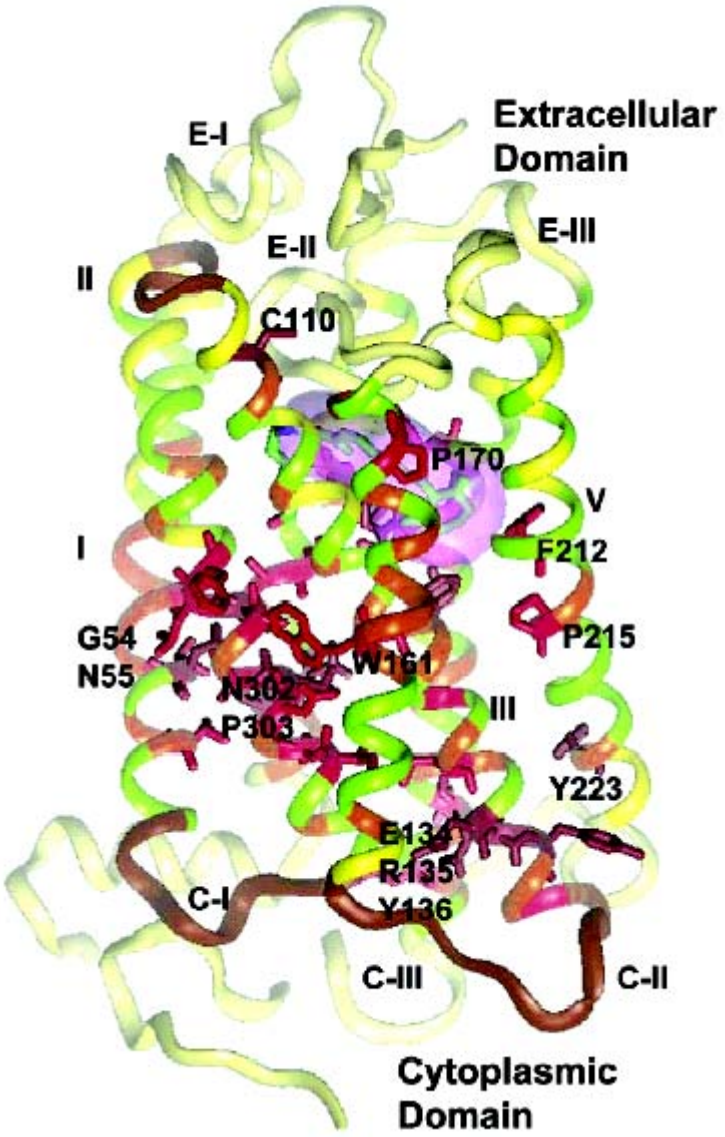

FIGURA 5. Estructura cristal·logràfica de la rodopsina bovina. Els residus tenen un color o altre en funció de la seva conservació dins la família de la rodopsina. Es mostra en color groc els residus que es conserven en un 10-20%, en color verd els residus que es conserven en un 20-40%, en color taronja els residus que es conserven en un 40-60 %, en color vermell els residus que es conserven en un 60-80% i en color marró els residus que es conserven en un 80-100%. El llaç extracel·lular conservat (ECL1) i els llaços intracel·lulars conservats (ICL1 i ICL2) es mostren en marró.

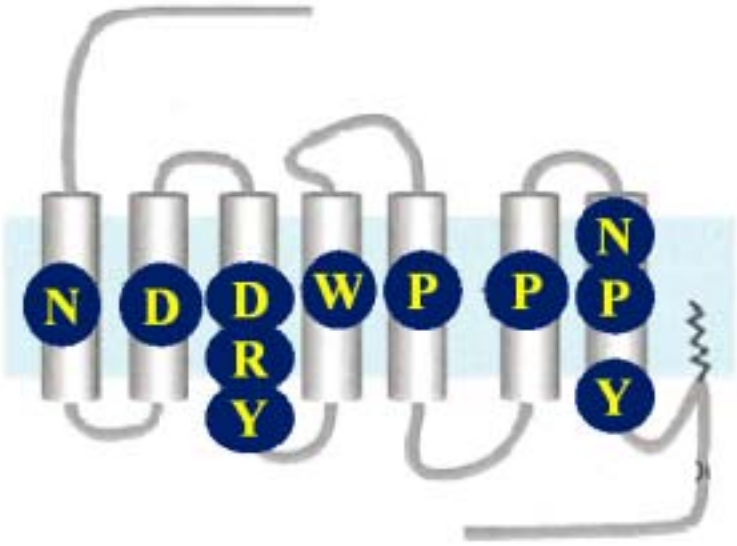

FIGURA 6. Patrons de conservació en les set hèlixs transmembràniques de la família A dels GPCRs. A la vegada aquests patrons de conservació serveixen per a enumerar els GPCRs de la família de la rodopsina. Així el residu d'asparagina conservat de la HTM1 definiria la posisció 1.50, el residu d'aspàrtic de la HTM2 marcaria la posició 2.50, l'arginina que forma el motiu conservat DRY de la HTM3 definiria la posició 3.50, el residu de triptòfan de la HTM4 definiria la posició 4.50, el residu de Prolina de la HTM5 definiria la posició 5.50, el residu de fenilalanina de la HTM6 definiria la posició 6.50 i el residu de prolina que constitueix el motiu conservat NPXXY a la HTM7 marcaria la posició 7.50.

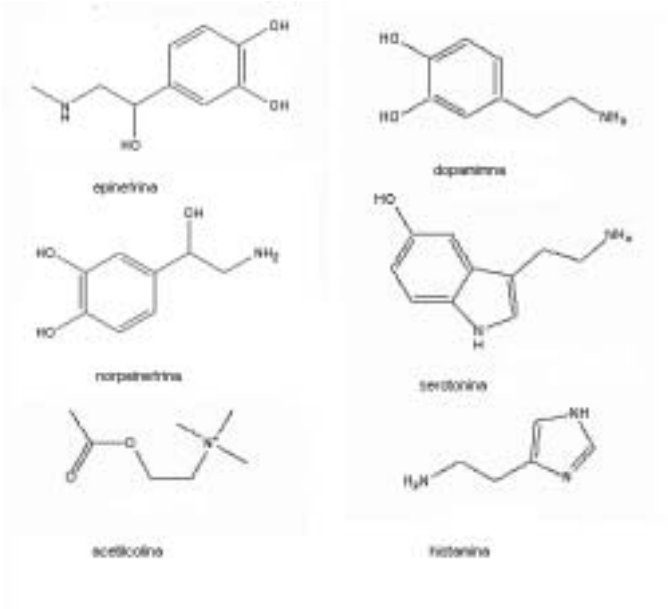

FIGURA 7. Lligands endògens dels receptors de les amines biogèniques. Els hidroxils dels anells de catecolamines dels lligand endògens de les amines biogèniques estan implicats en la unió amb residus de serina i treonina de les posicions 5.42, 5.43 i 5.46 dels receptors de les amines biogèniques. Una altra interacció important és entre l'amina protonada dels lligands i la cadena lateral del residu $Asp^{3.32}$.

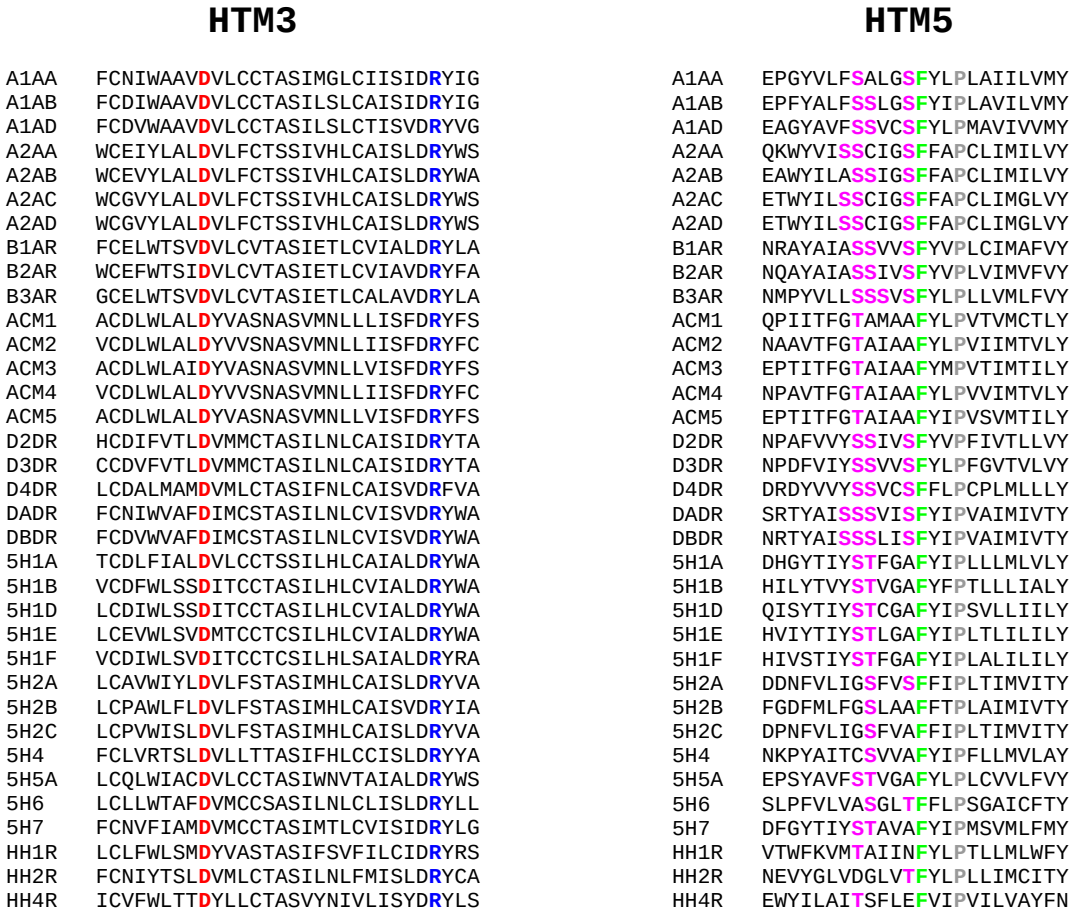

FIGURA 8. Alineament de les seqüències de les HTM3 i HTM5 dels receptors de les amines biogèniques. A la HTM3 hi trobem l'Asp$^{3.32}$ en vermell que es troba totalment conservat dins la família dels receptors de la família de les amines biogèniques i l'Arg$^{3.50}$ que forma part del motiu DRY, molt conservat en els GPCRs. A la HTM5 hi trobem els residus de Ser i Thr conservats al voltant de les posicions 5.42, 5.43 i 5.46 (en rosa). A més a més també hi trobem la Phe$^{5.47}$ (en verd) que també està implicat en la unió amb la part aromàtica dels lligands i que es troba totalment conservat en la família de les amines biogèniques. En gris hi trobem la Pro$^{5.50}$ que és el residu més conservat de la HTM5 en els receptors de la familia de la rodopsina.

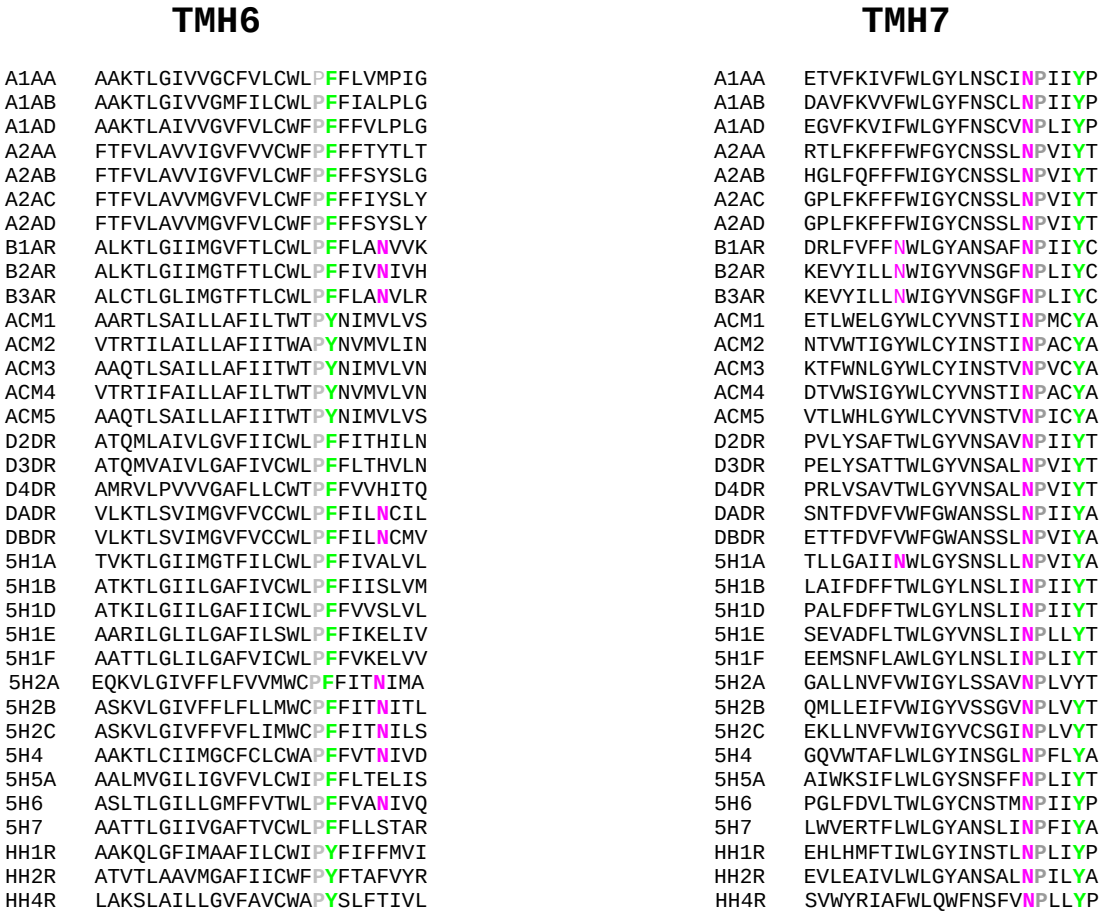

FIGURA 9. Alineament de les seqüències de les HTM 6 i 7 dels receptors de les amines biogèniques. A la HTM 6 hi trobem la Phe$^{6.51}$ (en verd) que es troba molt conservada, la Pro$^{6.50}$ que és el residu més conservat a la HTM6 dels receptors de la familia de la rodopsina i l'Asn$^{6.55}$ (en rosa) que està implicada en la unió d'agonistes en alguns receptors d'amines biogèniques.
A la HTM7 hi trobem el motiu molt conservat NPxxY (en rosa, gris i verd). També hi trobem l'Asn$^{7.39}$ que està implicat amb la unió d'antagonistes del receptor β_2-adrenèrgic.

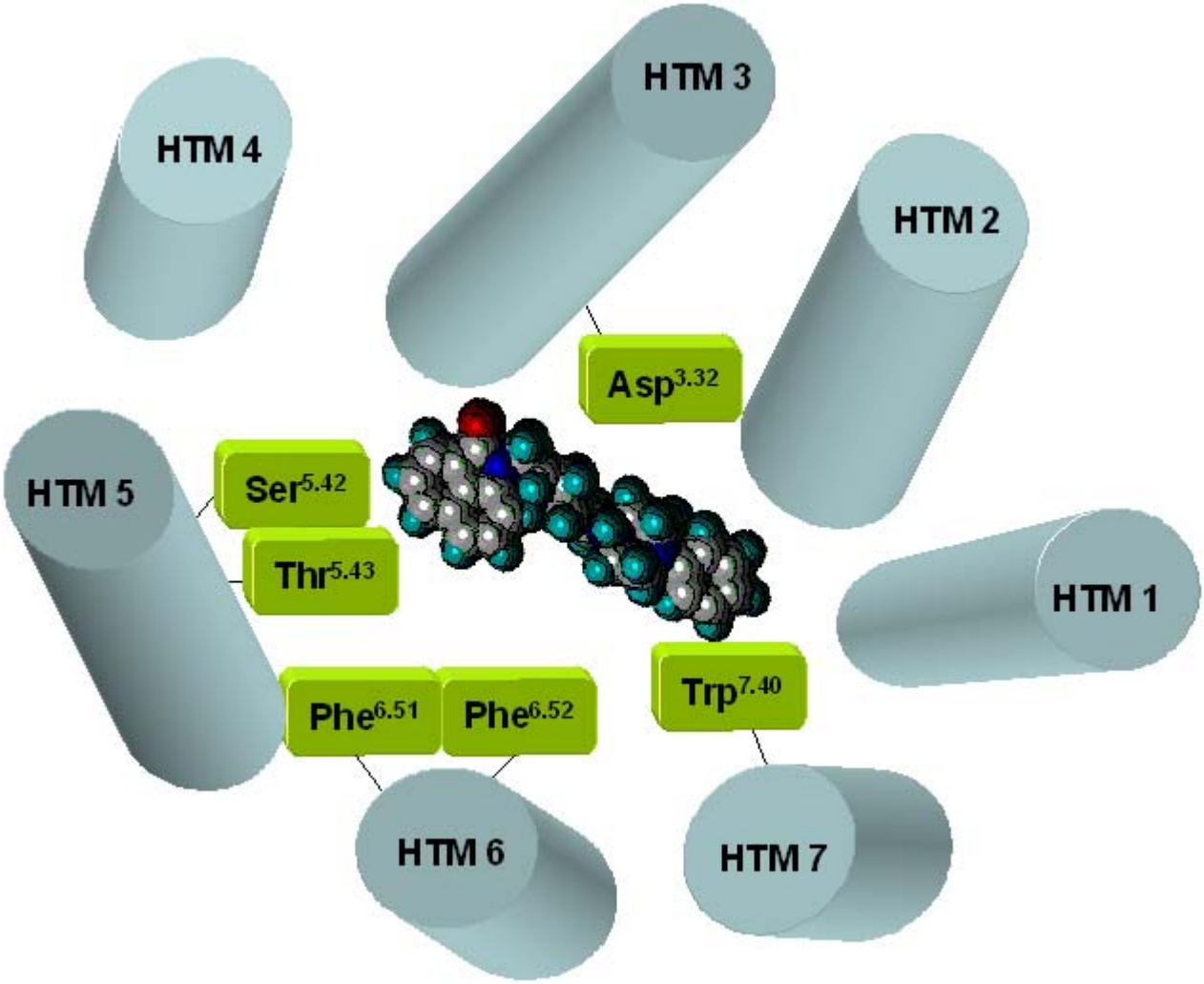

FIGURA 10. Representació de les set hèlixs transmembràniques dels receptors de les amines biogèniques (en blau) amb alguns dels principals residus (en verd) responsables de la interacció amb els seus lligands agonistes i antagonites.

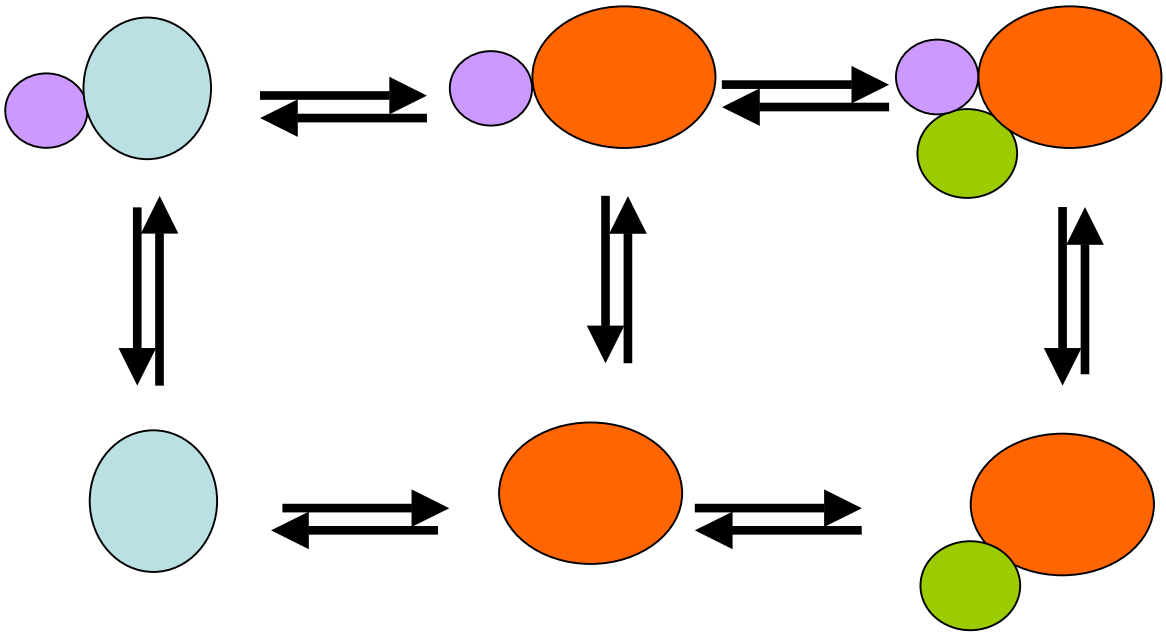

FIGURA 11. Model del complex ternari estès. El receptor es troba en equilibri entre l'estat inactiu (R) i l'estat actiu (R*). La unió de l'agonista (L) a R* estabilitzaria la conformació R* del receptor. El model del complex ternari estès permet la formació espontània de R* a partir de R independentment de la presència de l'agonista (L). R* pot interaccionar i activar la proteïna G (G) amb o sense la presència de l'agonista.

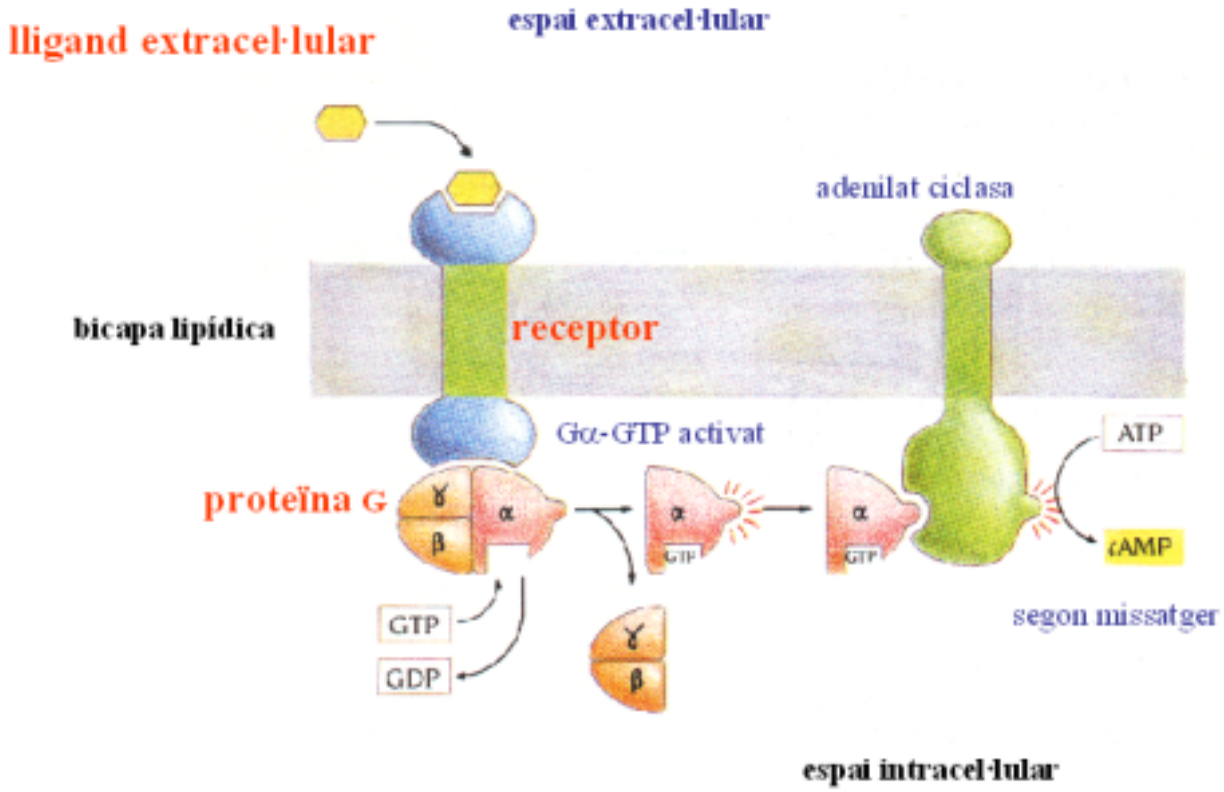

FIGURA 12. El lligand interacciona amb el receptor i trasmet el senyal cap a l'interior de la cèl·lula a través de la proteïna G. El receptor activat produeix un canvi conformacional a la subunitat α de la proteïna G tot provocant l'intercanvi de GDP a GTP. A continuació la subunitat α unida a GTP es dissocia del receptor i del dímer βγ; el dímer βγ pot modular diverses vies de senyalització cel·lular.

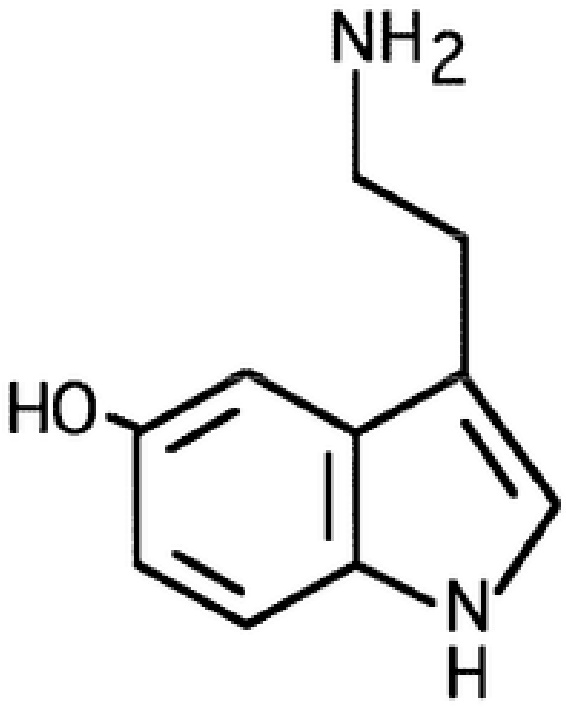

FIGURA 13. Estructura química de la serotonina (5-HT)

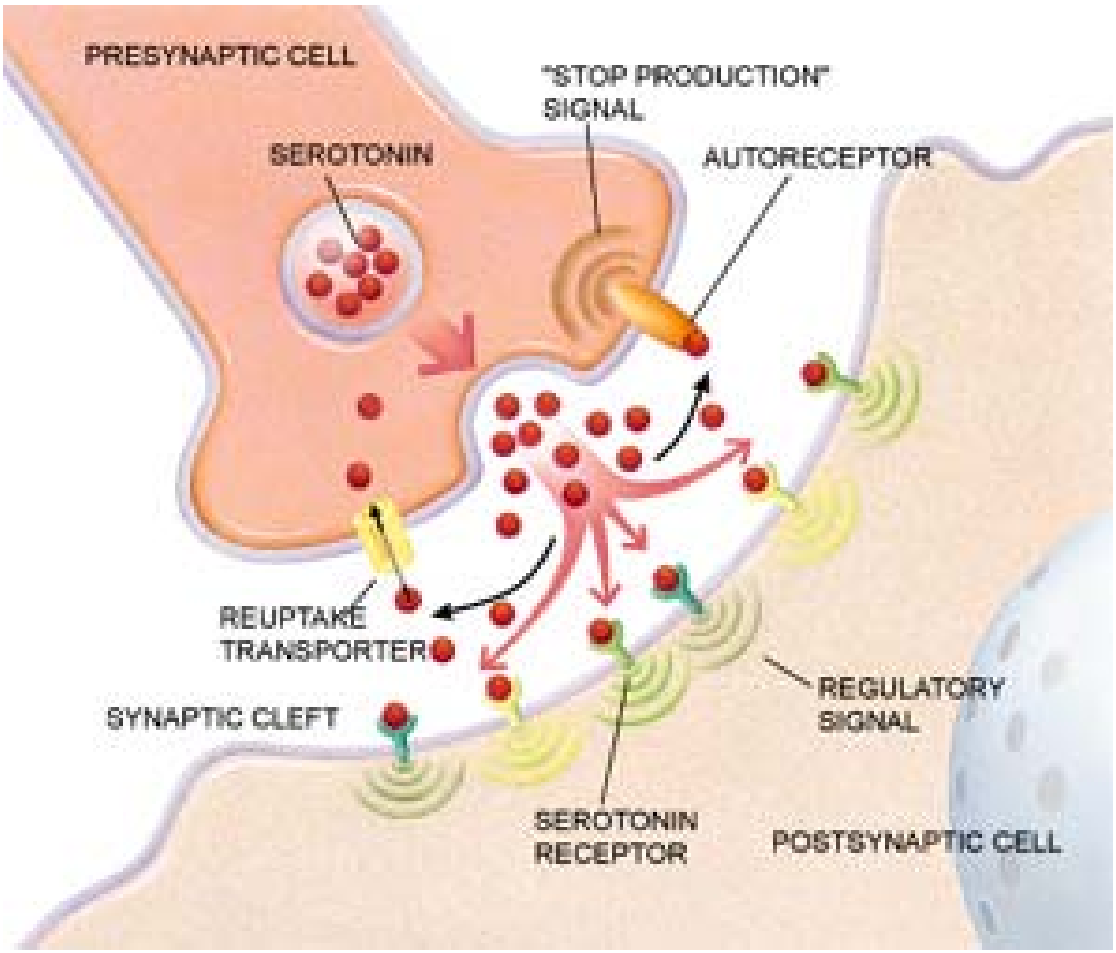

FIGURA 14. Respresentació gràfica de la sinapsis serotoninèrgica. La serotonina s'emmagatzema en vesícules i s'aboca a l'espai sinàptic on s'unirà als receptors serotoninèrgic postsinàptics per tal d'activar-los i començar el procés de transducció del senyal. Tot seguit comença el procés de recaptació de la serotonina cap a la neurona pre-sinàptica tot tancant el cicle.

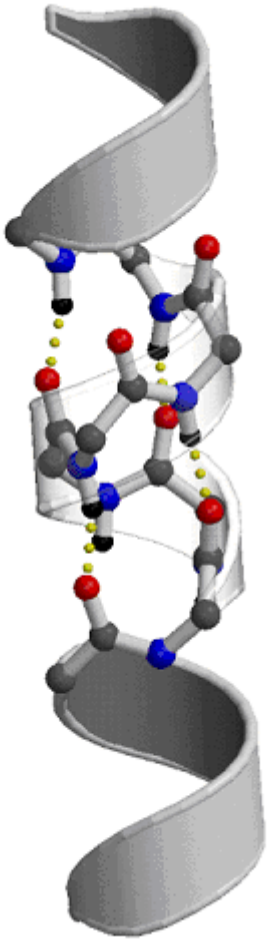

FIGURA 15. L'estabilitat de les hèlixs α ve donada per enllaços per pont d'hidrogen (en groc) entre els grups NH (blau i negre) i l'oxigen carbonílic (en vermell) de la volta anterior.

FIGURA 16. Estructura química dels residus de serina i treonina. El grup hidoxil (en blau) de la seva cadena lateral (en vermell) té la capacitat de formar ponts d'hidrogen.

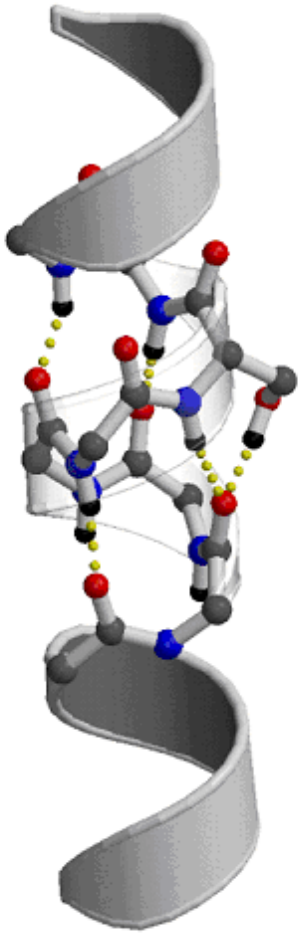

FIGURA 17. La Ser i Thr en la conformació g- distorsionen l'enllaç d'hidrogen intrahelical com a conseqüència de la formació d'un segon enllaç d'hidrogen entre la seva cadena lateral i el carbonil de la volta anterior

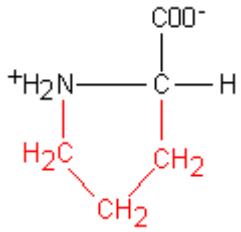

FIGURA 18. Estructura química del residu de Prolina.

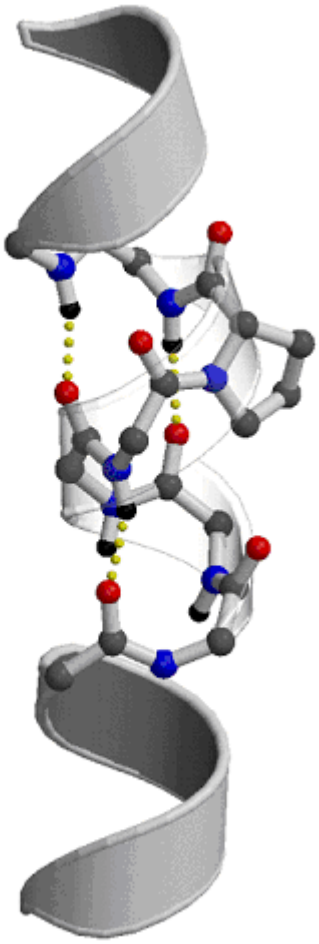

FIGURA 19. L'anell de pirrolidina no permet la formació de l'enllaç d'hidrogen intrahelical entre el grup NH i l'oxigen carbonílic en la posició i-4.

	Cerca en la base de dades PDB			Dinàmica molecular	
	$GLOB_{hidro\ fílic}$	GLOB-MEM_{cor}	$MEM_{hidrofòbic}$	Aigua	Metans
n	**252**	**510**	**97**	**1000**	**1000**
ϕ_i	**-63.5**/5.6	**-62.9**/5.3	**-61.8**/6.7	**-65.9**/10.0	**-61.2**/8.3
ψ_i	**-40.9**/5.4	**-41.6**/6.1	**-43.1**/7.0	**-39.3**/9.7	**-44.1**/8.5
$N_i \cdot\cdot O_{i-4}$	**3.04**/0.14	**2.98**/0.15	**2.96**/0.17	**3.10**/0.25	**2.93**/0.13
$N_i \cdot\cdot O_{i-4}=C_{i-4}$	**151.5**/6.0	**153.3**/7.1	**153.5**/7.5	**148.9**/10.5	**155.4**/8.3

POLARITAT DE L'ENTORN

(+) (-)

TAULA 1. Valors de Φ i Ψ i els paràmetres de l'enllaç d'hidrogen resultants de l'anàlisis d'estructures cristal·lines de proteïnes de membrana i de proteïnes globulars i fruit de les simulacions de dinàmica molecular. A mesura que augmenta la polaritat de l'entorn veiem com |Φ| augmenta i |Ψ| disminueix. A més a més veiem com els resultats de les simulacions de dinàmica molecular reprodueixen les tendències de Φ i Ψ i dels paràmetres de l'enllaç d'hidrogen de l'anàlisis d'estructures cristal·lines.

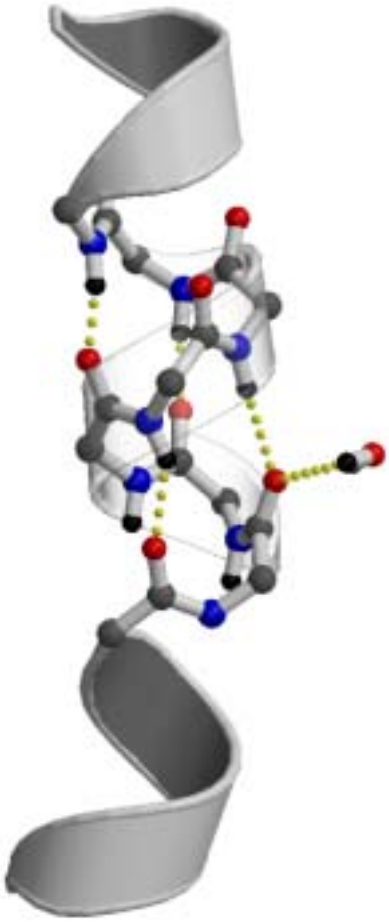

FIGURA 20. L'O de l'aigua és capaç de formar un enllaç d'hidrogen amb l'oxigen carbonílic de l'esquelet carbonat tot distorsionant l'enllaç d'hidrogen intrahelical entre aquest i el grup NH de l'esquelet carbonat de la volta posterior.

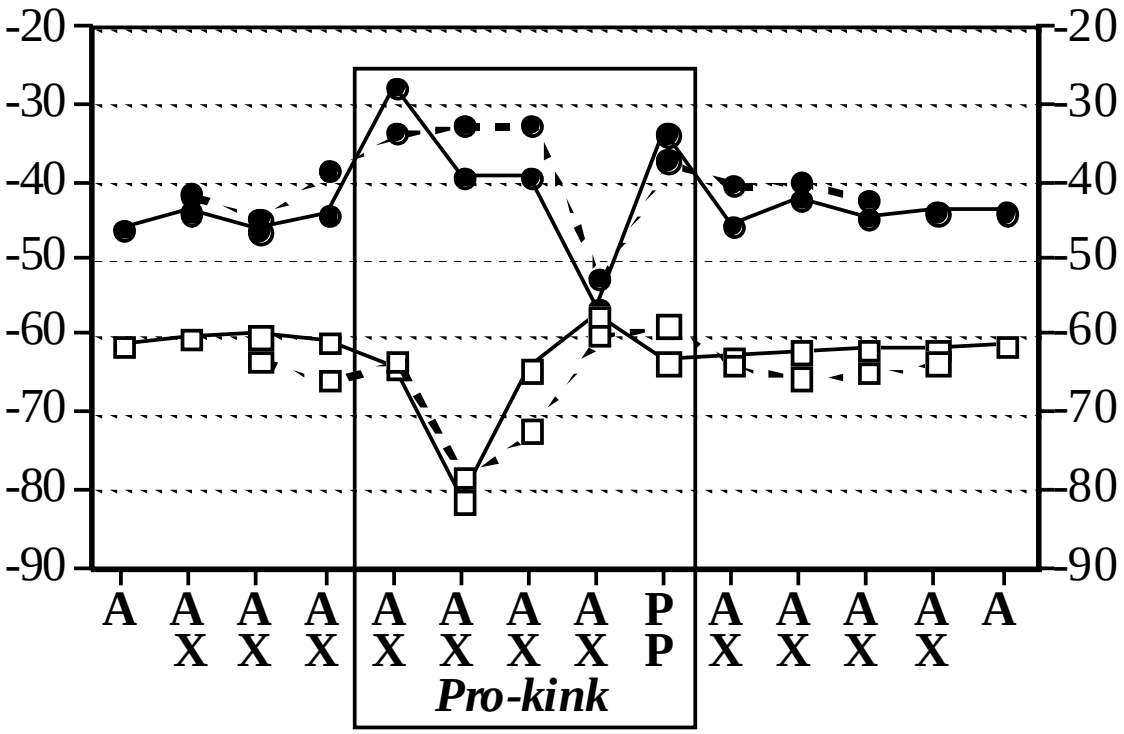

FIGURA 21. Valors mitjans dels angles diedres ϕ (en quadrats) i ψ (cercles) d'una hèlix α que conté el Pro kink fruit de la simulació de dinàmica molecular (línia negra) i de l'anàlisi d'estructures de proteïnes de membrana conegudes (línia discontínua). En els eixos X es representa la seqüència de l'hèlix α que es sotmet a la simulació de dinàmica molecular (part superior) i en l'anàlisi de proteïnes de membrana conegudes (part inferior). A significat Ala, P significa Pro i X és qualsevol residu excepte Pro.

```
5H1A    TCDLFIALDVLCCTSSILHLCAIALDRYWA
5H1B    VCDFWLSSDITCCTASILHLCVIALDRYWA
5H1D    LCDIWLSSDITCCTASILHLCVIALDRYWA
5H1E    LCEVWLSVDMTCCTCSILHLCVIALDRYWA
5H1F    VCDIWLSVDITCCTCSILHLSAIALDRYRA
5H2A    LCAVWIYLDVLFSTASIMHLCAISLDRYVA
5H2B    LCPAWLFLDVLFSTASIMHLCAISVDRYIA
5H2C    LCPVWISLDVLFSTASIMHLCAISLDRYVA
5H4     FCLVRTSLDVLLTTASIFHLCCISLDRYYA
5H5A    LCQLWIACDVLCCTASIWNVTAIALDRYWS
5H6     LCLLWTAFDVMCCSASILNLCLISLDRYLL
5H7     FCNVFIAMDVMCCTASIMTLCVISIDRYLG
```

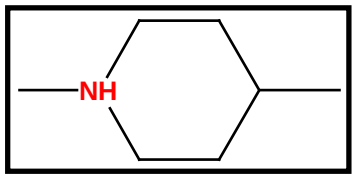

FIGURA 22. Alineament de seqüències de les HTM3 dels receptors de serotonina en humà. El residu Asp$^{3.32}$ (requadre negre, en vermell) interacciona amb amines protonades (requadre negre, en vermell) presents en molts lligands de serotonina.

```
5H1A    DHGYTIYSTFGAFYIPLLLMLVLY
5H1B    HILYTVYSTVGAFYFPTLLLIALY
5H1D    QISYTIYSTCGAFYIPSVLLIILY
5H1E    HVIYTIYSTLGAFYIPLTLILILY
5H1F    HIVSTIYSTFGAFYIPLALILILY
5H2A    DDNFVLIGSFVSFFIPLTIMVITY
5H2B    FGDFMLFGSLAAFFTPLAIMIVTY
5H2C    DPNFVLIGSFVAFFIPLTIMVITY
5H4     NKPYAITCSVVAFYIPFLLMVLAY
5H5A    EPSYAVFSTVGAFYLPLCVVLFVY
5H6     SLPFVLVASGLTFFLPSGAICFTY
5H7     DFGYTIYSTAVAFYIPMSVMLFMY
```

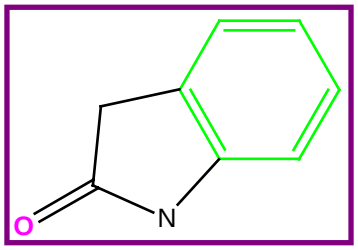

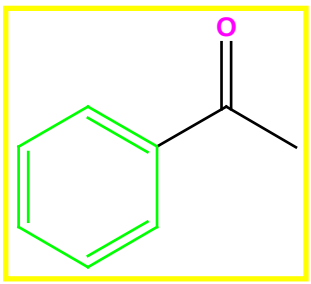

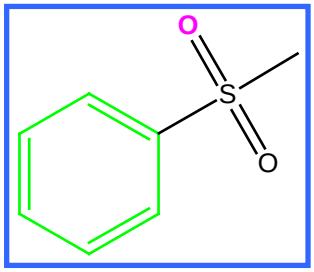

FIGURA 23. Alineament de les seqüències de la HTM5 dels receptors de serotonina en humà. Veiem com s'hi troben residus de Ser i Thr (en rosa). La situació i nombre d'aquests residus s'organitza en tres grups (requadres violeta, blau i groc), que a la vegada poden interaccionar amb tres grups funcionals diferents dels lligands respectivament (requadres violeta, blau i groc). La Phe$^{5.47}$ (en verd) interacciona amb motius aromàtics (en verd) pròxims als grups funcionals responsables d'interaccionar amb les Ser i Thr.

```
5H1A    TVKTLGIIMGTFILCWLPFFIVALVL
5H1B    ATKTLGIILGAFIVCWLPFFIISLVM
5H1D    ATKILGIILGAFIICWLPFFVVSLVL
5H1E    AARILGLILGAFILSWLPFFIKELIV
5H1F    AATTLGLILGAFVICWLPFFVKELVV
5H2A    ACKVLGIVFFLFVVMWCPFFITNIMA
5H2B    ASKVLGIVFFLFLLMWCPFFITNITL
5H2C    ASKVLGIVFFVFLIMWCPFFITNILS
5H4     AAKTLCIIMGCFCLCWAPFFVTNIVD
5H5A    AALMVGILIGVFVLCWIPFFLTELIS
5H6     ASLTLGILLGMFFVTWLPFFVANIVQ
5H7     AATTLGIIVGAFTVCWLPFFLLSTAR
```

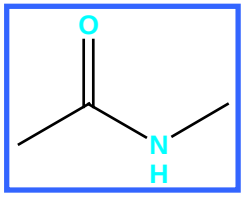

FIGURA 24. Alineament de les seqüències de la HTM6 dels receptors de serotonina en humà. En aquesta hèlix s'hi troben dos residus de Phe (requadre negre, en verd) totalment conservats. La Phe$^{6.51}$ interacciona amb la densitat de càrrega positiva de l'anell de piperidina que interaccoiona amb l'Asp$^{3.32}$ (veure FIGURA 23, requadre negre). La Phe$^{6.52}$ interacciona conjuntament amb Phe$^{5.47}$ amb grups funcionals aromàtics dels lligands (veure FIGURA 24, en verd).En els receptors 5HT$_{2A}$, 5HT$_{2B}$, 5HT$_{2C}$, 5HT$_4$ i 5HT$_6$ hi trobem l'Asn$^{6.55}$ (requadre blau, en blau cel) que pot interaccionar amb grups funcionals del tipus –NHCO- (requadre blau, en blau cel).

```
5H1A    LLGAIINWLGYSNSLLNPVIYA
5H1B    AIFDFFTWLGYLNSLINPIIYT
5H1D    ALFDFFTWLGYLNSLINPIIYT
5H1E    EVADFLTWLGYVNSLINPLLYT
5H1F    EMSNFLAWLGYLNSLINPLIYT
5H2A    ALLNVFVWIGYLSSAVNPLVYT
5H2B    MLLEIFVWIGYVSSGVNPLVYT
5H2C    KLLNVFVWIGYVCSGINPLVYT
5H4     QVWTAFLWLGYINSGLNPFLYA
5H5A    IWKSIFLWLGYSNSFFNPLIYT
5H6     GLFDVLTWLGYCNSTMNPIIYP
5H7     WVERTFLWLGYANSLINPFIYA
```

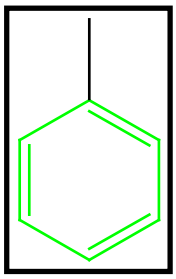

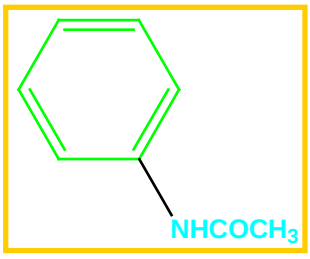

FIGURA 25. Alineament de les seqüències de la HTM7 dels receptors de serotonina en humà. Veiem la presència de residus aromàtics molt conservats com el Trp$^{7.40}$ i la Tyr$^{7.43}$ (requadre negre, en verd) que poden interaccionar amb motius aromàtics dels lligands (requadre negre, en verd). En el receptor 5-HT$_{1A}$ hi trobem l'Asn$^{7.39}$ (requadre ocre, en turquesa) que interacciona amb motius del tipus –NHCOCH$_3$ (requadre ocre, en turquesa). Aquesta interacció és molt important per a conferir selectivitat respecte a altres receptors.

Lligand	Estructura Química	K_i (nM) 5-HT_{1A}	K_i (nM) 5-HT_4	K_i (nM) 5-HT_7	Ki (nM) α_1
1	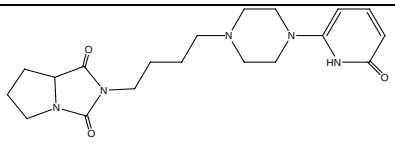	>10000			
2	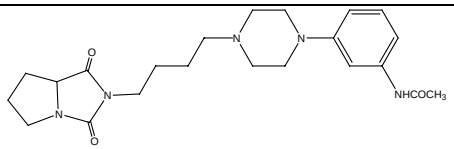	24			
3	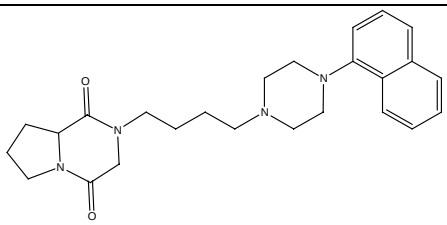	2.4			64.9
4	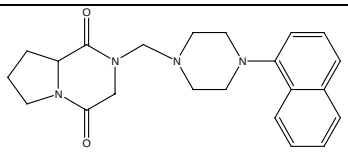	10.4			>1000
GR113808	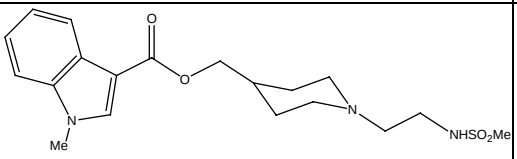		1.6		
5	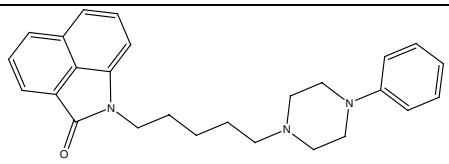			79.4	

TAULA 2. Dades d'unió dels lligands estudiats.

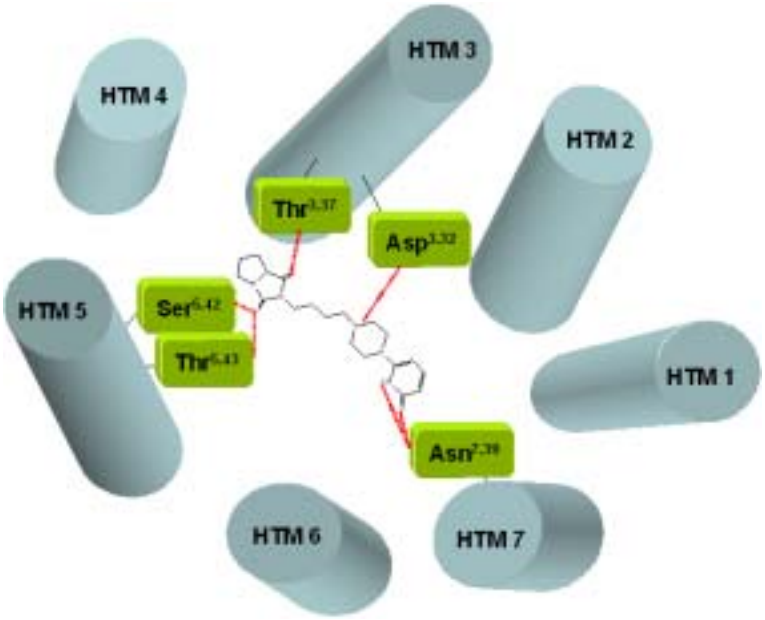

FIGURA 26. Representació de les set hèlixs α de la rodopsina i el lligand **1**. El lligand **1** interaccionaria òptimament amb el receptor 5-HT_{1A} si la disposicó de les set hèlixs α fos la mateixa que la de la rodopsina. El lligand interaccionaria amb el receptor a través dels residus $Asp^{3.32}$, $Ser^{5.42}$, $Thr^{5.43}$, $Thr^{3.37}$ i Asn $^{7.39}$.

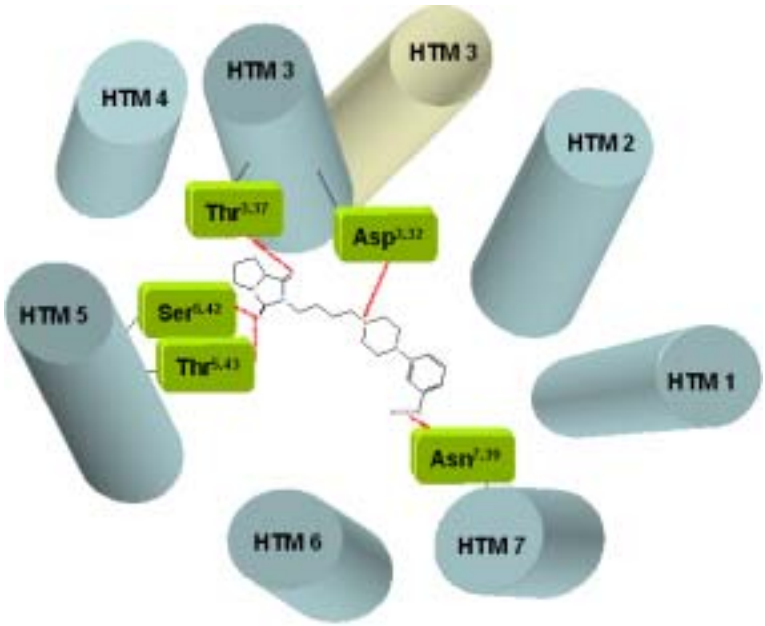

FIGURA 27. Representació de les set hèlixs α del receptor 5-HT_{1A} fruit de les simulacions de dinàmica molecular. Com a conseqüència del diferent motiu de la HTM3 entre la rodopsina i el receptor 5-HT_{1A}, la HTM3 es troba doblegada cap a la HTM5 allunyant-se de la HTM2. El lligand **2** interaccionaria òptimament amb el receptor 5-HT_{1A} que presenta la conformació de la HTM3 proposada en aquest treball.

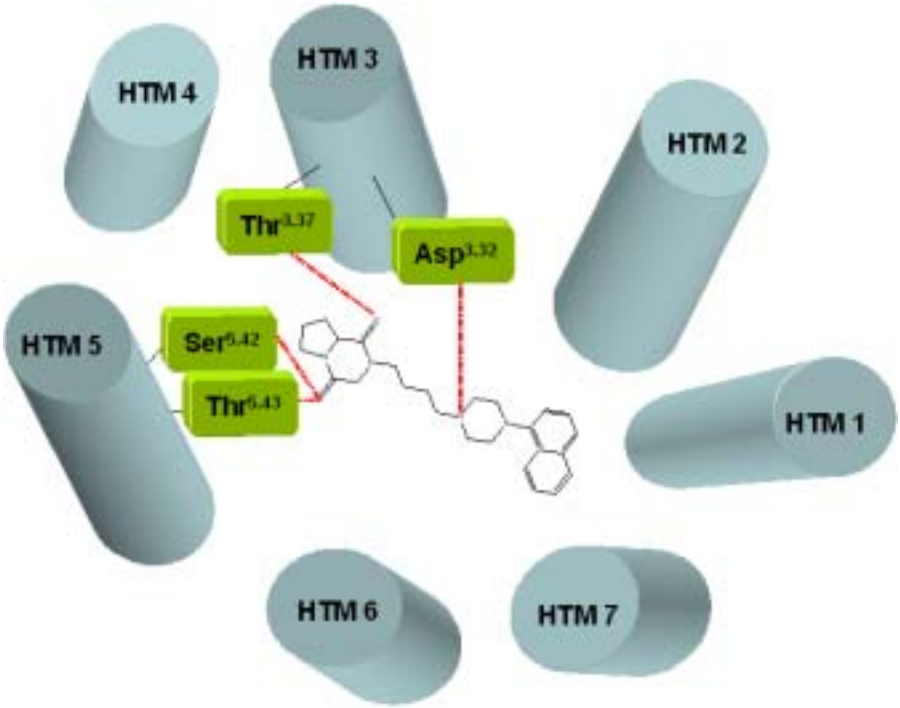

FIGURA 28. Esquema del mode d'unió del lligand **3** amb el receptor 5-HT_{1A}. La interacció es dóna entre el motiu hidantoïna i els residus $Thr^{3.37}$, $Ser^{5.42}$ i $Thr^{5.43}$ i entre l'$Asp^{3.32}$ i l'amina protonada del lligand.

	3.32	3.37	5.39	5.42	5.43
$5HT_{1A}$	CDLFIALDVLCCT		GYTIYST		FGA
α_{1A}	CNIWAAVDVLCCT		GYVLFSALGS		
α_{1B}	CDIWAAVDVLCCT		FYALFSSLGS		
α_{1D}	CDVWAAVDVLCCT		GYAVFSSVCS		

FIGURA 29. Seqüències aminoacídiques de la HTM3 i HTM5 del receptor 5-HT_{1A} i dels receptors α-adrenèrgics. Veiem que els residus que interaccionen amb el lligand **3** en el receptor 5-HT_{1A} es troben conservats en els receptors α-adrenèrgics. Per tal de guanyar selectivitat cal dissenyar un lligand que interaccioni amb residus presents en el 5-HT_{1A} i no en els α-adrenèrgics

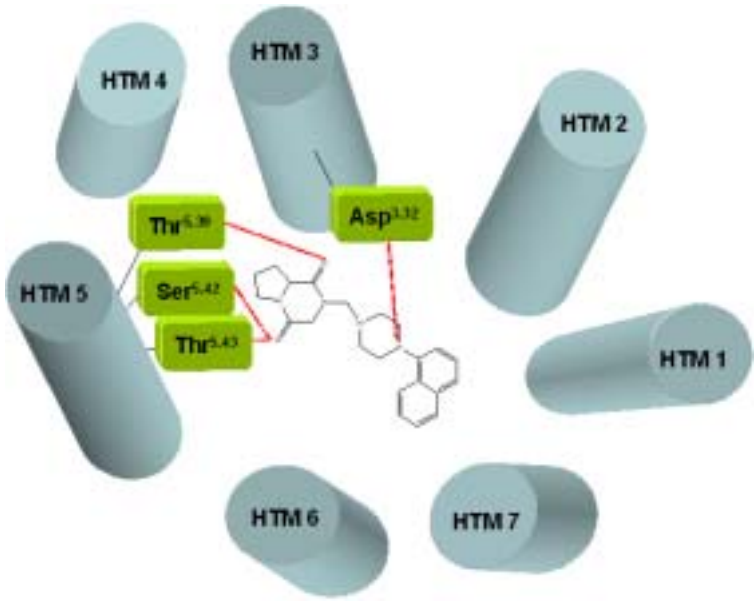

FIGURA 30. Mode d'unió del lligand **4** amb el receptor 5-HT_{1A}. El fet de tenir la cadena carbonada més curta que el lligand **3** fa que el lligand **4** interaccioni amb el motiu hidantoin a través dels residus $Thr^{5.39}$, $Ser^{5.42}$ i $Thr^{5.43}$. L'$Asp^{3.32}$ segueix interaccionant amb l'amina protonada del lligand. El fet que el residu $Thr^{5.39}$ es trobi present en el receptor 5-HT_{1A} i no en l'α_1-adrenèrgic, fa que aquest lligand sigui selectiu respecte el receptor α_1-adrenèrgic.

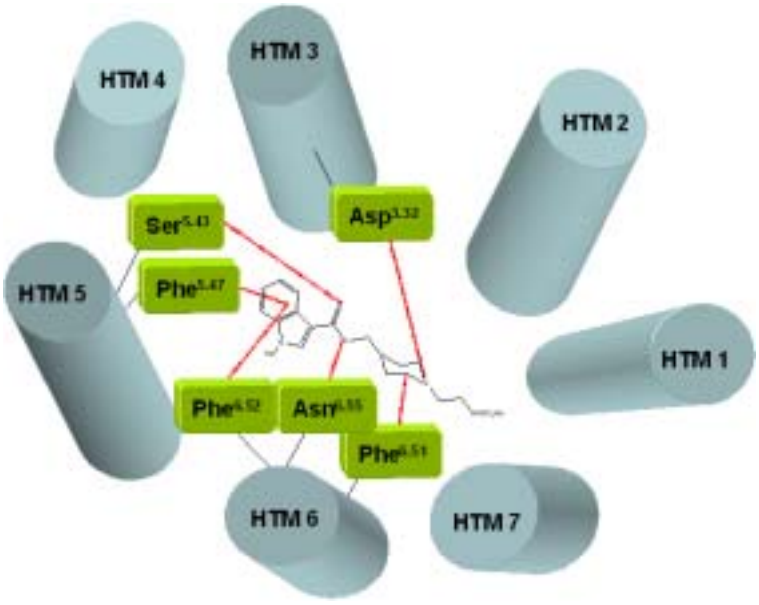

FIGURA 31. Esquema del mode d'unió del lligand **GR113808** amb el receptor 5-HT_4. El lligand **GR113808** interacciona amb el receptor 5-HT_4 a través de: (i) un enllaç per pont d'hidrogen entre l'oxígen carbonílic i el residu $Ser^{5.43}$,(ii) una interacció per pont d'hidrogen entre l'oxígen de l'éter i l'$Asn^{6.55}$, (iii) una interacció entre el residu $Asp^{3.32}$ i l'amina protonada, (iv) una interacció entre $Phe^{6.51}$ i l'anell de piperidina i (v) una interacció π-σ aromàtica-aromàtica entre $Phe^{6.52}$ i l'anell d'indol.

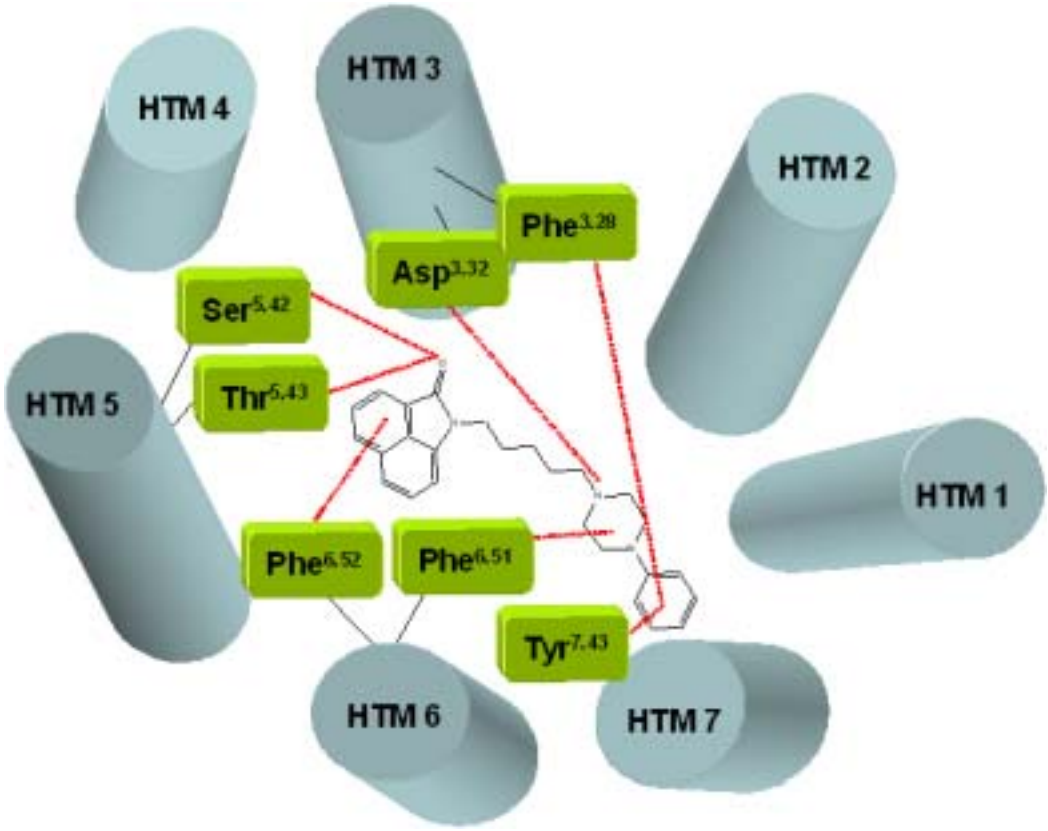

FIGURA 32. Esquema del mode d'interacció entre el lligand **5** i el receptor 5-HT_7. El lligand **5** intreacciona amb el receptor a través de (i) dues interaccions per pont d'hidrogen entre els residus $Ser^{5.42}$ i $Thr^{5.43}$ i l'oxígen carbonílic, (ii) una interacció entre l'$Asp^{3.32}$ i l'amina protonada de l'anell de piperidina, (iii) una interacció entre $Phe^{6.52}$ i l'anell de naftolactam, (iv) una intreacció entre $Phe^{6.52}$ i l'anell de piperidina i (v) una interacció entre l'anell de naftolactam i la $Tyr^{7.43}$ i la $Phe^{3.28}$.